

The Development of Novel Biocatalysts for the Asymmetric Hydroamination of Alkenes

A Thesis Submitted to the University of Manchester for the Degree of Doctor of
Philosophy in the Faculty of Engineering and Physical Sciences

2014

Sarah Louise Lovelock

School of Chemistry

Contents

List of Figures.....	5
List of Schemes.....	8
List of Tables.....	10
Abstract.....	12
Declaration.....	13
Copyright Statement.....	14
Acknowledgements.....	15
Abbreviations.....	16
Chapter 1: Introduction.....	18
1.1 Introduction to Directed Evolution.....	19
1.2 Biocatalysis in Amine Synthesis.....	20
1.3 Optically Active α -Amino Acids.....	24
1.3.1 Methods of α -Amino Acid Synthesis.....	25
1.4 Ammonia Lyases.....	29
1.4.1 Phenylalanine Ammonia Lyases.....	32
1.4.2 Catalytic Mechanism.....	41
1.4.3 Key Active Site Residues.....	47
1.4.4 Previous Mutagenesis Work.....	49
1.5 Objectives.....	49
Chapter 2: Identifying a Candidate for Directed Evolution.....	51
2.1 Introduction.....	52
2.2 Analytical Methods for the Determination of PAL Catalyzed Activity.....	52
2.2.1 HPLC Analysis.....	54
2.2.2 Spectrophotometric Analysis.....	56
2.2.3 L-Amino Acid Oxidase Coupled Assay.....	58
2.3 Optimization of PAL Expression.....	59
2.4 Optimization of PAL Catalyzed Reaction Conditions.....	63
2.4.1 Amination Reaction Conditions.....	63
2.4.2 Deamination Reaction Conditions.....	64
2.5 Determining the Kinetic Constants for PAL Catalyzed Reactions.....	65
2.5.1 Deamination Kinetics.....	65
2.5.2 Amination Kinetics.....	67
2.6 Comparison of <i>PcPAL</i> , <i>RgPAL</i> and <i>AvPAL</i> as Whole Cell Biocatalysts for the Production of Non-Proteinogenic Amino Acids.....	69
2.6.1 Analytical Scale Biotransformations.....	70
2.6.2 Large Scale Reactions and Product Isolation.....	74
2.6.3 D-Amino Acid Synthesis.....	74
2.7 Discussion and Conclusion.....	75
2.7.1 Chosen Target for Evolution.....	77
Chapter 3: Mechanistic Studies of PAL Catalyzed D-Amino Acid Formation.....	79
3.1 Introduction.....	79

3.2	Time Dependence on e.e.	80
3.3	Wild-type AvPAL Catalyzed Deamination of 4-Nitrophenylalanine	82
3.4	Thermodynamic Position of Equilibrium	83
3.5	Investigating the Activity of 4-Nitro- <i>cis</i> -Cinnamic Acid	85
3.6	Site-Directed Mutagenesis of Key Active Site Residues	85
3.6.1	Kinetic Constants for S168A Catalyzed Reactions	88
3.6.2	NaBH ₄ Reduced AvPAL	89
3.7	Isotope Labelling Studies to Determine the Stereoselectivity of AvPAL Catalyzed Amination and Deamination Reactions	91
3.7.1	Synthesis of Deuterated Standards	92
3.7.2	NMR Study of the Amination Reaction of Labelled Substrates	94
3.7.3	NMR Study of the Deamination Reaction of Labelled Substrates	96
3.8	Docking Study	99
3.9	Conclusions	101
Chapter 4: Testing the Substrate Promiscuity of Wild-type PALs		104
4.1	Introduction	104
4.2	Chemical Synthesis of Amine Substrates	106
4.3	Chemical Synthesis of Alkene Substrates	108
4.4	Analytical Methods	110
4.5	PAL Activity Towards Novel Substrates	111
4.6	Nucleophile Promiscuity	116
4.7	Conclusion	118
Chapter 5: Assay Development and Screening		119
5.1	Introduction	120
5.2	Assay Development	120
5.2.1	Measuring the Absorbance of Alkene Products	120
5.2.2	Derivatisation Methods	122
5.2.3	Enzyme Coupled Assays	123
5.2.4	Summary of Assays	132
5.3	Screening	134
5.3.1	Screening Variants for Enhanced D-Selectivity	134
5.3.2	Screening Variants for Activity Towards Amine Substrates	141
5.4	Conclusions and Future Work	143
Chapter 6: Materials and Methods		145
6.1	Chemicals and Reagents	146
6.2	Genes and Enzymes	146
6.3	Instruments	148
6.4	Buffers and Solutions	148
6.5	Protein Production and Purification	149
6.5.1	PAL Expression	149
6.5.2	<i>PpRac</i> Expression	149
6.5.3	MAO-N Expression	150
6.5.4	<i>E. coli</i> Amine Oxidase (EcAO) Expression and Purification	150

6.5.5	General Procedure for the Preparation of Cell Lysate	151
6.5.6	General Procedure for Protein Purification	151
6.6	Biotransformation Procedures.....	152
6.6.1	Preparation of Racemic Standards for HPLC Analysis.....	152
6.6.2	General Procedure for PAL Catalyzed Hydroamination of Cinnamic Acid Analogues	152
6.6.3	Large Scale PAL Catalyzed Hydroamination Reactions.....	152
6.6.4	D-Amino Acid Synthesis	153
6.6.5	General Procedure for PAL Catalyzed Deamination of Amine Substrates.....	153
6.6.6	General Procedure for PAL Catalyzed Hydroamination of Alkenes	153
6.7	Site Directed Mutagenesis	153
6.7.1	Sodium Borohydride Reduced PAL	155
6.7.2	Circular Dichroism	155
6.7.3	UV Difference Spectroscopy	155
6.8	Deuterium Isotope Labelling Study	155
6.8.1	Amination Reactions	155
6.8.2	Deamination Reactions	156
6.9	Determining the Kinetic Parameters of PAL catalyzed reactions	157
6.9.1	Measurement of Deamination Kinetic Constants.....	157
6.9.2	Measurement of Amination Kinetic Constants	158
6.10	Derivatisation Methods.....	158
6.10.1	Trinitrobenzene Sulphonic Acid (TNBS) Derivatisation	158
6.10.2	Dansyl Chloride (Dns-Cl) Derivatisation	158
6.10.3	Fluorescamine Derivatisation.....	158
6.11	Amine Oxidase Spectrophotometric Screen	158
6.12	General Procedures for the Amino Acid Oxidase Coupled Assays	159
6.12.1	Liquid Phase Amino Acid Oxidase Coupled Assay.....	159
6.12.2	Colony Based D-Amino Acid Oxidase Screen.....	159
6.12.3	Liquid Phase Transaminase/ D-Amino Acid Oxidase Screen	160
6.12.4	Colony Based Transaminase/D-Amino Acid Oxidase Screen	160
6.13	Chemical Synthesis.....	161
7	Appendix	171
7.1	DNA and Protein Sequences	171
7.2	PAL Catalyzed Hydroamination Reactions	181
7.3	Amino Acid Positions in Pools A-D	185
7.4	Publications.....	187
8	References	192

List of Figures

Figure 1: Stages of directed evolution for the development of biocatalysts with enhanced properties	19
Figure 2: Structures of therapeutic peptides and α -amino acid containing drug molecules	24
Figure 3: Methods for the synthesis of optically active α -amino acids.....	26
Figure 4: Non-proteinogenic amino acid substrates for <i>PcPAL</i> and <i>RgPAL</i>	34
Figure 5: The crystal structures of <i>AvPAL</i> and <i>RgPAL</i> showing the four interlocking monomers.	35
Figure 6: The six positive poles and one negative pole of the seven α -helices associated with the <i>RgPAL</i> active site	37
Figure 7: The structures of <i>AvPAL</i> and <i>RgPAL</i> , highlighting the extended C-terminal residues found in eukaryotic PALs	38
Figure 8: <i>AvPAL</i> crystal structure showing the inner catalytic loop and outer loop	39
Figure 9: Superimposed structures of <i>AvPAL</i> and <i>PcPAL</i> with catalytic loops	40
Figure 10: Two proposed intermediates in the PAL catalyzed L-phenylalanine deamination reaction.....	41
Figure 11: Schematics of the <i>PcPAL</i> active site with L-phenylalanine interactions.....	45
Figure 12: Sequence alignments for PALs, PAMs, TAMs and TALs.....	47
Figure 13: Conserved <i>AvPAL</i> active site residues.....	48
Figure 14: Panel of cinnamic acid derivatives screened for PAL activity	53
Figure 15: Chiral HPLC trace of the <i>PpRac</i> catalyzed racemization of L-2f.	56
Figure 16: The wavelength scans of A) cinnamic acid and phenylalanine B) 4-nitrocinnamic acid and 4-nitrophenylalanine	57
Figure 17: Plasmid map of the <i>RgPAL</i> gene cloned into pET-16b	60
Figure 18: The OD ₆₀₀ of <i>E. coli</i> BL21(DE3) whole cells expressing <i>RgPAL</i> grown in auto-induction media	61
Figure 19: Activity of <i>E. coli</i> BL21(DE3) whole cells expressing <i>RgPAL</i> produced using auto-induction media at different temperatures.....	62
Figure 20: Relative rate of cinnamic acid amination using different ammonia sources.....	64
Figure 21: pH profile for <i>AvPAL</i> , <i>RgPAL</i> and <i>PcPAL</i> catalyzed deamination of L-phenylalanine	65
Figure 22: The deamination of L-phenylalanine measured spectrophotometrically.....	66
Figure 23: The amination of cinnamic acid measured spectrophotometrically.....	68
Figure 24: Conserved active site residues of <i>RgPAL</i> , <i>PcPAL</i> and <i>AvPAL</i>	76
Figure 25: Superimposed structures of <i>PcPAL</i> and <i>AvPAL</i>	76
Figure 26: Chiral reverse phase HPLC traces from the <i>AvPAL</i> catalyzed hydroamination of 4-nitrocinnamic acid	81
Figure 27: The amination reaction of 4-nitrocinnamic acid mediated by whole cell <i>AvPAL</i> biocatalysts.....	82

Figure 28: HPLC traces for AvPAL catalyzed reactions starting from a) 4-nitro-L-phenylalanine b) 4-nitro-D-phenylalanine and c) 4-nitrocinnamic acid.....	84
Figure 29: SDS-PAGE of wild-type AvPAL and variants	86
Figure 30: CD spectra of wild-type AvPAL, Y78F, S168A and Y78F/S168A	87
Figure 31: UV difference spectra between wild-type and S168A AvPAL	87
Figure 32: CD spectra of S168A, wild-type and NaBH ₄ reduced AvPAL.....	90
Figure 33: L-Phenylalanine docked into the AvPAL active site and covalently bound via the substrate amine to the MIO cofactor	91
Figure 34: ¹ H NMRs of the AvPAL catalyzed hydroamination of 4-nitro-(3- ² H)-cinnamic acid	95
Figure 35: ¹ H NMR spectra of the AvPAL catalyzed deamination of isotopically labelled 4-nitro-D-phenylalanines 13 and 16	97
Figure 36: Proposed mechanism for the loss of deuterium incorporation in the AvPAL catalyzed deamination of 4-nitro-D-phenylalanine D-13	99
Figure 37: Modelling of a) L-phenylalanine and b) D-phenylalanine in the AvPAL active site	100
Figure 38: Proposed MIO-dependent and MIO-independent pathways for PAL catalyzed synthesis of amino acids.	102
Figure 39: Panel of substrates chosen to screen wild-type PAL deamination activity.....	105
Figure 40: Panel of substrates chosen to screen wild-type PAL hydroamination activity	109
Figure 41: GC-FID traces: β-methylstyrene reactions	115
Figure 42: LC-MS analysis of the RgPAL catalyzed deamination of N-methyl-L-phenylalanine	117
Figure 43: LC-MS analysis of the RgPAL catalyzed hydroamination of cinnamic acid	118
Figure 44: Wavelength scan of (R)-amphetamine and <i>trans</i> -β-methylstyrene	121
Figure 45: Wavelength scan of 4-nitro-(R)-amphetamine and 4-nitro- <i>trans</i> -β-methylstyrene	121
Figure 46: Method for the preparation of libraries and liquid phase screening using the L-AAO coupled assay	124
Figure 47: Method of screening libraries using the D-AAO coupled colony based assay	126
Figure 48: Screening MAO-N D5, D9 and D11 for activity towards amphetamine	128
Figure 49: The activity of ATA-117 towards different amine substrates	130
Figure 50: Transaminase coupled assay for the detection of <i>trans</i> -β-methylstyrene hydroamination activity.....	132
Figure 51: 4-Nitrocinnamic acid docked in the AvPAL active site.....	135
Figure 52: Screening of libraries G169NNK and A167NNK using the L-AAO assay.....	136
Figure 53: The percentage conversion and product e.e for the hydroamination of 4-nitrocinnamic acid	138
Figure 54: SDS-gels of purified wild-type AvPAL and variants.....	139
Figure 55: AvPAL amino acid positions incorporated into the library	142
Figure 56: Colony based D-AAO/transaminase screen for PAL activity towards <i>trans</i> -β-methylstyrene using Pool A.....	142

Figure 57: Plasmid map of the D-AAO and transaminase genes cloned into pRSF-Duet1 ... 147
Figure 58: SDS-PAGE of AvPAL purification..... 151

List of Schemes

Scheme 1: BASF lipase catalyzed resolution of α -methylbenzylamine	21
Scheme 2: The application of MAO-N in the deracemization of optically active intermediates for the synthesis of levocetirizine and solifenacin	21
Scheme 3: MAO-N catalyzed desymmetrization in the synthesis of telaprevir	22
Scheme 4: (<i>R</i>)-Transaminase catalyzed synthesis of sitagliptin	22
Scheme 5: LeuDH catalyzed synthesis of L- <i>tert</i> -leucine in the synthesis of atazanavir	23
Scheme 6: Chemoenzymatic synthesis of 2-indolinecarboxylic acid, a key intermediate in the synthesis of hypertension drugs	23
Scheme 7: Organocatalytic reactions using amino acid and amino acid derived catalysts	25
Scheme 8: The three-component asymmetric Strecker synthesis	26
Scheme 9: Asymmetric Strecker synthesis with a guanidine chiral catalyst	27
Scheme 10: Synthesis of α,α -disubstituted amino acids by asymmetric allylations using a molybdenum catalyst	27
Scheme 11: Transfer catalyzed asymmetric alkylation of glycine Schiff bases using a cinchoninium salt	27
Scheme 12: Example of an asymmetric Mannich-type reaction under aqueous conditions ...	28
Scheme 13: Asymmetric hydrogenation of dehydroamino acids catalyzed by a rhodium-DuPHOS complex	28
Scheme 14: The hydantoin process for the synthesis of enantiopure α -amino acids using a hydantoin racemase, hydantoinase and <i>N</i> -carbamoyl-amino acid hydrolase cascade	29
Scheme 15: The proposed mechanism for the deamination of aspartic acid and 3-methylaspartic acid catalyzed by the corresponding ammonia lyase	31
Scheme 16: Phenylalanine ammonia lyase catalyzed deamination of L-phenylalanine	32
Scheme 17: Phenylalanine aminomutases catalyze the interconversion of α -phenylalanine and β -phenylalanine	33
Scheme 18: The PAL catalyzed hydroamination of cinnamic acid analogues for the synthesis of optically active amino acids	33
Scheme 19: Proposed mechanism of autocatalytic MIO formation	37
Scheme 20: PAL catalyzed deamination of L-phenylalanine via different elimination mechanisms	42
Scheme 21: PAL catalyzed mechanism of deuterium washout in the elimination reaction of L-[5'- ² H]-histidine	43
Scheme 22: PAL catalyzed deamination of L-phenylalanine via a Friedel-Crafts type mechanism	44
Scheme 23: Racemization of L-amino acids using <i>PpRac</i>	56
Scheme 24: L-AAO coupled assay for the detection of PAL catalyzed amination activity	59
Scheme 25: <i>Av</i> PAL mediated synthesis of L-amino acids 2d and 2e	74
Scheme 26: Enzymatic kinetic resolution of phenylalanine derivatives 2b-n	75

Scheme 27: Proposed mechanism for the PAM catalyzed isomerization of (2 <i>S</i>)- α -phenylalanine	79
Scheme 28: Synthesis of 4-nitro- <i>cis</i> -cinnamic acid 7	85
Scheme 29: Synthesis of deuterium labelled enamide 11	92
Scheme 30: Synthesis of 4-nitro-(3 <i>S</i> - ² H)-D-phenylalanine 13	92
Scheme 31: Synthesis of 4-nitro-(3 <i>R</i> - ² H)-D-phenylalanine 16	93
Scheme 32: Stereoinversion and kinetic resolution to yield enantiopure α -amino acids	93
Scheme 33: Synthesis of deuterated 4-nitrocinnamic acid 18	93
Scheme 34: Amino acid oxidase catalyzed kinetic resolution of deuterated 4-nitrophenylalanine 13	96
Scheme 35: The reversible hydroamination of cinnamic acid methyl ester catalyzed by <i>R. glutinis</i> whole cells and the deamination of L-tyrosinol catalyzed by <i>PcPAL</i> F137H	104
Scheme 36: Aspartate ammonia lyase catalyzed hydroamination of fumarate using primary amine nucleophiles and the non-reversible <i>PcPAL</i> catalyzed deamination of <i>N</i> -methyl-L-phenylalanine	105
Scheme 37: Synthesis of 4-nitro-L-phenylalaninol 30	106
Scheme 38: Synthesis of nitro-substituted amphetamine	106
Scheme 39: Synthesis of Cbz-protected amines 42-45	107
Scheme 40: Deprotection of the amino ketone 42 and amino aldehyde 43	107
Scheme 41: Deprotection of <i>N</i> -Boc protected amino aldehyde 48	108
Scheme 42: Deprotection of amino acetals 44 and 45	108
Scheme 43: Synthesis of 4-nitro- <i>trans</i> -cinnamic acid methyl ester 49	109
Scheme 44: Synthesis of nitro-substituted <i>trans</i> - β -methylstyrene	109
Scheme 45: Synthesis of acetals 57 and 58	110
Scheme 46: Previously reported hydroamination reactions of <i>trans</i> - β -methylstyrene using a range of nucleophiles	112
Scheme 47: Synthesis of <i>N</i> -benzylidene methylamine from benzaldehyde and methylamine	114
Scheme 48: PAL catalyzed hydroamination of cinnamic acid using primary amine nucleophiles for the synthesis of chiral secondary amine products	116
Scheme 49: L-AAO coupled assay for the detection of L-amino acid formation	124
Scheme 50: D-AAO coupled assay for detection of D-amino acid formation	125
Scheme 51: Assay for the detection of oxidase activity towards (<i>R</i>)-amphetamine	127
Scheme 52: HRP catalyzed oxidation of 4-AAP and subsequent reaction with TBHBA	127
Scheme 53: Assay for the detection of (<i>R</i>)-amphetamine and (<i>S</i>)-phenylalaninol using a transaminase, D-AAO and HRP	129
Scheme 54: PAL catalyzed hydroamination of α - and β -substituted cinnamic acid analogues	143

List of Tables

Table 1: Key features of ammonia lyases	30
Table 2: Sequence identities and similarities between PAL enzymes from different sources	36
Table 3: Methods for reverse phase HPLC analysis	54
Table 4: Response factors for the calculation of percentage conversion	55
Table 5: Wavelengths and correction factors used to measure the kinetic constants	58
Table 6: The deamination activity of whole cells expressing <i>RgPAL</i> towards L-phenylalanine	62
Table 7: <i>AvPAL</i> kinetic constants for the deamination of substrates 2a-d , 2i-j & 2m-n	67
Table 8: Kinetic constants for the PAL catalyzed amination reactions of 1a-d , 1i-j & 1m-n	69
Table 9: Percentage conversion at the point of maximal product e.e. for the PAL catalyzed hydroamination reactions of substrates 1a-1n	71
Table 10: Percentage conversion and product e.e. for the PAL catalyzed hydroamination reactions of substrates 1a-1n after 22h reaction time	73
Table 11: Kinetic constants for the deamination of 4-nitrophenylalanine.....	82
Table 12: Kinetic constants for wild-type and S168A <i>AvPAL</i> catalyzed amination and deamination reactions	89
Table 13: Kinetic constants for NaBH ₄ treated <i>AvPAL</i> and S168A catalyzed amination and deamination reactions	90
Table 14: <i>AvPAL</i> catalyzed deamination of deuterated 4-nitro-D-phenylalanine substrates 13 and 16 under different reaction conditions.....	98
Table 15: Conditions for normal phase HPLC and GC-FID analysis	110
Table 16: Amines screened as potential substrates for <i>AvPAL</i> and <i>RgPAL</i> catalyzed deamination reactions	111
Table 17: Alkenes screened as potential substrates for <i>AvPAL</i> and <i>RgPAL</i> catalyzed hydroamination reactions	112
Table 18: Reaction conditions used for the PAL catalyzed hydroamination reaction of <i>trans</i> - β -methylstyrene.....	113
Table 19: Derivatizing agents and methods of detection	122
Table 20: Advantages and disadvantages of the newly developed screening methods	133
Table 21: Percentage conversion and product e.e. for the hydroamination reaction of 4-nitrocinnamic acid catalyzed by different <i>AvPAL</i> variants	137
Table 22: Kinetic constants for the deamination of 4-nitro-L-phenylalanine and 4-nitro-D-phenylalanine catalyzed by wild-type <i>AvPAL</i> and variants.....	140
Table 23: Kinetic constants for the amination of 4-nitrocinnamic acid	141
Table 24: Vectors containing different genes and restriction sites used for subcloning	146
Table 25: Mutagenic primer sequences for site directed mutagenesis	154
Table 26: Thermal cycling parameters for site directed mutagenesis.....	154
Table 27: Molar absorbance coefficient for cinnamic acid derivatives 1a-d , 1i-j & 1m-n	157

Table 28: Mutations in the protein sequence of each MAO-N variant	180
Table 29: <i>RgPAL</i> catalyzed amination reactions of cinnamic acid derivatives 1a-n	182
Table 30: <i>PcPAL</i> catalyzed amination reactions of cinnamic acid derivatives 1a-n	183
Table 31: <i>AvPAL</i> catalyzed amination reactions of cinnamic acid derivatives 1a-n	184

Abstract

The research presented in this thesis describes the application of phenylalanine ammonia lyase from the bacteria *Anabaena variabilis* (AvPAL), as a biocatalyst for the asymmetric hydroamination of cinnamic acid derivatives. PALs from eukaryotic sources such as the plant *Petroselinum crispum* (PcPAL) and yeast *Rhodotorula glutinis* (RgPAL) have been widely used as biocatalysts for the synthesis of non-natural amino acids. For example the PAL catalyzed hydroamination of 2'-chlorocinnamic acid has been implemented by DSM Pharma Chemicals on a tonne scale. However, there are very few examples of prokaryotic PALs and to our knowledge their activity towards unnatural substrates has not been investigated. Herein we explore the activity of AvPAL towards a panel of cinnamic acid analogues. For comparison, the activity of the commonly studied eukaryotic PcPAL and RgPAL towards the same substrate panel was also investigated. Although the difference in substrate conversions between the three PALs was fairly unremarkable, a significant reduction in product e.e. was observed following prolonged reaction times with all three PALs towards substrates bearing electron deficient aromatic rings. A time dependence on e.e. has not been previously reported for ammonia lyases and all previously described biotransformations have been reported to proceed with excellent e.e. in favour of the L-enantiomer. The mechanism leading to the formation of D-phenylalanine derivatives was explored through mutagenesis of key active site residues and isotopic labeling studies. The results obtained demonstrate that D-amino acid formation occurs via a previously unobserved competing MIO-independent pathway which proceeds in a non-stereoselective manner. In addition, the observations are consistent with amino acid deamination occurring via a stepwise E₁cB elimination mechanism.

In order to develop a more general biocatalytic method for asymmetric hydroamination reactions, the activity of PAL towards substrates lacking the carboxylic acid functionality was investigated. The synthesis of a panel of substrates and subsequent screening with AvPAL and RgPAL is described. Unfortunately, the wild-type enzymes demonstrated no activity towards any of the substrates screened. These enzymes were also screened for their promiscuity towards the nucleophilic amine partner and although deamination activity towards *N*-methyl-L-phenylalanine was observed, no hydroamination activity was detected using primary amines as nucleophiles. In order to broaden the substrate specificity of PAL enzymes, a number of screening methods have been developed. Herein we present both liquid phase and colony based colorimetric screens for the detection of PAL catalyzed hydroamination activity. Furthermore these screens have been used to screen libraries of variants for increased D-selectivity and hydroamination activity towards β -methylstyrene and cinnamyl alcohol derivatives.

Declaration

I hereby declare that I am the sole author of this thesis. No portion of the work referred to in the thesis has been submitted in support of an application for another degree or qualification of this or any other university or other institute of learning. I understand that my thesis may be made electronically available to the public.

Copyright Statement

- i. The author of this thesis (including any appendices and/or schedules to this thesis) owns certain copyright or related rights in it (the "Copyright") and she has given The University of Manchester certain rights to use such Copyright, including for administrative purposes.
- ii. Copies of this thesis, either in full or in extracts and whether in hard or electronic copy, may be made only in accordance with the Copyright, Designs and Patents Act 1988 (as amended) and regulations issued under it or, where appropriate, in accordance with licensing agreements which the University has from time to time. This page must form part of any such copies made.
- iii. The ownership of certain Copyright, patents, designs, trademarks and other intellectual property (the "Intellectual Property") and any reproductions of copyright works in the thesis, for example graphs and tables ("Reproductions"), which may be described in this thesis, may not be owned by the author and may be owned by third parties. Such Intellectual Property and Reproductions cannot and must not be made available for use without the prior written permission of the owner(s) of the relevant Intellectual Property and/or Reproductions.
- iv. Further information on the conditions under which disclosure, publication and commercialisation of this thesis, the Copyright and any Intellectual Property and/or Reproductions described in it may take place is available in the University IP Policy (see <http://www.campus.manchester.ac.uk/medialibrary/policies/intellectualproperty.pdf>), in any relevant Thesis restriction declarations deposited in the University Library, The University Library's regulations (see <http://www.manchester.ac.uk/library/aboutus/regulations>) and in The University's policy on presentation of Theses.

Acknowledgements

Firstly I would like thank my supervisor Prof Nicholas Turner, for giving me the opportunity to work on this project and for all his support and guidance.

I want to thank Dr. Richard Lloyd for his supervision throughout my PhD and giving me opportunity to work in the Labs at Dr. Reddy's. I would also like to acknowledge the CoEBio3 for funding.

To all members of the Turner Flitsch group both past and present, thank you for all your friendly advice and for making the lab an enjoyable place to work. In particular I am grateful to Rachel Heath for her help in the development of the colony based assays and to Rachel and Mark Corbett for helpful discussion as well as proof reading this thesis. A special mention goes to Anthony Green for his scientific input, numerous proof readings and unending support.

I would like to acknowledge Dominique Richardson, Shahed Hussain, Lucy Heap and Anthony Green whose friendship has always made Manchester feel like home.

Finally, I wish to thank my family, in particular my parents and all my close friends for their continuing support and encouragement.

Abbreviations

4-AAP	4-Aminoantipyrine
AAL	Aspartate ammonia lyase
AdmH	<i>Pantoea agglomerans</i> phenylalanine aminomutase
Av	<i>Anabaena variabilis</i>
BCA	Bicinchoninic acid
BLAST	Basic logical alignment search tool
cB	Conjugate base
CD	Circular dichroism
CmdF	<i>Chondromyces crocatus</i> tyrosine aminomutase
D-AAO	D-Amino acid oxidase
DAB	3,3'-Diaminobenzidine
DAO	Diamine oxidase
E ₁	Unimolecular elimination
E ₂	Bimolecular elimination
EcAO	<i>Escherichia coli</i> amine oxidase
<i>E. coli</i>	<i>Escherichia coli</i>
EncP	<i>Streptomyces maritimus</i> phenylalanine ammonia lyase
FDH	Formate dehydrogenase
HAL	Histidine ammonia lyase
HRP	Horse radish peroxidase
IPTG	Isopropyl-β-D-1-thiogalactopyranoside
L-AAO	L-Amino acid oxidase
LB	Luria broth
LeuDH	Leucine dehydrogenase

MAL	3-Methylaspartate ammonia lyase
MAO-N	Monoamine oxidase from <i>Aspergillus niger</i>
MIO	5-Methylene-3,5-dihydroimidazol-4-one
NAAAR	N-Acyl amino acid racemase
NADH	Nicotinamide adenine dinucleotide
NCBI	National centre for biotechnological information
<i>Np</i>	<i>Nostoc punctiforme</i>
OD ₆₀₀	Optical density at 600 nm
PAL	Phenylalanine ammonia lyase
PAM	Phenylalanine aminomutase
<i>Pc</i>	<i>Petroselinum crispum</i>
PCR	Polymerase chain reaction
PDB	Protein data bank
PKU	Phenylketonuria
PLP	Pyridoxal-5'-phosphate
<i>Pp</i>	<i>Pseudomonas putida</i>
Rac	Racemase
<i>Rg</i>	<i>Rhodotorula glutinis</i>
<i>Rs</i>	<i>Rhodobacter sphaeroides</i>
SDS-PAGE	Sodium dodecyl sulphate polyacrylamide gel electrophoresis
<i>Sg</i>	<i>Streptomyces globisporus</i>
TAL	Tyrosine ammonia lyase
TAM	Tyrosine aminomutase
TBHBA	2,4,6-tribromo-3-hydroxy-benzoic acid
<i>Tc</i>	<i>Taxus canadensis</i>
Wt	Wild-type

Chapter 1: Introduction

1 Introduction

Over the past ten years, biocatalysis has become an established technology for the generation of a wide variety of products, ranging from pharmaceutical and agrochemical intermediates to components of biofuels.[1] The application of enzymes in chemical synthesis offers a practical and environmentally friendly alternative to traditional metallo- and organocatalysis.[2] Biocatalysts are obtained from renewable sources, they are biodegradable and function effectively under mild temperatures and in aqueous solutions. An effective biocatalyst has high chemo-, enantio- or regioselectivity, is stable under the required reaction conditions and has a high catalytic turnover. Frequently, for an enzyme to be useful on either a lab or industrial scale process it must first undergo optimization, and directed evolution has emerged as a powerful tool enabling the development of biocatalysts with desirable properties.[3]

1.1 Introduction to Directed Evolution

Directed evolution combines several important steps including (i) identification of a suitable target (ii) methods of generating large random libraries of genes and (iii) methods for screening these libraries to allow identification of variants with improved characteristics (Figure 1). The first challenge of directed evolution is identifying an enzyme with relevant catalytic activity towards analogues of the targeted substrates. This can be achieved by screening microbial culture collections and libraries of available enzymes or by the application of bioinformatics tools such as genome mining, BLAST searches and sequence alignments. Enzymes which demonstrate good stability and are easily overexpressed make particularly attractive targets for mutagenesis.

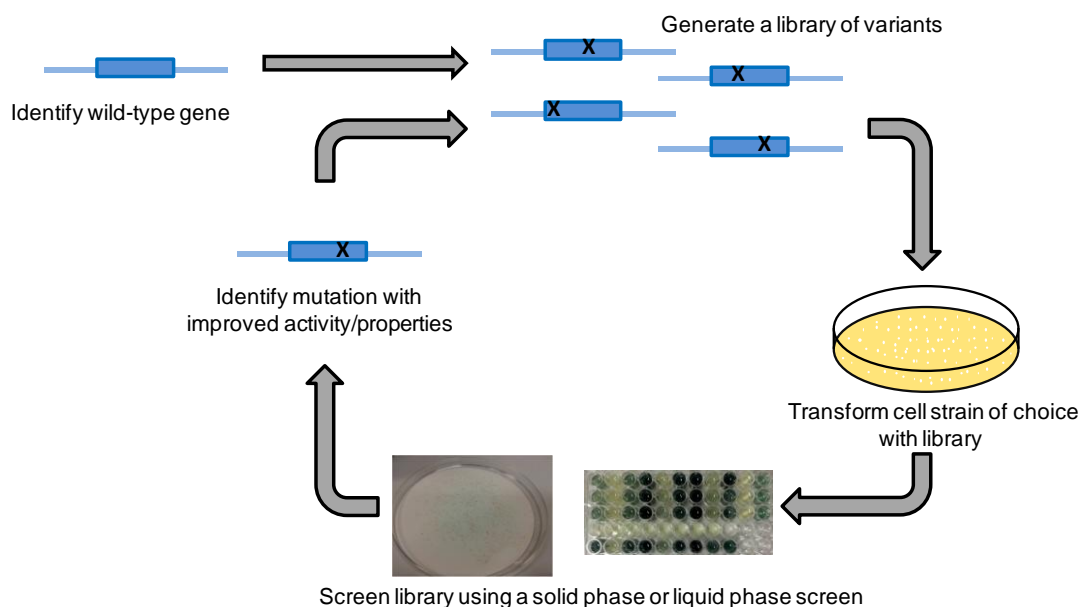


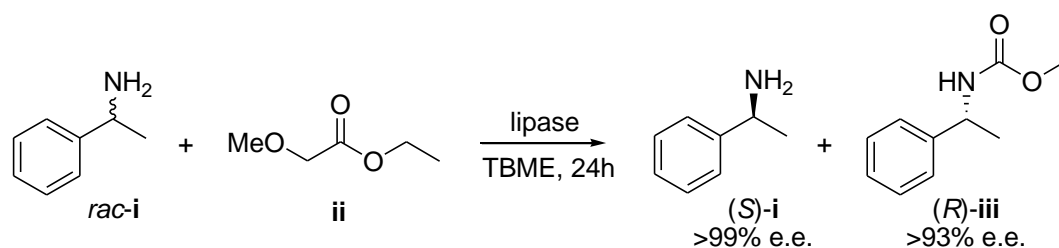
Figure 1: Stages of directed evolution for the development of biocatalysts with enhanced properties

The chosen method for generating libraries of genetic variants is dependent upon the capacity of the high-throughput screening methods.[4] Development of a robust high-throughput assay is vital to ensure all positive hits are identified with a low number of false positives. Libraries generated by DNA gene shuffling[5] or error-prone PCR are very large and require assays which are able to quickly screen a suitable number of variants such as colony based assays, fluorescence activated cell sorting (FACS),[6] phage-display[7] and yeast-display[8]. An example of an effective use of colony based screening is in the development of a toolbox of monoamine oxidase (EC 1.4.3.4) variants from *Aspergillus Niger* (MAO-N) which are able to catalyze the selective oxidation of a broad range of chiral amines.[9] To achieve this goal an assay based on detection of hydrogen peroxide co-product using horse radish peroxidase and a dye[10] allowed the effective screening of large libraries, generated first using a mutator strain and then by error-prone PCR.[11-13] The advantage of random mutagenesis is that it allows identification of previously unreported residues which influence catalysis, substrate binding or product release, which may be difficult to predict by rational design. When a high-throughput screen is unavailable, smaller, more focused libraries can be generated in order to reduce the screening effort. These libraries are designed using bioinformatics strategies, such as iterative combinatorial active site testing (CASTing)[14,15] and the use of reduced codons.[16,17] Abrahamson *et al.* utilized a CASTing approach to successfully engineer leucine dehydrogenase (EC 1.4.1.9 from *Bacillus stearothermophilus*) to function as an amine dehydrogenase.[18] A liquid phase spectrophotometric assay to detect the turnover of NADH cofactor was employed to effectively screen small libraries of variants.

1.2 Biocatalysis in Amine Synthesis

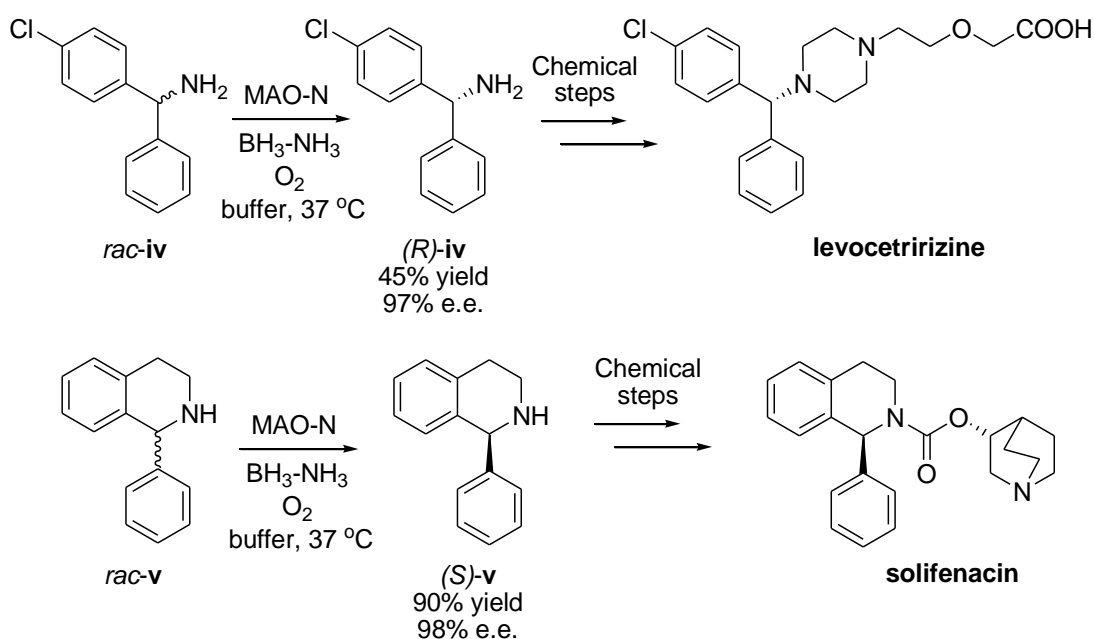
Recent innovations in the area of biocatalysis such as developments in screening and library design, have led to an increase in the industrial application of enzymes for the synthesis of a wide range of optically active compounds including amines, amides and amino acids.[19] Enzyme catalyzed synthesis is performed as either a kinetic resolution from racemic starting material or as an asymmetric synthesis from achiral substrates. The following section will focus on some specific industrial examples of biocatalysis in chiral amine synthesis.

BASF have developed a *Burkholderia plantarii* lipase (EC 3.1.1.1) catalyzed resolution of α -methylbenzylamine (**i**) using ethyl methoxyacetate (**ii**) as a donor substrate (Scheme 1).[20] The lipase stereoselectively acetylates the (*R*)-enantiomer to give access to enantiopure unreacted (*S*)-**i**. Removal of the amide product (*R*)-**iii** by distillation and subsequent hydrolysis allowed isolation of (*R*)-**i** in high optical purity.



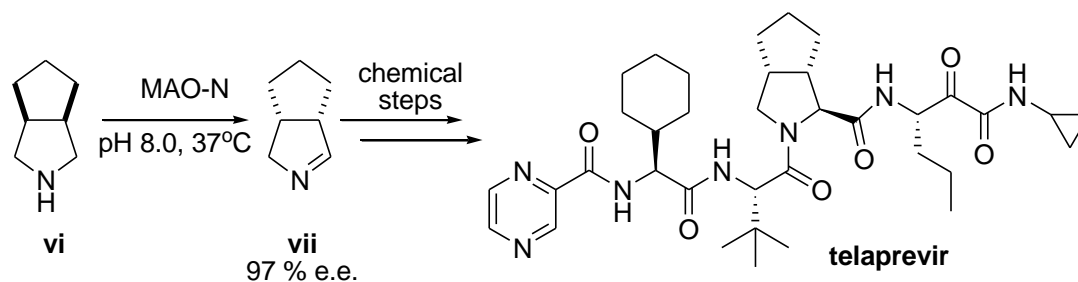
Scheme 1: BASF lipase catalyzed resolution of α -methylbenzylamine i

Although lipase catalyzed kinetic resolutions have been successful in the synthesis of a variety of enantiopure products, the method has the inherent disadvantage of maximum 50 % theoretical yields, which often renders this process uneconomic. To address this problem, methods have been developed for the dynamic kinetic resolution of racemic compounds. An example is the stereoselective oxidation of amines catalyzed by MAO-N, which when coupled with a non-selective chemical reducing agent leads to complete deracemization. Ghislieri *et al.* demonstrated the use of a MAO-N variant in the deracemization of two key pharmaceutical intermediates, 4-chlorobenzhydramine (**iv**) and 1-phenyl-tetrahydroisoquinoline (**v**) which are used in the synthesis of levocetirizine and solifenacin respectively (Scheme 2).[9]



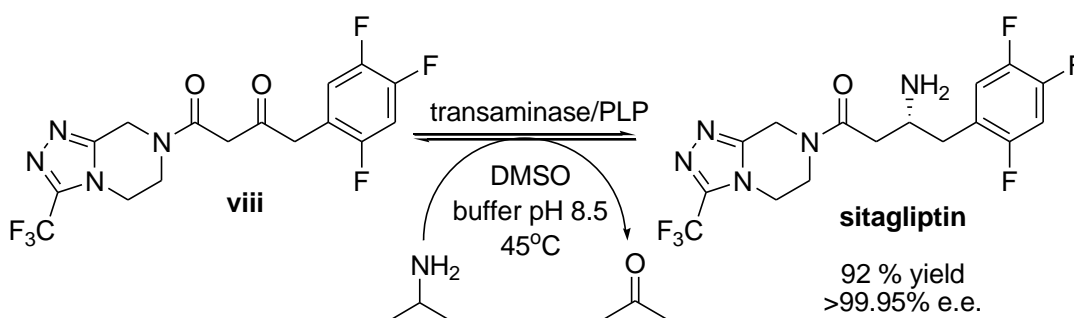
Scheme 2: The application of MAO-N in the deracemization of optically active intermediates for the synthesis of levocetirizine and solifenacin

A MAO-N variant has also been applied to the synthesis of the hepatitis C virus NS3 protease inhibitor, teleprevir (Scheme 3).[21] MAO-N catalyzes the oxidative desymmetrization of a prochiral bicyclic amine (**vi**) to the corresponding imine (**vii**) which is then reacted in a three-component Ugi-Passerini reaction with a carboxylic acid and an isocyanide intermediate. The new 11-step synthesis combining a biotransformation and a multi-component approach replaces a 24-step linear chemical synthesis, thereby improving both the atom and step economy of the process.



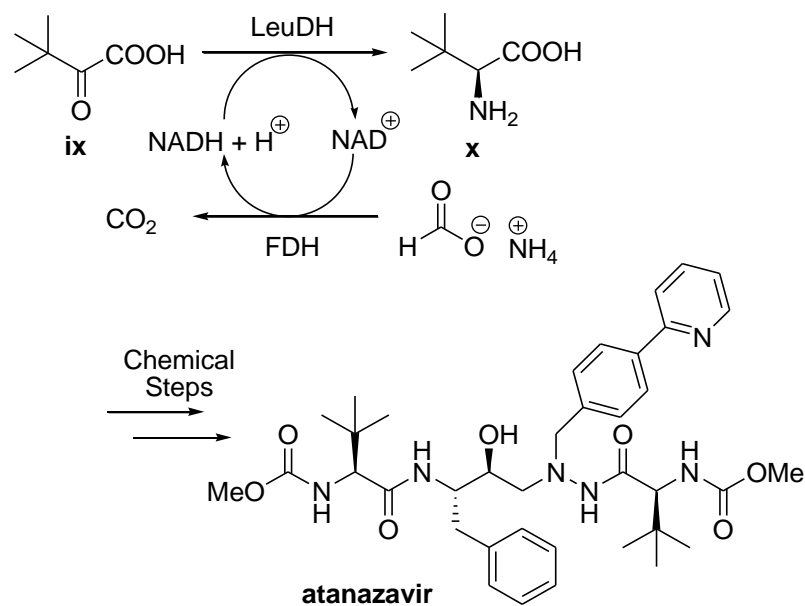
Scheme 3: MAO-N catalyzed desymmetrization in the synthesis of telaprevir

Biocatalysts can be utilized in asymmetric synthesis and a particularly significant example is the use of an engineered variant of an (*R*)-selective transaminase for the synthesis of the antidiabetic compound sitagliptin.[22] Codexis, in collaboration with Merck, engineered the PLP-dependent enzyme to catalyze the (*R*)-transamination of the ketone, prositagliptin (**viii**) using isopropylamine as an amine donor (Scheme 4). This biocatalytic transformation has been implemented in large scale production, replacing a high pressure rhodium-catalyzed asymmetric enamine hydrogenation which suffered from inadequate stereoselectivity. Moreover the biocatalytic process reduced the total waste and increased the productivity (kg/L per day) by 53 % compared to the previous chemical process.



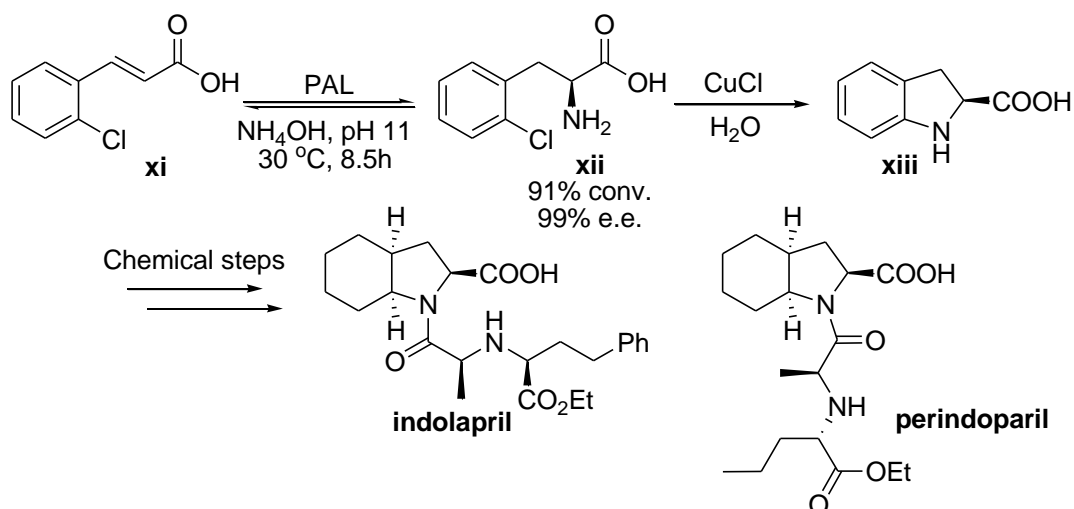
Scheme 4: (*R*)-Transaminase catalyzed synthesis of sitagliptin

Enzyme catalysis is an established method for industrial production of both proteinogenic and nonproteinogenic amino acids. Degussa utilize an L-leucine dehydrogenase (LeuDH) in the reductive amination of trimethylpyruvate (**ix**) for the synthesis of the non-natural amino acid L-*tert*-leucine (**x**) (Scheme 5).[23] L-*tert*-Leucine is an important synthetic building block in the manufacture of novel pharmaceutical active ingredients such as atazanavir, a protease inhibitor used in the treatment of HIV.



Scheme 5: LeuDH catalyzed synthesis of L-tert-leucine (x), coupled with formate dehydrogenase (FDH) cofactor recycling in the synthesis of atazanavir

A second biocatalytic method for asymmetric amino acid synthesis uses phenylalanine ammonia lyases (PAL, EC 4.3.1.24). DSM Pharma Chemicals have exploited the PAL catalyzed hydroamination reaction in the synthesis of 2'-chloro-L-phenylalanine (**xii**) on a tonne scale.[24] PAL from the yeast *Rhodotorula glutinis* is used to mediate the enantioselective addition of ammonia to 2'-chloro-cinnamic acid (**xi**), which undergoes subsequent copper catalyzed ring closure to yield (S)-2-indolinecarboxylic acid (**xiii**) (Scheme 6).[25] Compound **xiii** is an important building block for pharmaceuticals and is used in the synthesis of hypertension drugs such as indolapril and perindopril.



Scheme 6: Chemoenzymatic synthesis of 2-indolinecarboxylic acid **xiii, a key intermediate in the synthesis of hypertension drugs**

1.3 Optically Active α -Amino Acids

Proteinogenic amino acids have been produced industrially for more than 50 years for use in animal feedstocks and in the food industry.[23] L-Aspartic acid is required in large quantities for the manufacture of the dipeptide sweetener aspartame and is synthesized by the aspartase catalyzed addition of ammonia to fumaric acid. Optically active α -amino acids are also fundamental building blocks for the synthesis of a wide range of bioactive natural products and pharmaceuticals. In addition, non-proteinogenic amino acids have been used independently as drug molecules, including L-dopa (L-3,4-dihydroxyphenylalanine) the main drug used for the treatment of Parkinson's disease.[26]

There is significant interest in the development of therapeutic peptides and proteins which can contain both natural and non-natural amino acids (Figure 2). Protein therapeutics benefit from high specificity for their target due to a high number of interactions but can suffer from low bioavailability and low metabolic stability. To date more than one hundred peptide-based drugs have been produced commercially and the market for protein and peptide based therapeutics as of 2013 was estimated at more than \$40 billion per year.[27] Incorporation of D-amino acids into both peptides and small drug molecules can improve metabolic stability by increasing resistance to protease degradation.[28] For example the antibiotics ampicillin and amoxicillin contain the D-amino acid moieties, D-phenylglycine and *para*-hydroxy-D-phenylglycine respectively (Figure 2).

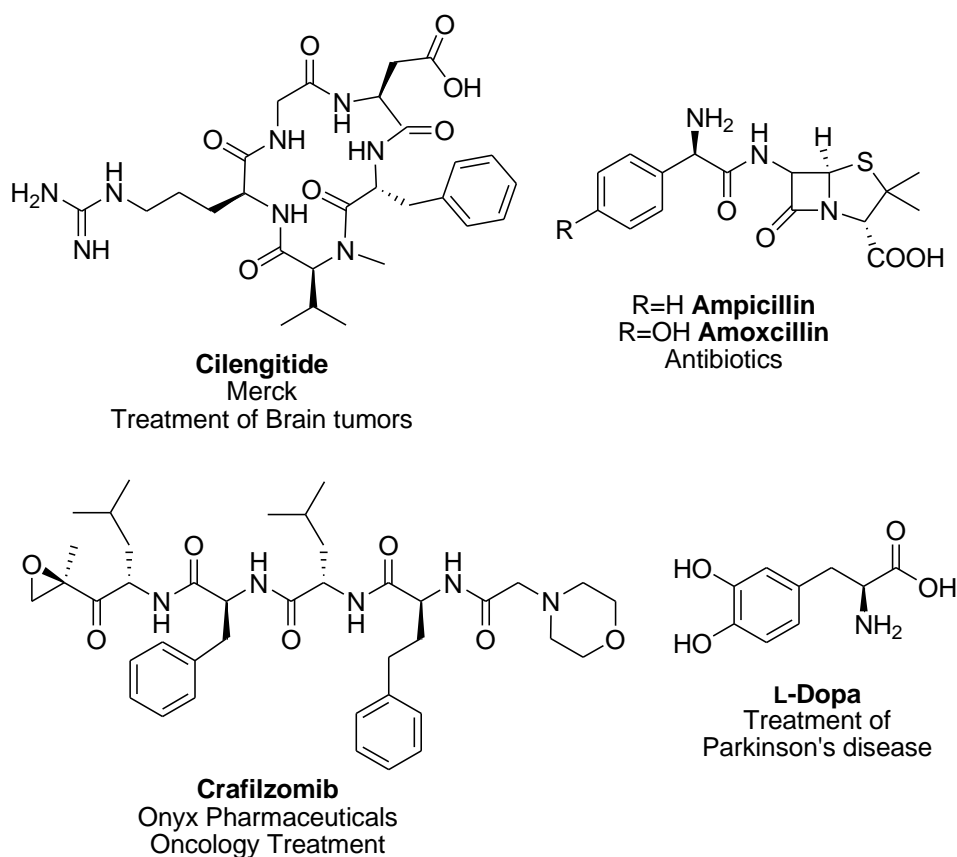
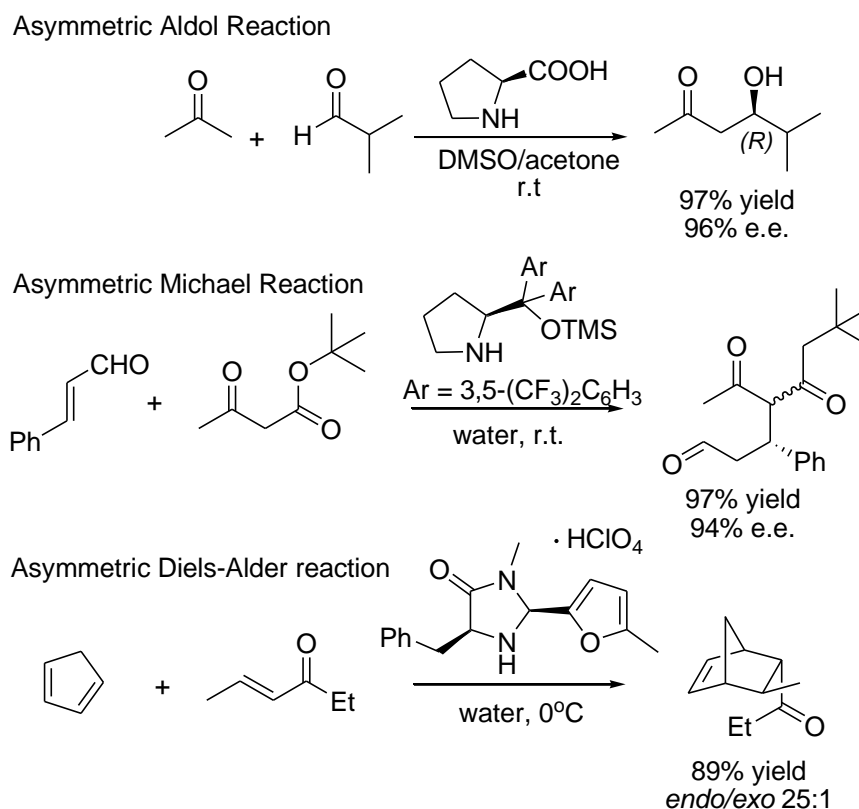


Figure 2: Structures of therapeutic peptides and α -amino acid containing drug molecules

Natural and non-natural amino acids are also frequently used in asymmetric synthesis as chiral starting materials and auxiliaries. List, Lerner and Barbas reported the first example of secondary amine promoted catalysis with the proline catalyzed direct intermolecular asymmetric aldol reaction.[29] Since then, numerous methodologies have been developed and amino acids and amino acid derived catalysts are now used to efficiently catalyze a whole range of asymmetric reactions (Scheme 7).[30,31]



Scheme 7: Organocatalytic reactions using amino acid and amino acid derived catalysts

1.3.1 Methods of α -Amino Acid Synthesis

The increasing demand to access amino acids in optically pure form has led to the development of several catalytic methods for their preparation,[32,33] including asymmetric Strecker reactions, C-C bond forming reactions and the hydrogenation of dehydroamino acids (Figure 3). The following section will discuss some current methods for the enantioselective synthesis of α -amino acids.

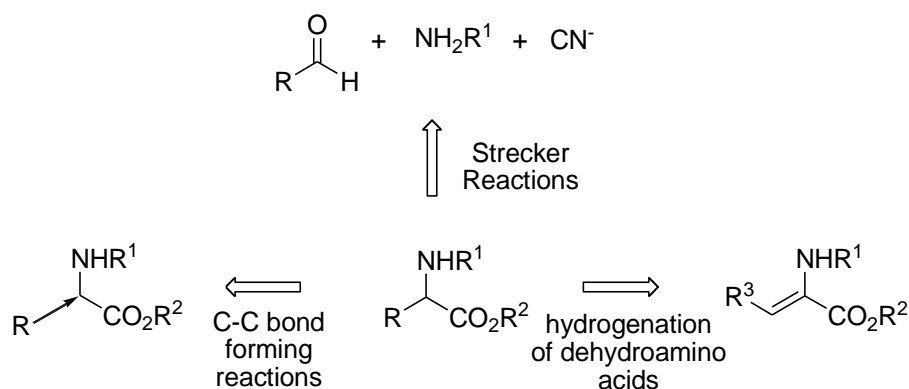
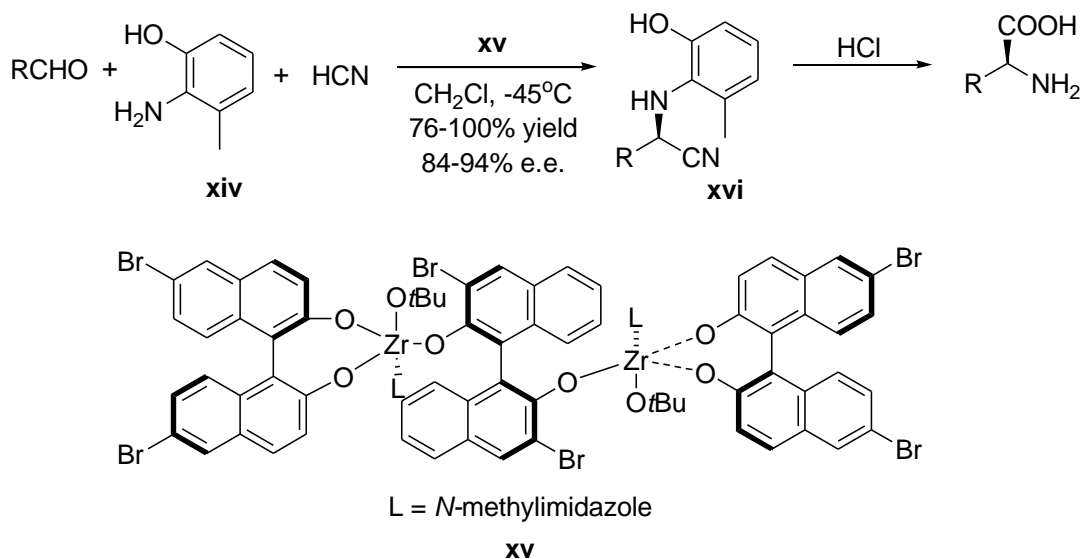


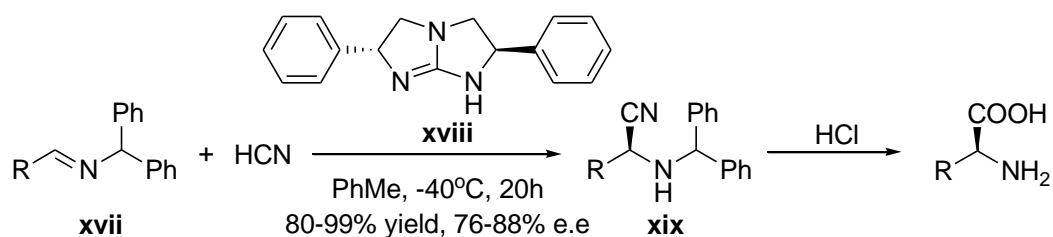
Figure 3: Methods for the synthesis of optically active α -amino acids

The direct hydrocyanation of imines and the three component Strecker synthesis are currently the simplest methods of α -amino acid synthesis.[34,35] The Strecker synthesis involves addition of cyanide onto an aldehyde followed by hydrolysis of the α -aminonitrile intermediate yielding both proteinogenic and non-proteinogenic amino acids. Both metal-based and metal-free chiral catalysts can be used to make this method enantioselective allowing access to either L- or D-products. Kobayashi *et al.* employed a chiral zirconium catalyst (**xv**) for the synthesis of α -amino acids starting from achiral aldehydes, an amine **xiv** and hydrogen cyanide (Scheme 8).[36] Treating the aminonitrile (**xvi**) with HCl gave access to the products in good yields with moderate to high enantioselectivity.



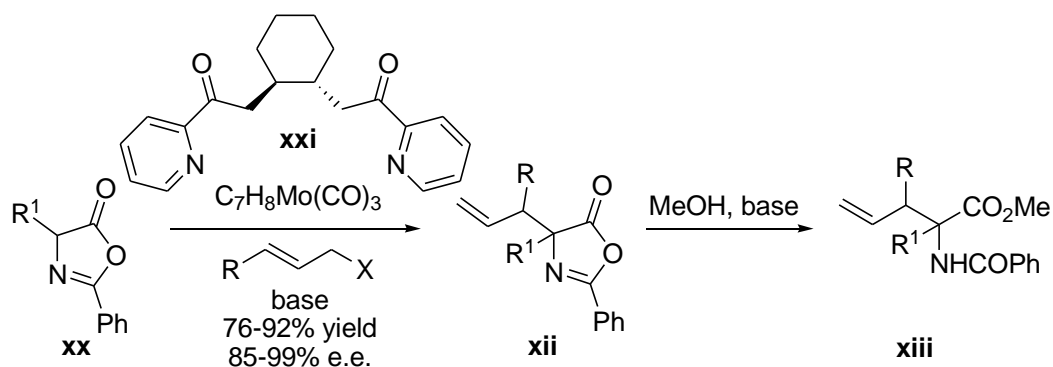
Scheme 8: The three-component asymmetric Strecker synthesis

Corey and Grogan developed a C_2 -symmetric bicyclic guanidine chiral catalyst (**xviii**) for the direct addition of hydrogen cyanide to achiral aromatic and aliphatic *N*-benzylideneamines (**xvii**) (Scheme 9).[37] This method was used to prepare a range of L-amino acids which were isolated in high yields but with only moderate enantioselectivity (76-88 % e.e).



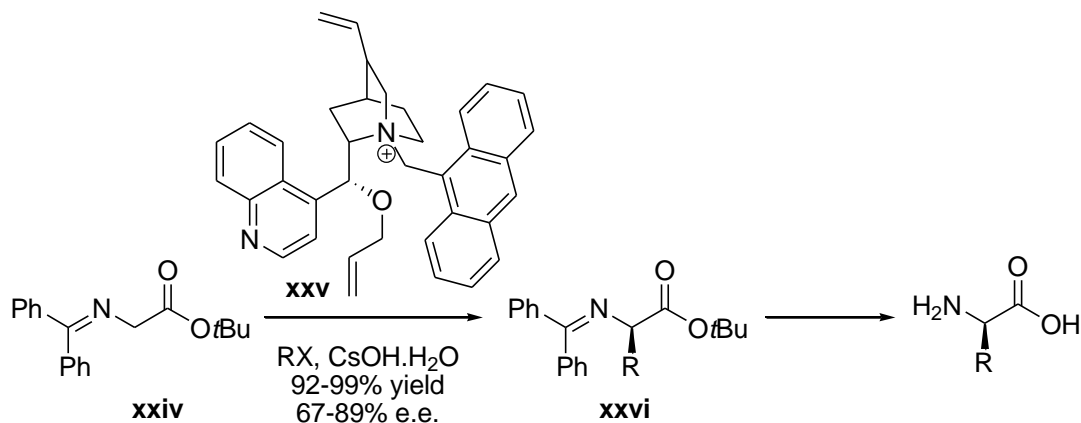
Scheme 9: Asymmetric Strecker synthesis with a guanidine chiral catalyst

An alternative method for amino acid synthesis involves C-C bond forming reactions which include asymmetric allylations, alkylations and Mannich type reactions. For example, Trost *et al.* developed a molybdenum catalyst (**xxi**) for the asymmetric allylic alkylation of substituted azalactones (**xx**). Dissolving the azalactone intermediate (**xii**) in methanol with a base yields optically active α,α -disubstituted amino acids (**xiii**) (Scheme 10).[38]



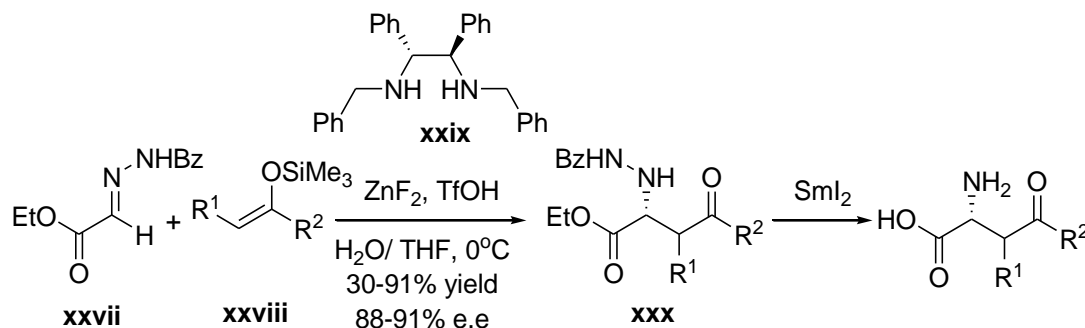
Scheme 10: Synthesis of α,α -disubstituted amino acids (xiii**) by asymmetric allylations using a molybdenum catalyst**

Another method of C-C bond formation in amino acid synthesis uses enantioselective alkylation of *tert*-butyl glycinate benzophenone Schiff bases (**xxiv**) with cinchona alkaloid type phase transfer catalysts (**xxv**) (Scheme 11).[39] Using bulky substituents at the quinuclidine nitrogen of the cinchona alkaloid, allows moderate stereocontrol in the reaction. Phase transfer catalysts of this type are commercially available and as shown in Scheme 11, they have been used to synthesize a range of protected D-amino acids.



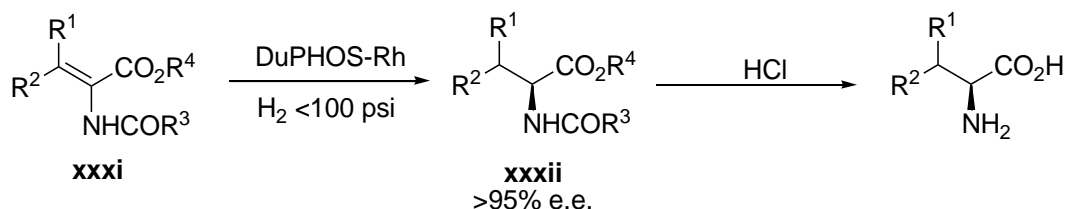
Scheme 11: Transfer catalyzed asymmetric alkylation of glycine Schiff bases using a cinchoninium salt

Kobayashi *et al.* have developed a Mannich-type reaction of silyl enol ethers (**xxviii**) derived from aromatic and aliphatic ketones (Scheme 12). The reaction is catalyzed by ZnF_2 and a chiral diamine catalyst (**xxix**) to yield hydrazines (**xxx**) which in the presence of Sml_2 can be converted to the corresponding amino acids in moderate yields (30-91 %) and enantioselectivities (88-91 % e.e.).[40]



Scheme 12: Example of an asymmetric Mannich-type reaction under aqueous conditions

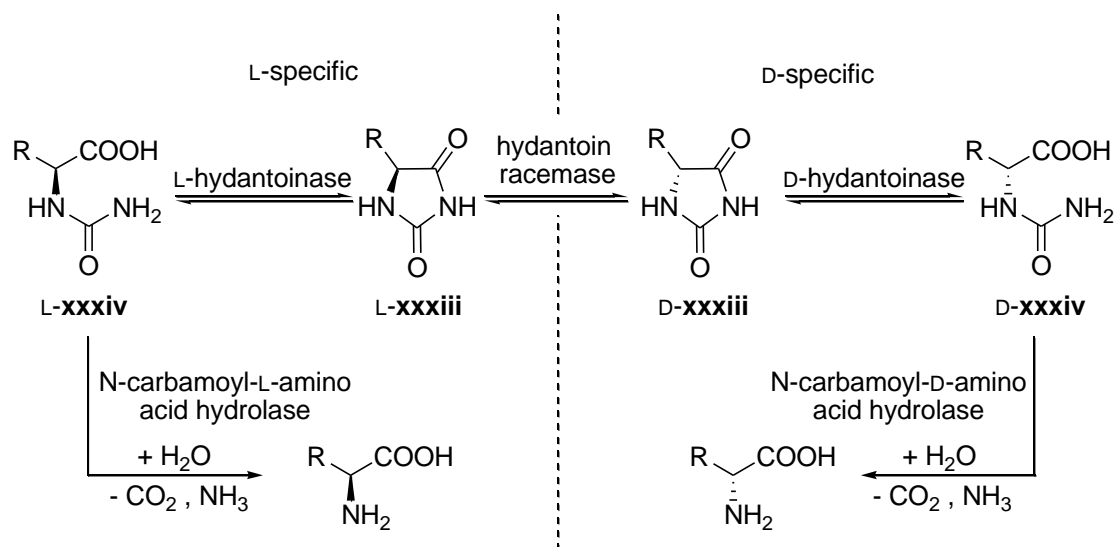
Asymmetric hydrogenation of dehydroamino acids catalyzed by rhodium or ruthenium complexes is an effective method for the synthesis of optically active α -amino acids (Scheme 13).[41,42] Catalysts such as rhodium-DuPHOS are made from chiral phosphorous ligands and enantio-complementary catalysts give access to both enantiomers of the products. Hydrogenation of *N*-acyl protected enamides (**xxx**) as carboxylic esters or acids is performed under reduced pressure and a broad range of β -substituents are tolerated including aromatic, alkyl and other functional groups. The hydrogenation products (**xxxii**) can be deprotected in acid and isolated with high enantiomeric excess, typically e.e.>95%.



Scheme 13: Asymmetric hydrogenation of dehydroamino acids (xxxi) catalyzed by a rhodium-DuPHOS complex

Although the described chemical methods of asymmetric α -amino acid synthesis are promising, they are still under investigation. For the wide use of these methodologies the chiral catalysts require improvements for increased stereoselectivity and generalization towards a broader substrate range. In addition, these methods often require the use of large protecting groups and as a result have low atom efficiency. Strecker reactions use hydrogen cyanide which is highly toxic and asymmetric hydrogenations require metal catalysts and reduced pressure. The use of transition metals on an industrial scale is limited by the significant cost and the pharmaceutical industry has strict limits on residual heavy metal concentrations in products.[43] As a result, these approaches are largely unsuitable for industrial application and new methods are demanded which use milder reaction conditions and proceed with higher

stereoselectivity. An alternative to these traditional chemical strategies is the use of biotechnological approaches, such as the hydantoin- process for the synthesis of α -amino acids from racemic hydantoin derivatives (**xxxiii**) (Scheme 14).[44] In the first step hydantoinases (EC 3.5.2.) catalyze the hydrolysis of the hydantoin ring system; secondly, *N*-carbamoyl-amino acid hydrolases (EC 3.5.1.87 and EC 3.5.1.77) catalyze the further hydrolysis of the hydantoic acids (**xxxiv**) to yield free amino acids. When used in combination with a hydantoin racemase (EC 5.1.99.5), a theoretical yield of 100 % enantiopure product can be achieved from racemic starting material.



Scheme 14: The hydantoin process for the synthesis of enantiopure α -amino acids using a hydantoin racemase, hydantoinase and *N*-carbamoyl-amino acid hydrolase cascade

Ammonia lyases are a second class of enzymes which can be exploited in the synthesis of α -amino acids.[45] Ammonia lyases catalyze the hydroamination of readily available achiral alkenes and they do not rely on any external cofactors or recycling systems making them particularly suitable as industrial biocatalysts. This has been demonstrated by the recent application of PAL in the synthesis of the non-natural amino acid, 2'-chloro-L-phenylalanine on a tonne scale by DSM Pharma Chemicals (see 1.2: *Biocatalysis in amine synthesis*). Ammonia lyases are the focus of this project and will be discussed in more detail in the following sections.

1.4 Ammonia Lyases

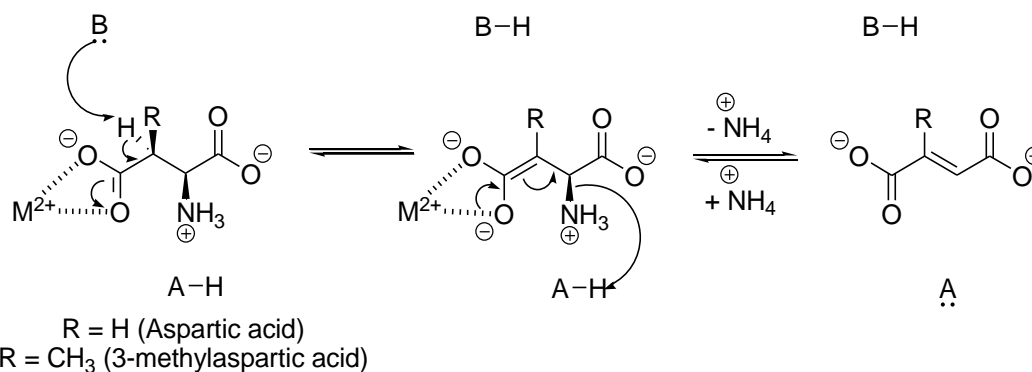
Ammonia lyases catalyze the reversible non-oxidative deamination of α -amino acids to yield *trans*- α,β -unsaturated alkenes and ammonia. These enzymes are particularly intriguing, as lyase catalyzed amination occurs selectively at the α -position and represents a method of amino acid synthesis which to date is not accessible using chemical approaches, since the addition of ammonia would be expected to occur at the β -position. Yet, there are two families of ammonia lyases which have evolved to catalyze this unusual transformation. The first family of ammonia lyases share an MIO-cofactor formed by a post-translational modification and in

nature, catalyze the deamination of the aromatic amino acids, L-phenylalanine, L-histidine and L-tyrosine.[46] The second family show similarities to the fumerase/ enolase superfamily and do not undergo post-translational modification, but instead utilize divalent metal cations, these include aspartate and 3-methylaspartate ammonia lyases (EC 4.3.1.1 and EC 4.3.1.2).[47,48] Some key features of ammonia lyases from each family are summarised in Table 1.

Table 1: Key features of ammonia lyases

Enzyme	Typical Sources	Reaction	Cofactor
phenylalanine ammonia lyase (PAL)	<i>Petroselinum crispum</i> <i>Rhodotorula glutinis</i> <i>Anabaena variabilis</i>	L-phenylalanine ↔ cinnamic acid + NH ₃	
tyrosine ammonia lyase (TAL)	<i>Rhodobacter sphaeroides</i>	L-tyrosine ↔ coumaric acid + NH ₃	MIO
histidine ammonia lyase (HAL)	<i>Pseudomonas putida</i>	L-histidine ↔ urocanic acid + NH ₃	
aspartate ammonia lyase (AAL)	<i>Escherichia coli</i> <i>Pseudomonas fluorescens</i> <i>Bacillus sp.</i>	L-aspartate ↔ fumerate + NH ₃	Mg ²⁺
3-methylaspartate ammonia lyase (MAL)	<i>Citrobacter amalonaticus</i> <i>Citrobacter freundii</i> <i>Enterobacter sp.</i>	(S)-threo-(2S,3S)-3-methyl aspartic acid ↔ mesaconic acid + NH ₃	divalent cation
threo-3-hydroxy aspartate ammonia lyase	<i>Pseudomonas sp.</i> <i>Saccharomyces cerevisiae</i> <i>Delftica sp.</i>	threo-3-hydroxy-L-aspartic acid ↔ oxaloacetate + NH ₃ threo-3-hydroxy-D-aspartic acid ↔ oxaloacetate + NH ₃	PLP and divalent cation
erythro-3-hydroxy aspartate ammonia lyase	<i>Micrococcus denitrificans</i>	erythro-3-hydroxy-L-aspartic acid ↔ oxaloacetate + NH ₃	

Aspartate ammonia lyases are found in bacteria and are involved in microbial nitrogen metabolism. 3-Methylaspartate ammonia lyase (MAL) is the second enzyme in the catabolic pathway in which L-glutamate is metabolised via L-threo-3-methylaspartate to yield acetyl-coenzyme A. The likely mechanism involves a general base catalyzed formation of an enzyme-stabilized enolate anion intermediate, followed by a rearrangement to form fumerate and mesaconic acid products (Scheme 15). A lysine residue acts as a general base and the enolate intermediate is stabilized by interactions with active site residues and either Mg²⁺ or another divalent metal ion.



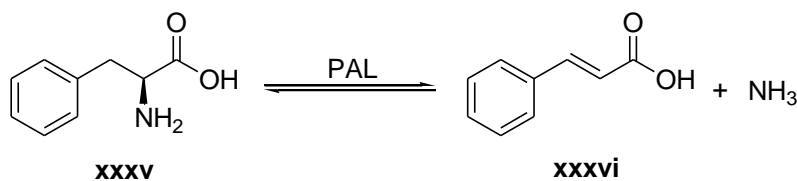
Scheme 15: The proposed mechanism for the deamination of aspartic acid and 3-methylaspartic acid catalyzed by the corresponding ammonia lyase and a divalent metal cation

The *threo*- and *erythro*-3-hydroxyaspartate ammonia lyases (EC 4.3.1.27 and EC 4.3.1.20) deaminate the two epimers of 3-hydroxyaspartic acid and are involved in the glycolate and glyoxylate degradation pathways. Interestingly, both L- and D- specific *threo*-3-hydroxyaspartate ammonia lyases have been identified from different organisms, however there is little known about this family of enzymes.

Aromatic amino acid ammonia lyases have been well characterized and share an MIO-cofactor. Histidine ammonia lyases (HALs, EC 4.3.1.3) are found in humans, mammals and bacteria but are absent in fungi and plants and are responsible for the degradation of histidine. The first product of histidine degradation is urocanate,[49] which is believed to act as a photoprotectant in human and mammalian skin.[50] One of the most thoroughly characterized HALs is from the bacteria *Pseudomonas putida* (*PpHAL*) and the MIO-cofactor was first identified from the X-ray crystal structure of this enzyme, solved in 1999.[51] Tyrosine ammonia lyases (TAL, EC 4.3.1.23) are found in some plants and bacteria and catalyze the degradation of tyrosine to yield coumaric acid. In photobacteria such as *Rhodobacter sphaeroides* (*RsTAL*), coumaric acid is used in the synthesis of a photosensory protein chromophore.[52,53] Whereas in a limited number of higher plants, coumaric acid is utilized as a starting material for resveratrol, an antimicrobial defence compound.[54] Phenylalanine ammonia lyases (PAL) are found in plants, fungi and bacteria and catalyze the degradation of phenylalanine to cinnamic acid. PALs are the focus of this thesis and will be described in more detail in the following sections.

1.4.1 Phenylalanine Ammonia Lyases

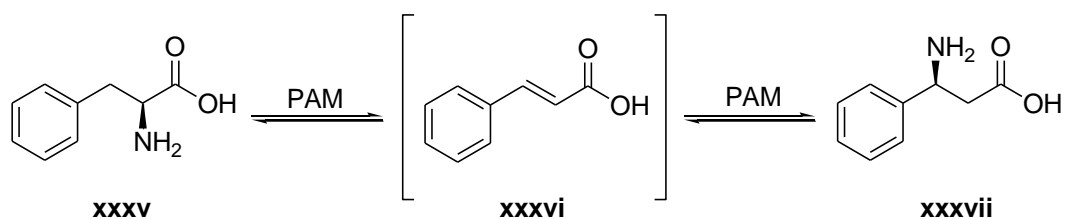
In Nature, PAL enzymes catalyze the deamination of L-phenylalanine (**xxxv**) to yield *trans*-cinnamic acid (**xxxvi**) and ammonia (Scheme 16).



Scheme 16: Phenylalanine ammonia lyase catalyzed deamination of L-phenylalanine

These enzymes are frequently found in fungi, such as the yeast *Rhodotorula glutinis* and function as catabolic enzymes, utilizing L-phenylalanine as a carbon and nitrogen source.[55] PALs are ubiquitous in plants and represent the first enzyme in the phenylpropanoid biosynthetic pathway.[56] *Trans*-cinnamic acid (**xxxvi**) is the precursor of a number of phenylpropanoids and these include lignin, coumarins, and flavonoids.[57] Lignin is a major constituent of wood (commonly 15-30 %), it is used for mechanical support and acts as a physical barrier against pathogens.[58] Coumarins have antimicrobial properties and are used in the biosynthesis of anticoagulants[59] and flavonoids function as the colourful components of many flowers.

There are very few examples of bacterial ammonia lyases known which display activity towards L-phenylalanine (**xxxv**). In prokaryotes, PALs are involved in the biosynthesis of various natural products such as 3,5-dihydroxy-4-isopropylstilbene in *Photobacterium luminescens*,[60] cinnamamide in *Streptomyces verticillatus*[61] and enterocin in *Streptomyces maritimus*. [62] Recently, PAL from the thermotolerant marine bacterium *S. maritimus* (EncP) was identified as a bifunctional PAL and phenylalanine aminomutase (PAM, EC 5.4.3.11). Aminomutases are mechanistically related MIO-dependent enzymes, which catalyze the isomerisation of α - and β - amino acids. EncP shows optimum lyase activity at 74 °C consistent with the environment of its host, however at low temperatures the enzyme displayed mutase activity catalyzing the isomerisation of (*S*)- α -phenylalanine (**xxxv**) to (*S*)- β -phenylalanine (**xxxvii**) (Scheme 17).[63] Similarly, a PAM from *Pantoea agglomerans* (AdmH) which shows optimum mutase activity at 25 °C demonstrated high thermostability and a temperature dependent activity switch, resulting in lyase activity at high temperatures.

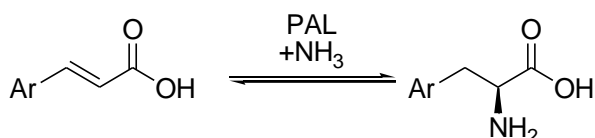


Scheme 17: Phenylalanine aminomutases catalyze the interconversion of α-phenylalanine (xxxv) and β-phenylalanine (xxxvii)

Moffitt *et al.* recently identified two PALs from the cyanobacteria *Anabaena variabilis* (AvPAL) and *Nostoc punctiforme* (NpPAL) using a bioinformatics search of the genomes in the NCBI database.[64] Their biological function is unknown, however the lyase genes were found associated with secondary metabolite biosynthetic gene clusters.[65] AvPAL is currently under investigation for use as a therapeutic enzyme for the treatment of phenylketonuria (PKU) disease.[66] PKU is an inherited metabolic disorder caused by loss or impairment of phenylalanine hydroxylases, which are responsible for phenylalanine metabolism. The result of PKU is phenylalanine can accumulate in the body, which causes neurotoxic effects. Prokaryotic PALs are smaller than eukaryotic PALs and are believed to be more metabolically stable making them more suitable as therapeutic proteins (see 1.4.1.2: Structure).

1.4.1.1 PALs as Biocatalysts

Although the natural lyase reaction involves the elimination of ammonia, the reaction is reversible at high ammonia concentrations.[67] Therefore PALs represent potentially attractive biocatalysts for the synthesis of enantiomerically pure non-natural L-amino acids from substituted cinnamic acid analogues and ammonia (Scheme 18). PALs have the advantage of using readily available achiral cinnamic acid derivatives as starting materials, and they do not rely on any external cofactors or recycling systems making them particularly suitable as industrial biocatalysts.



Scheme 18: The PAL catalyzed hydroamination of cinnamic acid analogues for the synthesis of optically active amino acids

There have been a number of studies investigating the substrate range of eukaryotic PALs from the plant *Petroselinum crispum* (PcPAL) and yeast *Rhodotorula glutinis* (RgPAL), however bacterial PALs have never been previously exploited as biocatalysts. A selection of compounds which show good conversion with PcPAL and RgPAL biocatalysts are shown in

Figure 4.[57,68-72] Rétey and co-workers investigated a range of fluoro -and chloro-substituted cinnamic acid derivatives, and the products were isolated in yields of 37-99% with an enantiomeric excess of >99% in favour of the L-enantiomer. A range of aromatic groups

were also investigated including furans, thiophenes, benzofurans and benzothiophenes: these were all well tolerated when bound to L-alanine at the 2'-position on the ring but were not substrates when substituted at the 3'-position. In general, substrates with electron withdrawing groups at any of the 2'- 3'- or 4'-positions are well tolerated whilst electron donating groups such as methoxy- and amino substitutions are poor substrates.

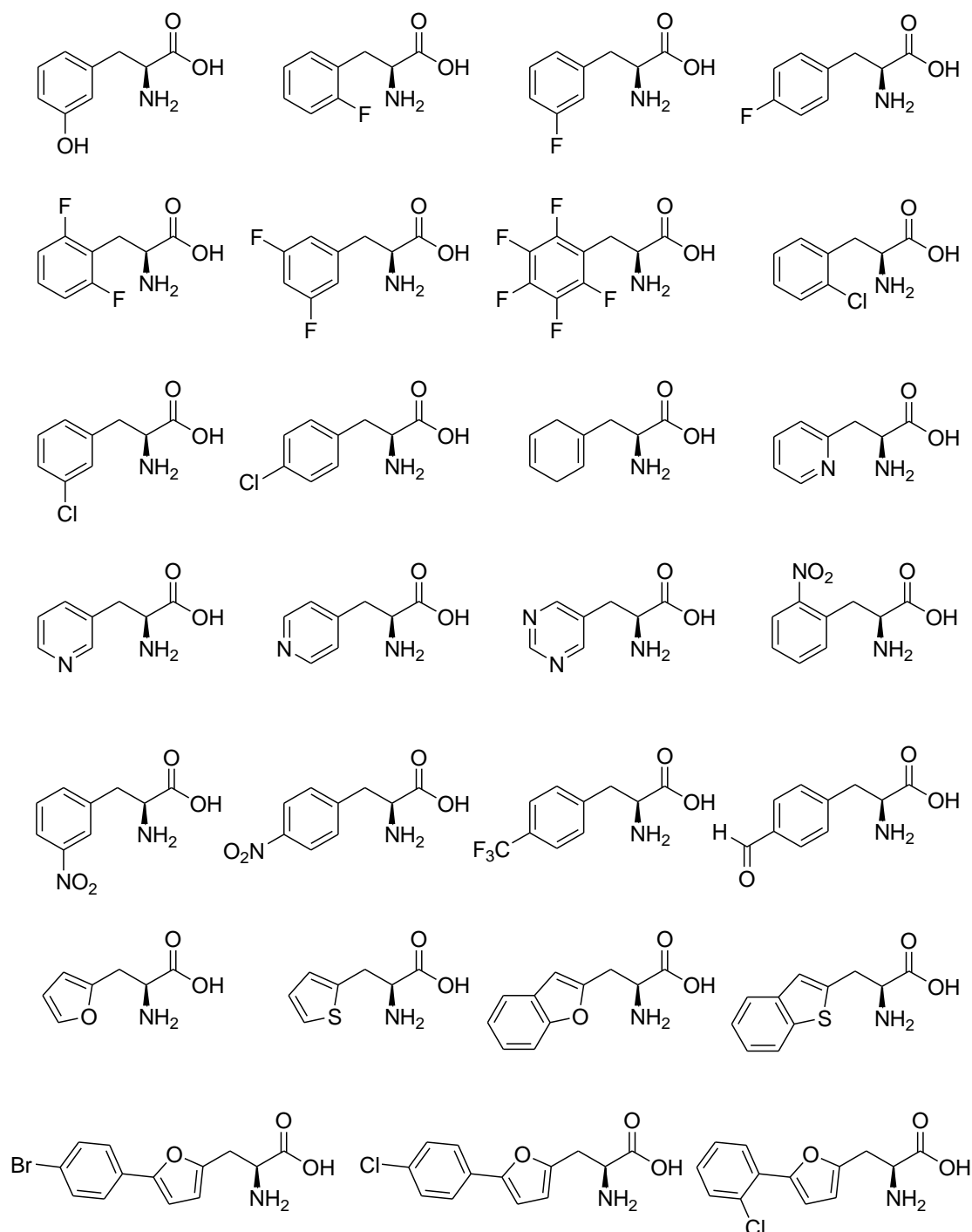


Figure 4: Non-proteinogenic amino acid substrates for *PcPAL* and *RgPAL*

1.4.1.2 Structure

PAL is a homotetramer, of closely interlocking monomers with 222 symmetry and approximately half of their combined surface area is buried within the structure (58% in *RgPAL*).^[73] Each tetramer contains four catalytic sites and each active site is comprised of residues from three different monomers and one cofactor. Each MIO-cofactor is anchored to each monomer by non-covalent bonding to three central α -helices, which are coiled together and form a rigid central core and funnel into the active site.

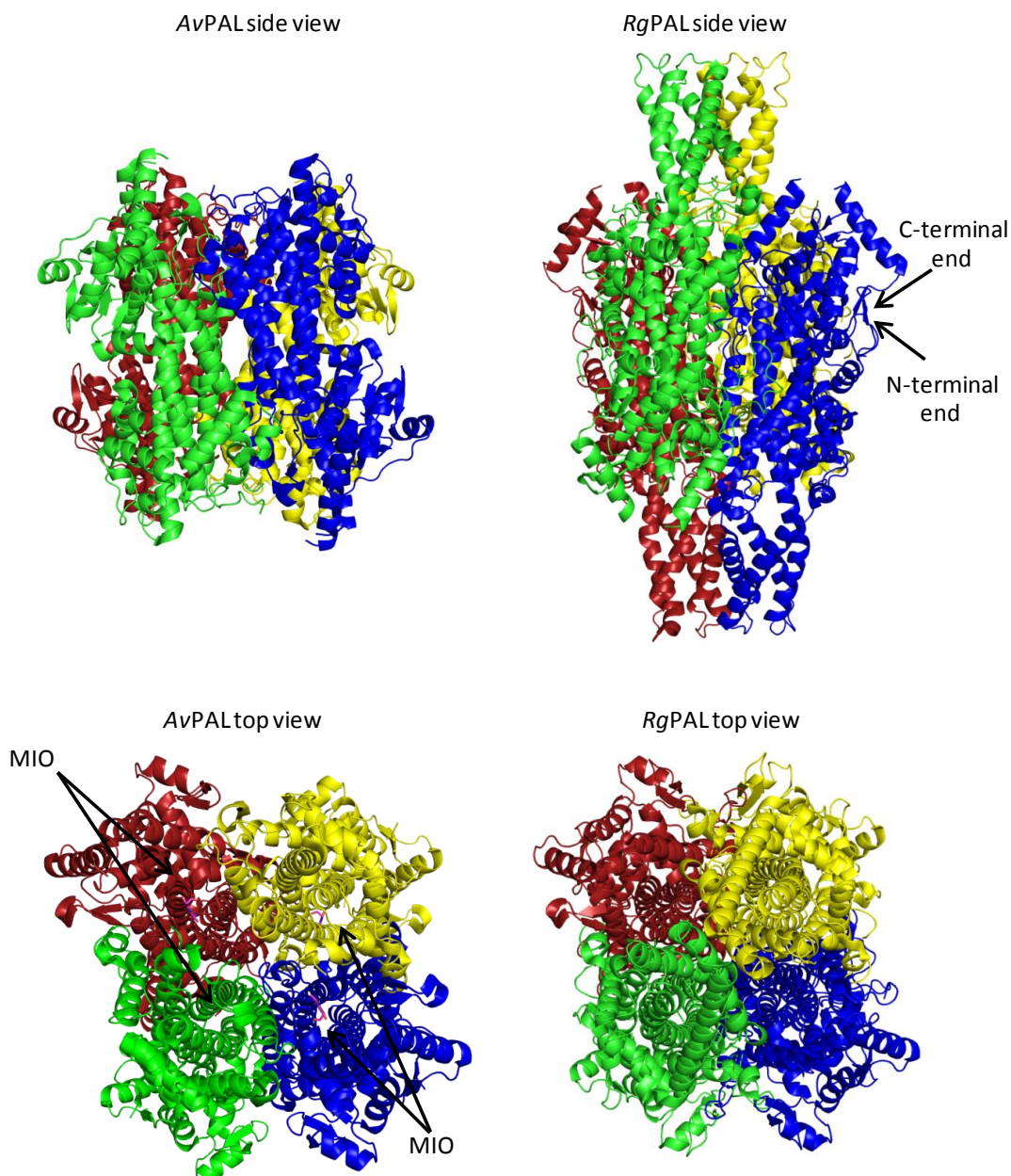


Figure 5: The crystal structures of AvPAL (PDB code 2NYN) and *RgPAL* (PDB code 1T6P) at 2.2 Å resolution showing the four interlocking monomers. Structures were generated using Pymol

The crystal structures of several PAL enzymes have been solved including the eukaryotic PALs from *R. glutinis*[73] and *P. crispum*[74] and the slightly smaller prokaryotic PAL from *A. variabilis*. [64] The eukaryotic PALs are approximately 77 kDa per monomer and the prokaryotic AvPAL is 64 kDa per monomer. The extra residues in the eukaryotic PALs are largely located at the N-terminal and at the C-terminal of the protein and stretch above and below the main body of the protein in a fan-like arrangement (Figure 5), for more details on the loop structures see section 1.4.1.4: *Mobile Loops*. AvPAL is more similar in size to the prokaryotic HAL enzymes however it has high sequence identity to the eukaryotic PALs (Table 2).

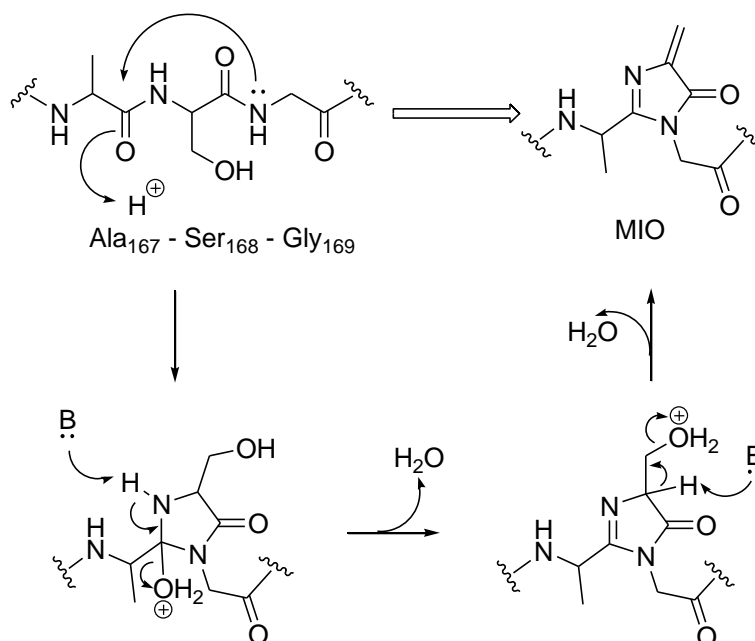
Table 2: Sequence identities and similarities between PAL enzymes from different sources

PAL sources	Percentage identity	Percentage similarity
<i>A. variabilis</i> - <i>P. crispum</i>	35	53
<i>A. variabilis</i> – <i>R. glutinis</i>	35	51
<i>P. crispum</i> – <i>R. glutinins</i>	37	54

1.4.1.3 MIO-Cofactor

The presence of an essential electrophilic prosthetic group was first identified in *Pp*HAL by Abeles *et al.* who identified enzyme inactivation in the presence of the strong nucleophiles KCN, NaBH₄, phenylhydrazine, NaHSO₃ and NH₂OH.[75] The isotope labeled nucleophile, sodium borotritide was used to inactivate *Pp*HAL and subsequent acid hydrolysis afforded [³H]alanine as the only labeled material.[50] From these results it was postulated that the cofactor was a dehydroalanine residue (2-aminoacrylic acid), a moiety previously identified in some peptide based antibiotics.[76] The natural occurrence of dehydroalanine is believed to derive from a base catalyzed dehydration at a serine residue.[77] However it wasn't until almost thirty years later that the first crystal structure was solved with sufficient resolution to show the true identity of the cofactor. The X-ray crystal structure of *Pp*HAL variant C273A was solved at 2.1 Å resolution and revealed the cofactor was in fact a modified dehydroalanine, 5-methylene-3,5-dihydroimidazol-4-one (MIO).[51] The presence of the cofactor was confirmed in *Pp*HAL and *Pc*PAL by comparing the UV difference spectra between wild-type enzyme and variants S143A and S203A respectively. The wild-type enzymes showed a discrete maxima at 308 nm which was absent in the variants which have disrupted MIO-formation.[78] Based on sequence alignments, all aromatic amino acid lyases and mutases were believed to share this unique MIO-cofactor, and this was later confirmed as further crystal structures were solved.[73,74] Using site-directed mutagenesis, Rétey *et al.* showed that the cofactor is formed by a post-translational internal cyclisation of a conserved tripeptide Ala-Ser-Gly.[77,79] The mechanism proceeds via nucleophilic attack of the backbone amide nitrogen at the neighboring amino acid carbonyl, this is followed by dehydration and the elimination of two molecules of water (Scheme 19). A study of the crystal structures of some *Pp*HAL variants

suggest that the formation of the MIO-cofactor is triggered by mechanistic compression in a late stage chain folding of the already rigid protein. The authors suggest F329-C_β and D145 residues serve as anchoring points against which the bulk protein presses down on the MIO-forming loop.[80]



Scheme 19: Proposed mechanism of autocatalytic MIO formation (AvPAL numbering)

The MIO-cofactor is much more electrophilic than a dehydroalanine residue as the lone pair on the cofactor's imidazole nitrogen cannot delocalize. In addition, the MIO group is located on an electropositive platform formed from six α -helices which are associated with the active site and are oriented with their positive resultant dipoles aligned similarly, increasing the MIO electrophilicity further (Figure 6).[73]

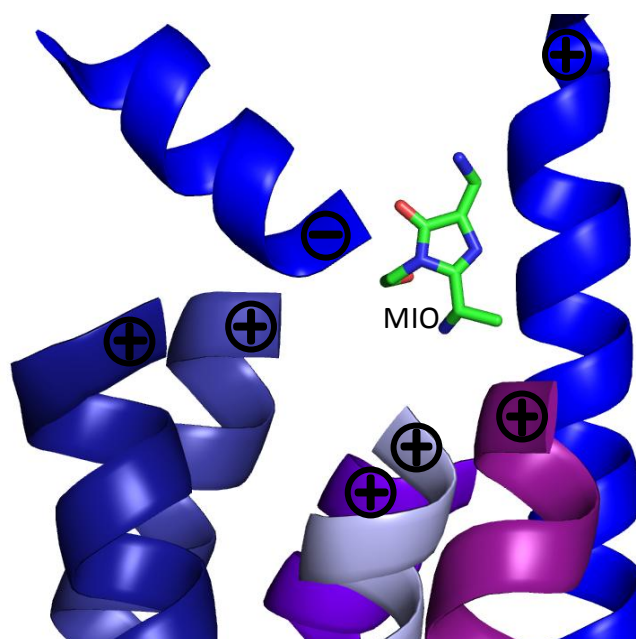
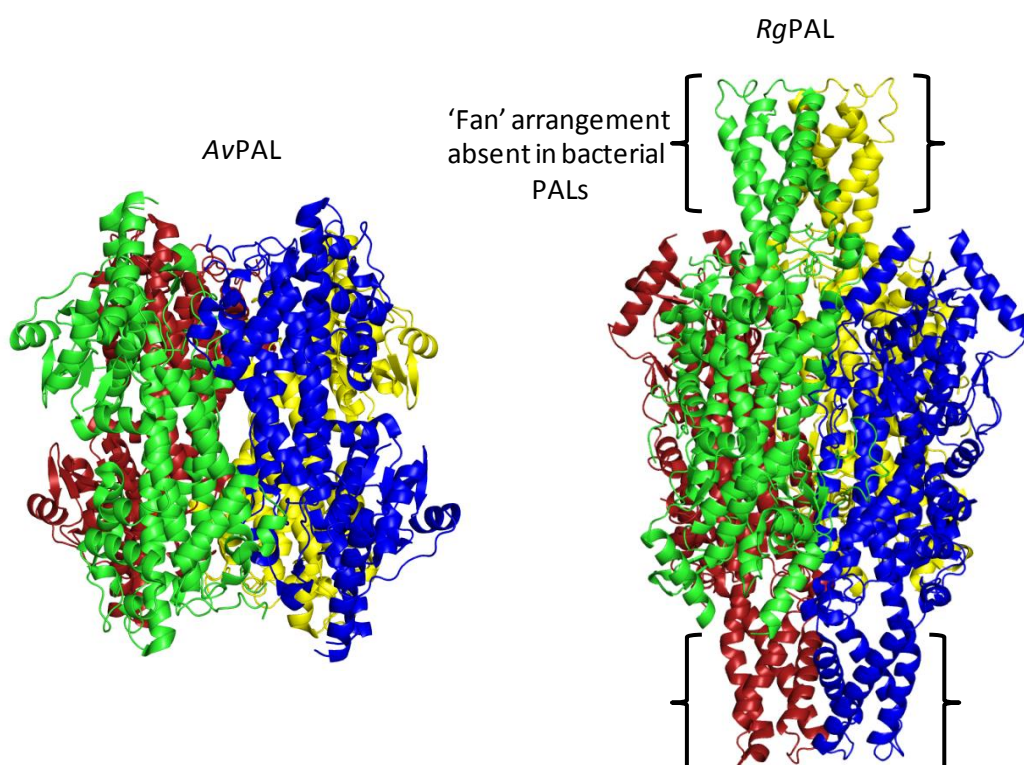


Figure 6: The six positive poles and one negative pole of the seven α -helices associated with the RgPAL active site (PDB code 1T6P). The structure was generated using Pymol

1.4.1.4 Mobile Loops

Eukaryotic PALs are approximately 215 residues larger than the prokaryotic PALs and these extra residues are largely located at the N-terminal (ca. 60 residues) and at the C-terminal (ca. 120 residues) ends of the protein. The inserted C-terminal residues in the eukaryotic PALs stretch above and below the main body of the protein in a fan-like arrangement and arch above the enzyme's active site (Figure 7).[73] These extra residues have been associated with controlling substrate entry and product release.[74] The C-terminal residues have also been suggested to affect the conformation of the active site lid loop.[81]



C-terminal residues

PcPAL	---MENGNGAITNGHVNGNGMDFCMKTEDPLYWGIAAEAMTGSHLDEVKKMVAEYRKPVV	57
RgPAL	MAPSLDSISHSFANGVASAKQAVNGASTNLAVAGSHLPTTQVTQVDIVEKMLAAPTDSL	60
AvPAL	-----MKTLSQAQSKTSSQQFSFTGNSSANV	26

N-terminal residues

PcPAL	TFEDELKALLPKEVESARAALES-GNPAIPNRIEBCRSYPLYKFVRKELGIEYLT---	677
RgPAL	VAAAESAISLTRQVRETFWSAASTSSPALS--LSPRTQILYAFVREELGVKARRGDV	687
AvPAL	DILPCLH-----	

PcPAL	--GEKVTSPGEEFDKVFIAMSKGEIIDPLLECLESWNGAPLPIC-----	716
RgPAL	FLGKQEVTVIGSNVSKIYEAIKSGRINNVLLKMLA-----	716
AvPAL	-----	567

Figure 7: The structures of AvPAL (PDB code 2NYN) and RgPAL (PDB code 1T6P), highlighting the extended C-terminal residues found in eukaryotic PALs. Structures were generated using Pymol. The sequence alignments showing the extended C-terminal and N-terminal residues in the eukaryotic PALs

AvPAL is similar in size to PpHAL but has an additional 21 residues at its N-terminal. To investigate the function of these residues an N-terminally truncated (21 residues) AvPAL variant was generated which resulted in soluble protein with no significant change in activity.[64] The N-terminal residues are therefore believed to have a role in anchoring the proteins to other cell components.

Each active site is capped by two flexible loops; an inner loop which is packed tightly in the active site and forms interactions with the substrate and an outer loop which serves as an external cap (Figure 8). The outer loop is attributed to forming a barrier to bulk solvent preventing access to the active site. The inner loop contains an essential catalytic tyrosine residue Tyr78 (AvPAL numbering) which is conserved between all eukaryotic and prokaryotic PALs.[78] The loop moves between a closed conformation, allowing the Tyr78 catalyzed abstraction of the substrate's β -proton and an open conformation allowing product release and substrate entry.[81]

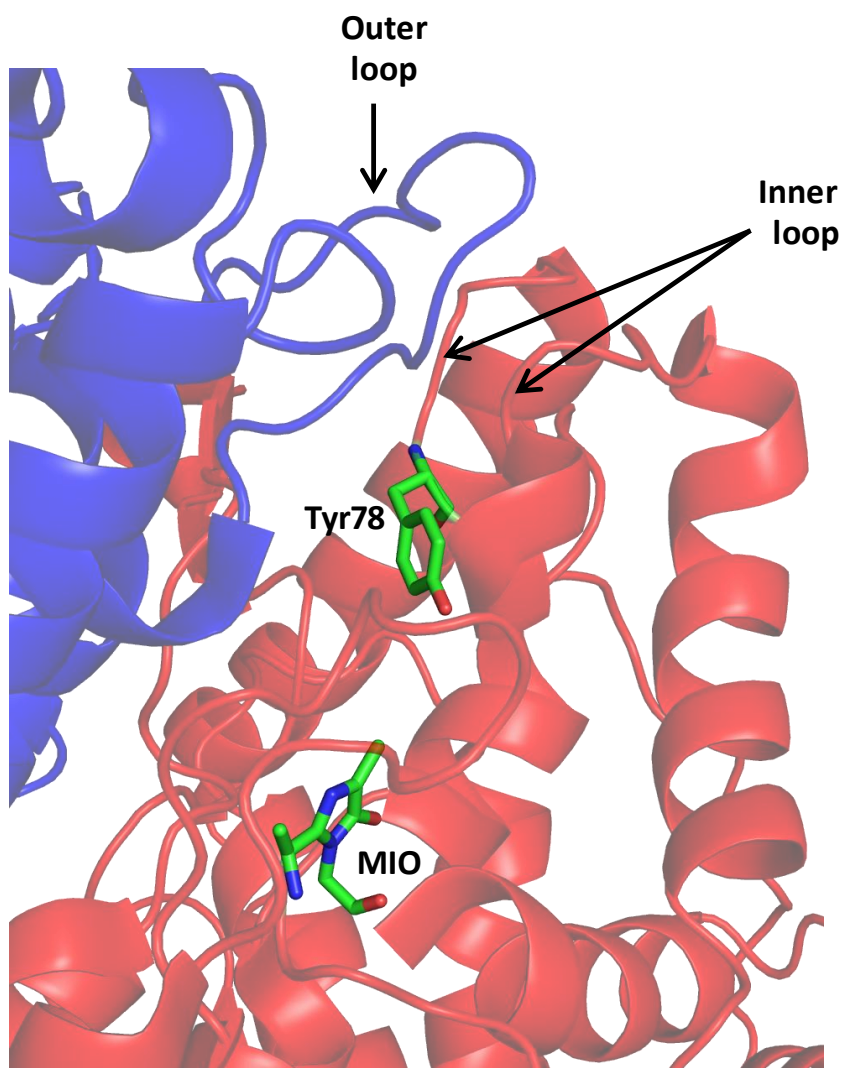


Figure 8: AvPAL crystal structure (PDB code 3CZO) showing the inner catalytic loop from monomer 1 (red) and outer loop from the adjacent monomer (blue). The structure was generated using Pymol

The catalytic loops are highly mobile and in various crystal structures, including that of *RgPAL*, the loops are often unresolved.[73] The crystal structure of *PcPAL* shows the loops well resolved however they are believed to be in the inactive loop out conformation.[74] Recently, Wang and coworkers solved the first crystal structure of a PAL showing the loop residues ordered and in the closed active conformation for catalysis. The crystal structure was generated from an *AvPAL* variant (C503S/C565S) with two mutated surface cysteine residues which increased the protein solubility and prevented aggregation.[65] Ordered loops have also been observed in the X-ray crystal structures of *PpHAL*,[51] *Streptomyces globisporus* tyrosine aminomutase (*SgTAM*, EC 5.4.3.6)[82] and a *RsTAL* variant H89F.[83]

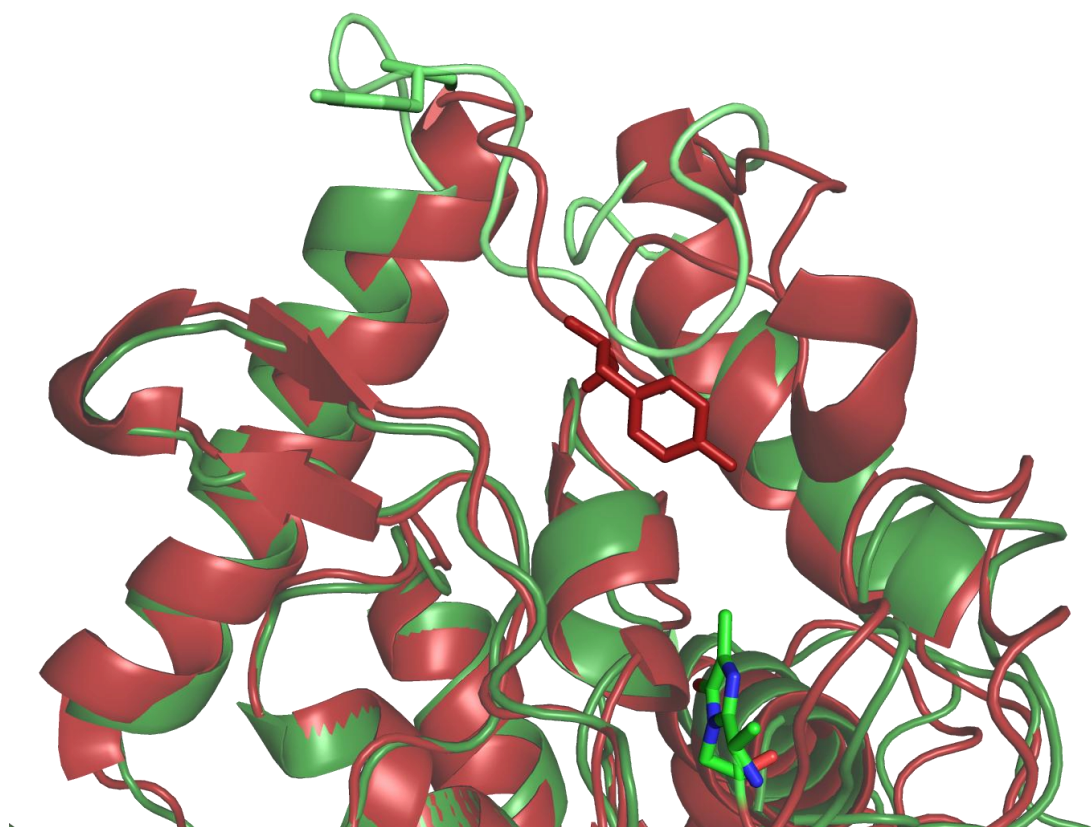


Figure 9: Superimposed structures of *AvPAL* (PDB code 3CZO, red) and *PcPAL* (PDB code 1W27, green). *AvPAL* shows the active site loop in the closed conformation and *PcPAL* shows the flexible catalytic loop in the open conformation. Structures were generated using Pymol

There is strong sequence homology between ammonia lyases and aminomutases. *SgTAM* and *PcPAL* show 32% identity with very little variation of the active site residues. In fact *SgTAM*,[84] *Taxus canadensis* PAM (*TcPAM*)[85] and *Chondromyces crocatus* TAM (*CmdF*)[86] have all been shown to produce small amounts of α,β -unsaturated products which in some cases can accumulate over time. A significant difference between the structures of lyases and mutases is in the loop regions. Mutases generally have a more rigid catalytic loop than lyases, to ensure the re-addition of ammonia onto the α,β -unsaturated intermediate before product release. The temperature dependent activity of the bifunctional PAL *EncP* and PAM *AdmH* is thought to be a consequence of catalytic loop mobility.[63] These

thermotolerant enzymes act as PALs at high temperatures as there is high mobility in the loop, and PAMs at low temperatures. In addition, Bartsch and coworkers identified a single point mutation Arg92Ser in *TcPAM* which increases the catalytic loop flexibility by destabilizing the closed conformation and converts mutase activity to lyase activity.[87]

The inner catalytic loop in eukaryotic PALs contain protease cleavage sites and it has been suggested that in plant PALs these may play a role in feedback systems providing control of the phenylpropanoid pathway.[65] The flexible catalytic loop in *AvPAL* lacks these cleavage sites, it is shorter and more rigid than the eukaryotic PALs and shows similarities to the mutase active site loop, nonetheless *AvPAL* does not show any mutase activity.[64]

1.4.2 Catalytic Mechanism

The exact mechanism of the PAL catalyzed L-phenylalanine deamination reaction has been under investigation for more than 50 years.[88] There have been two suggested catalytic mechanisms; one is based on an amine-MIO cofactor intermediate and elimination pathway and the other on a Friedel-Crafts type reaction. In both proposed mechanisms, MIO forms a covalent intermediate with the phenylalanine substrate, which is subsequently deprotonated at the β -position. Isotope labelling studies confirmed that stereospecific proton abstraction is at the *pro*-(S) position.[89]

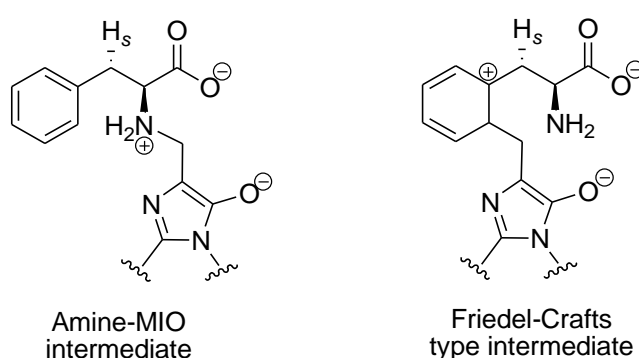
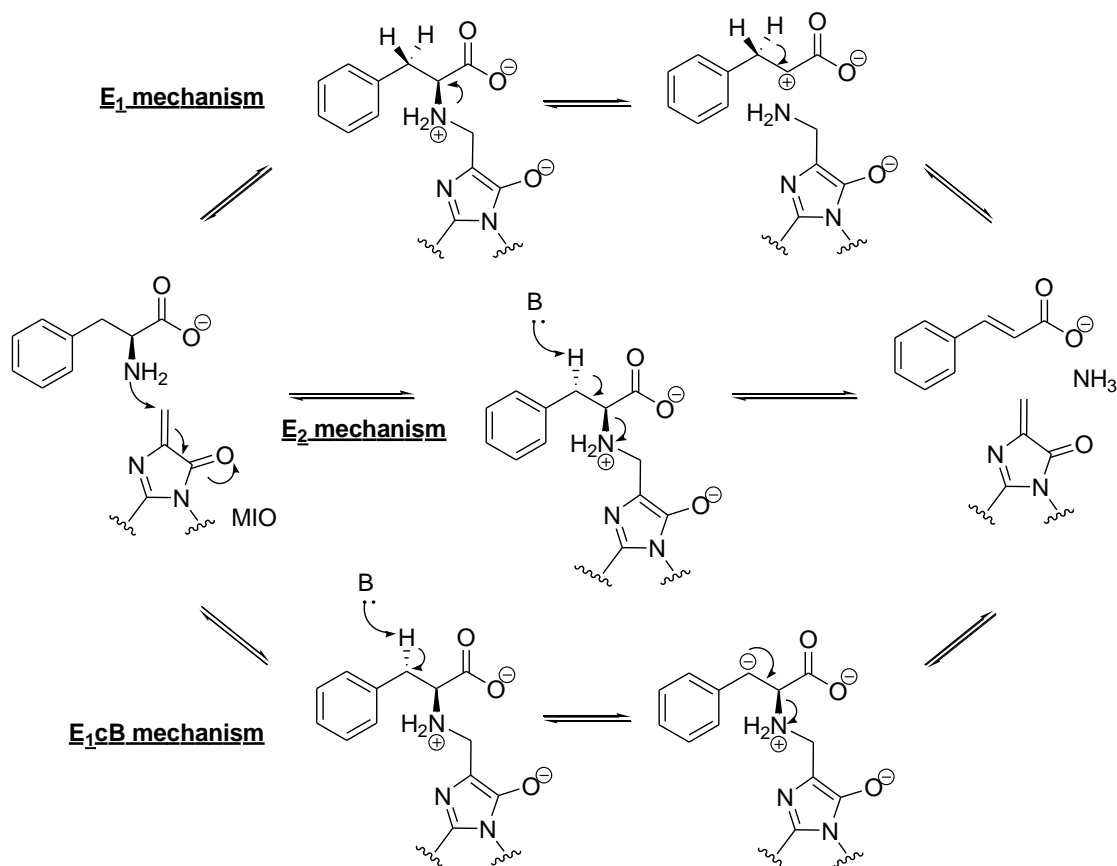


Figure 10: Two proposed intermediates in the PAL catalyzed L-phenylalanine deamination reaction

1.4.2.1 Elimination Mechanism

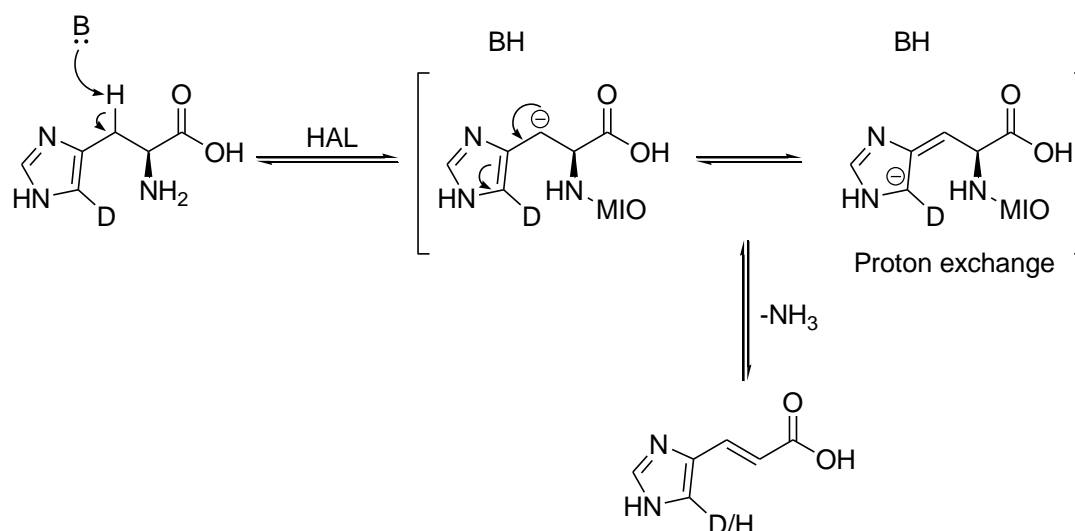
The first PAL catalyzed mechanism was proposed by Abeles *et al.* in 1967 which suggests that the α -amine group of phenylalanine nucleophilically attacks the prosthetic electrophile to give a secondary amine-MIO complex.[75] Abstraction of the β -proton by an enzymatic base and elimination of the substrates amine yields the cinnamic acid product. Lastly the amine bound to the MIO is protonated by an acidic active site residue, ammonia is eliminated and the cofactor regenerates to complete the cycle. This mechanism supports the work of Peterkofsky, who found that ammonia is released after the α,β -unsaturated product.[90]



Scheme 20: PAL catalyzed deamination of L-phenylalanine via different elimination mechanisms

The elimination step in this mechanism is unlikely to proceed via E₁-elimination as the resulting α-carbocation intermediate would be too high in energy. Instead, the elimination has been proposed to proceed via either a stepwise E_{1cB} or E₂ mechanism (Scheme 20).

An E_{1cB}-type elimination was initially proposed by Abeles and coworkers and this mechanism is supported by a study of ¹⁵N-kinetic isotope effects with both C₃-dideuterated and unlabeled phenylalanine and an alternative slow substrate, 3-(1,4-cyclohexadienyl)alanine.[91] A deuterium labeling study using the substrate L-[5'-²H]-histidine and *Pseudomonas fluorescens* HAL also suggest an E_{1cB}-type mechanism.[92] Deuterium washout at the C5' position in both the substrate and product was observed in the elimination reaction and this was explained by deuterium exchange of the stable carbanion intermediate (Scheme 21). The loss of deuterium incorporation in the starting material was explained as a result of a reversible reaction. The extent of deuterium washout was affected by the pH which indicated that the stability of the carbanion intermediate is pH dependent.



Scheme 21: PAL catalyzed mechanism of deuterium washout in the elimination reaction of L-[5'-²H]-histidine

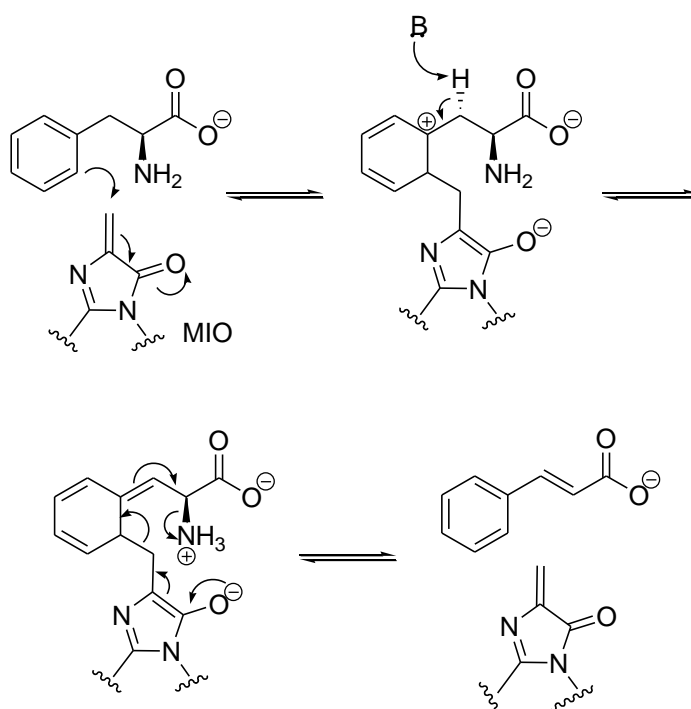
The E₁cB mechanism results in the formation of a carbanion intermediate which is relatively unstable and as a result some studies suggest an E₂-elimination is more likely. A recent quantum mechanics and molecular mechanics study of TALs suggests that an E₂-like transition state would have the lowest energy out of all possible intermediates.[93] Regardless of the mechanism of elimination, there is a general consensus that the mechanism for both aromatic amino acid lyases and mutases proceeds via an amine-MIO intermediate. A theoretical computational study of the *Pp*HAL catalyzed reaction proposes the mechanism can only proceed via an amine-MIO intermediate.[94] Some of the strongest evidence supporting an amine-MIO intermediate is from crystallographic data. A crystal structure of *Rs*TAL bound to coumarate, caffeate and cinnamate complexes allowed modelling of L-tyrosine suggesting the substrate amine would be appropriately positioned for attack at the MIO cofactor.[95] *Sg*TAM has been co-crystallized together with cinnamate epoxides and α,α-difluoro-β-tyrosine which are non-hydrolysable mechanistic probes and substrate and product analogues. The X-ray crystal structures of the trapped intermediates indicate the presence of covalently bound MIO-amine adducts.[96,97] Walker *et al.* solved the X-ray crystal structure of the bifunctional amino-mutase *AdmH*, which shows electron density in two different monomer subunits, consistent with both α- and β-phenylalanine bound via the substrate amine to the MIO-cofactor.[98] Lastly the recent detailed crystal structure of *Av*PAL showing the active site loops well resolved allowed docking studies, which together with *N*-hydroxysuccinimide-biotin binding studies suggested the phenylalanine amino group directly attacks the MIO-prosthetic group.[65]

The elimination step is chemically challenging and this mechanism needs to account for deprotonation of the non-acidic hydrogen residue (pK_a 40). Several factors are believed to contribute to the lowering of the pK_a of the benzylic proton. Firstly the amine-MIO adduct is believed to enhance the leaving ability of the amine and the helical dipole moments strengthen the electrophilicity of the MIO cofactor. The dipole moments also create a positively charged

active site environment which can effectively lower the pKa of the benzylic proton. In addition, co-complex structures indicate the enzyme binds substrates in a conformation favouring orbital alignment for periplanar elimination.[46] The phenyl ring binding site is very hydrophobic and is believed to polarise electrons away from the carbanion intermediate enhancing the electron withdrawing ability of the ring.

1.4.2.2 Friedel-Crafts Type Mechanism

It is argued that the elimination mechanism does not sufficiently explain how the enzyme facilitates abstraction of the non-acidic β -proton or stabilization of the carbanion intermediate.[73] An alternative Friedel-Crafts type mechanism was proposed on the basis that the benzylic proton has a pKa of approximately 40 and therefore abstraction by an enzymatic base is unlikely.[99] *Pp*HAL and *Pc*PAL variants which cannot form a dehydroalanine cofactor were found to retain activity towards the deamination of 4-nitro-L-histidine and 4-nitro-L-phenylalanine respectively.[77,100] This led to the hypothesis that the 4-nitro substituent must have an analogous role to the MIO cofactor, which is to acidify the β -protons for abstraction. A similar result was observed for wild-type enzymes which were chemically reduced using sodium borohydride.

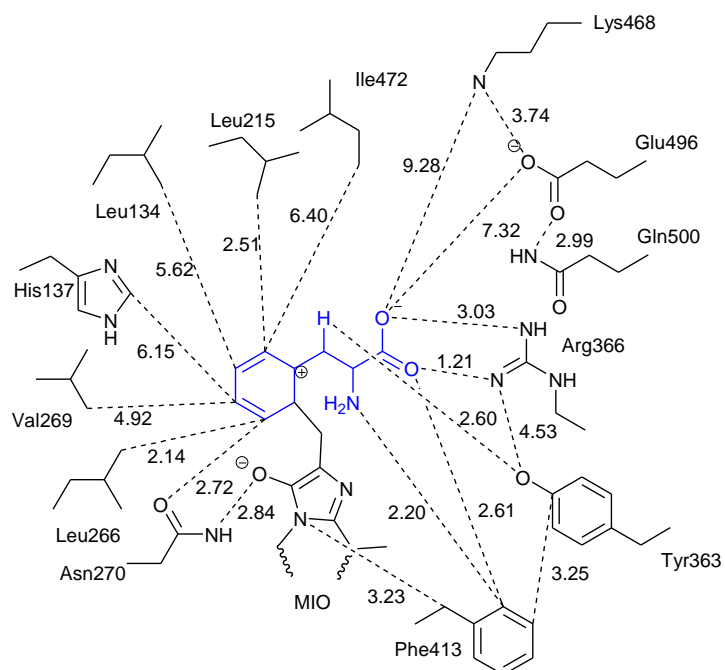


Scheme 22: PAL catalyzed deamination of L-phenylalanine via a Friedel-Crafts type mechanism

The alternative mechanism involves a 1,4-addition of the substrate's phenyl group onto the MIO methylene group to give a carbocation intermediate. The β -proton is now activated and stereospecific abstraction of the *pro*-(S) proton leads to the formation of an exocyclic double bond, subsequently ammonia is eliminated and the MIO cofactor reforms (Scheme 22). A putative *Pc*PAL active site model was used in a computational docking study and an

alternative substrate binding mode was proposed based on this mechanism (Figure 11). It is proposed that for a Friedel-Crafts type reaction the substrate's phenyl ring must be stacked between the cofactor-MIO and a conserved residue Phe413 (*PcPAL* numbering) allowing maximal π -overlap.[70] Attack of the L-phenylalanine aromatic ring is believed to occur from the *ortho*-position as it has been shown that dihydrophenylalanine is a substrate.[91]

A) Binding mode according to the Friedel-Crafts mechanism



B) Binding mode according to the E₁cB mechanism

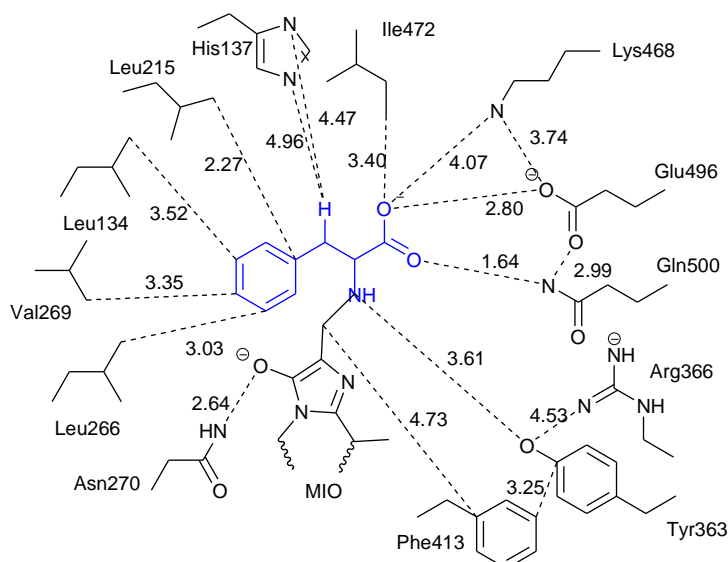


Figure 11: Schematics of the *PcPAL* active site with L-phenylalanine interactions[73] (distances are given in Å)

A study using labeled [²H₅]-phenylalanine as a substrate showed deuterium isotope effects which are consistent with attack at the aromatic ring.[69] Further support for this proposal is provided by Rétey and coworkers who have studied the effects of different substituted phenylalanine derivatives on PAL catalyzed activity. They found that *meta*-tyrosine was a slightly better substrate for PcPAL than the natural substrate, due to increased ring electrophilicity which stabilizes the Friedel-Crafts intermediate more easily.[101] Similarly, phenylalanine derivatives halogenated at the *meta*-position reacted faster than phenylalanine as these substituents would facilitate attack at the *ortho*-position on the ring.[70] Lastly benzofuran- and benzothiophenyl- alanines were screened as PAL substrates and, although substrates with the alanyl side chains attached at the 2'-position were good substrates, those with side chains at the 3'-position were strong competitive inhibitors.[57] Modeling substrates with alanyl chains at the 3'-position suggests that the *ortho*-position to the alanyl chain is sterically hindered to Friedel-Crafts attack.

This proposed pathway is the first biological mechanism of its kind; nonetheless the high energy complex formed provides means to sufficiently lower the pK_a of the β-proton.[102] The major criticism of the Friedel-Craft type mechanism regards the formation of the carbocation intermediate, which suffers a loss of aromaticity.[73] In addition, although there is an absence of basic residues in the phenyl binding pocket to prevent re-aromatization, chemically it would be more intuitive than abstraction of the benzylic proton. This mechanism was originally proposed on the basis that the formation of an amine bound substrate-dehydroalanine cofactor complex is not sufficient to activate the β-proton. However this was prior to the first lyase crystal structure and the discovery of the MIO-cofactor. MIO is more electrophilic than a dehydroalanine cofactor and is located on an electropositive platform formed from the resultant dipoles of six α-helices which direct their positive dipoles towards the active site. The electropositive environment surrounding the cofactor supports the development of a carbanion intermediate over the formation of a carbocation intermediate. Furthermore evidence for the Friedel-Crafts mechanism is largely based on the relative activities of various substituted phenylalanine substrates, but although the described observations are consistent with this proposal they do not provide conclusive proof. The most active substrates are derivatives with substituents which activate the β-proton towards abstraction and this can be interpreted in favor of either mechanism. Moreover, recently a wealth of crystallographic data has been made available showing various lyases and mutases with ligands bound which provides substantial support for the original amine-MIO mechanism.

1.4.2.3 Catalytic Promiscuity

Despite the growing amount of published experimental data there is not a general consensus regarding the PAL catalyzed mechanism. A study by Bornscheuer *et al.* suggests this is due to the fact lyases and mutases are catalytically promiscuous and can proceed via either an amine-MIO intermediate or a Friedel-Crafts type mechanism.[103] The authors propose the catalytic mechanism is dependent on a highly conserved glutamic acid residue (Glu484,

PcPAL numbering) in PALs and PAMs, which is an asparagine in TALs and TAMs. The glutamic acid residue in TALs and TAMs interacts strongly with the substrates' amine group resulting in an unfavorable conformation for the formation of an amine-MIO interaction. Mutating this glutamic acid residue to asparagine, allows a change in the substrate binding resulting in an amine-MIO interaction. However, this study fails to discuss HALs which have a conserved serine residue and the enzymes AdmH and EncP, which have a threonine residue at the analogous positions. Furthermore, a recent X-ray structure of wild-type SgTAM with an asparagine residue at the switch position, co-crystallized with different ligands, supports an elimination mechanism.[96,97]

1.4.3 Key Active Site Residues

The active site residues which are highly conserved between PALs, TALs, PAMs and TAMs from different sources are discussed in the following section. There are several highly conserved catalytic residues aside from the conserved Ala167-Ser168-Gly169 (AvPAL numbering) triad which forms the MIO cofactor (

Figure 12).[46,79] The catalytic base which abstracts the phenylalanine β -proton is an essential Tyr78 residue which is located on the flexible catalytic loop.[65,81] Mutating the tyrosine residue in PcPAL to a phenylalanine residue led to complete enzyme inactivation.[104] Another key catalytic residues is Phe363 which is found in close proximity to the MIO-cofactor, indicating a possible role in stabilizing the amine-MIO intermediate via interactions between the amine's lone pair and the residues aromatic π -system. Asn223 hydrogen bonds to the developing enolate on the MIO cofactor and Tyr314 protonates the MIO-amine after release of the cinnamic acid product to allow cofactor regeneration.

	78	167	223	314	366					
AvPAL	EPIYGVTS	FGSIGASG	DLVPL	KEGLAMN	NGTSVMTG	IQDRYSLR	CPLPQYLG	YHGGNF	LGQYV	
AdmH	RVIYGVNT	SMG KGS	SLGTSG	DLGPL	KEGLALIN	GTSGMVG	IEDAYSIR	CTPQILG	FHNGHF	HGQYV
EncP	RVIYGVNT	SMG KGS	SLGTSG	DLGPL	KDGLALIN	GTSGMVG	IEDAYSIR	CTPQILG	FHNGHF	HGQYV
SgTAM	IPIYGVTT	GYG IGS	LGASG	DLAPL	KEGLALIN	GTSGMTG	LQKAYSL	RAIPQVVG	FHGANE	HGQPI
cmdF	HPIYGVNT	TGFG QGS	LGASG	DLSP	LDALALVN	GTSGMVG	LQDAYTL	RAVPQILG	FHGANE	HGQYV
RsTAL	RHVGGLTT	TGFG RGT	VGASG	DLTPL	RDALALVN	GTSGMVG	GQDAYSL	RCAVQVVG	LHGGNF	MGQHV
PcPAL	TDSYGVTT	TGFG RGT	TITASG	DLVPL	KEGLALVN	GTAVGSG	KQDRYAL	RTSPQWLG	IHGGNF	QGTPI
TcPAM	ADIYGVTT	TGFG RGS	VASG	DLIPL	KEGLALVN	GTSGMVG	KQDRYAL	RSSPQWLA	LHGANE	QGSVA
RgPAL	MSVYGVTT	TGFG RGT	TITASG	DLSP	KEGLALVN	GTAVSAS	RQDRYPL	RTSPQWLG	HHGGNF	QAAAV

Figure 12: Sequence alignment for *Anabaena variabilis* PAL (AvPAL), *Pantoea agglomerans* PAM (AdmH), *Streptomyces maritimus* PAL (EncP), *Streptomyces globisporus* TAM (SgTAM), *Chondromyces crocatus* TAM (cmdF), *Rhodobacter sphaeroides* TAL (RsTAL), *Petroselinum crispum* PAL (PcPAL), *Taxus Canadensis* PAM (TcPAM) and *Rhodotorula glutinis* PAL (RgPAL) showing highly conserved active site residues (AvPAL numbering)

PALs have several conserved residues responsible for substrate recognition and binding, such as the flexible Lys419 residue which binds to the substrate carboxylate and chaperones the substrate into the correct binding orientation. Lys419 is adjacent to a glycine residue which allows high mobility at the lysine position. F107 is key residue for substrate recognition and interacts with the substrates *para*-position; it has been attributed to selectivity for

phenylalanine over tyrosine as a substrate, however this residue is a histidine in *RgPAL*.^[83] The aromatic binding pocket is very hydrophobic and is made up of multiple leucine residues, whilst the carboxylate binding pocket is made up from a very sensitive network of hydrogen bonding. The residues which make up the funnel leading into the active site are mainly hydrophobic residues; however the residues are not conserved between PALs from different sources (Figure 12).

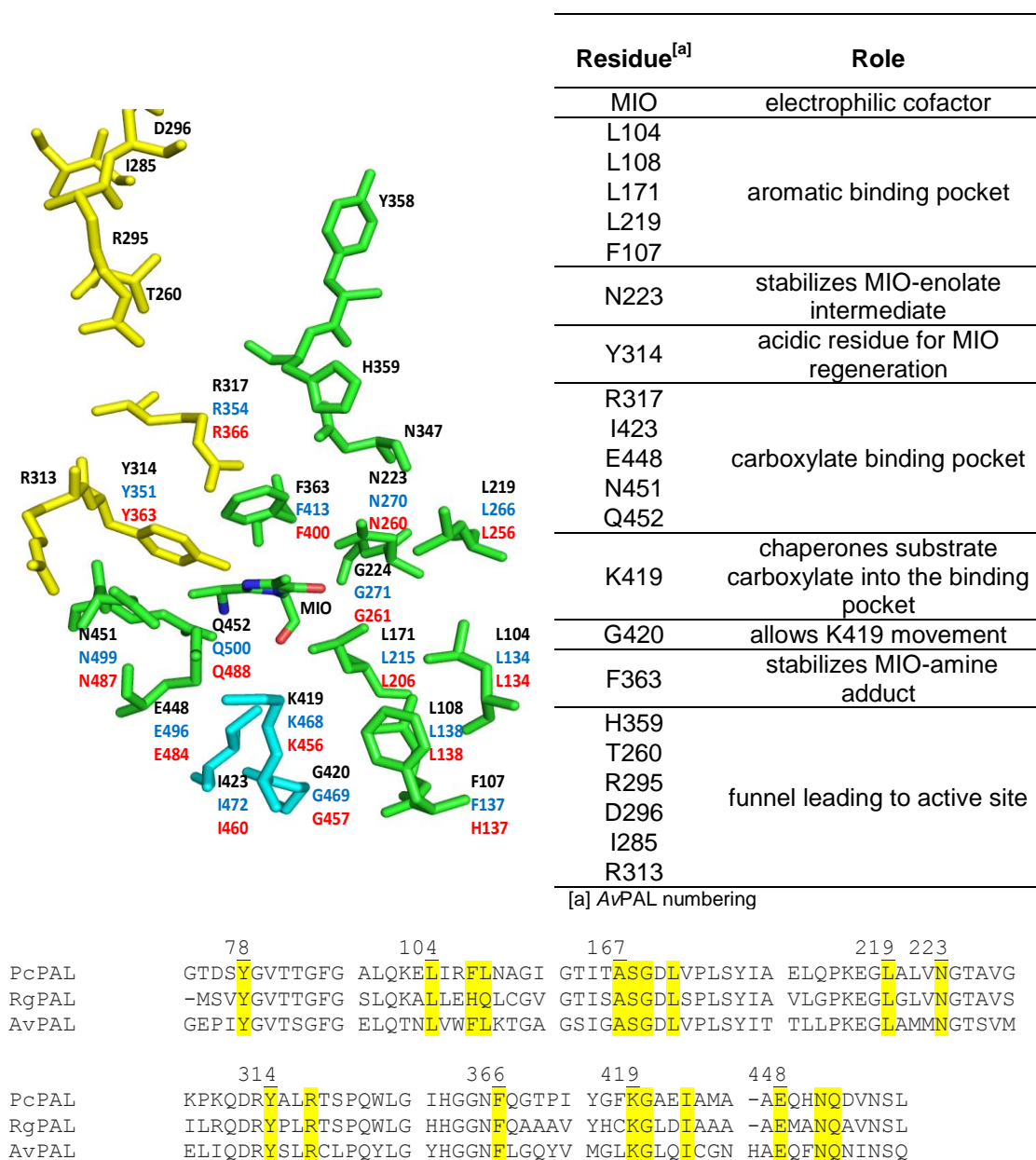


Figure 13: Conserved AvPAL active site residues from three adjacent monomers (shown in yellow, green and blue, PDB code 3CZO). Conserved active site residues are shown in black (AvPAL), blue (PcPAL) and red (RgPAL). Residues leading into the active site are not conserved and only the AvPAL residues are shown. The structure was generated using Pymol. Sequence alignments highlight the conserved active site residues (AvPAL numbering)

1.4.4 Previous Mutagenesis Work

Phe107 has been described as the substrate selectivity switch which distinguishes between PAL and TAL activity.[83] The residue is a conserved phenylalanine in PALs but a histidine residue in TALs, and mutating the analogous residue His89 in *RsTAL* to a phenylalanine changed the enzymes selectivity from tyrosine to phenylalanine. However, the fungal *RgPAL* has a histidine residue in the corresponding position but accepts phenylalanine substrates preferentially. Nonetheless this residue is known to interact with the *para*-position of the substrates' phenyl ring and has been mutated to increase activity towards *para*-substituted phenylalanine derivatives. Bartsch *et al.* mutated the corresponding residue Phe137 in *PcPAL* using saturation mutagenesis and screened variants for increased activity towards 4-nitrocinnamic acid.[71] They identified the variant F137V, which has 1.7-fold higher activity towards 4-nitrocinnamic acid than the wild-type enzyme, explained by the smaller side chain increasing the available space within the active site. Furthermore, a *PcPAL* F137H variant was found to show deamination activity towards tyrosinol (4-(2-amino-3-hydroxypropyl)phenol), a substrate with no wild-type activity.[103] The histidine residue in the F137H variant hydrogen bonds to the tyrosinol *para*-hydroxy group positioning the substrate appropriately for activity.

1.5 Objectives

PALs represent potentially attractive biocatalysts for the synthesis of enantiomerically pure L-amino acids from substituted cinnamic acids and ammonia. The substrate range of eukaryotic PALs from the plant *PcPAL* and yeast *RgPAL* have been well characterized and these enzymes show activity towards a range of non-natural substituted phenylalanine derivatives.[57,70,71] However, there is great interest in the development of PAL enzymes with enhanced substrate scope and suitable properties for biocatalytic applications.

The aims of this project are as follows:

- 1) Identify a suitable PAL candidate to target by directed evolution

To date, there have been few reported examples of bacterial PALs and they have not been previously exploited as biocatalysts for amino acid synthesis. Herein the activity and substrate specificity of wild-type bacterial PALs will be determined alongside well characterized eukaryotic PALs. This work includes development of analytical methods as well as the optimization of expression and reaction conditions. These studies revealed previously unreported features regarding the stereochemistry of the PAL catalyzed reaction and consequently the catalytic mechanism was investigated in more detail.

- 2) Determine the wild-type PAL substrate specificity towards previously unreported substrates

Substrates of interest include phenylalanine derivatives with alternate aromatic moieties or different functional groups at the carboxylic acid position, *N*-substituted analogues and D-

amino acids. Before variants can be developed for increased activity towards a broad range of substrates, it is useful to analyze the wild-type activity towards these substrates. This work includes the synthesis of a panel of substrates and their corresponding products and the development of analytical methods for the detection of novel activity.

3) Develop high-throughput screening methods

Several screening methods have been developed for the detection of hydroamination activity towards a variety of different substrates including cinnamic acid derivatives, cinnamyl alcohols, and β -methylstyrenes. Both liquid phase and colony based screens have been investigated.

4) Generate libraries and screen for improved PAL catalyzed activity

A number of libraries were generated using a variety of methods which were chosen based on the screening capacity of the assays. The aim was to screen libraries for increased activity and substrate specificity and then subject any positive hits to further rounds of evolution.

The successful development of variants with increased substrate promiscuity will have valuable applications in a range of biotechnological processes for pharmaceutical and agrochemical industries. PAL catalyzed hydroamination reactions for the synthesis of chiral amines offers a practical, atom efficient and environmentally friendly alternative to traditional methods using metallo- and organocatalysis.

Chapter 2: Identifying a Candidate for Directed Evolution

2 Identifying a Candidate for Directed Evolution

2.1 Introduction

The broad use of PALs as biocatalysts for amine synthesis is limited by their relatively narrow substrate specificity. The long term aim of this project is to develop the substrate range of PALs beyond substituted phenylalanine derivatives towards substrates with different functional groups at the carboxylic acid position, alternative aromatic moieties and *N*-substituted derivatives. To achieve this goal a suitable PAL must be identified, which will be subjected to rounds of evolution. The substrate ranges of the yeast *Rhodotorula glutinis* PAL (*RgPAL*) and parsley *Petroselinum crispum* PAL (*PcPAL*) have been well characterized and these enzymes show hydroamination activity towards a range of cinnamic acid analogues.[57,70,71] However, to our knowledge the activity of prokaryotic PALs towards unnatural substrates has not been previously investigated. Herein we examine the activity and enantioselectivity of *Anabaena variabilis* PAL (*AvPAL*) towards a broad range of non-natural substrates and compare this activity with the eukaryotic *RgPAL* and *PcPAL*. These enzymes were selected as they represent the three known sources of PALs, bacteria, fungi and plants. In addition, the crystal structures for these enzymes have been solved making them compatible with future rational design.

This chapter describes the development of analytical methods for the detection of PAL catalyzed activity towards cinnamic acid and phenylalanine derivatives. These methods were used firstly, to determine the optimal conditions for high level protein expression in *E. coli* and secondly to discover the most favourable reaction conditions for catalysis. Lastly, the activity of *RgPAL*, *PcPAL* and *AvPAL* were compared under these conditions using both whole cell biocatalysts and purified enzymes.

2.2 Analytical Methods for the Determination of PAL Catalyzed Activity

The aim of this chapter is to identify a PAL with a broad substrate specificity and high activity towards the amination of cinnamic acid analogues for the synthesis of non-natural phenylalanine derivatives. A panel of substrates (**1a-q**) were selected which possess both electron withdrawing and donating substituents at the 2'-, 3'-, and 4'- positions on the aromatic ring (Figure 14). HPLC and spectrophotometric methods have been developed to analyze the conversion between cinnamic acid derivatives (**1a-q**) and their corresponding α -amino acid products (**2a-q**) and vice versa.

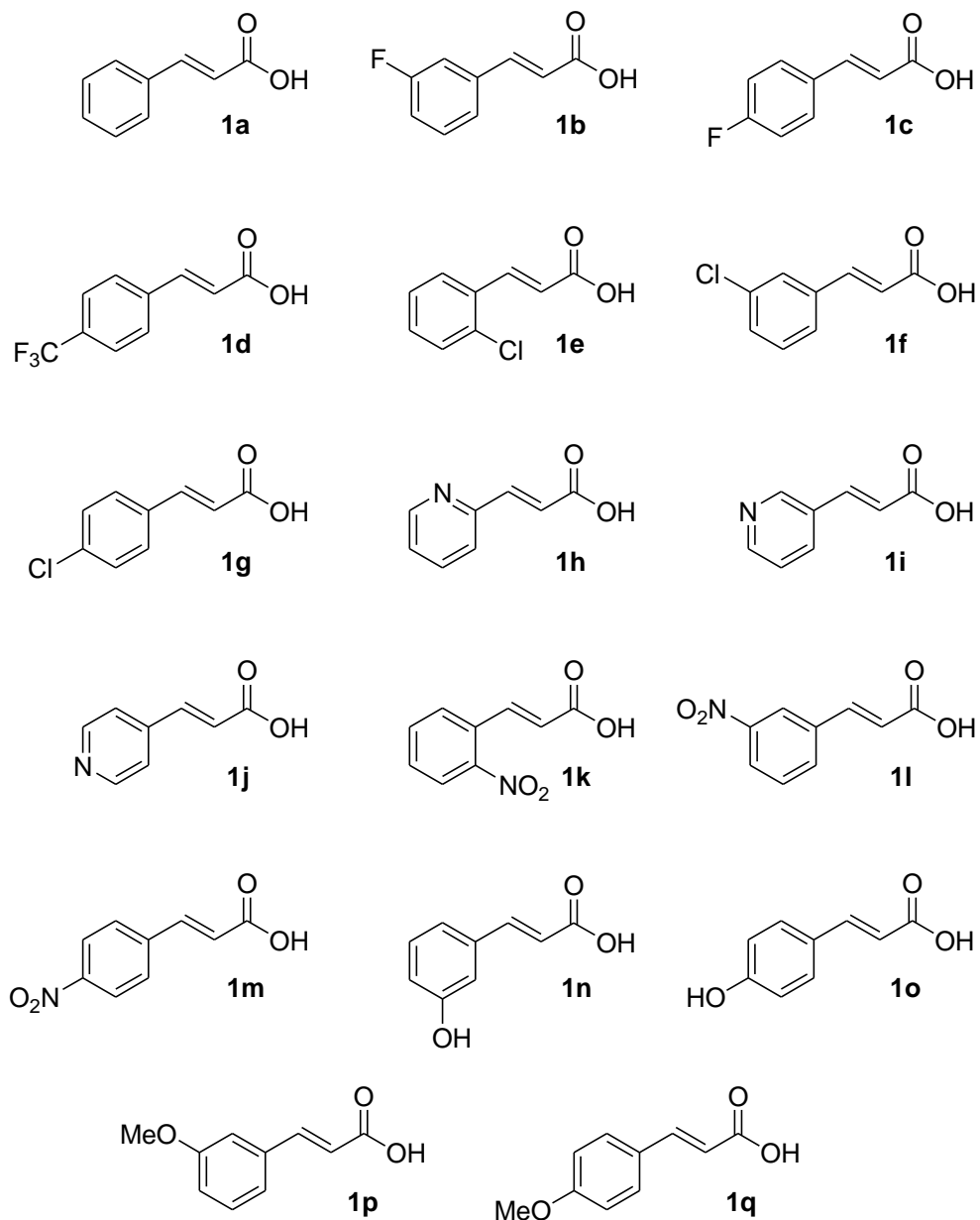
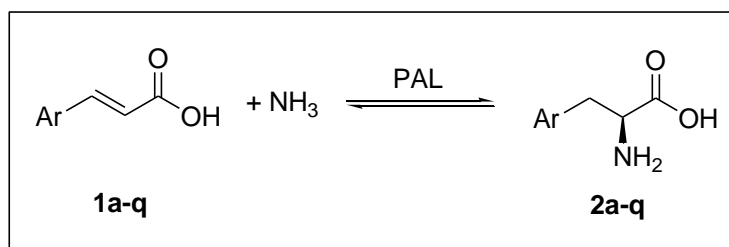


Figure 14: Panel of cinnamic acid derivatives screened for PAL activity

2.2.1 HPLC Analysis

Non-chiral (methods A-E) and chiral (method F) reverse-phase HPLC methods were developed which allow measurement of the percentage conversion and amino acid enantiomeric excess (Table 3).

Table 3: Methods for reverse phase HPLC analysis

Method	Conditions
A-D	Luna phenyl-hexyl column 4.6 mm x 150 mm, 5.0 μ m mobile phase: 40 % methanol/ 60 % 0.1 M NH_4OH pH 10 flow rate: 0.5 mL/min, 20 $^\circ\text{C}$, 15 min A: 50% methanol, B: 40% methanol, C: 20% methanol, D: 10% methanol
E	Zorbax extend C18 column 4.6 mm x 50 mm, 3.5 μ m mobile phase: 40% methanol/ 60% 0.1 M NH_4OH pH 10 flow rate: 1 mL/min, 40 $^\circ\text{C}$, 10 min
F-G	Astec Chirobiotic T column 4.6 mm x 250 mm, 5.0 μ m mobile phase: 60% methanol/ 40% water 40 $^\circ\text{C}$, 20 min F: flow rate 0.8 mL/min G: flow rate 1.5 mL/min

To calculate the percentage conversion between cinnamic acid and phenylalanine derivatives by HPLC the peaks areas from the UV traces are measured. Cinnamic acid derivatives (**1a-q**) absorb more strongly at the wavelengths measured than their corresponding phenylalanine derivatives (**2a-q**). As a result the response factor for each substrate and product were calculated from standards of known concentration (Table 4). The measured peak area for the cinnamic acid derivative is corrected by dividing by the calculated response factor.

Table 4: Response factors for substrates 1a-q, for the calculation of percentage conversion
n.d = not determined, a standard of amino acid 2p was not commercially available

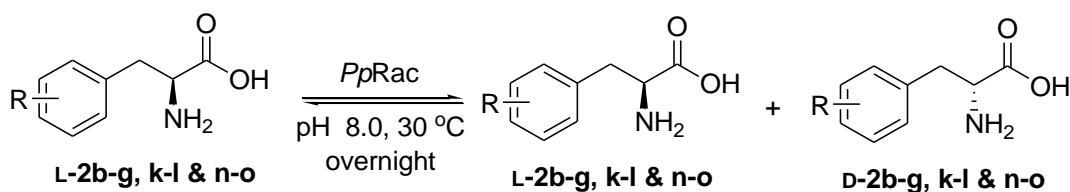
Substrate	Method	Wavelength (nm)		Response Factor
		Cinnamic Acid Derivative (1)	Phenylalanine Derivative (2)	
a	B,E,F	222	222	6.15
b	B,E,F	275	222	7.4
c	B,E,F	275	222	15.2
d	A,E,F	275	222	7.8
e	B,E,F	222	222	7.8
f	B,E,F	222	222	3.8
g	B,E,F	222	222	1.3
h	C,E,G	254	254	5.9
i	C,E,F	254	254	10.5
j	C,E,G	254	254	10.3
k	B,E,F	275	275	2.4
l	B,E,F	275	275	3.6
m	B,E,F	320	275	1.4
n	D,E,F	275	222	3.2
o	D,E,F	275	222	1.4
p	B,E,F	222	n.d	n.d
q	B,E,F	275	222	1.0

These HPLC methods are compatible with reactions using whole cell biocatalysts, cell lysate and purified enzymes. For HPLC analysis, methanol (300 μ l) is added to biotransformation samples (300 μ l), whole cell and protein material is cleared by centrifugation (1 minute, 13,000 rpm) and the supernatant is filtered using HPLC filter vials (0.45 μ m, Thomson). The percentage conversion is calculated from the integration of the UV peak areas and corrected using the appropriate response factor.

2.2.1.1 Preparation of Racemic Standards

To determine the enantiomeric excess of the amino acid products by HPLC, standards of both the L- and D-enantiomer are required. Non-proteinogenic D-amino acids are generally not available commercially therefore racemic standards for HPLC analysis were prepared from the corresponding L-amino acids using the PLP-dependent phenylalanine racemase (EC 5.1.1.10) from *Pseudomonas putida* (*PpRac*) (Scheme 23). *PpRac* was overexpressed in LB with IPTG induction and the His-tagged protein was purified by nickel affinity chromatography (See section 6: *Materials and Methods* for details). Purified protein was used for biotransformations in order to minimize background signals in the HPLC traces. *PpRac* (100 μ L, 2 mg/mL) was

added to L-amino acid solutions **2b-g, k-l & n-o** (10 mM) in phosphate buffer (100 mM, pH 8.0, 5 ml) and the reactions were incubated at 30 °C overnight with shaking (120 rpm).



Scheme 23: Racemization of L-amino acids using *PpRac*

Samples from the biotransformations were analyzed by chiral HPLC which showed that for each reaction a new product was formed in a 1:1 ratio with the starting L-amino acid. This suggests that the reactions had reached equilibrium and the new peak was assumed to be the corresponding D-amino acid (Figure 15). Comparison with standards of the L-amino acids (**L-2b-g, k-l & n-o**) showed that in each case the L-enantiomer eluted before the D-enantiomer.

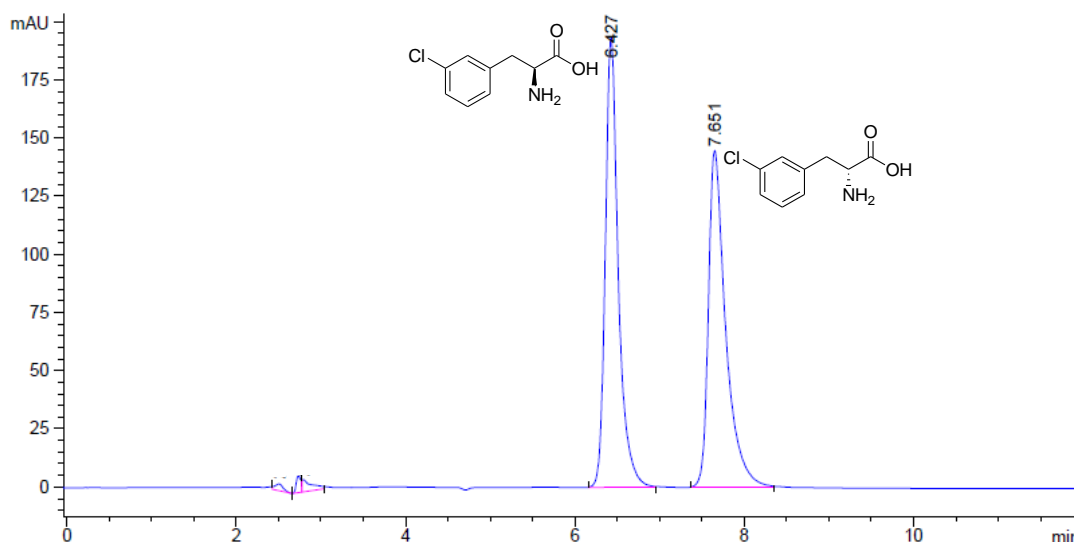


Figure 15: Chiral HPLC trace of the *PpRac* catalyzed racemization of L-2f (HPLC Method F).

2.2.2 Spectrophotometric Analysis for the Determination of PAL Catalyzed Activity

The deamination of phenylalanine **2a** to cinnamic acid **1a** using purified PAL can be measured spectrophotometrically and has been reported by Khan and Vaidyanathan.[105] The change in absorbance is measured over time at a wavelength corresponding to the cinnamic acid derivative. Using a calibration curve, the change in absorbance with time can be converted to change in substrate or product concentration with respect to time. This method allows the measurement of kinetic parameters (V_{max} , k_{cat} and K_M) for accurate comparison of PALs from different sources with different substrates. Using a spectrophotometer a scan of the absorbance over a range of wavelengths (210 nm- 450 nm in 10 nm steps) was performed for a solution of each substrate and product. From the scan, a suitable wavelength was chosen at

which only the cinnamic acid analogue has an absorbance (some examples are shown in Figure 16) which will allow the change in concentration to be measured without interference for the amino acid.

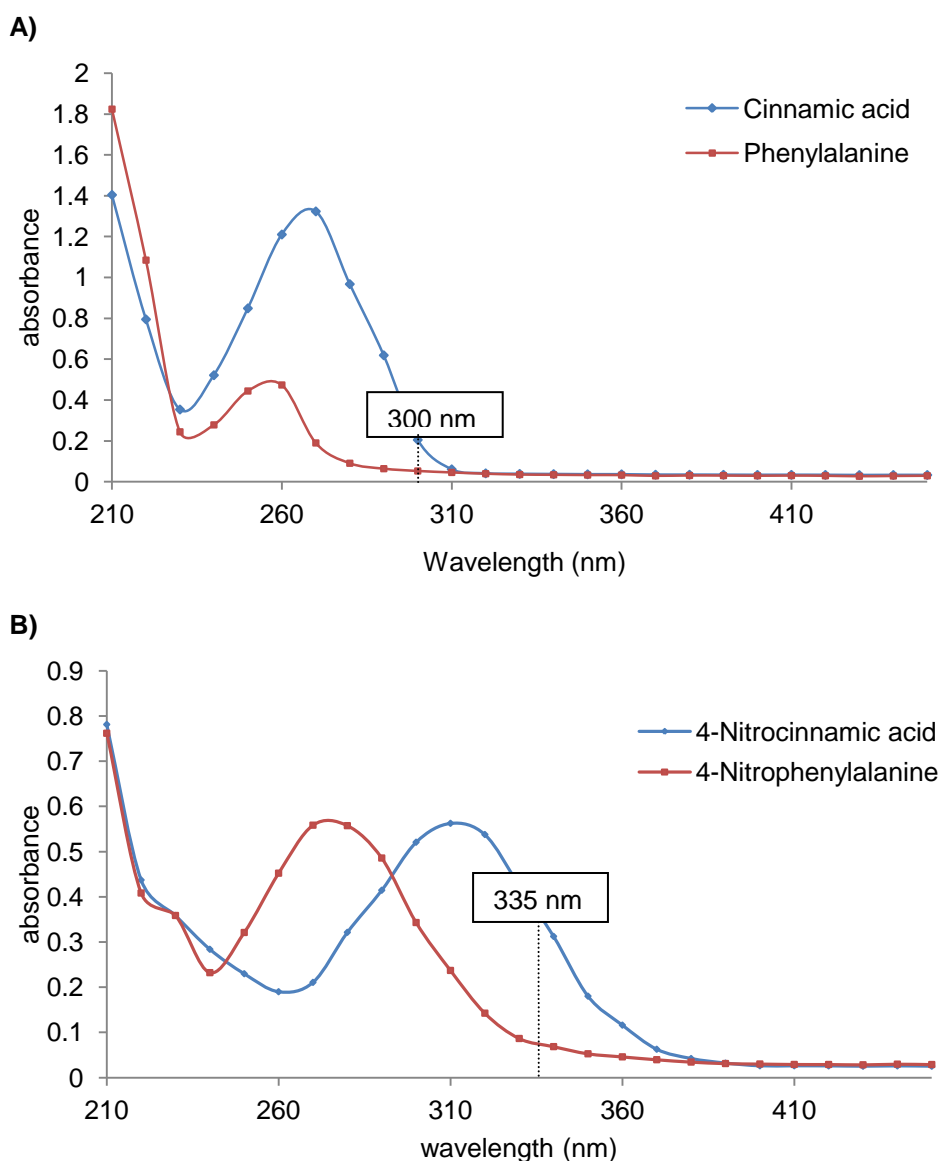


Figure 16: The wavelength scans of A) cinnamic acid 1a and phenylalanine 2a and B) 4-nitrocinnamic acid 1m and 4-nitrophenylalanine 2m, with the chosen wavelength for the measurement of kinetic parameters

Unfortunately, the chloro-substituted substrates **1e-g** and nitro-substituted substrates **1k-l** do not show a significant difference in the absorbance spectra between the cinnamic acid derivative and phenylalanine derivative at any wavelength. Therefore the kinetics for these substrates could not be determined accurately using this method.

The absorbance of cinnamic acid derivatives (**1a-d**, **1i-j** & **1m-n**) at different substrate concentrations were measured in triplicate. The gradient of the calibration line represents the correction factor used to calculate the turnover of substrate (mM/min) from the change in

absorbance (OD/min). These values are reported in Table 5 with the wavelength at which they were measured.

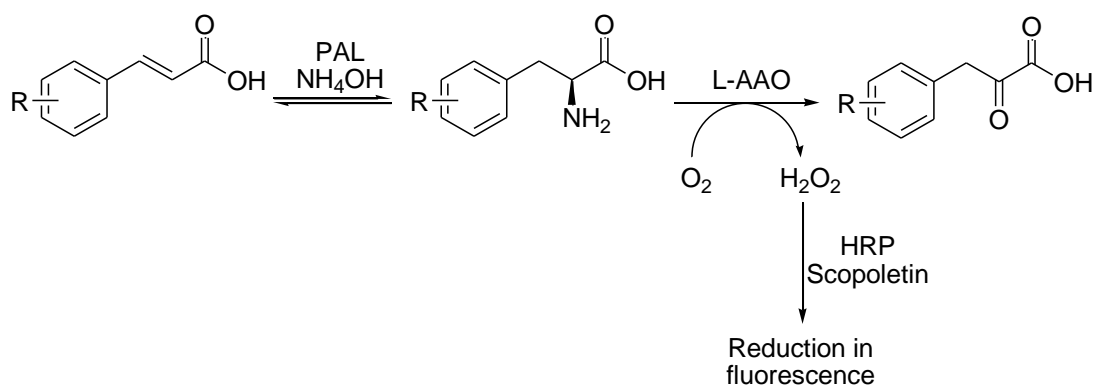
Table 5: Wavelengths and correction factors used to measure the kinetic constants for substrates 2a-d, 2i-j & 2m-n

Substrate	wavelength (nm)	correction factor
2a	300	1.35
2b	295	2.82
2c	295	3.36
2d	285	5.43
2i	295	3.10
2j	280	4.23
2m	335	6.42
2n	300	2.53

The deamination kinetics can be calculated from the increase in absorbance corresponding to the formation of the cinnamic acid analogue. Reactions can be measured in 96-well microtitre plates using a range of substrates concentrations (0-10 mM). Amination kinetics can also be measured using the spectrophotometric method, however lower concentrations of the cinnamic acid derivative are required (typically <0.4 mM) so that the absorbance is within the limits of detection. In order to measure the small changes in absorbance at the low substrate concentrations, a sensitive Cary-Series spectrophotometer was used and reactions were performed in cuvettes.

2.2.3 L-Amino Acid Oxidase Coupled Assay

The method developed in the previous section for measuring PAL catalyzed hydroamination activity is not compatible with screening in 96-well plates and requires the use of purified enzymes, as changes in absorbance are small and sensitive to background interference. An L-amino acid oxidase (L-AAO) (EC 1.4.3.2) coupled assay has been developed to allow the measurement of PAL catalyzed amination activity and is compatible with screening in a 96-well microtitre plate. In this screen, commercially available L-AAO from *Crotalus adamanteus* is used to oxidize the amino acid product from the PAL catalyzed reaction (Scheme 24). Hydrogen peroxide is formed as a co-product and is detected using horse radish peroxidase (HRP, EC 1.11.1.7). Assays based on hydrogen peroxide detection using HRP and coloured dyes, such as 2,4,6-tribromo-3-hydroxy-benzoic acid (TBHBA) and 4-aminoantipyrine (4-AAP) have been previously described.[10] However, the use of coloured dyes is not compatible with PAL catalyzed hydroamination reactions as no colour formation is observed at high pH. Instead, this assay utilizes the fluorescent compound scopoletin. Formation of hydrogen peroxide in the presence of HRP leads to a reduction in fluorescence which can be detected spectrophotometrically (excitation 380 nm, emission 460 nm).



Scheme 24: L-AAO coupled assay for the detection of PAL catalyzed amination activity using the fluorescent compound scopoletin

Unfortunately, the fluorescence is very sensitive to changes in buffer concentration, ammonia, pH and the substrates present in the assay affecting the reproducibility of this method. Furthermore, this method is not compatible with whole cell biocatalysts or cell lysate as the L-AAO can react with L-amino acid contaminants from the cell. Nonetheless, if the same assay mixture is used to screen PAL catalyzed activity using purified enzymes, normalizing the results allows comparison between parallel reactions. This method has been used to successfully determine the optimal hydroamination reaction conditions using purified *RgPAL* (see section 2.4.1: *amination reaction conditions*). Additionally, this assay can be performed as an endpoint assay for detecting hydroamination activity using whole cell biocatalysts (see section 5.2.3.1: *L-amino acid oxidase coupled assay*).

2.3 Optimization of PAL Expression

Previous work on the optimization of *Rhodotorula graminis* PAL expression showed that protein production using *E. coli* BL21(DE3) cells grown in LB with IPTG induction (1 mM at OD₆₀₀ = 0.6-1.0) at 26 °C for 18 hours yielded soluble active protein.[106] In order to improve the overproduction of PAL, different *E. coli* host strains and the use of auto-induction media were studied. The results were compared to the level of protein produced under the previous conditions.

Auto-induction media was developed in 2005 and is based on the ability of sugars present in the growth media to induce protein expression of genes controlled by a *lac* promoter, when cells reach saturation.[107] Glucose is used as an early energy source and represses protein production by preventing lactose uptake. Once glucose is depleted, which usually coincides with the mid to late log phase of growth, lactose uptake can occur which leads to protein induction. Lactose is converted to allolactose which binds to the *lac* repressor and triggers transcription of the *lac* operon to induce expression of genes under the control of the *lac* operator (Figure 17). Glycerol present in the media serves as a late energy source. The advantages of this system are there is no need to monitor the OD₆₀₀ of the culture, the final amount of biomass produced from each culture is greater than with IPTG induction and generally protein yields are higher.

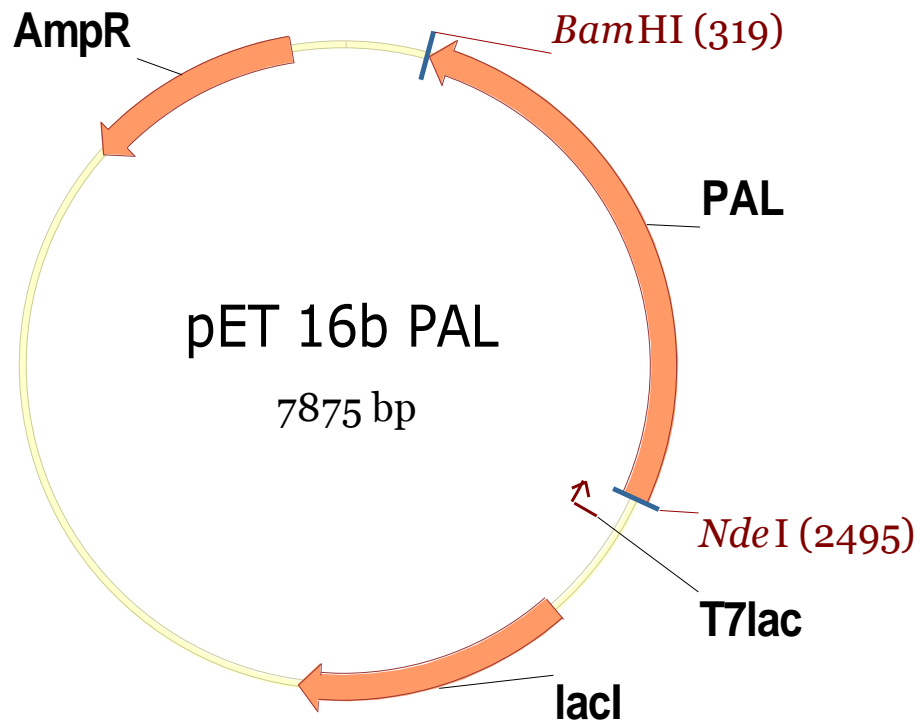


Figure 17: Plasmid map of the *RgPAL* gene cloned into pET-16b using *NdeI* and *BamHI* restriction sites

Of the three PAL enzymes investigated in this chapter, *RgPAL* (from *Rhodotorula glutinis*) was chosen for optimization as it has the highest identity to *Rhodotorula graminis* PAL (72%) used previously. Overnight starter cultures (1 mL) of *E. coli* BL21(DE3) cells carrying the plasmid for *RgPAL* expression were used to inoculate auto induction media (100 mL) which was prepared according to the method of Studier.[107] The cultures were incubated at four different temperatures, 18 °C, 26 °C, 30 °C and 37 °C and samples (2 mL) were taken each day for 7 days. The OD₆₀₀ of each sample was measured and the results are shown in Figure 18. Expression in auto-induction media at 18 °C gave significantly higher cell mass after 5 days incubation than at the other temperatures studied. In addition, the overall cell mass from a culture of auto induction media at 18 °C was approximately 8 times higher than the yield from a culture of cells grown under the previously optimized conditions.

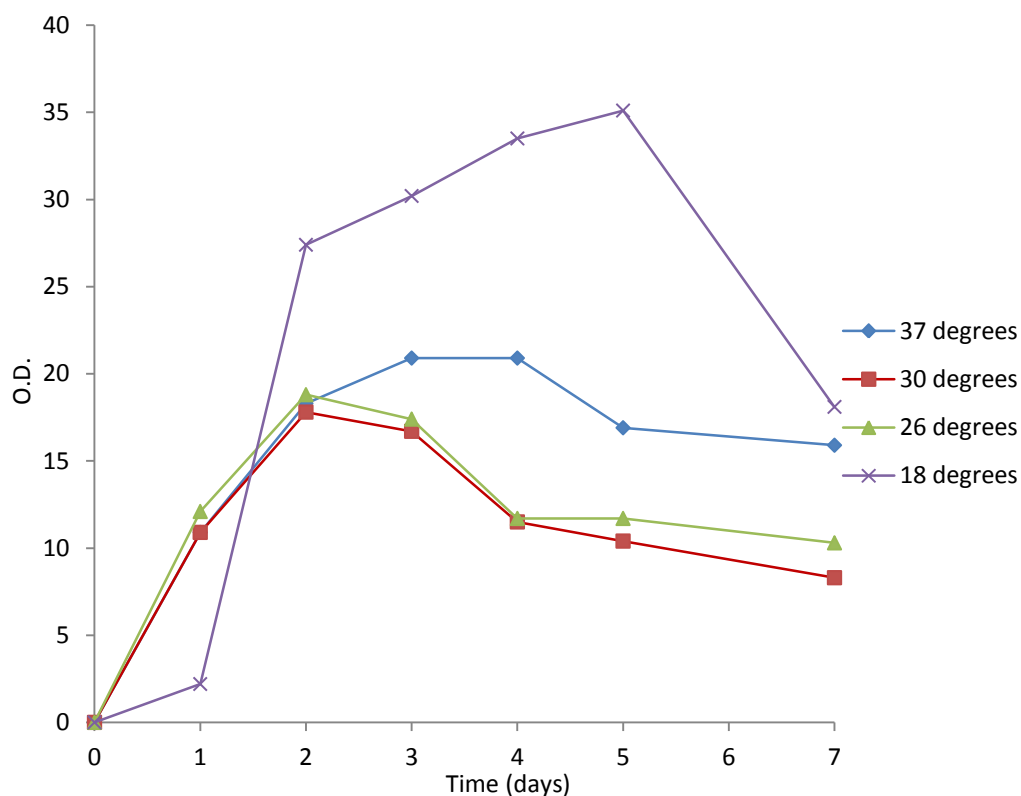


Figure 18: The OD₆₀₀ of *E. coli* BL21(DE3) whole cells expressing *RgPAL* grown in auto-induction media

To determine the levels of active protein, a sample (20 μ L, 2 O.D units) from each time point was assayed spectrophotometrically. The deamination activity towards L-phenylalanine (8 mM) was determined by measuring the formation of *trans*-cinnamic acid at 300 nm. The results show that the highest activity which corresponds to the highest production of active protein, is found in cells grown at 18 °C for 5 days ($V_{max} = 67.9 \pm 4.6 \mu\text{M}/\text{min}$, Figure 19). Under these conditions *E. coli* BL21(DE3) cells expressing *RgPAL* have twice the activity of those prepared using IPTG induction (V_{max} of $34.2 \pm 3.4 \mu\text{M}/\text{min}$). Furthermore, the same volume of culture yields 8 times more cell mass leading to an overall 16-fold increase in the amount of soluble active protein per litre of culture.

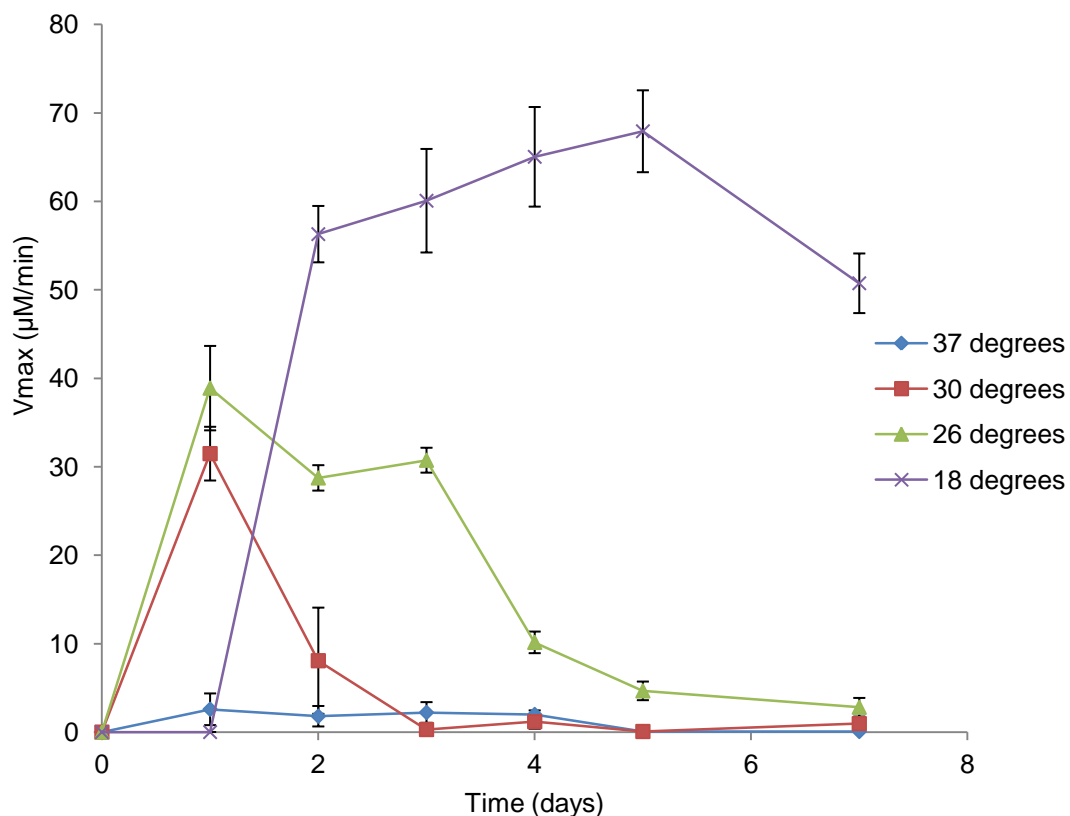


Figure 19: Activity of *E. coli* BL21(DE3) whole cells expressing *RgPAL* produced using auto-induction media at different temperatures. The results show the average of three measurements and the error bars represent the standard deviation

In addition to studying the effect of auto-induction media on protein yield, *E. coli* Rosetta and C43(DE3) cells were investigated as alternative hosts to further increase protein production. Rosetta is a strain of *E. coli* which carries preferred rare tRNAs for efficient translation of eukaryotic genes and C43(DE3) is a strain developed to increase expression levels of toxic proteins. These cells were transformed with the pET-16b plasmid carrying the gene for *RgPAL* and were grown in LB with IPTG induction (1 mM at $OD_{600} = 0.8$) at 26 °C for 18 hours. The whole cells were assayed as before and the results are shown in Table 6.

Table 6: The deamination activity of whole cells expressing *RgPAL* towards L-phenylalanine

<i>E. coli</i> strain	V_{max} (µM/min)
BL21(DE3)	34.2 ± 3.4
C43(DE3)	23.9 ± 2.67
Rosetta	42.7 ± 6.74

Rosetta cells expressing *RgPAL* showed higher activity than BL21(DE3) and C43(DE3) cells. However, the use of BL21(DE3) cells with auto-induction media at 18 °C yielded sufficient levels of PAL expression and therefore further optimization using Rosetta cells with auto-induction media was not explored. *PcPAL* and *AvPAL* were expressed using the newly optimized conditions and a high concentration of soluble active protein was achieved at a similar level to *RgPAL* as judged by subsequent protein purifications.

2.4 Optimization of PAL Catalyzed Reaction Conditions

Reactions of proteinogenic and non-proteinogenic amino acids catalyzed by eukaryotic PALs have been previously reported.[57,70-72,108] Hydroamination reactions were typically performed in 5-6 M NH_4OH , pH 10 and deamination reactions in 100 mM buffer, pH 8-9, at 30 °C or 37 °C. Herein the optimal reaction conditions are investigated, including the effects of the ammonia source on the rate of amination and the optimal pH for deamination reactions.

2.4.1 Amination Reaction Conditions

2.4.1.1 Effect of Ammonia Concentration

Initial attempts to achieve HAL catalyzed hydroamination using 10-60 mM ammonia failed and led to the erroneous assumption that lyase catalyzed reactions are irreversible.[90] It has since been determined that the K_M value for ammonia in the *PcPAL* catalyzed amination of *trans*-cinnamic acid is 4.4 M and 2.6 M at pH 8.8 and pH 10 respectively.[109] The concentration of ammonia has a significant effect on the rate of reaction and position of equilibrium and in order to achieve good conversions, 5-6 M ammonia is typically used in literature procedures. Hydroamination reactions in this thesis will be carried out in the presence of 5 M ammonia.

2.4.1.2 Effect of Ammonia Source

The effect of different ammonia sources on PAL catalyzed cinnamic acid amination was measured using purified *RgPAL* and the L-AAO coupled assay (see 2.2.3 *L-Amino acid oxidase coupled assay*). The results show that the initial rate of hydroamination is slightly lower at 2 M ammonia concentration than at 5 M ammonia (Figure 20). The use of ammonium carbamate as an ammonia source resulted in the fastest initial rate of amination. Nonetheless, reactions using *E. coli* BL21(DE3) whole cells expressing *RgPAL* showed that varying the ammonia source had little effect on the final substrate conversion (as determined by HPLC). Therefore to maintain consistency with current literature, NH_4OH was selected as the ammonia source for this work.

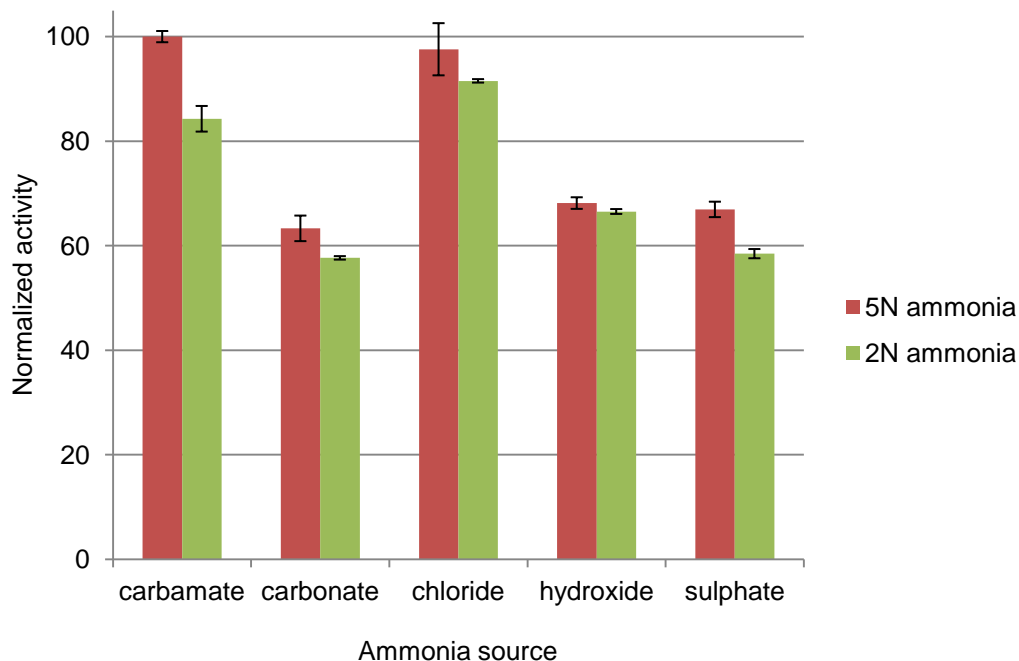


Figure 20: Relative rate of cinnamic acid amination using different ammonia sources. The activity measurements are normalized to the highest activity. Measurements were made in triplicate and the error bars represent the standard deviation

2.4.1.3 Effect of pH

In the literature, hydroamination reactions have typically been performed at *ca.* pH 10 which leads to a favourable equilibrium position.[57,71,72,108] However, using purified PAL in 5 M NH_4OH , pH 10 at 30 °C with shaking at 250 rpm leads to significant protein precipitation and inactivation of the enzymes resulting in poor substrate conversions. The pH was reduced to 9.5 and shaking was reduced to 120 rpm, which allowed the PAL enzymes to retain activity and yield comparable conversions to reactions using whole cell biocatalysts. Further reactions using purified enzymes, cell lysate and whole cell biocatalysts were all performed at pH 9.5.

2.4.2 Deamination Reaction Conditions

Eukaryotic *PcPAL* and *RgPAL* catalyzed deamination reactions have been previously reported, however to our knowledge the activity of prokaryotic *AvPAL* towards non-natural amino acids has not been studied. For this reason, the optimal conditions were determined for *AvPAL* mediated deamination reactions.

2.4.2.1 Effect of pH

The pH profile for *AvPAL* catalyzed deamination of L-phenylalanine was measured using the spectrophotometric assay (2.2.2: *Spectrophotometric analysis*) and cell lysate. The results show that the optimal pH for *AvPAL* catalyzed deamination of L-phenylalanine is pH 8.3 (Figure 21) and above this pH the activity significantly decreases. Interestingly, the eukaryotic

PALs have a higher pH optimum than AvPAL and maintain a high level of activity above the optimum. For further reactions pH 8.3 was used as all three PALs showed a high level of activity at this pH.

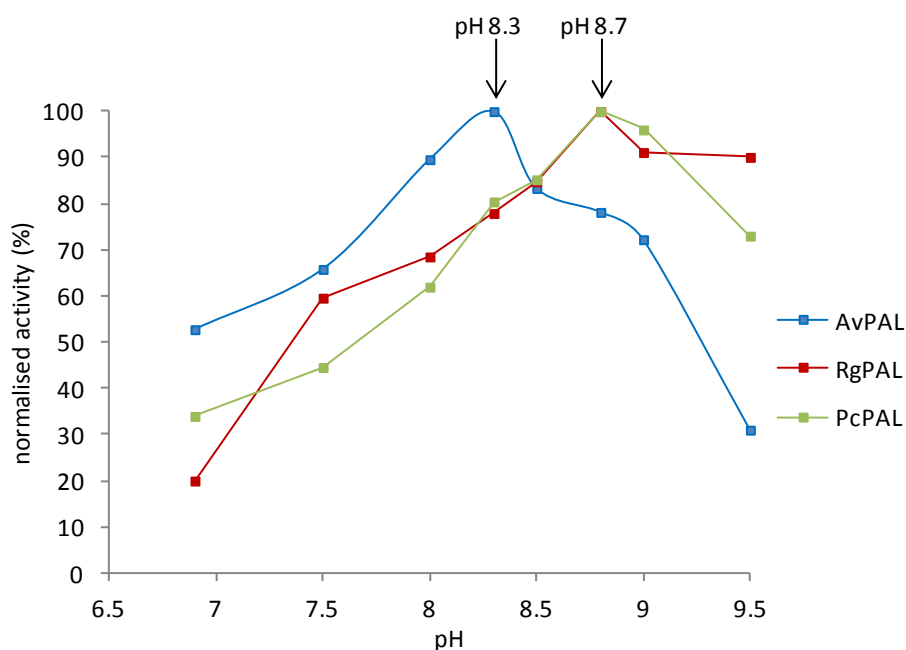


Figure 21: pH profile for AvPAL (blue), RgPAL (red) and PcPAL (green) catalyzed deamination of L-phenylalanine (10 mM) in 100 mM Tris-buffer at 30 °C using cell lysate (10 μ L, prepared from the lysis of 500 mg whole cells in 2 mL water)

2.5 Determining the Kinetic Constants for PAL Catalyzed Reactions

2.5.1 Deamination Kinetics

Kinetic constants for AvPAL catalyzed deamination of the natural substrate (**2a**) and a series of non-natural substrates (**2b-d**, **2i-j** & **2m-n**) were measured spectrophotometrically (see section 2.2.2: *Spectrophotometric analysis* for details) in triplicate. Purified AvPAL (100 μ L, 0.3 mg/mL) was added to L-amino acid solutions at eight different concentrations (0-20 mM, 100 μ L) and the increase in absorbance corresponding to the formation of the cinnamic acid derivative was measured (Figure 22). The initial rate (mM/min) was calculated from the initial change in OD per minute using the molar absorption coefficient calculated from a standard calibration curve for each product (see experimental section **Error! Reference source not found.**). The kinetic constants were determined from non-linear regression analysis using the Microsoft Excel add-in, Solver.[110]

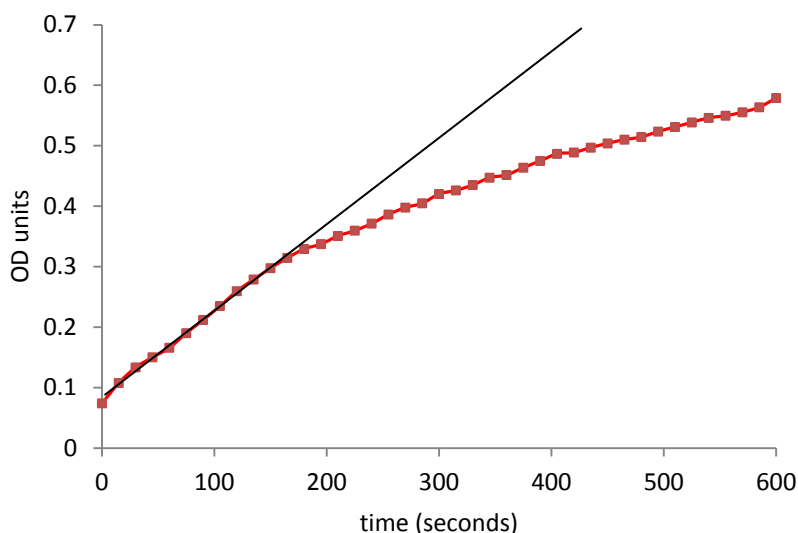
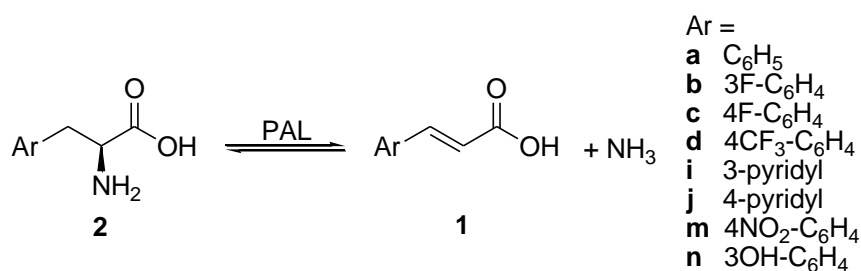


Figure 22: The deamination of L-phenylalanine (5 mM) measured spectrophotometrically at 300 nm (shown in red). The initial rate was measured from the linear portion of the graph and the linear regression analysis is shown in black

Surprisingly, all non-natural amino acids screened show enhanced turnover rates (k_{cat}) compared to the natural substrate L-phenylalanine (**2a**) (Table 7). The substrates 3-fluoro-L-phenylalanine (**2b**), 4-fluoro-L-phenylalanine (**2c**), 3-pyridyl-L-alanine (**2j**) and 4-nitro-L-phenylalanine (**2m**) had the highest k_{cat} values which were two times larger than for **2a**. Interestingly, all non-proteinogenic amino acids also had larger K_{M} values than **2a**, with 3-substituted substrates **2b** and **2i** displaying higher K_{M} values than the corresponding 4-substituted amino acids **2c** and **2j**. This result suggests that the shape of the active site may bind 4-substituted structures more easily than 3-substituted structures. As a result of their high values of K_{M} most substrates with the exception of **2b** and **2e**, resulted in catalytic efficiencies ($k_{\text{cat}}/K_{\text{M}}$) that were lower than for L-phenylalanine.

Table 7: AvPAL kinetic constants for the deamination of substrates 2a-d, 2i-j & 2m-n



Substrate	k_{cat} (s ⁻¹)	K_{M} (mM)	$k_{\text{cat}}/K_{\text{M}}$ (s ⁻¹ mM ⁻¹)
2a	0.49 ± 0.01	0.29 ± 0.06	1.68
2b	1.01 ± 0.17	0.75 ± 0.15	1.46
2c	1.06 ± 0.06	0.56 ± 0.01	1.89
2d	0.82 ± 0.01	1.05 ± 0.06	0.78
2i	0.91 ± 0.04	3.39 ± 0.26	0.27
2j	0.61 ± 0.003	0.48 ± 0.03	1.27
2m	1.08 ± 0.03	0.23 ± 0.02	4.69
2n	0.89 ± 0.01	1.11 ± 0.05	0.80

Reactions performed in triplicate (0.1 M borate buffer, pH 8.3 at 30 °C). The error represents the standard deviation calculated from the measurements which were made in triplicate.

2.5.2 Amination Kinetics

The synthetic utility of PALs lies in their applications in the conversion of cinnamic acid analogues to their corresponding amino acids. The kinetic constants for the AvPAL, PcPAL and RgPAL catalyzed amination of a panel of cinnamic acid derivatives (**1a-d**, **1i-j** & **1m-n**) were measured to allow direct comparison between PALs from different sources (Table 8). Purified PAL (0.8 mg/mL, 50 µL) was added to substrate solutions at six different concentrations (0-0.4 mM, 850 µL) in NH₄OH (5 M, pH 9.5) and the initial decrease in absorbance was measured spectrophotometrically corresponding to substrate consumption (Figure 23). The kinetic constants were determined from non-linear regression analysis using the Microsoft Excel add-in, Solver (Table 8).

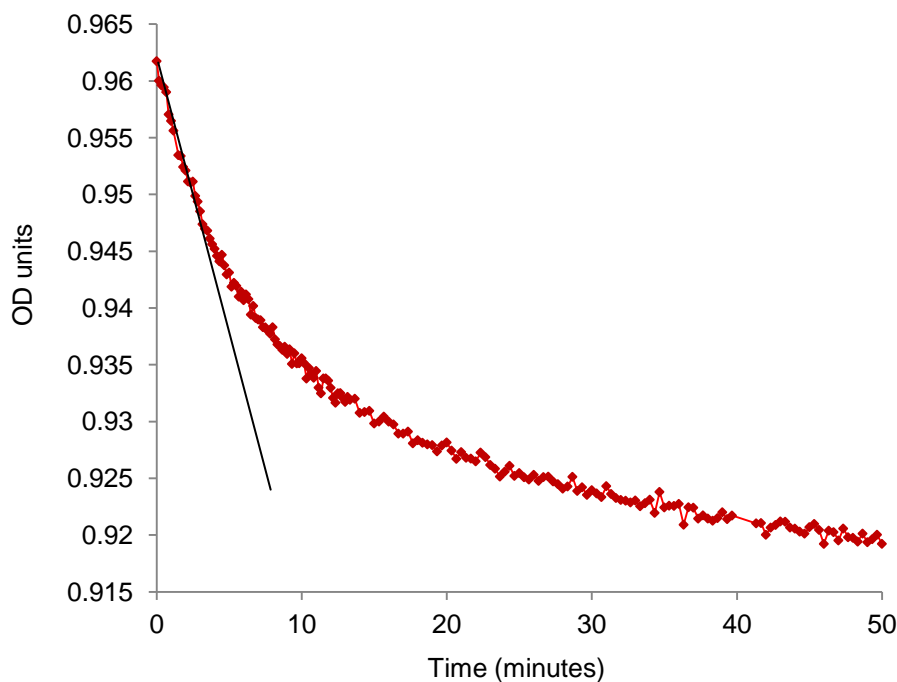
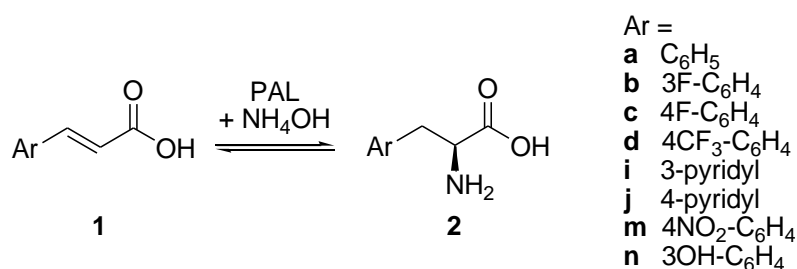


Figure 23: The amination of cinnamic acid (0.2 mM) in 5 M NH₄OH, pH 9.5 at 30 °C measured spectrophotometrically at 300 nm (shown in red). The initial rate is measured from the gradient of the linear portion of the graph (shown in black)

The amination of cinnamic acid (**1a**) by AvPAL is approximately three and ten times slower than PcPAL and RgPAL respectively (Table 8). However, AvPAL shows a higher initial turnover rate (k_{cat}) and clear preference towards all non-natural cinnamic acid derivatives compared to cinnamic acid itself. PcPAL also showed enhanced activity towards the non-natural substrates compared to cinnamic acid however RgPAL showed only a preference towards the pyridyl compounds **1i** and **1j**.

Interestingly AvPAL showed higher catalytic turnover towards substrates 4-trifluoromethylcinnamic acid (**1d**), 4-pyridylacrylic acid (**1j**), 4-nitrocinnamic acid (**1m**) and 3-hydroxycinnamic acid (**1n**) compared to the eukaryotic PALs. Significantly, the turnover of substrate **1m** is approximately forty and twenty times faster with AvPAL than with PcPAL and RgPAL respectively. In addition, substrate **1d**, which is a poor substrate for both eukaryotic PALs, shows excellent activity with AvPAL. Furthermore, cinnamic acid derivatives **1d**, **1j** and **1m** were better substrates (higher k_{cat} values) in the synthetically useful amination direction than the physiological deamination direction.

Table 8: Kinetic constants for the PAL catalyzed amination reactions of 1a-d, 1i-j & 1m-n



	RgPAL		PcPAL		AvPAL	
	k_{cat} (s ⁻¹)	K_{M} (mM)	k_{cat} (s ⁻¹)	K_{M} (mM)	k_{cat} (s ⁻¹)	K_{M} (mM)
1a	0.31 ± 0.05	0.33 ± 0.08	0.07 ± 0.002	0.30 ± 0.001	0.03 ± 0.0004	0.03 ± 0.01
1b	0.27 ± 0.04	0.06 ± 0.02	0.46 ± 0.08	0.18 ± 0.06	0.08 ± 0.01	0.07 ± 0.02
1c	0.21 ± 0.03	0.19 ± 0.04	0.25 ± 0.05	0.25 ± 0.1	0.09 ± 0.03	0.12 ± 0.07
1d	0.05 ± 0.03	0.39 ± 0.01	0.06 ± 0.01	1.85 ± 0.001	3.14 ± 0.09	1.51 ± 0.003
1i	0.66 ± 0.003	1.87 ± 0.001	0.07 ± 0.007	0.38 ± 0.0001	0.14 ± 0.01	0.39 ± 0.001
1j	0.85 ± 0.02	1.42 ± 0.0004	0.28 ± 0.06	1.85 ± 0.006	1.06 ± 0.04	0.38 ± 0.12
1m	0.17 ± 0.02	1.86 ± 0.0004	0.10 ± 0.004	3.31 ± 0.001	3.81 ± 0.08	0.66 ± 0.13
1n	0.18 ± 0.002	0.30 ± 0.02	0.27 ± 0.05	0.27 ± 0.07	0.61 ± 0.01	3.30 ± 0.001

Reactions performed in triplicate (in 5 M NH₄OH, pH 9.5 at 30 °C). The error represents the standard deviation calculated from the measurements which were made in triplicate.

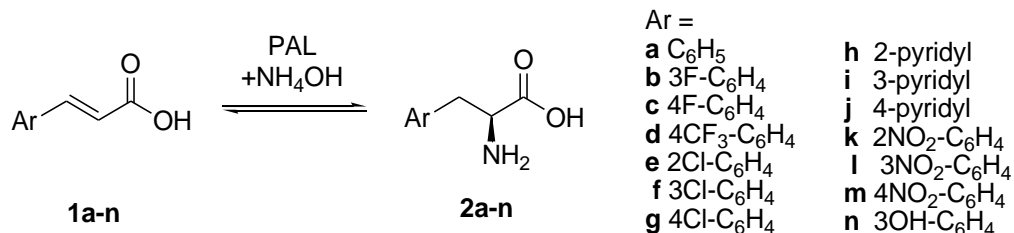
2.6 Comparison of PcPAL, RgPAL and AvPAL as Whole Cell Biocatalysts for the Production of Non-Proteinogenic Amino Acids

The application of eukaryotic PALs as whole cell biocatalysts for the amination of cinnamic acid analogues has been described previously.[57,71,72,108] However, to our knowledge the activity of prokaryotic PALs towards unnatural substrates has not been investigated. In order to investigate the suitability of AvPAL as a biocatalyst for amino acid synthesis, the substrate specificity and activity of wild-type AvPAL was determined alongside the eukaryotic PcPAL and RgPAL.

2.6.1 Analytical Scale Biotransformations

The conversion of a panel of cinnamic acid derivatives (**1a-q**) to their corresponding amino acids was carried out using *E. coli* BL21(DE3) whole cells expressing the individual PAL enzymes AvPAL, RgPAL and PcPAL. The reactions were monitored over time by chiral HPLC and the percentage conversion at the point of maximal product e.e. is reported in Table 9. All PALs including AvPAL show very low to no conversion of coumaric acid (**1o**) to tyrosine (**2o**), confirming their classification as PALs and not TALs. Furthermore, electron rich structures, 3-methoxy and 4-methoxy cinnamic acid (**2p** and **2q**) were poor substrates for all three PALs. In general, the activity of AvPAL was largely comparable to that of the eukaryotic PcPAL and RgPAL, with all three enzymes catalyzing the conversion of substrates **1a-n**. PAL catalyzed synthesis of non-natural amino acids has been reported to proceed with >98 % enantioselectivity. However, although the majority of substrates initially yielded products with high e.e. in favour of the L-amino acid (see appendix for percentage conversions at different time points) substrates **1f** & **1k-m** yielded products with a lower e.e. Interestingly, these substrates demonstrated a high turnover rate and had reached their maximum conversion after short reaction times. AvPAL demonstrated superior stereoselectivity towards 3'-substituted substrates 3-fluorocinnamic acid (**1b**), 3-chlorocinnamic acid (**1f**) and 3-nitrocinnamic acid (**1l**) compared to PcPAL and RgPAL under the reaction conditions employed. However, for these substrates the time taken to reach maximal conversion with AvPAL was longer than with the eukaryotic PALs. Whole cell PAL activity is affected by varying levels of protein overexpression which can occur from small changes in the expression conditions. Furthermore, there is an inherent source of error when weighing wet cell mass, so direct comparison between whole cell biocatalysts is problematic. However, an accurate comparison between the activities of the three PAL enzymes has already been provided in section 2.5.2 *Amination kinetics*, where the kinetic constants were measured using purified enzymes.

Table 9: Percentage conversion at the point of maximal product e.e. for the PAL catalyzed hydroamination reactions of substrates 1a-1n



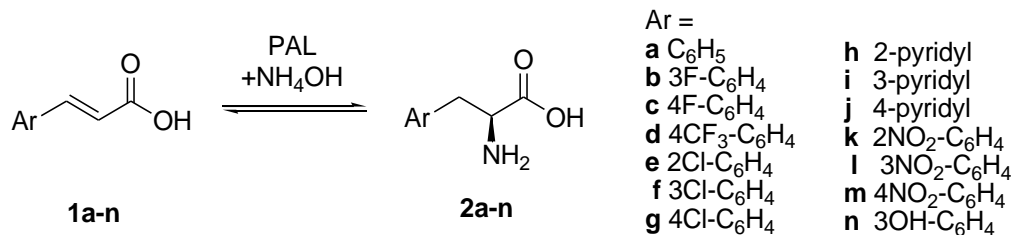
	RgPAL			PcPAL			AvPAL		
	conv.	e.e. ^a	time (h)	conv.	e.e. ^a	time(h)	conv.	e.e. ^a	time(h)
1a	55	>99	22	58	>99	22	49	>99	22
1b	61	96	0.33	62	88	0.33	59	>99	22
1c	61	>99	22	61	>99	0.33	59	>99	22
1d	73	>99	6	62	>99	0.66	69	>99	0.66
1e	80	96	0.33	90	>99	0.33	91	>99	6
1f	66	72	0.33	74	43	0.33	62	>99	22
1g	52	<99	2	50	>99	0.66	53	>99	6
1h	54	89	2	46	>99	2	61	>99	2
1i	81	<99	1	82	>99	0.66	80	>99	22
1j	82	<99	0.66	82	>99	0.33	85	>99	1
1k	86	57	0.33	87	51	0.33	38	50	0.33
1l	82	46	0.33	84	35	0.33	65	>99	6
1m	48	72	0.33	61	71	0.33	81	72	0.33
1n	48	<99	6	50	>99	2	50	>99	6

[a] e.e. of the L-enantiomer. Reactions performed using *E. coli* BL21(DE3) whole cells (20 mg/mL) expressing each PAL with 5 mM substrate in 5 M NH₄OH, pH 9.5 at 30 °C

Surprisingly, after prolonged reaction times (22 hours) the e.e. of the amino acid products **2b**, **2d-f** & **2h-m** diminished significantly with all three PAL biocatalysts (Table 10). The substrates **1b**, **1d-1f** & **1h-1m** all possess electron-withdrawing substituents on the aromatic ring, suggesting that PALs are able to catalyze the formation of the D-enantiomer for these electron-deficient structures. D-amino acid formation is especially prominent with substrates which are able to stabilize negative charge at the benzylic position, for example in the cases of substrates **1k** and **1m** which possess *ortho* and *para* nitro-substituents respectively. Furthermore, these substrates show a slight preference for formation of the D-enantiomer after 22 hours.

Control reactions were performed in parallel using *E. coli* BL21(DE3) whole cells carrying an empty pET-16b vector and ruled out the possibility of background chemical reactions. Furthermore, in the absence of PAL enzyme no racemization of α -amino acids was observed. A time dependence on e.e has not been previously reported for PAL catalyzed reactions and this result will be studied in more detail in the next chapter.

Table 10: Percentage conversion and product e.e. for the PAL catalyzed hydroamination reactions of substrates 1a-1n after 22h reaction time

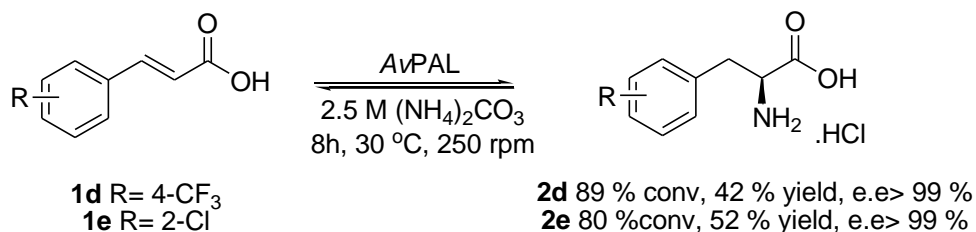


	RgPAL		PcPAL		AvPAL	
	conv.	e.e. ^a	conv.	e.e. ^a	conv.	e.e. ^a
1a	55	>99	58	>99	49	>99
1b	71	2	75	6	59	>99
1c	61	>99	60	>99	59	>99
1d	75	93	75	96	76	71
1e	93	13	94	0	91	>99
1f	76	7	72	14	62	>99
1g	51	>99	50	>99	53	>99
1h	62	38	49	-8	61	76
1i	85	28	87	10	80	>99
1j	89	1	89	0	77	75
1k	86	-14	87	-11	86	-9
1l	83	7	84	7	78	92
1m	85	5	86	-4	79	-6
1n	48	>99	50	>99	50	>99

[a] e.e. of the L-enantiomer. Reactions performed using *E. coli* BL21(DE3) whole cells (20 mg/mL) expressing each PAL incubated with 5 mM substrate in 5 M NH₄OH, pH 9.5 at 30 °C

2.6.2 Large Scale Reactions and Product Isolation

The results presented in Table 9 and Table 10 demonstrate that the choice of biocatalyst and reaction conditions can have a significant effect on the e.e. of the amino acid products, in particular for those with electron withdrawing substituents on the aromatic ring. To demonstrate the applicability of these enzymes in preparative scale reactions, the AvPAL catalyzed amination of 4-trifluoromethyl-cinnamic acid (**1d**) and 2-chloro-cinnamic acid (**1e**) were performed on a one gram scale (Scheme 25).

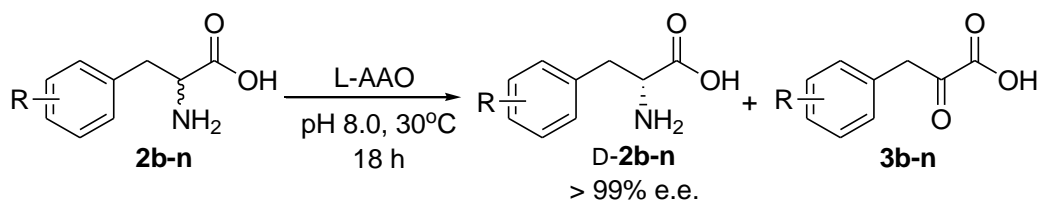


Scheme 25: AvPAL mediated synthesis of L-amino acids 2d and 2e

Whole cell *E. coli* BL21(DE3) expressing AvPAL (7.5 g) was resuspended in a solution of substrate (1g, 5.5 mmol) in ammonium carbonate (2.5 M, 500 mL) which was used without adjusting the pH (9.1) to avoid the formation of unwanted salts. The reactions were incubated with shaking (250 rpm) at 30 °C and the conversion and product e.e were monitored closely over time by chiral HPLC. After 8 hours the reactions had reached full conversion to yield 4-trifluoro-L-phenylalanine **2d** (89 % conversion, e.e. >99 %) and 2-chloro-L-phenylalanine **2e** (80 % conversion, e.e. >99 %). The whole cells were removed by centrifugation and the supernatant was lyophilized. The hydrochloride salt of the amino acid was formed by the addition of HCl and the solution was lyophilized for a second time. The solids were washed with diethyl ether and recrystallized from water with the addition of 5 M NH₄OH until pH 7.0 to yield **2d** (42 % isolated yield) and **2e** (52 % isolated yield).

2.6.3 D-Amino Acid Synthesis

D-Amino acids are important building blocks in the production of pharmaceuticals due to their enhanced metabolic stability and they are frequently used as chiral auxiliaries and chiral synthons in organic synthesis.[111] Enzymatic kinetic resolution using a commercially available L-AAO from *Crotalus adamanteus* can be used to access optically pure D-amino acids from mixtures of enantiomers produced following prolonged PAL catalyzed hydroamination reactions. L-AAO was used in the kinetic resolutions of racemic amino acids **2b-n** to yield D-amino acids in > 99 % e.e. as determined by chiral HPLC (Scheme 26).



Scheme 26: Enzymatic kinetic resolution of phenylalanine derivatives 2b-n

2.7 Discussion and Conclusion

The expression conditions have been optimized and auto-induction media has been used to increase the levels of active protein by 16-fold per litre of culture. The amination and deamination reaction conditions have also been optimized. The kinetic constants determined for AvPAL catalyzed deamination reactions showed that all non-proteinogenic amino acids screened had a higher turnover (k_{cat}) and higher K_M value than L-phenylalanine. The K_M values were also significantly higher for 3-substituted derivatives than 4-substituted substrates. The amination kinetic constants have been measured for each of the three PAL enzymes and highlight clear differences in activity between AvPAL, PcPAL and RgPAL. However, it is interesting to note that the active sites between these enzymes are highly conserved (Figure 24). A key structural difference between eukaryotic and prokaryotic PALs lies in the active site loop, which has been attributed to controlling substrate entry and product release and contains the essential catalytic tyrosine residue (Figure 25).[81] In eukaryotic PALs the loop, which is highly mobile and unresolved in the crystal structures of PcPAL and RgPAL, must move into an active conformation for catalysis.[73,74] The corresponding loop in AvPAL is more rigid and in the crystal structure of this enzyme, the loop is well resolved and in the active conformation.[65] It is believed that differences in the rigidity of the loop account for the difference in activity between structurally similar ammonia lyases and aminomutases.[63] As the catalytic loop is significantly different between the eukaryotic PcPAL and RgPAL and prokaryotic AvPAL, it is possible it is also involved in controlling substrate specificity.

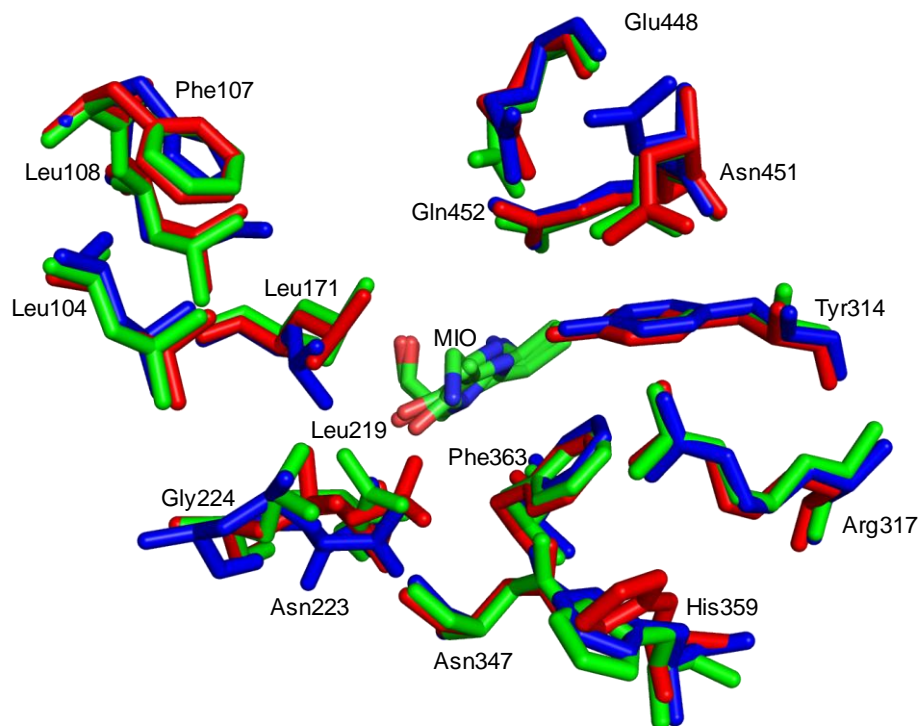
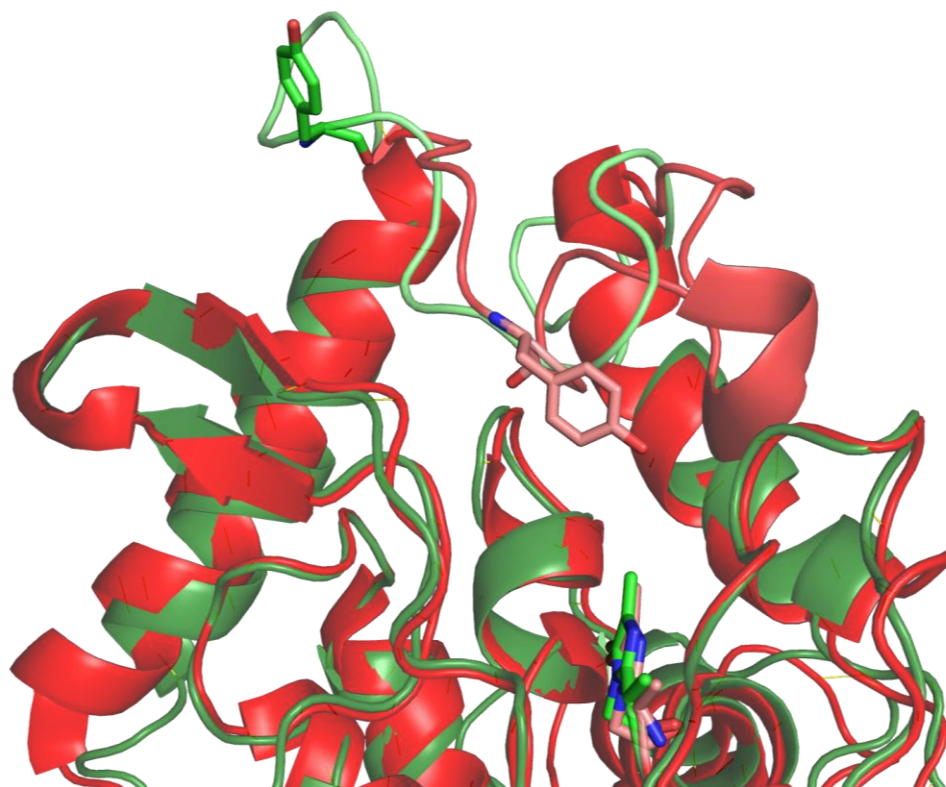


Figure 24: Conserved active site residues of *Rg*PAL (PDB code 1T6P, blue), *Pc*PAL (PDB code 1W27, green) and *Av*PAL (PDB code 3CZO, red) *Av*PAL numbering



```

RtPAL: 95 SVEFLRSQLS--MSVYGVTTGFGGSA--DTRTEDAISLQKALL 135
PcPAL: 94 SSDWVMSMNKGTDSYGVTTGFGATS--HRRTKQGGALQKELI 135
AvPAL: 63 SCDYINNAVESGEPIYGVTSGFGGMANVAISREQASELQTNLV 104

```

Figure 25: Superimposed structures of *Pc*PAL (pdb code 1W27, green) and *Av*PAL (pdb code 3CZO, red) showing the catalytic tyrosine bases. The structure of *Pc*PAL shows the catalytic loop in the open conformation and *Av*PAL in the closed conformation. The structures were generated using Pymol. The sequence alignments show the loop residues highlighted in red

Lastly, comparing the whole cell activity between *PcPAL*, *RgPAL* and *AvPAL* showed that the difference in substrate specificity is fairly unremarkable. However a time dependence on e.e has been observed which to our knowledge has not been previously reported and this will be studied in more detail in the following chapter (*Chapter 3: Mechanistic Studies of PAL Catalyzed D-Amino Acid Formation*).

2.7.1 Chosen Target for Evolution

The turnover (k_{cat} values) of non-natural substrates **1b**, **1d**, **1m** & **1n** were significantly faster with *AvPAL* than with the eukaryotic PALs screened. Therefore the bacterial *AvPAL* has been chosen as the primary candidate for directed evolution. Moreover, the suitability of *AvPAL* as an industrial biocatalyst has been demonstrated by the large scale hydroamination of substrates **1d** and **1e** to yield L-amino acid products in good yields and with high enantiomeric excess. Furthermore, there is a detailed X-ray crystal structure of *AvPAL* which, unlike the eukaryotic PALs shows the catalytic loop well resolved and in the active conformation for catalysis. A detailed crystal structure is beneficial for directed evolution as it allows the use of rational design.

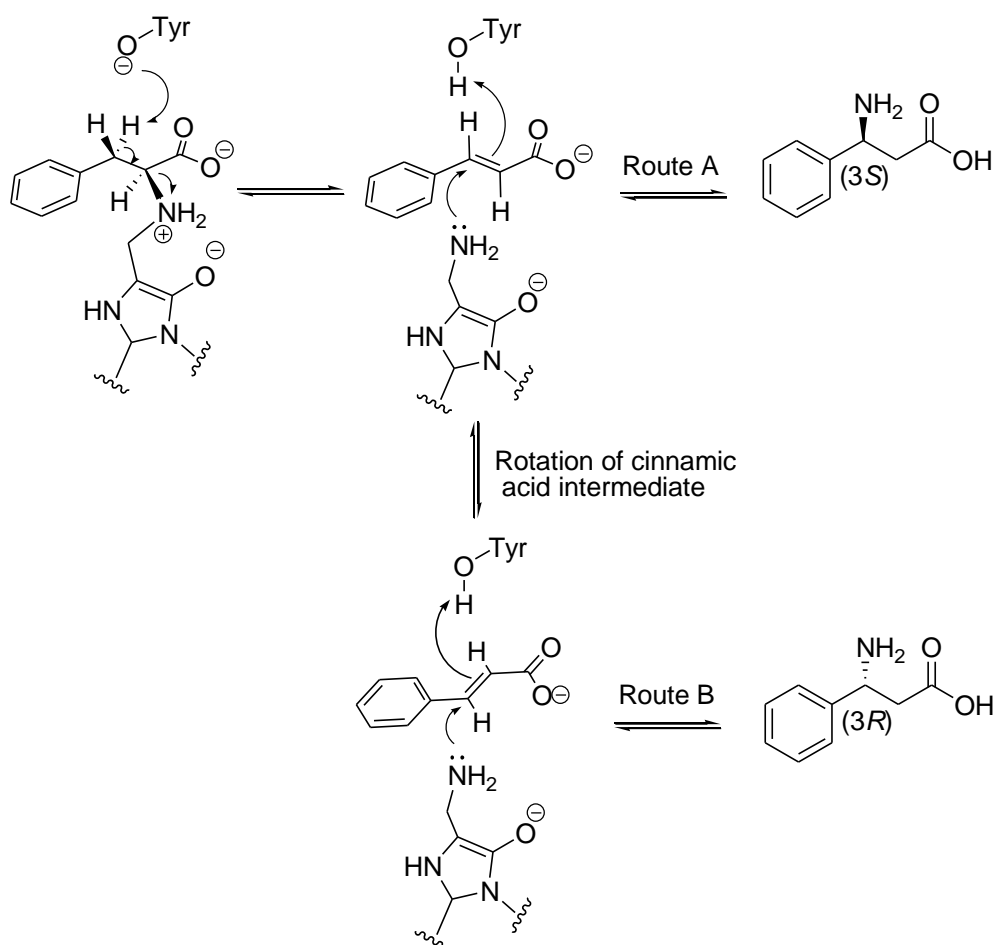
Chapter 3: Mechanistic Studies of PAL Catalyzed D-Amino Acid Formation

3 Mechanistic Studies of PAL Catalyzed D-Amino Acid Formation

3.1 Introduction

To the best of our knowledge, the data presented in the previous chapter represents the first report showing PAL catalyzed D-amino acid formation. Furthermore, this is the first report to demonstrate a time dependence on enantiomeric excess. In general, the PAL mediated synthesis of non-natural amino acids has been reported to proceed with >98 % enantioselectivity.[57,70,71,108]

Although ammonia lyase catalyzed D-amino acid formation has never been reported there are examples of enantio-complimentary aminomutases which can produce either (3*S*)- or (3*R*)- β -phenylalanines. AdmH and TcPAM catalyze the stereoselective isomerization of (2*S*)- α -phenylalanine to (3*S*)- β -phenylalanine and (3*R*)- β -phenylalanine respectively.[112] The TcPAM catalyzed formation of (3*R*)- β -phenylalanine is believed to occur via a rotation of the cinnamate intermediate at the C₁-C _{α} and C_{*ipso*}-C _{β} bonds following deamination of α -phenylalanine (Scheme 27).



Scheme 27: Proposed mechanism for the PAM catalyzed isomerization of (2*S*)- α -phenylalanine Route A) catalyzed by PaPAM Route B) catalyzed by TcPAM

TAMs display a similar activity to PAMs and SgTAM and CmdF catalyze reactions with opposite stereoselectivity. CmdF has been shown to produce (S)- β -tyrosine preferentially although upon prolonged periods of incubation significant amounts of (R)- β -tyrosine have been observed.[86] A Glu399 residue was identified which had an effect on the stereoselectivity at the β -position. A Glu399Met variant led to a decrease in stereoselectivity and the formation of racemic product, whilst Glu399Lys led to increased (R)-selectivity. The analogous residue in AvPAL is Lys419, which is believed to play a role in substrate-directing. Although aminomutases have demonstrated different stereoselectivities at the β -position, until now the formation of D- α -amino acids has not been observed.

As described in chapter 2, the AvPAL mediated hydroamination of 4-nitrocinnamic acid (**1m**) showed preference for 4-nitro-D-phenylalanine formation after prolonged reaction times. Therefore this compound was chosen as a model substrate to investigate the origin of D-amino acid formation. This chapter explores the mechanism of D-amino acid synthesis through mutagenesis of key active-site residues and isotopic labelling studies.

3.2 Time Dependence on e.e.

In order to confirm that the variation in e.e. over time did not occur as a result of background reactions taking place in the *E. coli* whole cells, control reactions were performed with cells transformed with empty pET-16b vectors. Reactions in the absence of PAL were analyzed by chiral HPLC and showed (i) no conversion of **1m** to either L- or D- product (ii) no racemization of either L- or D-amino acids and (iii) no deamination of L- or D-amino acids, eliminating the possibility of non-selective background reactions.

The amination of **1m** (5 mM, in NH₄OH 5M, pH 9.5, 30 °C) was repeated using a lower concentration of *E. coli* BL21(DE3) whole cells expressing AvPAL (15 mg/mL), in order to allow the conversion and product e.e. to be monitored more closely over time (Figure 26). After three hours the reaction had reached maximum substrate conversion however the e.e. continued to decrease over 48 hours (Figure 27). The reaction profile is consistent with initial (reversible) formation of the L-amino acid as the kinetic product followed by a slower process in which formation of the D-enantiomer occurs.

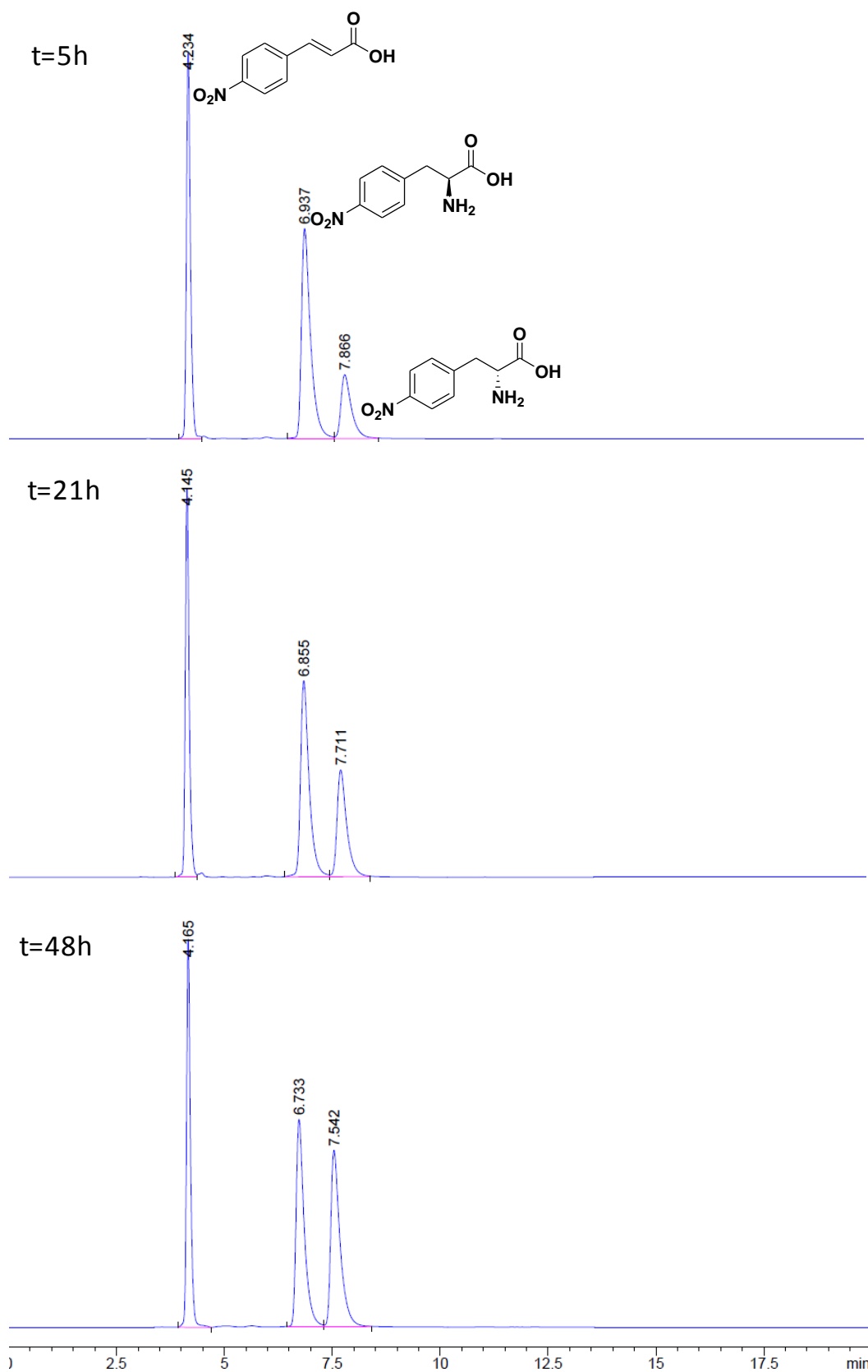


Figure 26: Chiral reverse phase HPLC traces from the AvPAL catalyzed hydroamination of 4-nitrocinnamic acid after 5 hours, 21 hours and 48 hours reaction time

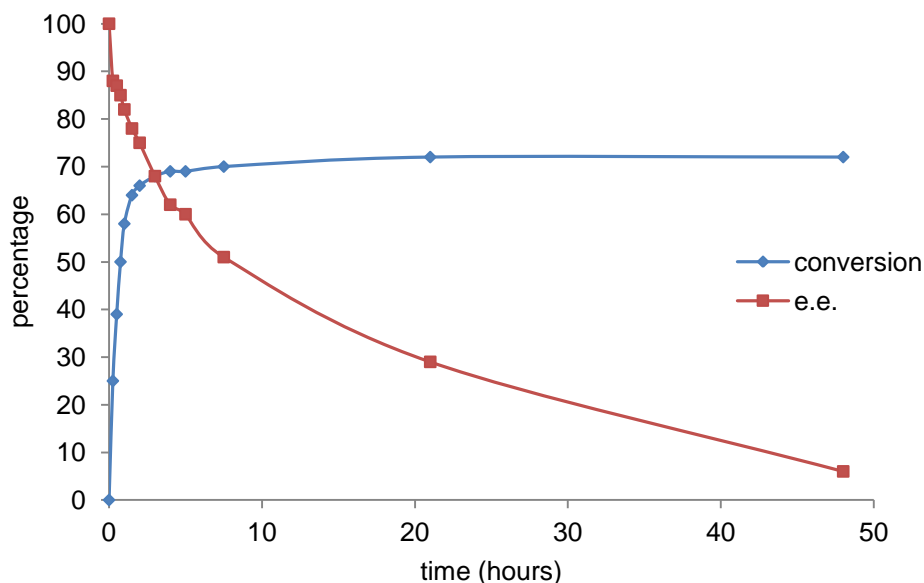


Figure 27: The amination reaction of 4-nitrocinnamic acid (**1m**) mediated by whole cell AvPAL biocatalysts

3.3 Wild-type AvPAL Catalyzed Deamination of 4-Nitrophenylalanine

To confirm the reversibility of the amination reaction under conditions of high ammonia concentration, the kinetic constants for wild-type AvPAL deamination reactions of both enantiomers of 4-nitrophenylalanine **2m** were measured under different reaction conditions.

Table 11: Kinetic constants for the deamination of both enantiomers of 4-nitrophenylalanine catalyzed by AvPAL

Reaction conditions	4-nitro-L-phenylalanine			4-nitro-D-phenylalanine		
	k_{cat} (s^{-1})	K_{M} (mM)	$k_{\text{cat}}/K_{\text{M}}$ ($\text{s}^{-1}\text{mM}^{-1}$)	k_{cat} (s^{-1})	K_{M} (mM)	$k_{\text{cat}}/K_{\text{M}}$ ($\text{s}^{-1}\text{mM}^{-1}$)
0.1 M borate buffer pH 8.3	1.38	0.48	2.88	0.09	0.09	1.0
2 M NH_4OH pH 9.5	1.32	0.65	2.03	0.06	0.16	0.38
5 M NH_4OH pH 9.5	1.29	1.08	1.19	0.06	0.14	0.43

The standard optimized deamination reaction conditions (0.1 M borate buffer pH 8.3) gave the highest overall catalytic efficiency ($k_{\text{cat}}/K_{\text{M}}$). The presence of increasing concentrations of ammonia and high pH increased the values of K_{M} (most significantly for the L-**2m** reactions) which led to a decrease in the catalytic efficiency. Nonetheless, the kinetic data shows that not only is the deamination reaction possible in the presence of high concentrations of ammonia but the value of k_{cat} is also largely unaffected.

3.4 Thermodynamic Position of Equilibrium

To determine whether the AvPAL catalyzed reaction is under thermodynamic control and to establish the position of equilibrium, transformations were performed starting from each of the three components (*i.e.* **1m**, L-**2m**, D-**2m**). The three reactions were performed under the same standard amination reactions conditions (5 mM substrate in 5M NH₄OH, pH 9.5, 30 °C) and after incubation with AvPAL for 48 hours the mixture of components was analyzed by chiral HPLC. Within experimental error the same composition (4-nitrocinnamic acid **1m** 14%, 4-nitrophenylalanine **2m** 86%, e.e = 9% D-enantiomer) was obtained starting from each of the three compounds (Figure 28), demonstrating that the equilibrium position of the reactions had been reached.

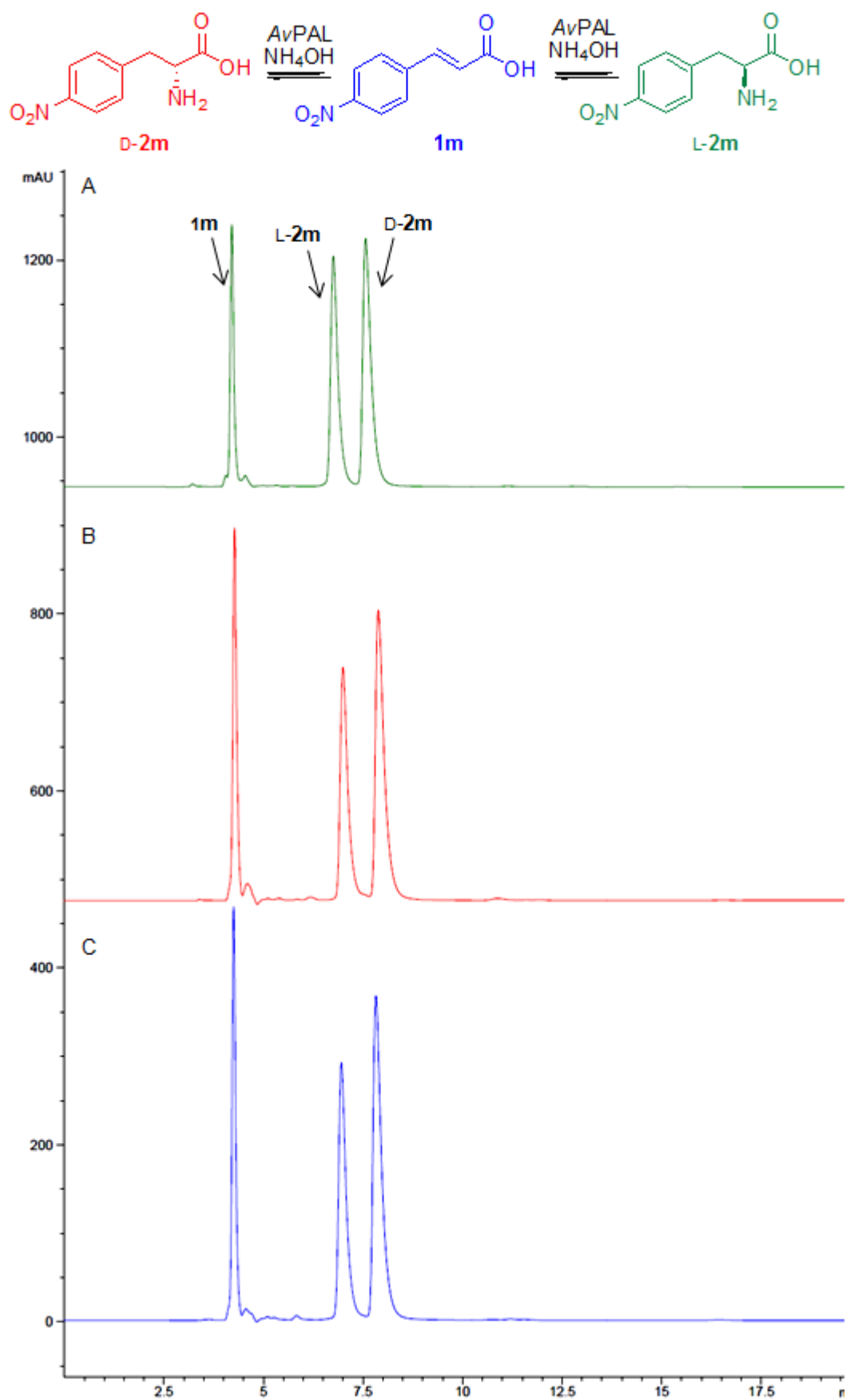
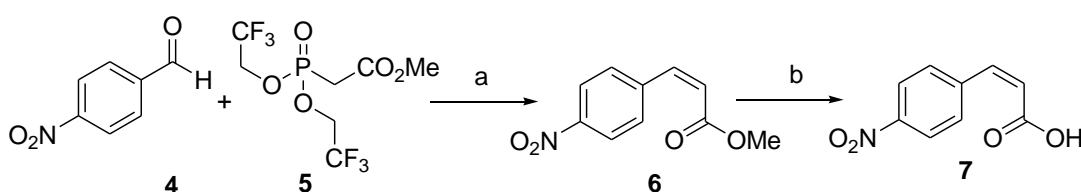


Figure 28: HPLC traces for AvPAL catalyzed reactions starting from a) 4-nitro-L-phenylalanine L-2m b) 4-nitro-D-phenylalanine, D-2m and c) 4-nitrocinamic acid, 1m after 48 hours

3.5 Investigating the Activity of 4-Nitro-*cis*-Cinnamic Acid

A proposed mechanism for the formation of D-amino acids involves the amination of 4-nitro-*cis*-cinnamic acid, following an isomerization of the *trans*-cinnamic acid starting material. (Isomerization could occur from the amination of 4-nitro-*trans*-cinnamic acid, followed by a rotation of the L-amino acid product and deamination to yield the *cis*-cinnamic acid derivative). To rule out the possibility that D-amino acids are derived from the *cis*-isomer, 4-nitro-*cis*-cinnamic acid **7** was synthesized and screened as a PAL substrate.

Compound **7** was synthesized in two steps from 4-nitrobenzaldehyde **4** following a Still-Gennari modified Horner-Wadsworth-Emmons coupling reaction[113] and subsequent hydrolysis.



Scheme 28: Synthesis of 4-nitro-*cis*-cinnamic acid **7** a) 18-crown-6, KHMDS, -78 °C, 4h, 84% b) LiOH, r.t, 18 h, 98 %

The amination of **7** (5 mM in 5M NH₄OH, pH 9.5) using whole cell *E. coli* BL21(DE3) expressing AvPAL was carried out at 30 °C for 48 hours. Chiral HPLC showed no conversion of the *cis*-isomer **7** to 4-nitrophenylalanine. This suggests that the mechanism leading to the formation of D-amino acids does not occur via a 4-nitro-*cis*-cinnamic acid intermediate.

3.6 Site-Directed Mutagenesis of Key Active Site Residues

To investigate the role of the MIO-cofactor and catalytic base (Tyr78) in the synthesis of D-amino acids, key catalytic residues were mutated. The essential Tyr78 residue is located on the active-site loop and is reported to be responsible for abstraction of the substrate's C-3 benzylic proton.[65] In order to assess the role of this residue in D-amino acid formation, a Y78F variant was generated. To examine the role of the MIO cofactor in D-amino acid synthesis a S168A mutation was made, so that the prosthetic group can no longer form by post-translational modification. Each of these mutations together with a Y78F/S168A double mutation were made using QuikChange site directed mutagenesis (Stratagene). The correct mutant sequences were verified, the variants were overexpressed in *E. coli* BL21(DE3) and proteins were purified according to the standard procedures (Figure 29).

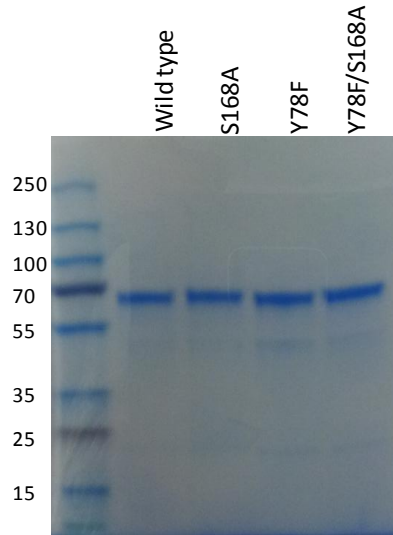


Figure 29: SDS-PAGE of wild-type *AvPAL* and variants purified by nickel affinity column chromatography lane 1: molecular weight markers, lane 2-4: purified proteins

Circular dichroism (CD) spectroscopy was used to ensure that the mutations had not affected the protein structure. CD measures the differences in the absorption of left and right handed polarized light which arises due to the enzymes secondary structure. The trough observed in the spectra between 200-240 nm (Figure 30) is characteristic of a protein with a predominantly α -helical structure. The spectrum for each variant is the same as that of the wild-type enzyme showing that each protein is correctly folded. This confirms that the mutations have not affected the overall protein structure which may have led to protein inactivation.

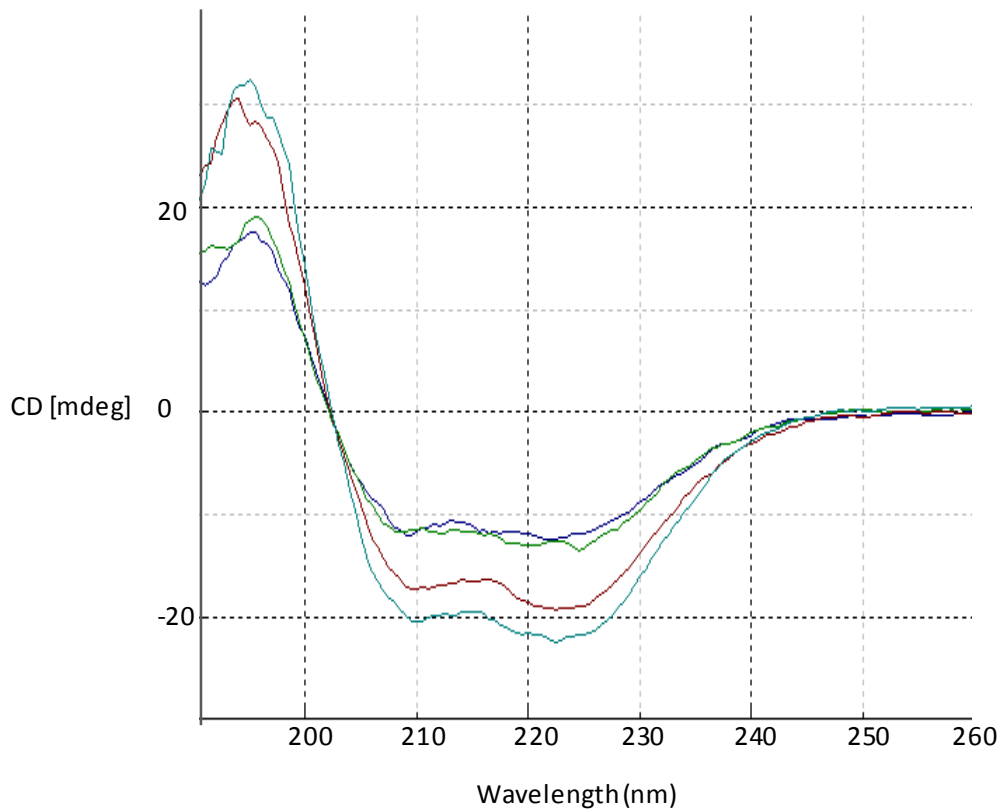


Figure 30: CD spectra of wild-type AvPAL (dark blue), Y78F (green), S168A (red) and Y78F/S168A (light blue), protein concentration 1 mg/ml

The absence of the MIO-cofactor in S168A AvPAL was confirmed by measuring the UV difference spectra between the wild-type enzyme and variant at two different protein concentrations (0.8 and 0.4 mg/mL). A discrete maxima at ca. 310 nm was observed which corresponds to the presence of MIO in the wild-type enzyme but not the S168A variant.[78]

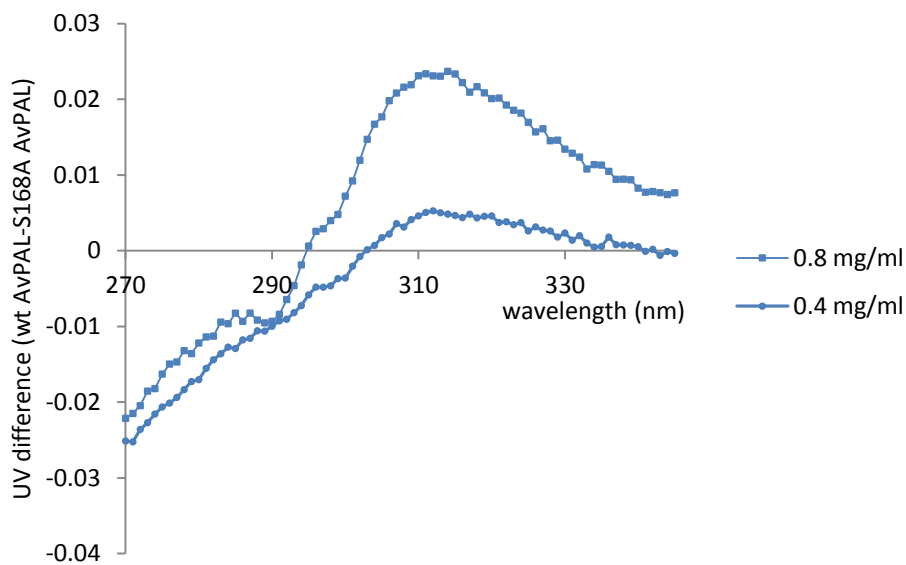


Figure 31: UV difference spectra between wild-type and S168A AvPAL

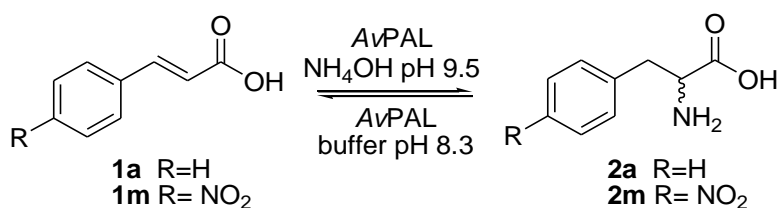
Y78F and Y78F/S168A variants were screened for activity towards the amination of cinnamic acid (**1a**) and 4-nitrocinnamic acid (**1m**) as well as the deamination of both enantiomers of phenylalanine (**2a**) and 4-nitrophenylalanine (**2m**). Reactions using whole cell biocatalysts expressing the variants were analyzed by chiral HPLC whilst reactions with purified enzymes were analyzed spectrophotometrically (see 2.2.2: *Spectrophotometric analysis*). Neither Y78F nor Y78F/S168A variants showed activity towards the amination of **1a** and **1m** or towards the deamination of **2a** and **2m**. The equivalent mutation in *PcPAL* (Y110F) was previously shown to significantly reduce the deamination activity towards L-phenylalanine (L-**2a**).^[104] In agreement, our results confirm that Tyr78 plays a crucial role in the *AvPAL* catalyzed deamination of L-**2a** and significantly, also shows that it is an essential catalytic residue for activity towards production and deamination of D-amino acids. Furthermore this result demonstrates that D-amino acid catalysis occurs at the active site rather than an alternative binding site.

The MIO-deficient variant S168A displayed no activity towards the substrates cinnamic acid (**1a**) and phenylalanine (**2a**). However S168A maintained activity towards the corresponding nitro-substituted analogues **1m** and **2m**. S168A catalyzed transformations starting from each of the three components (*i.e.* **1m**, L-**2m**, D-**2m**) under the same standard amination reactions conditions were carried out in an attempt to determine the thermodynamic equilibrium position. However, the reaction rates were low and transformations failed to reach the equilibrium position despite the use of high concentrations of whole cell biocatalyst (100 mg/mL).

3.6.1 Kinetic Constants for S168A Catalyzed Reactions

The kinetic parameters for S168A and the wild-type enzyme were determined spectrophotometrically according to the standard procedures. The S168A mutation resulted in complete loss of activity towards the amination of cinnamic acid (**1a**) and deamination of L-phenylalanine (L-**2a**) (Table 12). However, S168A retained low level activity towards the amination of 4-nitrocinnamic acid (**1m**) and towards the deamination of 4-nitro-L-phenylalanine (L-**2m**); although a significant reduction (293 and 31 fold respectively) in k_{cat} values were observed. This result is in agreement with a previous study using the homologous S202A *PcPAL* variant.^[101] Interestingly, the k_{cat} for 4-nitro-D-phenylalanine (D-**2m**) deamination catalyzed by S168A *AvPAL* was not significantly affected by the absence of the cofactor. These results demonstrate that the dominant pathway for the formation or consumption of L-amino acids is dependent on MIO, whereas the analogous reactions involving the D-enantiomer occur predominantly via an MIO-cofactor independent pathway. The values of k_{cat} for the deamination of both enantiomers of **2m** catalyzed by S168A are similar, which suggests that the cofactor-independent pathway leading to the formation of D-amino acids proceeds in a non-selective manner.

Table 12: Kinetic constants for wild-type and S168A AvPAL catalyzed amination and deamination reactions



	wt AvPAL			S168A AvPAL		
	k_{cat} (s^{-1})	K_M (mM)	R^2	k_{cat} (s^{-1})	K_M (mM)	R^2
amination^a						
cinnamic acid 1a	0.029	0.039	0.99	n.d.	n.d.	n.d.
4-nitrocinnamic acid 1m	4.106	0.720	0.97	0.014	0.062	0.90
deamination^b						
L-phenylalanine L- 2a	0.491	0.298	0.99	n.d.	n.d.	n.d.
D-phenylalanine D- 2a	n.d. ^c	n.d.	n.d.	n.d.	n.d.	n.d.
4-nitro-L-phenylalanine L- 2m	1.38	0.478	0.93	0.045	0.137	0.90
4-nitro-D-phenylalanine D- 2m	0.090	0.089	0.99	0.025	0.329	0.86

[a] amination reactions in 5 M NH_4OH , pH 9.5, 30 °C [b] deamination reactions in 0.1 M borate buffer, pH 8.3, 30 °C [c] n.d. = the kinetic constants could not be measured. The R^2 values are calculated from the linear regression analysis from the Hanes-Woolf plot

3.6.2 $NaBH_4$ Reduced AvPAL

An alternative method reported to inactivate the MIO cofactor involves reduction of the exocyclic alkene.[101] $NaBH_4$ was added to a solution of purified wild-type AvPAL and incubated overnight at 4 °C. Following buffer exchange using a PD10 desalting column, the eluted reduced protein was characterized using CD, which showed that the protein was correctly folded.

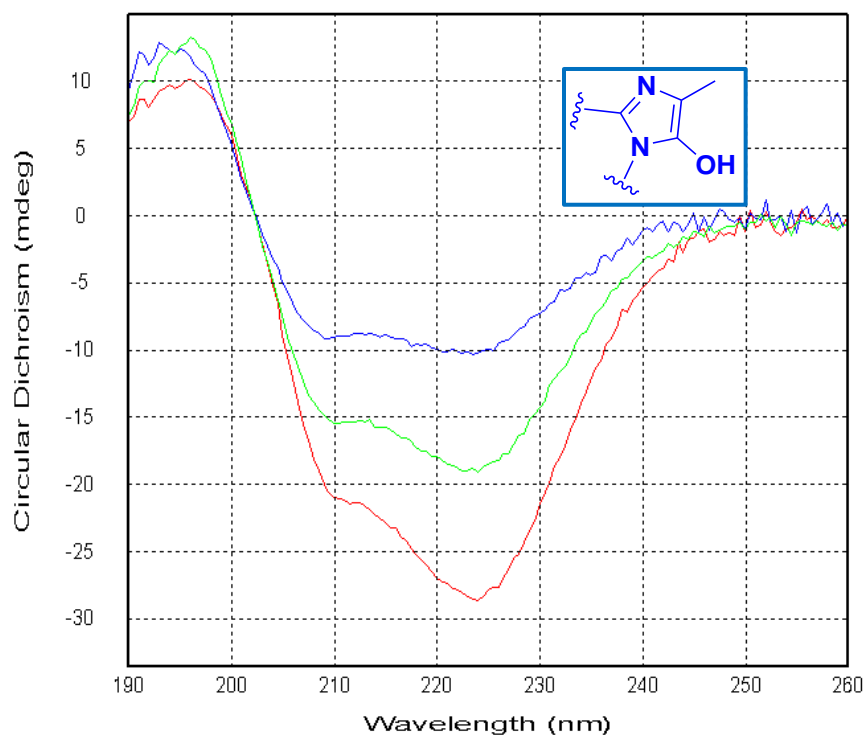
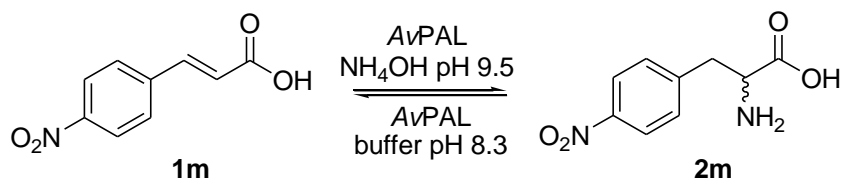


Figure 32: CD spectra of S168A (1.2 mg/ml, in red), wild-type (1.0 mg/ml, in green) and NaBH₄ reduced AvPAL (0.8 mg/ml in blue). The structure of the reduced cofactor is shown in blue.

The NaBH₄ reduced AvPAL showed comparable activity to the S168A variant and was inactive towards the natural substrates cinnamic acid and phenylalanine but retained low level activity towards the nitro-substituted compounds **1m**, L-**2m** and D-**2m**. The kinetic constants were determined and are shown in Table 13.

Table 13: Kinetic constants for NaBH₄ treated AvPAL and S168A catalyzed amination and deamination reactions



	red AvPAL			S168A		
	k_{cat} (s ⁻¹)	K_M (mM)	R^2	k_{cat} (s ⁻¹)	K_M (mM)	R^2
Amination:						
4-nitrocinnamic acid 1m	0.017	0.16	0.93	0.014	0.062	0.90
Deamination:						
4-nitro-L-phenylalanine L- 2m	0.010	0.91	0.80	0.045	0.137	0.90
4-nitro-D-phenylalanine D- 2m	0.013	1.37	0.77	0.025	0.329	0.86

The R^2 values are calculated from the linear regression analysis of the Hanes-Woolf plots.

The kinetic constants for the reduced AvPAL mediated amination of 4-nitrocinnamic acid show a similar trend to those determined for S168A. Both NaBH₄ reduced AvPAL and S168A have similar k_{cat} values for the deamination of both enantiomers of **2m**. This suggests that the MIO-independent pathway leading to the formation of D-amino acids is non-selective. The different methods of cofactor inactivation will have different effects on the active site environment which may explain the lower k_{cat} values and higher K_M values for reduced AvPAL catalyzed deamination reactions compared to S168A catalyzed reactions.

3.7 Isotope Labelling Studies to Determine the Stereoselectivity of AvPAL Catalyzed Amination and Deamination Reactions

It has been previously shown that PAL mediated deamination of L-phenylalanine proceeds in a stereoselective manner.[89] The essential catalytic base Tyr78 selectively abstracts the pro-(S) benzylic proton of the amine-bound MIO-intermediate (Figure 33). (The dominant binding interaction of the substrate within the active site is dominated by the formation of a salt-bridge with Arg317 and the substrate's aromatic ring lies in a large hydrophobic binding pocket).

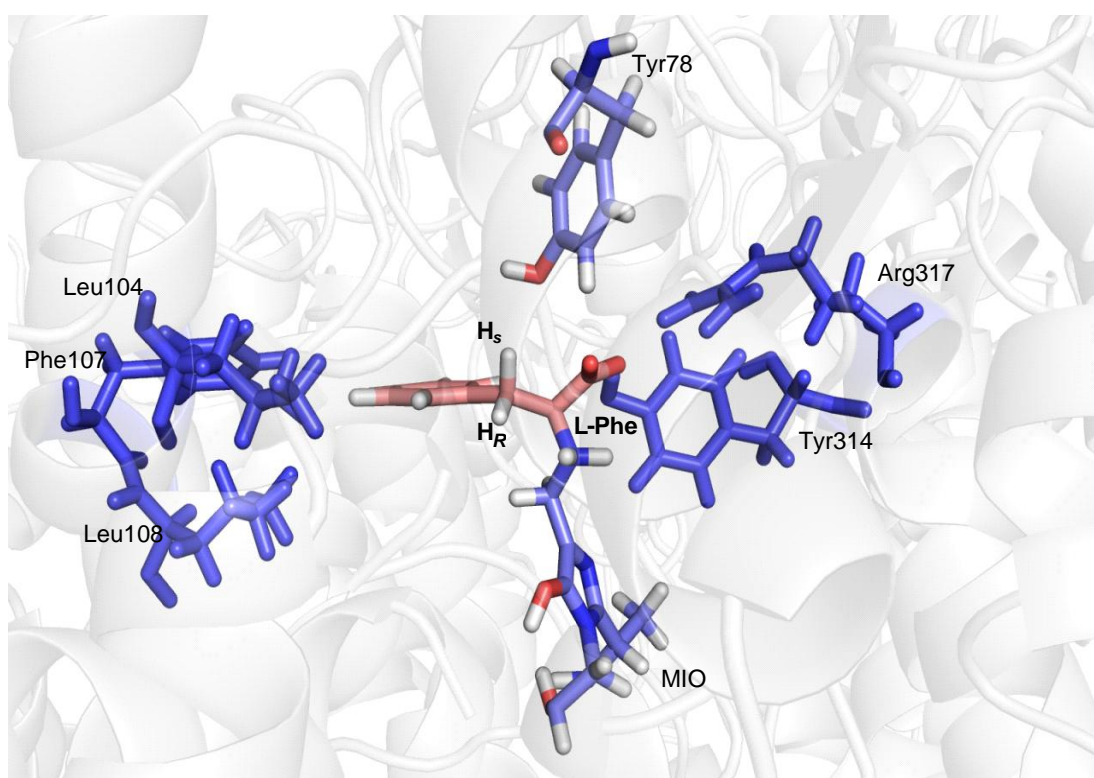
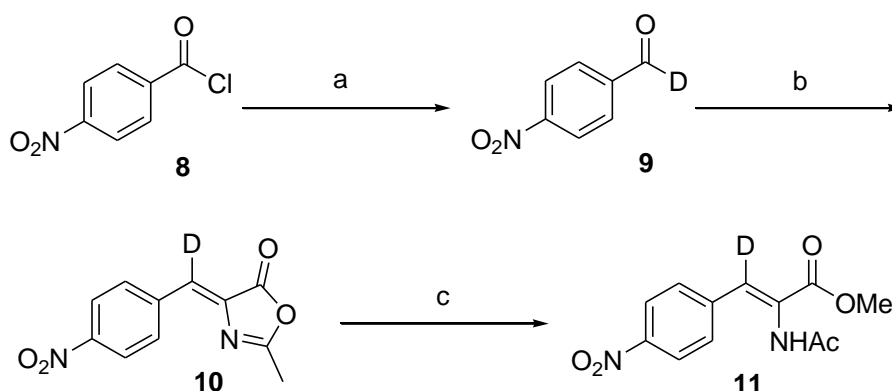


Figure 33: L-Phenylalanine docked into the AvPAL active site and covalently bound via the substrate amine to the MIO cofactor. Docking was performed by Jason Schmidberger using the AvPAL X-ray crystal structure (PDB code 3CZO) and the figure was generated using Pymol

In order to investigate the stereoselectivity of D-amino acid (synthesis/deamination) reactions, samples of 4-nitro-D-phenylalanine and 4-nitrocinnamic acid stereospecifically deuterated at the benzylic position were chemically synthesized. The labelled compounds were used as substrates in AvPAL catalyzed biotransformations which were monitored by ¹H NMR.

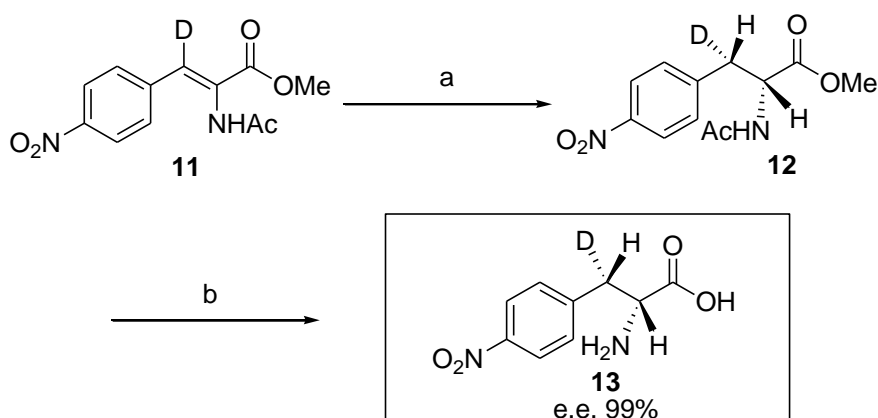
3.7.1 Synthesis of Deuterated Standards

^2H -Labelled enamide **11** was synthesized in three steps from 4-nitrobenzyl chloride **8** (Scheme 29) and was used for the synthesis of both deuterated 4-nitro-D-phenylalanine diastereoisomers D-**13** and D-**16**. Reduction of acid chloride **8** with lithium aluminium deuteride gave deuterated 4-nitrobenzaldehyde **9** which was subsequently converted to **10** via an Erlenmeyer-Plöchl azalactone synthesis.[114] The azalactone **10** was ring-opened with NaOMe/MeOH to generate ^2H -enamide **11** with 80 % deuterium incorporation (determined by ^1H NMR). Loss of deuterium incorporation occurs in the azalactone synthesis and has been demonstrated previously in the analogous reaction with benzaldehyde.[115]



Scheme 29: Synthesis of deuterium labelled enamide **11** a) LiAlD_4 , $-78\text{ }^\circ\text{C}$, 30 min b) N-acetylglycine, NaOAc, Ac_2O , $100\text{ }^\circ\text{C}$, 18 h, 52 % c) MeOH, NaOMe, r.t., 15 min, 46 %

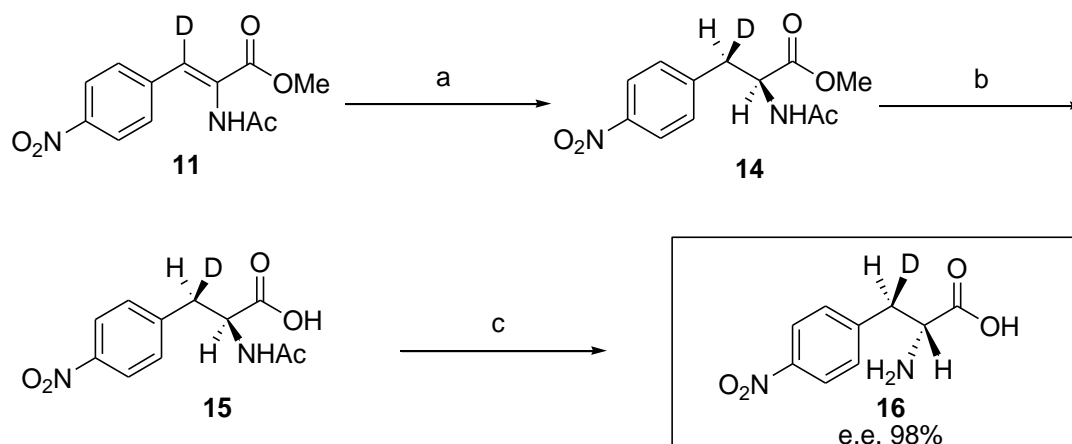
Enamide **11** was stereoselectively reduced using a chiral rhodium catalyst, $[\text{Rh}(\text{R,R})\text{-Et-DuPhos}(\text{COD})]\text{BF}_4$ [116] to give the amide (2*R*,3*S*)-**12** which was deprotected by refluxing in 4 N HCl (Scheme 30). The product 4-nitro-(3*S*- ^2H)-D-phenylalanine **13** (80 % ^2H -incorporation) was achieved with high enantiopurity (e.e. 99 %) determined by chiral HPLC.



Scheme 30: Synthesis of 4-nitro-(3*S*- ^2H)-D-phenylalanine **13** a) $[\text{Rh}(\text{R,R})\text{-EtDuPhos}(\text{COD})]\text{BF}_4$, H_2 , 100 psi, 90 min, 99 % b) 4 N HCl, reflux, 7h, 67 %

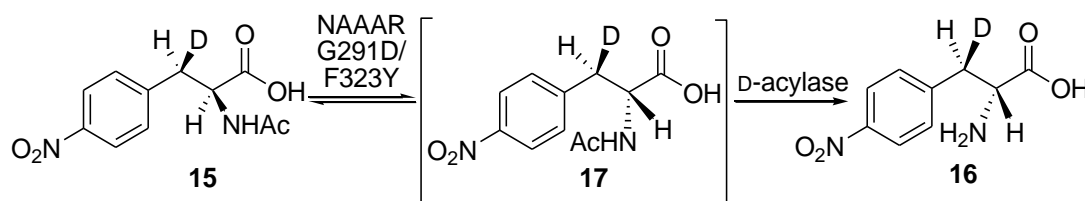
In order to access the second diastereoisomer D-**16**, stereoselective reduction of ^2H -enamide **11** with $[\text{Rh}(\text{S,S})\text{-Et-DuPhos}(\text{COD})]\text{BF}_4$ was followed by lithium hydroxide hydrolysis of the methyl ester product **14** to yield *N*-acetyl-4-nitro-L-phenylalanine **15** (Scheme 31). Inversion of

the C2-stereocentre to the required (*R*)-configuration, was achieved by combining a variant of *N*-acetyl amino acid racemase (NAAAR G291D/F323Y)[117] with a commercially available *D*-acylase in a one-pot reaction.



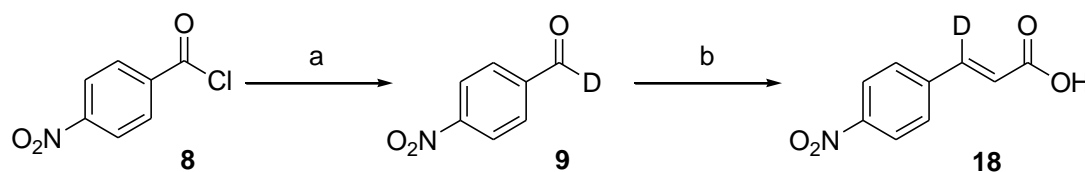
Scheme 31: Synthesis of 4-nitro-(3*R*-²H)-D-phenylalanine 16 a) Rh(*S,S*)-EtDuPhos, H₂, 100 psi, 90 min, 99 % b) LiOH, r.t, 2 h, 99 % c) NAAAR G291D/F323Y, *D*-acylase, CoCl₂ pH 8.0, 37 °C, 23 h, 78%

The NAAAR variant (G291D/F323Y) from the actinobacterium *Amycolatopsis sp.* Ts-1-60 (EC 5.1.1.10) was developed by Campopiano and co-workers using directed evolution and shows increased activity towards a range of *N*-acetylated amino acids.[117] NAAAR (G291D/F323Y) catalyzed racemization of *N*-acetyl-4-nitro-(3*R*-²H)-L-phenylalanine **15** was coupled with a *D*-acylase (EC 3.5.1.14) catalyzed kinetic resolution to yield the deuterium labelled product 4-nitro-(3*R*-²H)-D-phenylalanine **16** (e.e. 98 %, 80 % deuterium incorporation) (Scheme 32).



Scheme 32: Stereoinversion and kinetic resolution to yield enantiopure α -amino acids

The substrate, 4-nitro-(3-²H)-cinnamic acid **18** was synthesized from 4-nitro-(²H)-benzaldehyde **9** via a Knoevenagel condensation (Doebner modification) with malonic acid (<99% deuterium incorporation) (Scheme 33).[118]



Scheme 33: Synthesis of deuterated 4-nitrocinnamic acid 18 a) LiAlD₄, -78 °C, 30 min b) malonic acid, piperidine, pyridine, 80 °C, 18 h, 79 %

3.7.2 NMR Study of the Amination Reaction of Labelled Substrates

To investigate the stereoselectivity of D-amino acid synthesis, the amination of deuterated 4-nitrocinnamic acid **18** (12 mM) was carried out in the presence of whole cell *E. coli* BL21(DE3) expressing AvPAL (20 mg/mL) in NH₄OH (100 mL, 5M, pH 9.5) at 30 °C for 18 hours. Chiral HPLC showed the reaction had reached 83 % conversion to the corresponding 4-nitrophenylalanine (e.e. = 6 % in favour of the L-enantiomer). The whole cell biocatalyst was removed by centrifugation, the supernatant was lyophilized and the mixture of enantiomers was isolated using ion-exchange chromatography with acidic Dowex resin (50 x 8, 50-100 mesh). The mixture of enantiomers was shown to be a single diastereoisomer as evidenced by presence of a doublet at 2.94 ppm and the absence of a doublet at 2.85 ppm in the ¹H NMR spectrum (Figure 34). Comparison with the chemo-enzymatically synthesized standards D-**13** and D-**16** show the products from the biotransformation are consistent with *anti*-addition of ammonia across the cinnamic acid double bond.

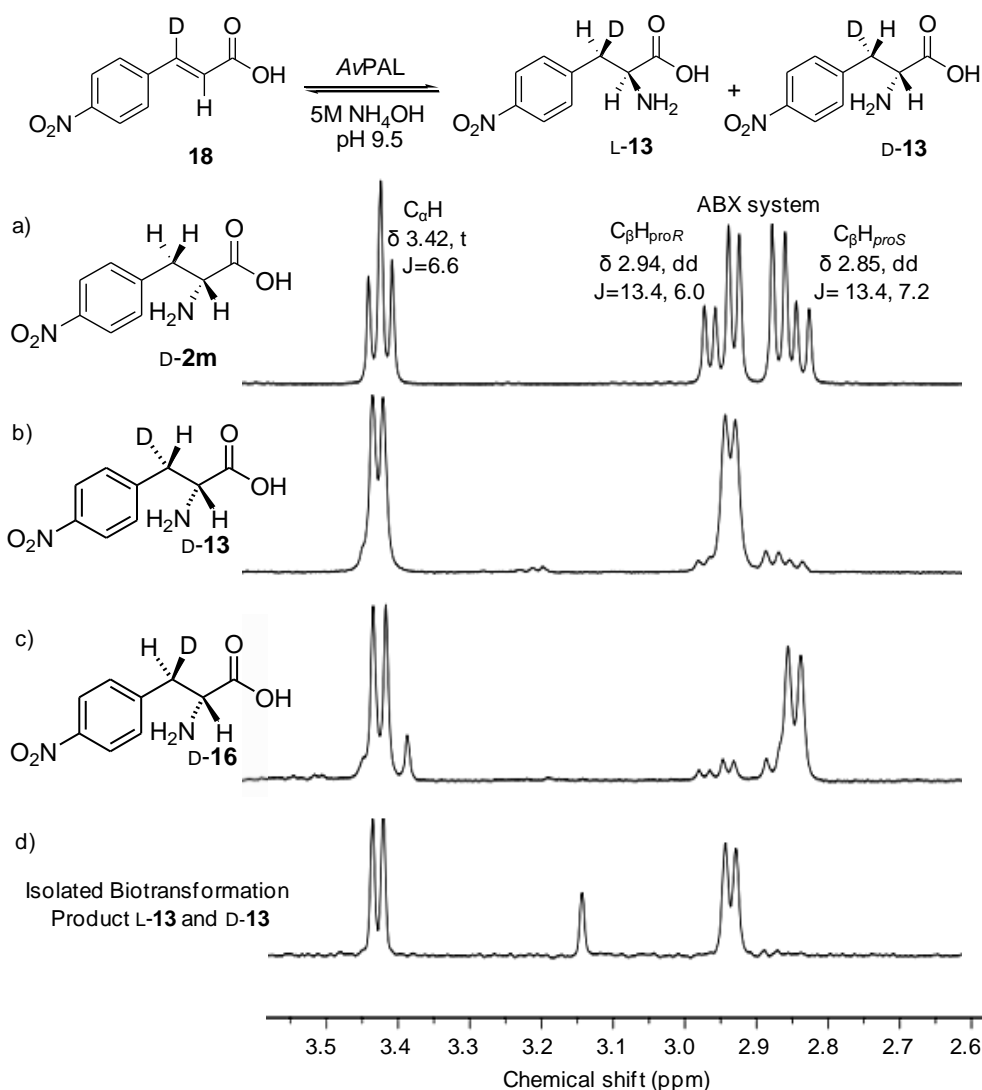
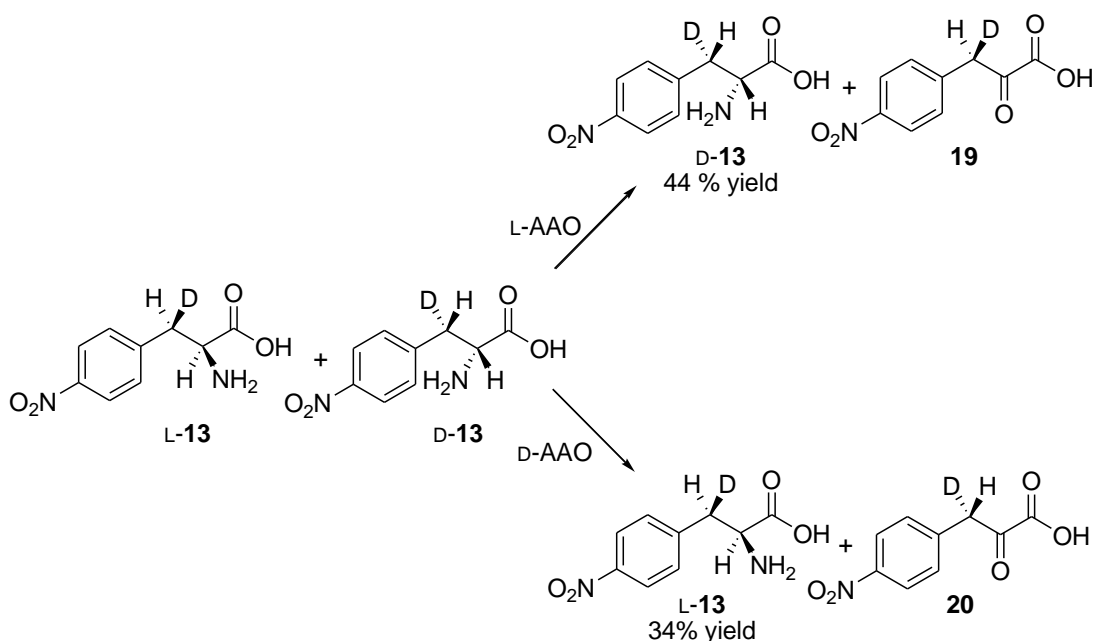


Figure 34: ^1H NMRs (400 MHz) of the AvPAL catalyzed hydroamination of 4-nitro-(3- ^2H)-cinnamic acid **18** and amino acid standards (a) unlabeled 4-nitro-D-phenylalanine (D-**2m**), showing a classical ABX spin system (b and c) deuterated 4-nitro-D-phenylalanine standards **13** and **16** and (d) the isolated product from the AvPAL catalyzed amination of **18**

The single enantiomers (e.e. >99 %) of the deuterated biotransformation products (L-**13** and D-**13**) were isolated individually by kinetic resolution using commercially available L-amino acid oxidase from *Crotalus adamanteus* (purified enzyme) or D-amino acid oxidase from porcine kidney (lyophilized purified enzyme) (Scheme 34). The mixture of enantiomers (5 mM in phosphate buffer 0.1 M, pH 8.0) were incubated with the amino acid oxidases at 30 °C overnight and reached full conversion as shown by chiral HPLC. The amino acid oxidase biotransformations were lyophilized and the remaining solids were washed with acetone to remove the keto-acid products (**19** and **20**). The amino acids were redissolved in 1 N HCl, filtered to remove any protein and the final solution was lyophilized to yield enantiopure hydrochloride salts of 4-nitro-(3S- ^2H)-D-phenylalanine (D-**13**) and 4-nitro-(3R- ^2H)-L-phenylalanine (L-**13**) as confirmed by comparison with the synthesized standards D-**13** and D-**16**. This confirms AvPAL catalyzed synthesis of D-amino acids proceeds via stereospecific *anti*-addition of ammonia across the substrate double bond.



Scheme 34: Amino acid oxidase catalyzed kinetic resolution of deuterated 4-nitrophenylalanine **13** (pH 8.0, 30 °C, 18 h).

3.7.3 NMR Study of the Deamination Reaction of Labelled Substrates

The stereoselectivity of AvPAL deamination reactions were also investigated using the isotopically labelled D-amino acid substrates **D-13** and **D-16** (10 mM). Deamination reactions were catalyzed by whole cell *E. coli* BL21(DE3) expressing AvPAL under standard conditions (0.1 M borate buffer pH 8.3). After incubation at 30 °C for 48 hours, chiral HPLC showed 89 % conversion to the corresponding 4-nitrocinnamic acid product for each reaction. The whole cell biocatalysts were removed by centrifugation, the supernatant was acidified to pH 1.0 with 1 N HCl and the precipitate was collected by filtration. Analysis by ^1H NMR showed the substrate **D-16** yielded a single fully protiated product **1m** consistent with the exclusive *anti*-elimination of the (3*R*)-deuterium, however substrate **D-13** gave a mixture of products **1m** and **18** (Figure 35).

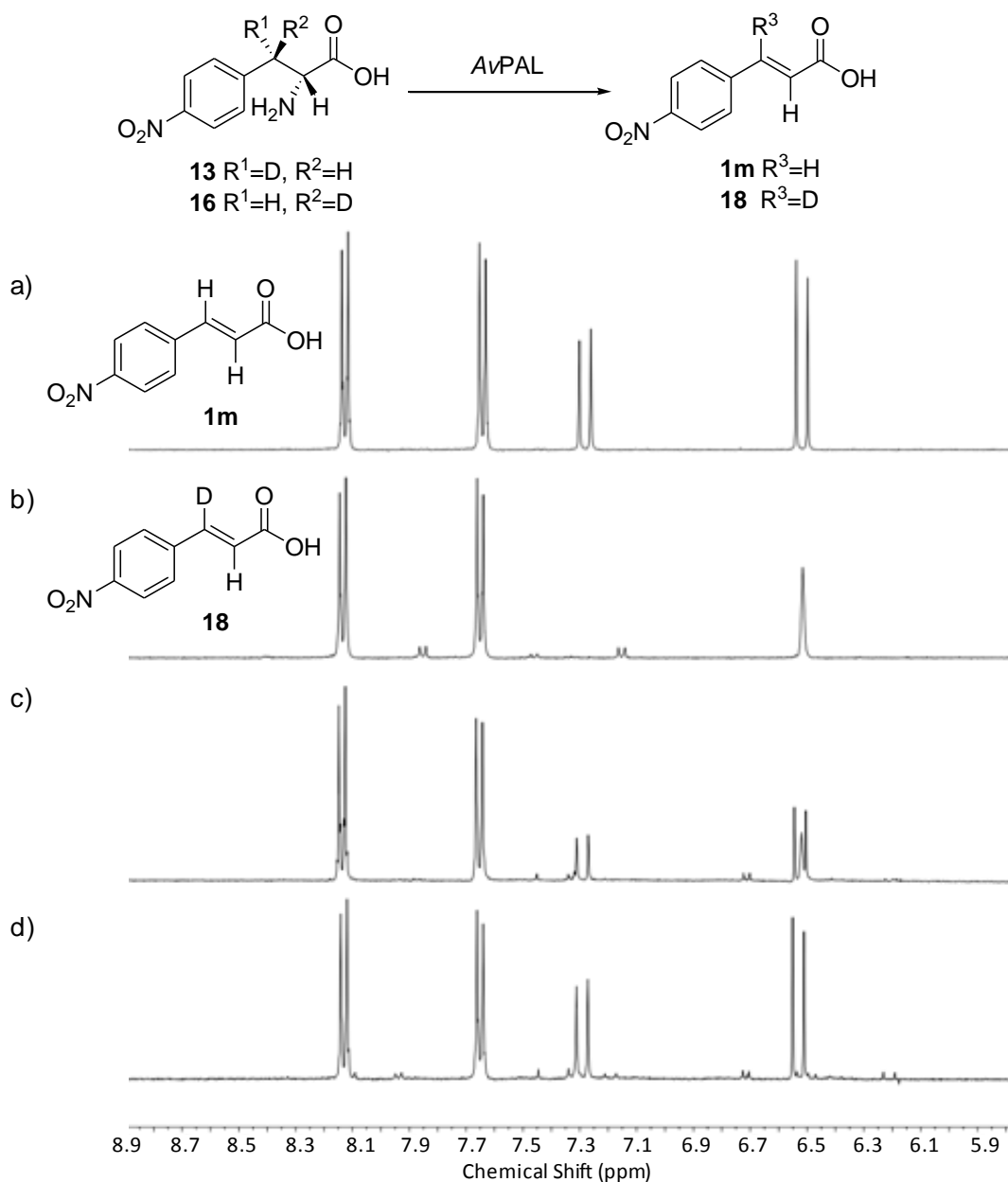


Figure 35: ^1H NMR spectra of the AvPAL catalyzed deamination of isotopically labelled 4-nitro-D-phenylalanines **13** and **16** a) commercially available fully protiated 4-nitro-*trans*-cinnamic acid **1m** b) *trans*-3- $[\text{H}^2]$ -3(4-nitrophenyl)acrylic acid **18** c) Mixture of products from the AvPAL catalyzed deamination of 4-nitro-D-phenylalanine **13** d) product from the AvPAL catalyzed deamination of 4-nitro-D-phenylalanine **16**.

The deamination reaction with substrate D-**13** was repeated and the ratio of products produced was variable (49 % and 71 % loss of deuterium incorporation from two repeats). The loss of deuterium incorporation appears to be influenced by subtle changes in reaction conditions. This result was somewhat unexpected considering the (reversible) amination of 4-nitro-(3- ^2H)-cinnamic acid **18** (5M NH_4OH , pH 9.5) was completely stereoselective to produce isomer **13**. PAL catalyzed deamination reactions are generally carried out at pH 8.3 whereas reactions in the amine synthesis direction are conducted at pH 9.5 which leads to a more favourable equilibrium position. To investigate whether the stereoselectivity of deamination is

influenced by changes in pH, reactions were repeated at pH 9.5 and were shown to result in the formation of a single product due to *anti*- elimination of the (3*R*)-proton. Similarly, previous isotopic studies following the stereochemistry of the mechanism of CcTAM and TcPAM also report a loss in the product deuterium incorporation and suggest that proton exchange with bulk solvent is pH dependent.[119,120] The PAL catalyzed deamination of D-**13** and D-**16** were carried out at pH 8.3 in D₂O. Partial loss of the (3*R*)-proton of D-**16** was expected to occur based on the analogous deamination of D-**13** in H₂O. Surprisingly in this case, only products arising from elimination of the (3*R*)-proton/deuterium of D-**13** and D-**16** respectively were observed (Table 14).

Table 14: AvPAL catalyzed deamination of deuterated 4-nitro-D-phenylalanine substrates **13 and **16** under different reaction conditions**

D-**13** R¹=D, R²=H
D-**16** R¹=H, R²=D

1m R³=H
18 R³=D

Substrate	Reaction conditions	Product
D- 13	0.1 M borate buffer pH 8.3	Mixture of 1m and 18
	0.1 M borate buffer pH 9.5	18
	D ₂ O pH 8.3	18
D- 16	0.1 M borate buffer pH 8.3	1m
	0.1 M borate buffer pH 9.5	1m
	D ₂ O pH 8.3	1m

Deamination of substrates D-**13** and D-**16** catalyzed by the S168A variant (lacking the MIO cofactor) showed a similar trend to wild-type AvPAL. At both pH 8.3 and pH 9.5 substrate D-**16** yielded fully protiated product **1m** exclusively, whereas deamination of substrate D-**13** gave a mixture of products **1m** and **18**. The loss of deuterium incorporation was significantly higher at pH 8.3 than at pH 9.5 (63% and 30% loss respectively).

These results suggest that the deamination of D-amino acids proceed via a stepwise E₁cB mechanism, with initial stereoselective deprotonation (pro-*R* proton) at the benzylic position catalyzed by Tyr78, followed by elimination of ammonia (Figure 36). We propose that the MIO-independent elimination step is slow (relative to the MIO-dependent pathway), and reprotonation of the carbanion intermediate from either bulk solvent or active-site residues can occur. At pH 8.3 non-stereoselective reprotonation competes with amine elimination resulting

in partial loss of the deuterium in the final product. The rate of reprotonation is pH dependent and is slower at pH 9.5 than at pH 8.3.

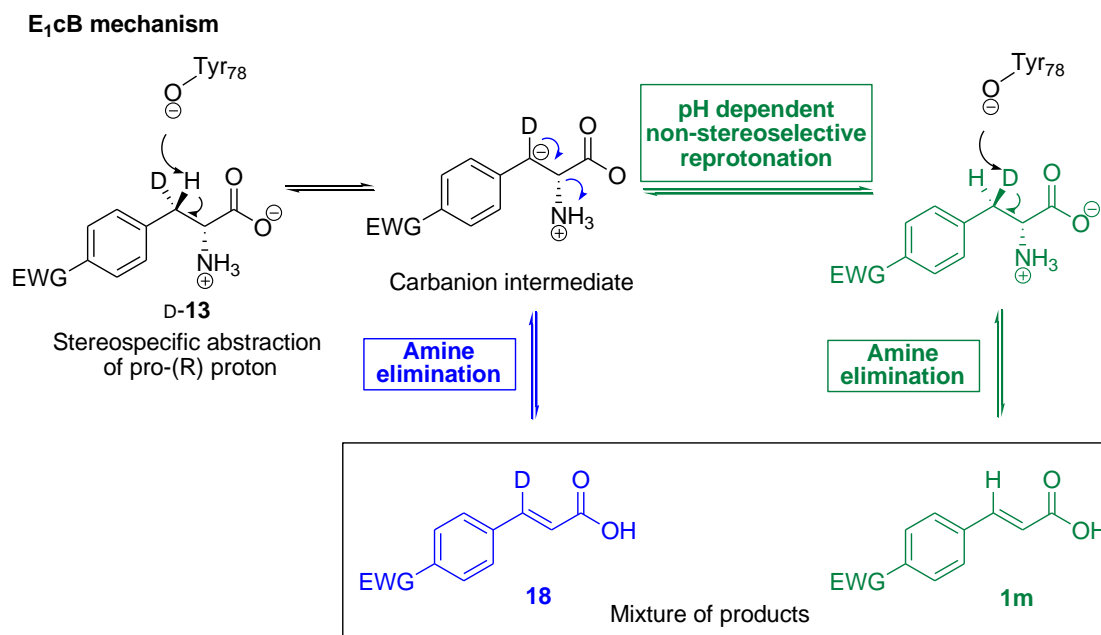


Figure 36: Proposed mechanism for the loss of deuterium incorporation in the AvPAL catalyzed deamination of 4-nitro-D-phenylalanine D-13

The carbanion intermediate formed during the reaction will be stabilized by the presence of electron withdrawing substituents on the substrates aromatic ring. However, it is possible that the reaction may not proceed via a carbanion intermediate and instead the mechanism may lie between a classical E₁cB and E₂ elimination.

3.8 Docking Study

Docking L- and D-phenylalanine into the AvPAL active-site showed that the main difference between the two bound enantiomers is the position of C_β, which allows only the pro-S benzylic proton of L-phenylalanine or pro-R proton of D-phenylalanine to interact with the catalytic Tyr78 residue (

Figure 37). The computational modelling supports the results of the isotopic labelling study, which shows that the Tyr78 catalyzed deprotonation of D-amino acids is stereoselective favouring abstraction of the pro-R proton. The dominant binding interactions between the substrate carboxylic acid group and Arg317 were maintained for both enantiomers. Similarly the aromatic moieties of each enantiomer lie in virtually the same orientation and sit in the hydrophobic binding pocket. However, the docking study does not conclusively show why the reaction of D-amino acids is independent of the MIO cofactor as it appears that the amine is in sufficiently close proximity to the methylene group of the cofactor for the formation of a covalent intermediate. Detailed molecular modelling and molecular dynamics studies are required to further investigate the origins of this observation.

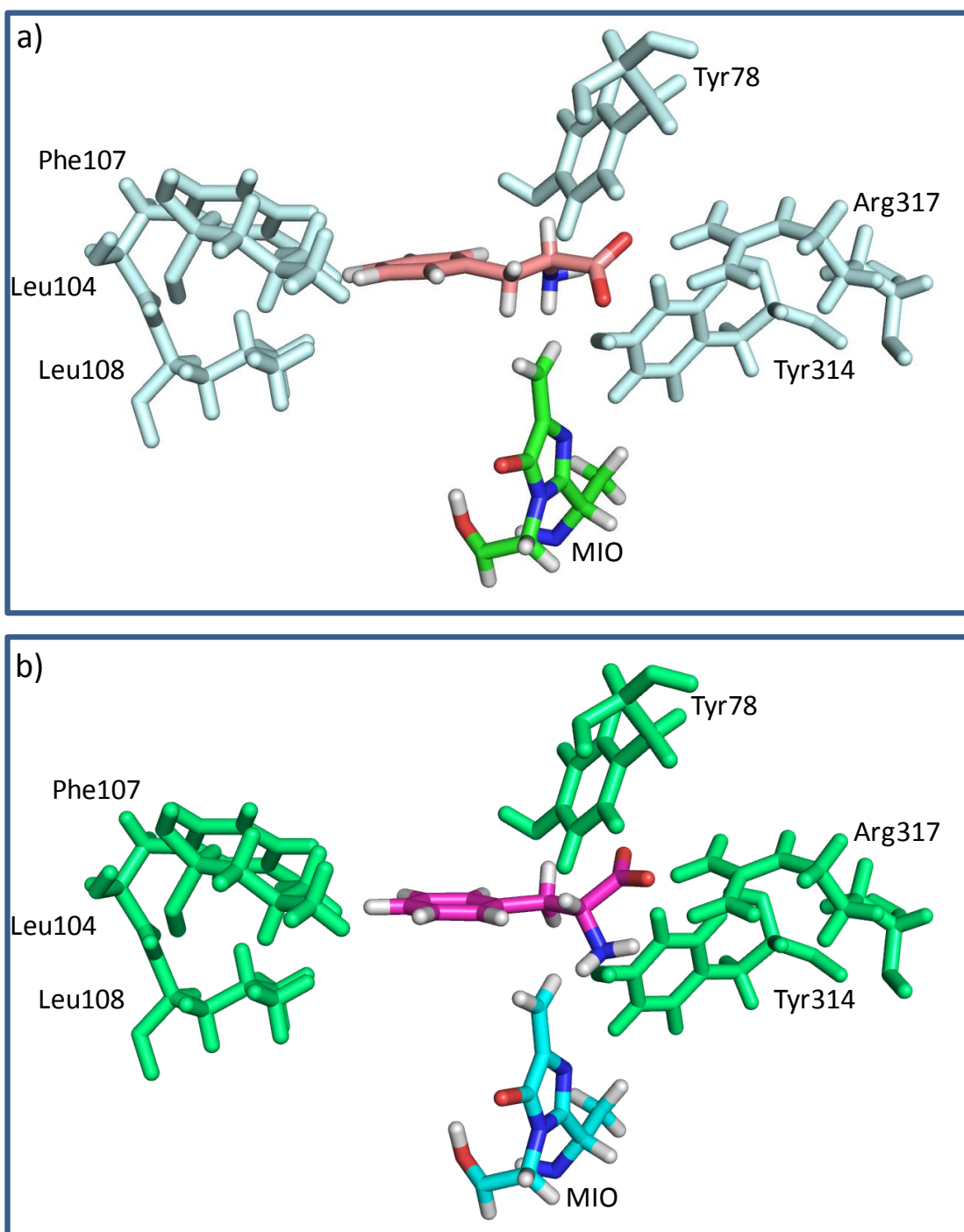
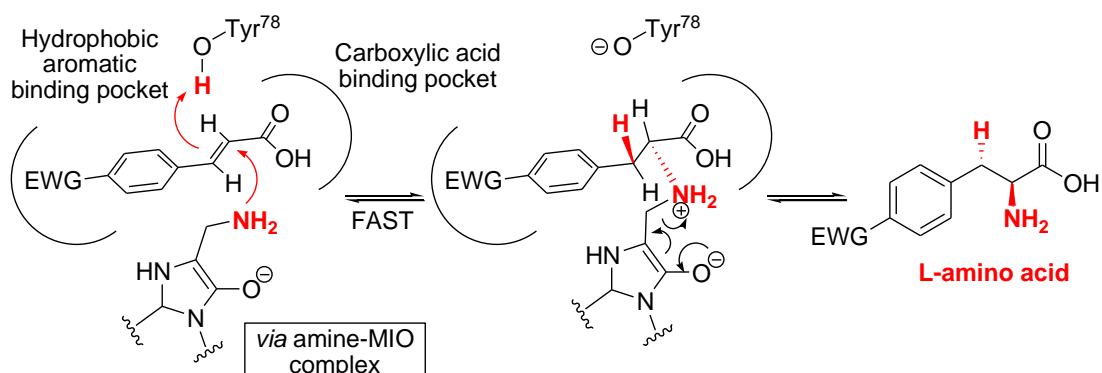


Figure 37: Modelling of a) L-phenylalanine and b) D-phenylalanine in the AvPAL active site pdb CZO3.

3.9 Conclusions

Combined, the kinetic data obtained with wild-type AvPAL and selected variants together with isotopic labelling studies and molecular modelling have provided significant mechanistic insights into a newly discovered MIO-independent pathway (Figure 38). This competing pathway proceeds in a non-selective manner, leading to the formation of both L- and D-amino acids. Hydroamination has been shown to occur via *anti*-addition of the amine and the benzylic proton for the synthesis of both the L- and D-enantiomers. The key catalytic base (Tyr78) in the well established MIO-dependent pathway remains an essential catalytic residue in the cofactor-independent pathway, demonstrating that this 'enzyme assisted' reaction occurs within the PAL active site. The deamination of D-amino acids proceeds via an elimination mechanism with deprotonation at the benzylic position catalyzed by Tyr78. We propose that electron deficient substrates increase the stability of this intermediate carbanion with respect to reprotonation, allowing a slow MIO-independent amine elimination step to occur. Our observations further suggest that cinnamic acid derivatives adopt two possible binding modes in the PAL active site (Figure 38). Although two binding modes of cinnamic acid have been reported to occur in the closely related mutases, a second binding conformation has not been described for lyases.[112,119]

MIO-dependent pathway



MIO-independent pathway

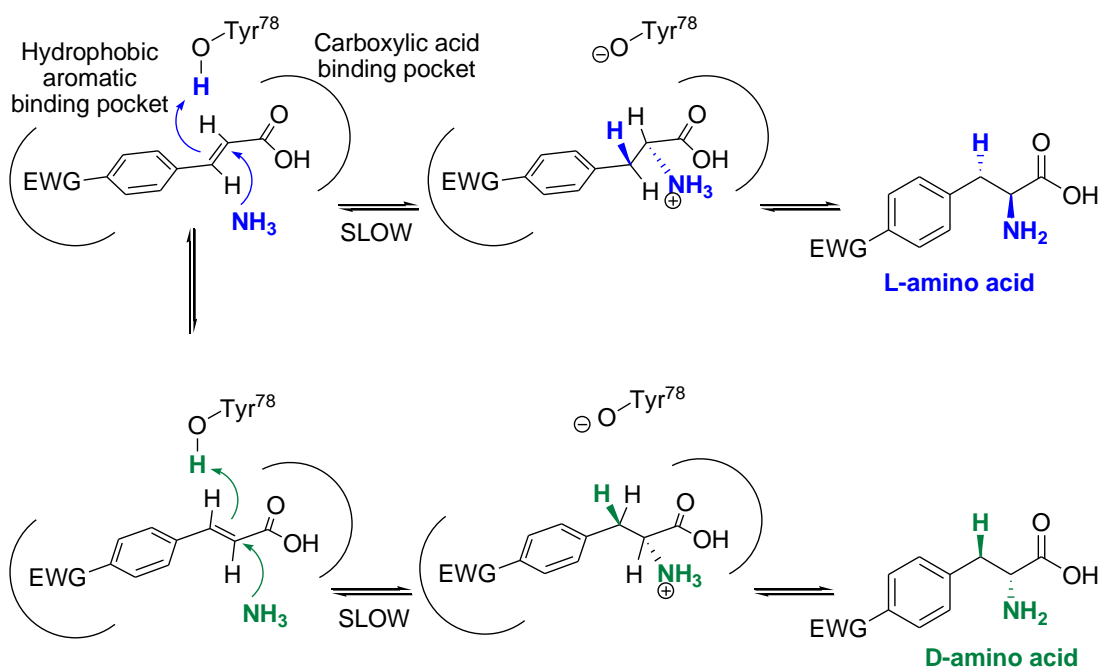


Figure 38: Proposed MIO-dependent and MIO-independent pathways for PAL catalyzed synthesis of amino acids.

The discovery of this alternative pathway may provide insights for future studies on the mechanism of the MIO-dependent pathway; in addition these results have broader implications for the future development of selective biocatalysts for the synthesis of non-natural amino acids.

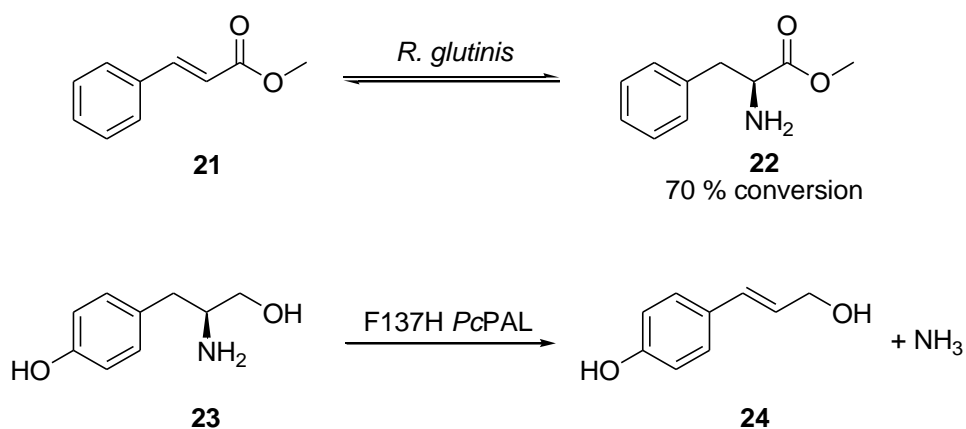
Chapter 4: Testing the Substrate Promiscuity of Wild-type PALs

4 Testing the Substrate Promiscuity of Wild-type PALs

4.1 Introduction

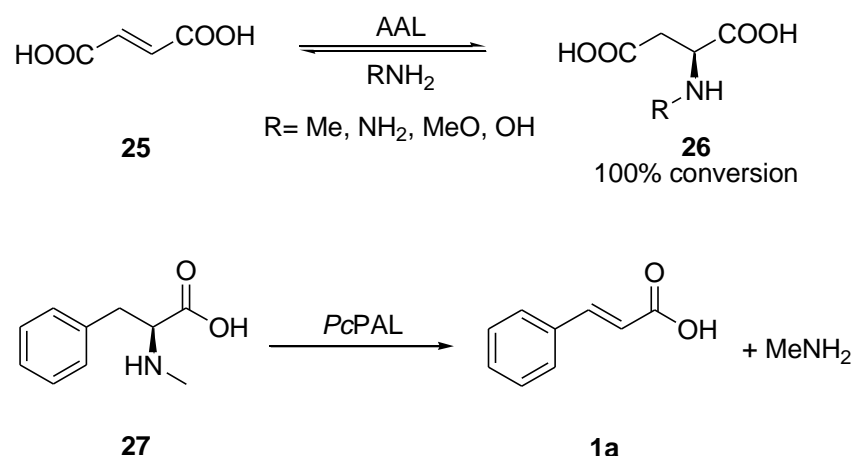
The activity of the eukaryotic PALs from the plant *Petroselinum crispum* (PcPAL) and yeast *Rhodotorula glutinis* (RgPAL) towards non-proteinogenic amino acids have been previously reported.[57,70-72,108] Furthermore, this work has investigated the activity of a prokaryotic PAL from the cyanobacteria *Anabaena variabilis* (AvPAL) with non-natural amino acids (chapter 2). However, there are very few reports which investigate alternative substrates which lack carboxylic acid functionality. The objective of this thesis is to develop a more general method of asymmetric hydroamination for the synthesis of structures other than amino acids.

D’Cunha *et al.* describe the synthesis of L-phenylalanine methyl ester **22** using *Rhodotorula glutinis* whole cells expressing a phenylalanine ammonia lyase using a biphasic system.[121,122] In addition, Bornscheuer *et al.* have investigated the activity of PcPAL towards amino alcohol substrates and found the variant F137H showed a very low turnover (k_{cat}) of L-tyrosinol **23** (281 times lower than the wild-type PcPAL catalyzed deamination of L-phenylalanine).[103] Attempts to increase the activity towards amino alcohols by screening single and multiple site-directed saturation mutagenesis libraries which were predicted using computational modelling were unsuccessful.[71]



Scheme 35: The reversible hydroamination of cinnamic acid methyl ester catalyzed by *R. glutinis* whole cells (heptane: 100 mM Tris-buffer, 1 M $(\text{NH}_4)_2\text{SO}_4$, pH 9.0, 30 °C) and the deamination of L-tyrosinol catalyzed by the PcPAL variant F137H (50 mM Tris-buffer, pH 8.8, 30 °C)

A second objective is to broaden the nucleophile specificity to include primary amines which can be used to synthesize chiral *N*-substituted phenylalanine derivatives. A variety of nucleophiles including methylamine, hydrazine, methoxyamine and hydroxylamine have been previously used in the aspartate ammonia lyase (AAL) catalyzed hydroamination of fumarate **25**. [123] Furthermore, Rétey *et al.* investigated *N*-methylated phenylalanine derivatives as substrates for PcPAL and found that *N*-methyl-L-phenylalanine **27** was accepted as a reluctant substrate ($k_{\text{cat}} = 0.22 \text{ s}^{-1}$, $K_M = 6.6 \text{ mM}$). However no hydroamination activity was observed using cinnamic acid and methylamine (Scheme 36).[109]



Scheme 36: Aspartate ammonia lyase (AAL) catalyzed hydroamination of fumarate using primary amine nucleophiles (phosphate buffer, pH 7-8) and the non-reversible PcPAL catalyzed deamination of *N*-methyl-L-phenylalanine (100 mM Tris-buffer, pH 8.8, 37 °C)

This chapter will investigate the promiscuity of prokaryotic AvPAL and eukaryotic RgPAL towards a broad range of amines and *N*-substituted phenylalanines. A panel of substrates were selected with a range of functional groups in place of the natural substrate's carboxylic acid moiety (Figure 39). In addition, some substrates were chosen which incorporate a *para*-nitro substituent on the aromatic ring as it has been shown that nitro-substituents activate cinnamic acid derivatives towards hydroamination (see 2.5: *Determining the kinetic constants for PAL catalyzed reactions*). This chapter describes the synthesis of a number of substrates and their corresponding products and the development of analytical methods for their detection. Finally the wild-type PAL substrate specificity was determined by screening for activity towards these compounds.

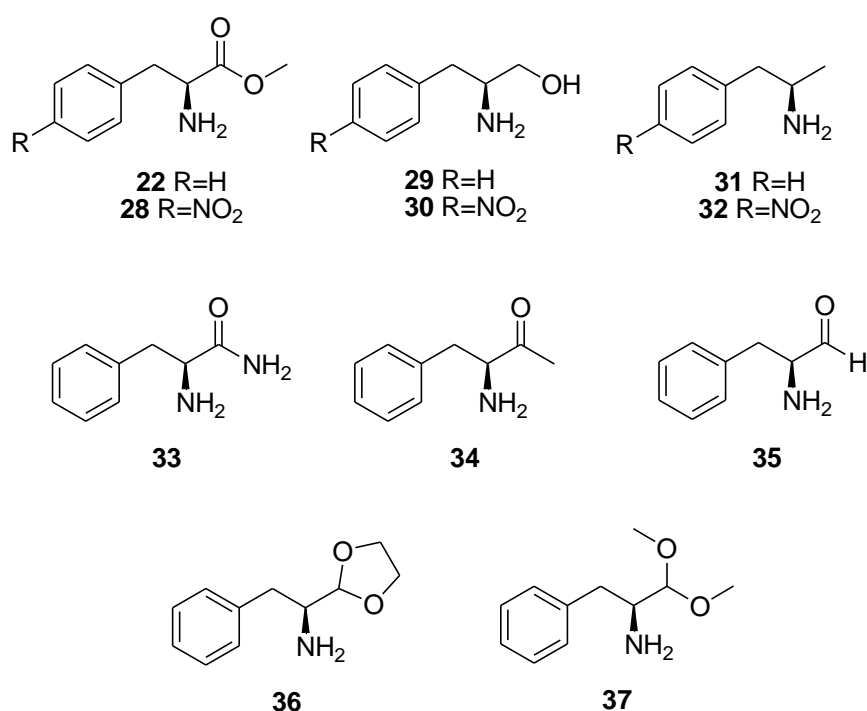
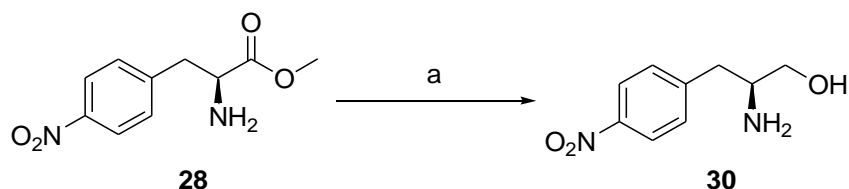


Figure 39: Panel of substrates chosen to screen wild-type PAL deamination activity

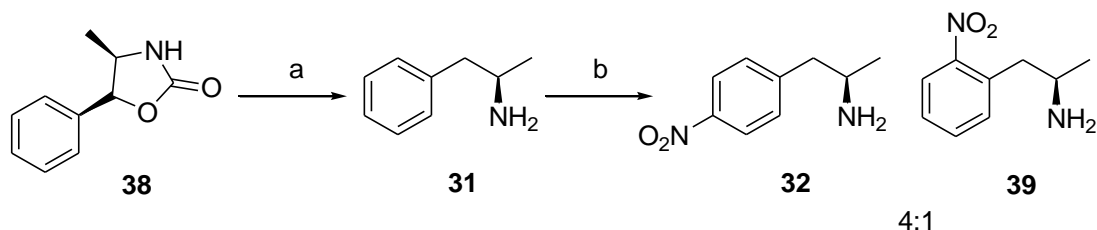
4.2 Chemical Synthesis of Amine Substrates

Amine compounds **30** & **34-37** were not commercially available and were therefore synthesized chemically. 4-Nitro-L-phenylalaninol (**30**) was synthesized in one step by the reduction of 4-nitro-L-phenylalanine methyl ester (**28**) using sodium borohydride (Scheme 37).[124]



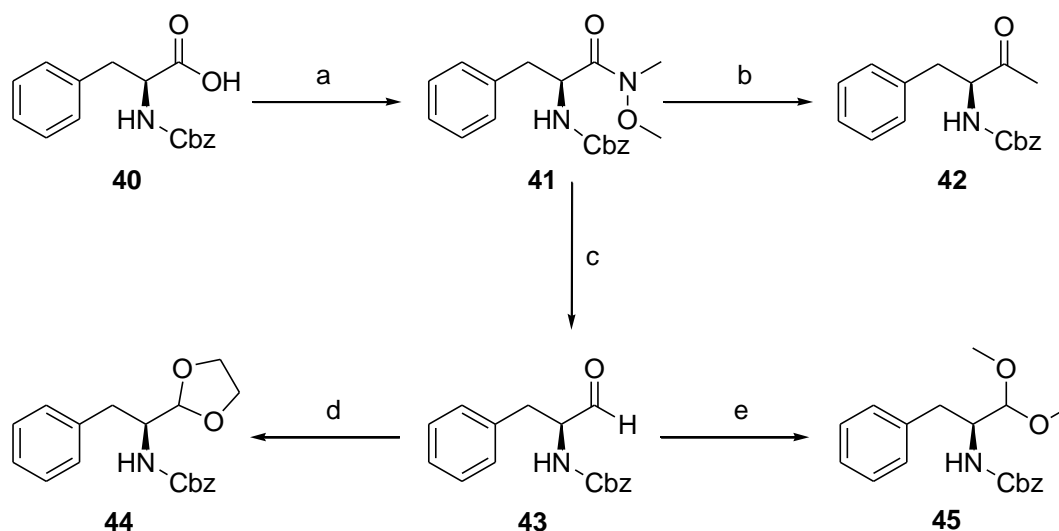
Scheme 37: Synthesis of 4-nitro-L-phenylalaninol 30 a) NaBH₄, H₂O, 5 °C, 4 h, 47 %

(*R*)-amphetamine (**31**) was synthesized from (4*R*,5*R*)-4-methyl-5-phenyloxazolidin-2-one (**38**) following palladium mediated hydrogenation followed by subsequent decarboxylation (Scheme 38) according to the patent by Mencil *et al.*[125] Nitration of **31** yielded a mixture of 2- and 4-nitro-(*R*)-amphetamine in a 1:4 ratio (determined by ¹H NMR).[126] The regioisomers were not separated and were used in the PAL catalyzed deamination reactions as a mixture.



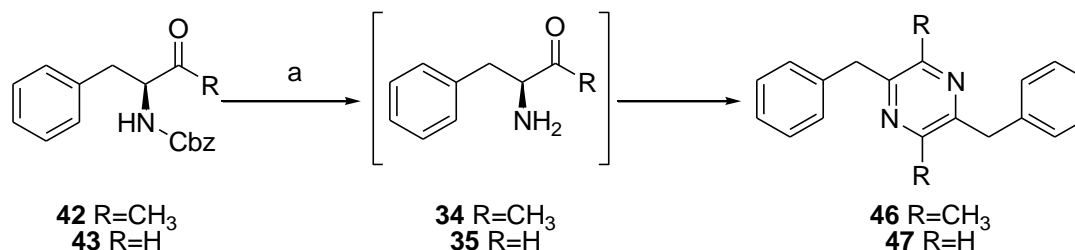
Scheme 38: Synthesis of nitro-substituted amphetamine a) H₂, Pd/C 10 %, EtOH, rt, 95 % b) HNO₃, -20 °C, 18 h, 60 %

The carboxybenzyl (Cbz) protected amines **42-45** were synthesized from the Weinreb amide intermediate **41** which in turn was synthesized by condensation of acid **40** with *N,O*-dimethylhydroxylamine (Scheme 39). Using the Weinreb amide prevents a second addition of methyl lithium in the synthesis of the desired ketone **42** as the tetrahedral intermediate formed in the reaction is stabilized.[127] Similarly, reaction of intermediate **41** with lithium aluminium hydride yields the desired aldehyde **43**, as the stabilized intermediate cannot undergo further reduction.[128] Treatment of the Cbz-protected aldehyde **43** with ethylene glycol in the presence of catalytic amounts of *p*-toluene sulphonic acid yielded the cyclic acetal **44**. [128] Alternatively, treatment of **43** with catalytic amounts of *p*-toluene sulphonic acid in the presence of methanol and trimethylorthoformate provided the dimethyl acetal **45**.



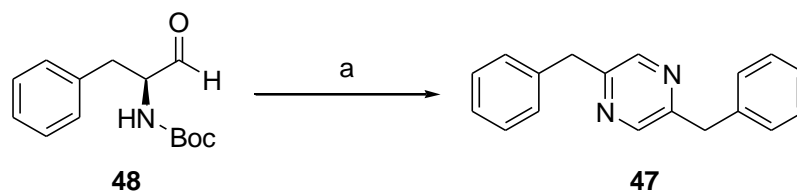
Scheme 39: Synthesis of Cbz-protected amines 42-45 a) HN(Me)OMe.HCl, HBTU, HOBT, DIEA, DMF, rt, 2 h, 100 % crude b) MeLi, THF, -30 °C, 1 h, 47 % c) LiAlH₄, THF, 0 °C, 1 h, 30 % d) (CH₂OH)₂, TsOH, toluene, reflux, 6 h, 58 % e) trimethylorthoformate, TsOH, MeOH, rt, overnight 47 %

Next, the compounds **42-45** were deprotected to achieve the required amine substrates. Deprotection of the amino ketone **42** and amino aldehyde **43** by transfer hydrogenation using cyclohexadiene and Pearlman's catalyst yielded the intermediates **34** and **35**. However, the desired products dimerised to form 2,5-dihydropyrazines which spontaneously aromatised to pyrazines **46** and **47** (Scheme 40) which were characterized by NMR and GC-MS.



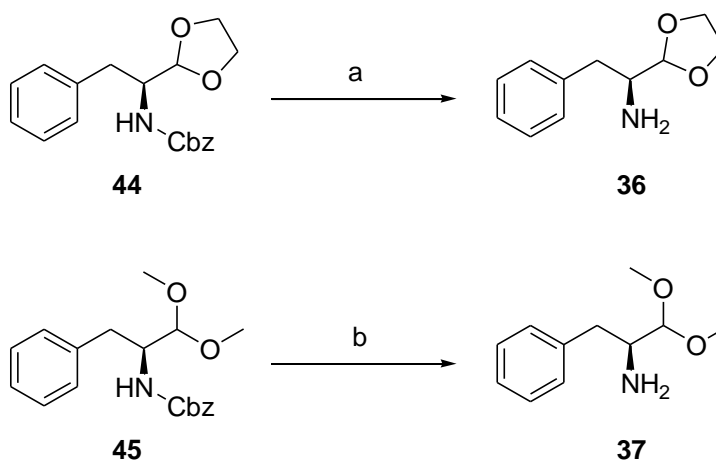
Scheme 40: Deprotection of the amino ketone 42 and amino aldehyde 43 a) Pd(OH)₂/C, 1,4-cyclohexadiene, EtOAc, rt, overnight

In an attempt to avoid dimerisation of the amino aldehyde, an alternative method was investigated using a *tert*-butoxycarbonyl (Boc) protecting group. Commercially available Boc-protected amino aldehyde **48**, was deprotected under acidic condition in an attempt to form the amino aldehyde hydrochloride salt. Unfortunately the reaction yielded the dimerised product **47**, and as a result amino aldehydes and ketones were omitted from the substrate panel due to their instability.



Scheme 41: Deprotection of *N*-Boc protected amino aldehyde 48 a) 4 N HCl in dioxane, rt, overnight

The carboxybenzyl protecting groups were successfully cleaved from compounds **44** and **45** by transfer hydrogenation, following the optimized reaction conditions determined by Kappel and Barany (Scheme 42).[128]



Scheme 42: Deprotection of amino acetals 44 and 45 a) Pd(OH)₂/C, 1,4-cyclohexadiene, EtOAc, rt, 5 h, 45 % b) Pd(OH)₂/C, 1,4-cyclohexadiene, EtOAc, rt, 5 h, 41 %

4.3 Chemical Synthesis of Alkene Substrates

The panel of alkene substrates chosen to investigate the substrate promiscuity of PAL enzymes corresponds to the panel of amine substrates (Figure 39). The alkenes **49**, **53**, **57** & **58** were not commercially available and were chemically synthesized.

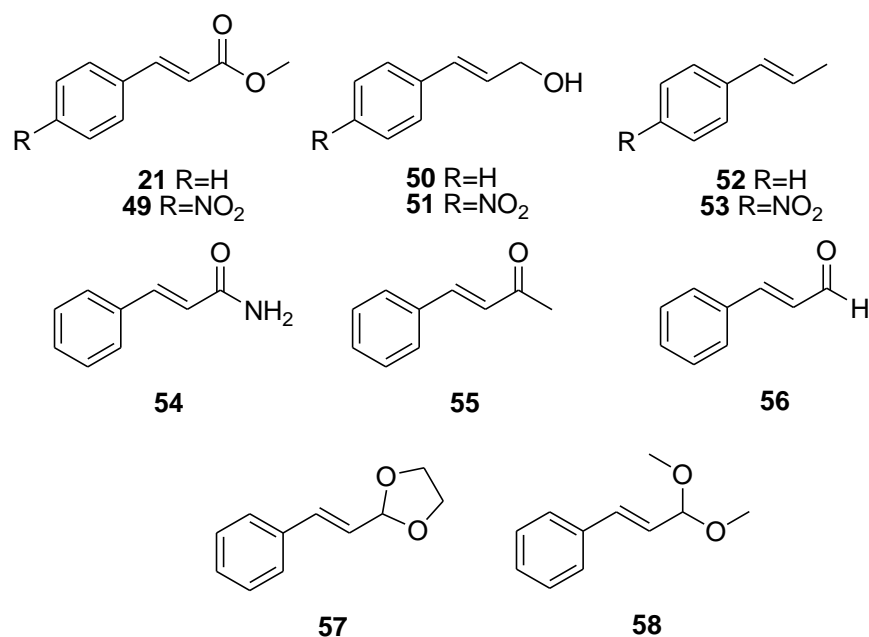
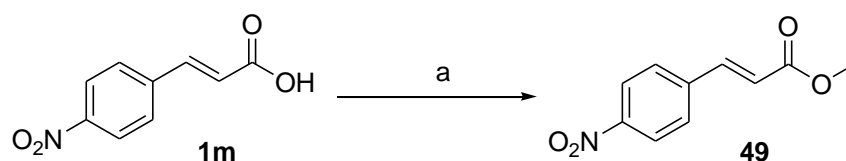


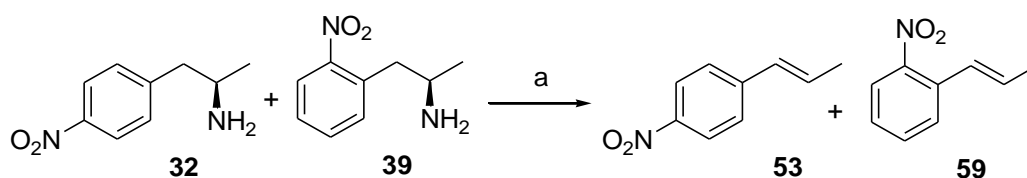
Figure 40: Panel of substrates chosen to screen wild-type PAL hydroamination activity

4-Nitrocinnamic acid methyl ester **49** was synthesized in a single step by the esterification of 4-nitrocinnamic acid **1m** using thionyl chloride in methanol (Scheme 43).



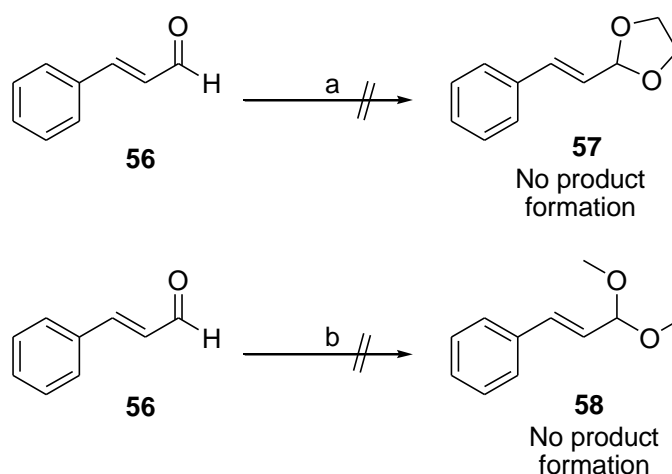
Scheme 43: Synthesis of 4-nitro-*trans*-cinnamic acid methyl ester **49 a) SOCl₂, MeOH, overnight, rt, 78%**

4-Nitro-*trans*- β -methylstyrene **53** was synthesized from 4-nitro-(*R*)-amphetamine **32** following a trimethylation with iodomethane followed by base catalyzed elimination of the amine according to the procedure of Millian *et al.*[129] The starting material used was a mixture of *ortho*- and *para*-nitro substituted regioisomers (1:4) and as a result the alkene product was achieved in the same ratio of isomers (Scheme 44). The desired alkene **53** was subsequently isolated following purification by column chromatography.



Scheme 44: Synthesis of nitro-substituted *trans*- β -methylstyrene a) MeI, K₂CO₃, rt, 48 h, 73 %

The synthesis of the cyclic acetal **57** and dimethyl acetal **58** were unsuccessful as the compounds were prone to hydrolysis (Scheme 45) and as a result, these compounds were omitted from the alkene substrate panel.



Scheme 45: Synthesis of acetals 57 and 58 a) ethylene glycol, TsOH, toluene, reflux, 6 h b) trimethylorthoformate, camphor sulphonic acid, MeOH, r.t, overnight

4.4 Analytical Methods

L-Phenylalaninamide **33** and cinnamamide **54** were analyzed using the reverse-phase HPLC methods developed for analyzing amino acids and cinnamic acid derivatives. All other alkene compounds in this study suffer from low solubility in aqueous media and therefore alternative analytical techniques are required. Normal-phase HPLC and GC-FID conditions have been successfully established for the identification of the amines and alkenes screened in this chapter. For analysis, the substrate and product from PAL catalyzed biotransformations must be extracted into organic media. The reactions (typically 5 mL) are firstly pH adjusted with sodium hydroxide (10 N) to approximately pH 12 and then the compounds are extracted three times with *tert*-butyl methyl ether (3 x 10 mL). The organic extracts are combined, dried over magnesium sulphate and concentrated, before injection onto the HPLC or GC-FID columns. The parameters for the analytical methods are shown in Table 15.

Table 15: Conditions for normal phase HPLC and GC-FID analysis

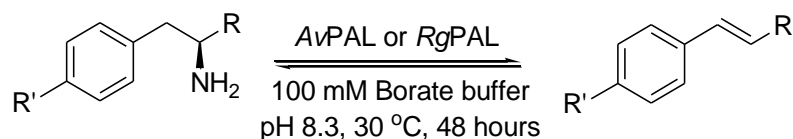
Method	Conditions
Normal-phase HPLC	Chiralpak IC column (Daicel chemical industries), 25 cm x 4.6 mm, 20 μ m Mobile phase: 80 % hexane (+ 0.1 % diethyl amine)/ 20% propan-2-ol flow rate: 0.5 mL/min, 20 $^{\circ}$ C, UV detection: 222, 254, 270, 320 nm, 30 min
GC-FID	Chirasil-Dex CB column (Agilent), 25 nm x 250 μ m x 0.26 μ m Inlet temp: 200 $^{\circ}$ C, FID @ 200 $^{\circ}$ C, Carrier: He Oven: 150 $^{\circ}$ C for 10 mins, increase 5 $^{\circ}$ C/min for 2 min, 180 $^{\circ}$ C for 5 min

4.5 PAL Activity Towards Novel Substrates

The prokaryotic AvPAL and eukaryotic RgPAL were screened for activity towards amine substrates **22**, **28-33** & **36-37** and alkene substrates **49**, **21** & **50-56** with modifications at the carboxylic acid position. AvPAL was chosen as it showed a higher catalytic turnover (k_{cat}) of selected non-proteinogenic amino acids compared to the eukaryotic PALs, significantly those with 4-nitro substituents (chapter 2). The difference in activity between the eukaryotic RgPAL and PcPAL towards various phenylalanine analogues was shown to be fairly unremarkable, therefore only RgPAL was investigated herein.

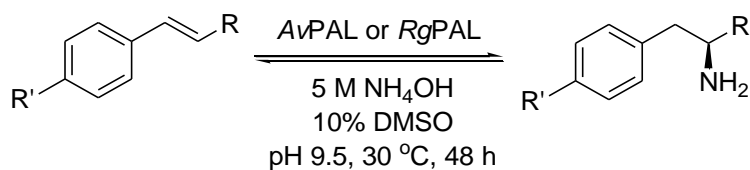
Some of the substrates screened in this chapter are particularly polar and diffusion across the cell walls of whole cell biocatalysts can present a potential problem. Consequently, to test the substrate specificity of AvPAL and RgPAL, purified enzyme preparations were used (0.3 mg total protein per 5 mL reaction). The enzymes were screened for both deamination and hydroamination activity towards the panel of available substrates (Table 16 and 17). The reactions were incubated for 48 hours, extracted with *tert*-butyl methyl ether and analyzed by both normal phase and GC-FID methods.

Table 16: Amines screened as potential substrates for AvPAL and RgPAL catalyzed deamination reactions



Amine	R	R'
22	COOMe	H
28	COOMe	NO ₂
29	CH ₂ OH	H
30	CH ₂ OH	NO ₂
31	CH ₃	H
32	CH ₃	NO ₂
33	CONH ₂	H
36	CH(OCH ₂ CH ₂ O)	H
37	CH(OMe) ₂	H

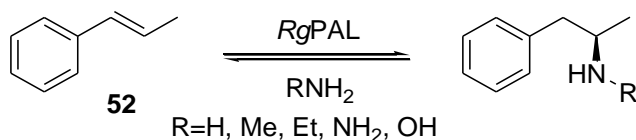
Table 17: Alkenes screened as potential substrates for AvPAL and RgPAL catalyzed hydroamination reactions



Alkene	R	R'
21	COOCH ₃	H
49	COOCH ₃	NO ₂
50	CH ₂ OH	H
51	CH ₂ OH	NO ₂
52	CH ₃	H
53	CH ₃	NO ₂
54	CONH ₂	H
55	COCH ₃	H
56	COH	H

Unfortunately the two PAL enzymes screened showed no conversion of any of the substrates tested, in either deamination or hydroamination reactions. For each biotransformation the remaining starting material was detected using both normal phase HPLC and GC-FID but no product peaks were observed.

In contrast to the results presented above, a previous investigation of wild-type *RgPAL* catalyzed hydroamination of *trans*- β -methylstyrene **52** reported the formation of the desired amphetamine product (**31**), which was observed by GC-MS (unpublished results). Furthermore, product peaks had been observed in the hydroamination reactions of **52** using the alternative nucleophiles methylamine, ethylamine, hydroxylamine and hydrazine (Scheme 46).



Scheme 46: Previously reported hydroamination reactions of *trans*- β -methylstyrene using a range of nucleophiles

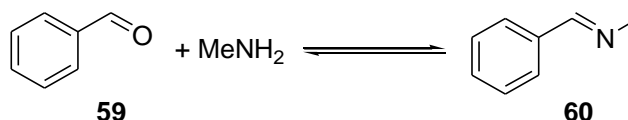
To investigate the discrepancy between previous results and the results presented in this thesis, the *RgPAL* gene was sequenced to rule out the possibility of mutations responsible for a loss in activity; however results showed the gene had the correct DNA sequence. Next, the PAL catalyzed hydroamination reaction was repeated under different reaction conditions (Table 18). For each reaction the amination of cinnamic acid served as a positive control and a

reaction with no enzyme as a negative control. Nonetheless, amphetamine product formation could not be detected under any of the reaction conditions tested.

Table 18: Reaction conditions used for the PAL catalyzed hydroamination reaction of *trans*- β -methylstyrene

Condition	Parameters Tested
permeabilizing agents - increases permeability of cell walls and increases substrate solubility - reported to increase PAL activity[130]	Triton X-100 (0-10 %), Tween (0-5 %), gluteraldehyde (0.1 %), glycerol (10 %), PEG (0.5 %), toluene (3 %)
cosolvents - increases the substrate solubility - PAL maintains good activity towards cinnamic acid in < 20% DMSO	DMSO 0 - 20%
biphasic system - increases substrate solubility - parameters determined by D'Cunha <i>et al.</i> [121]	Heptane: 0.1 M Tris buffer (2:1) 1 M (NH ₄) ₂ SO ₄
ammonia source - previous investigation observed product formation using a range of nucleophiles	ammonium sulphate, carbonate, carbamate, hydroxide, acetate, chloride; methylamine, ethylamine, hydroxylamine, hydrazine
biocatalyst – different PAL sources and types of biocatalysts	Resting whole cells, lyophilized whole cells, cell lysate, purified protein, lyophilized purified protein, AvPAL, RgPAL, PcPAL, commercially available purified RgPAL
pH range	pH 8.5 - 11.0
speed of shaking	100- 250 rpm
reaction time - biocatalysts generally found to be inactive after 48 hours - increased reaction time may highlight the presence of slow background reactions	up to 9 days
Scale up – allows identification of very low level activity	5 x 10 mL reactions: purified RgPAL (5 mg per reaction), 5 mM substrate Reactions extracted with TBME, extracts were combined and concentrated

GC-MS spectra of an *Rg*PAL catalyzed hydroamination reaction of *trans*- β -methylstyrene and methylamine from the previous investigation was compared to the mass spectra of compounds in the NIST database (National Institute of Standards and Technology). The product formed in the reaction was identified by the database search as *N*-benzylidene methylamine (**60**), which can be formed from the chemical reaction between benzaldehyde and methylamine (Scheme 47). It was suspected that the *trans*- β -methylstyrene sample used in the previous study may have been contaminated with a benzaldehyde impurity. This was later confirmed by ^1H NMR analysis of the original starting material.



Scheme 47: Synthesis of *N*-benzylidene methylamine from benzaldehyde and methylamine

A reaction of benzaldehyde, **59** (10 mM) with methylamine (5 M, pH 9.5) was incubated at 30 °C for 24 hours, the reaction was basified with sodium hydroxide (10 N), extracted with *tert*-butyl methyl ether and analyzed by GC-FID. As suspected, the results showed the formation of a product peak with the same retention time (2.8 min) as a commercial standard of *N*-benzylidene methylamine, **60** (Figure 41A). Biotransformations were performed with purified *Rg*PAL and two samples of *trans*- β -methylstyrene (contaminated sample and a pure sample) in 5 M methylamine (pH 9.5, 30 °C). Work up of these reactions and analysis by GC-FID confirmed that the product peak observed in the reaction using contaminated starting material is a result of a background chemical reaction between benzaldehyde and methylamine (Figure 41B and Figure 41C). Similarly the contaminating benzaldehyde can react with all primary amines and ammonia. No new product peaks were observed in the reaction of pure *trans*- β -methylstyrene starting material with either primary amine nucleophiles or ammonia, confirming *trans*- β -methylstyrene is not a PAL substrate.

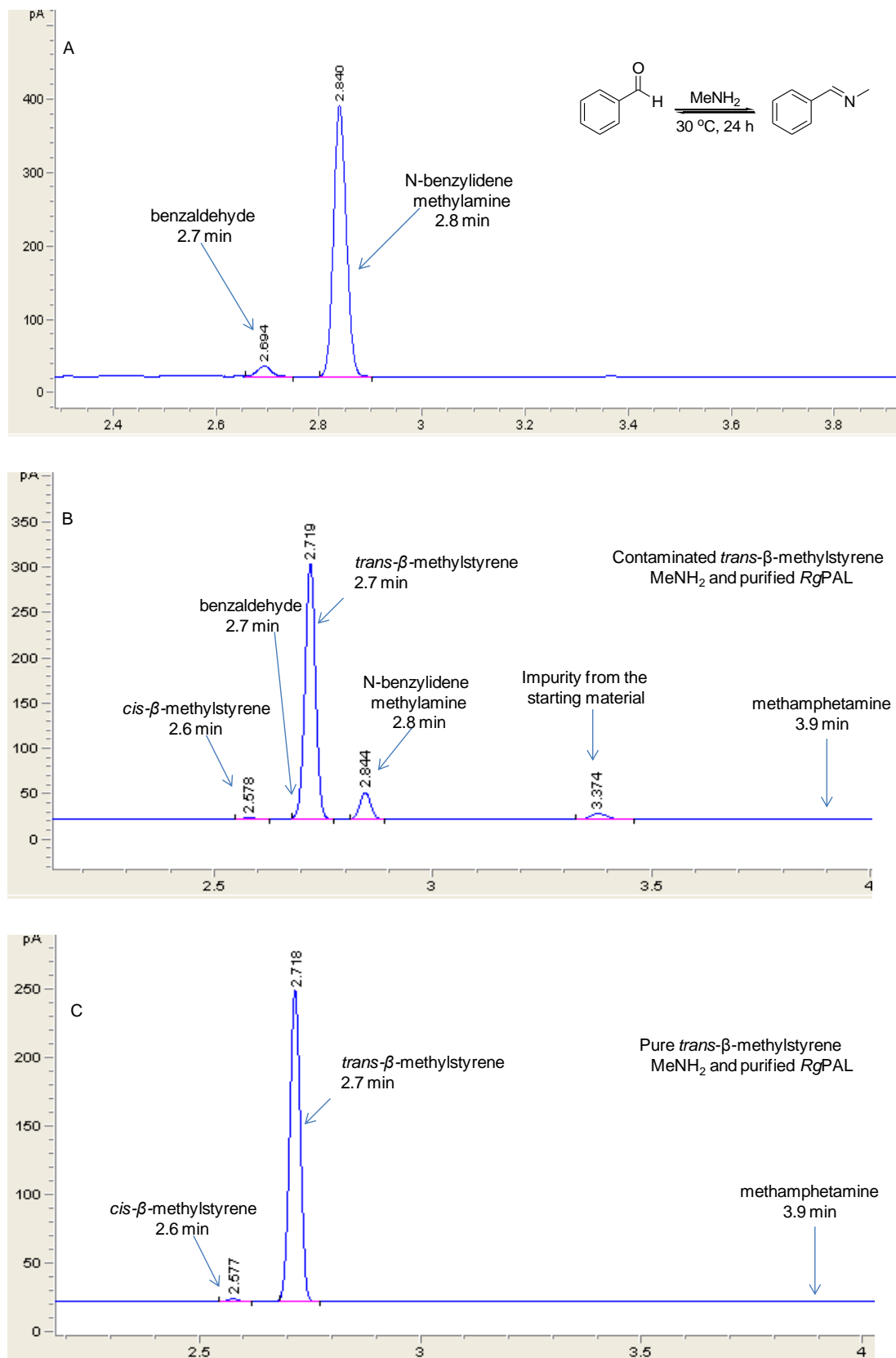


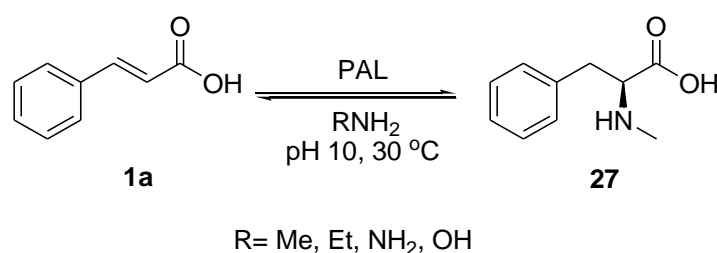
Figure 41: GC-FID traces A) Reaction of 10 mM benzaldehyde with MeNH₂ (5 M) B) RgPAL incubated with MeNH₂ (5 M) and 10 mM *trans*- β -methylstyrene contaminated with benzaldehyde. B) RgPAL incubated with MeNH₂ (5 M) and 10 mM *trans*- β -methylstyrene (no impurities). Purified RgPAL from a commercial source was used. *cis*-Methylstyrene (2.6 min) is an impurity found in both samples of the starting material. The expected product methamphetamine has a retention time of 3.9 min

This work has highlighted the importance of using high purity substrates, as impurities have the potential to perform competing reactions or could potentially inhibit enzyme activity. Adequate controls are also essential to eliminate the possibility of product formation from background reactions. In addition, when it is not possible to isolate new products due to low conversions, it is beneficial to obtain a standard of the product so that adequate analysis can be performed.

4.6 Nucleophile Promiscuity

The aspartate ammonia lyase (AAL) catalyzed hydroamination of fumarate with small primary amines has been successfully achieved by Feringa *et al.*[123] However AALs belong to the fumarase/ enolase superfamily and react via an alternative catalytic mechanism which does not involve an MIO-cofactor. The PAL catalyzed deamination of *N*-methyl phenylalanine has been achieved by Rétey *et al.*[109] however hydroamination reactions using a variety of primary amine nucleophiles have not been reported.

With the exception of *N*-methyl-L-phenylalanine, the desired *N*-substituted phenylalanine derivatives are not commercially available. Therefore the PAL catalyzed hydroamination activity was investigated using LC-MS analysis, so that any newly formed product peaks could be characterized by mass spectrometry. Nucleophiles methylamine, ethylamine, hydrazine and hydroxyl amine were screened for activity using the substrate cinnamic acid (**1a**) (Scheme 48). Various amine concentrations (100 mM to 10 M) were used with *E. coli* whole cell biocatalysts, cell lysate and purified enzymes (*Rg*PAL and *Av*PAL) however no product formation was observed.



Scheme 48: PAL catalyzed hydroamination of cinnamic acid using primary amine nucleophiles for the synthesis of chiral secondary amine products

In agreement with previous results,[109] the deamination of *N*-methyl-L-phenylalanine (**27**) was achieved using *E. coli* BL21(DE3) whole cells expressing *Rg*PAL and the biotransformation reached 26 % substrate conversion (the deamination of L-phenylalanine performed in parallel reached 82 % conversion). In the presence of high ammonia concentrations the deamination of α -amino acids is reversible. However, although *N*-methyl-L-phenylalanine (**27**) was a substrate in the deamination reaction, hydroamination with methylamine was not possible. This result can be explained by examination of the values of K_M . Rétey *et al.* determined that the K_M value for ammonia in the PAL catalyzed hydroamination of cinnamic acid at pH 8.8 and 10 is 4.4 M and 2.6 M respectively.[109] Based

on the analogy that the K_M value for *N*-methyl-L-phenylalanine **27** is 55 times higher than L-phenylalanine **2a**, it is predicted that the K_M for methylamine would be considerably higher than for ammonia.[109] Therefore, the absence of hydroamination activity with methylamine as a nucleophile can be explained by a prohibitively high K_M which leads to a concentration required for activity which is unachievable.

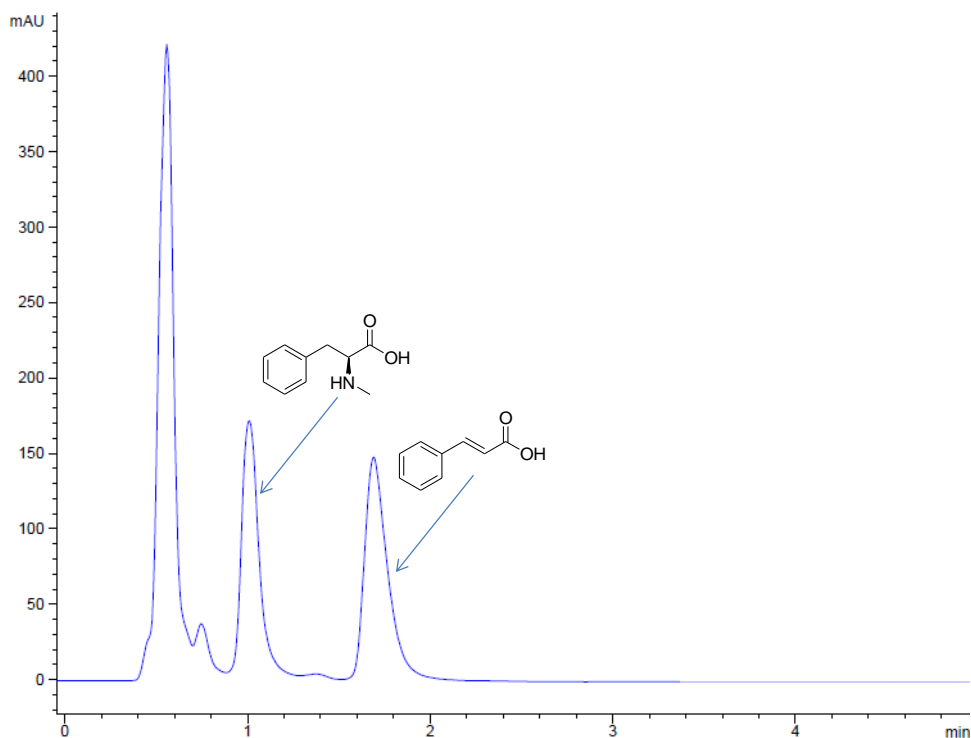


Figure 42: LC-MS analysis of the *Rg*PAL catalyzed deamination of *N*-methyl-L-phenylalanine (5 mM) in 0.1 M borate buffer (pH 8.3, 30 °C, 22 hours). The reaction was heated to 95 °C for 5 minutes to stop the reaction which led to the release of whole cell contaminants which appear as a peak at 0.5 minutes. These contaminants were also observed in the control reaction using whole cell *E. coli* BL21(DE3) transformed with empty pET-16b vector

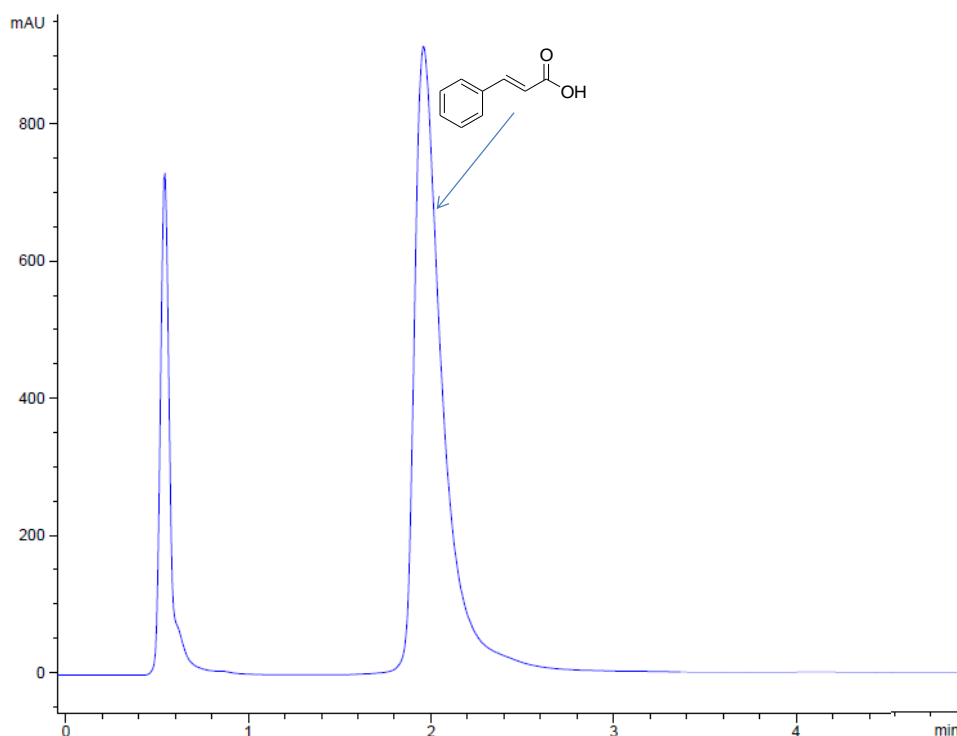


Figure 43: LC-MS analysis of the *RgPAL* catalyzed hydroamination of cinnamic acid (5 mM) with 5 M MeNH₂ (pH 9.5, 30 °C for 22 hours) showing no product formation. The reaction was heated to 95 °C for 5 minutes to stop the reaction which led to the release of whole cell contaminants which appear as a peak at 0.5 minutes

4.7 Conclusion

A range of amines and their corresponding alkenes were synthesized and screened as substrates for *RgPAL* and *AvPAL*. Substrates without carboxylic acid functionality were not tolerated and no activity was detected by either HPLC or GC. Many of the alkenes screened suffer from low solubility which can lead to low substrate availability. For future work, it may be beneficial to synthesis and screen pyridyl analogues which will have improved solubility. Furthermore, future work will focus on screening libraries using the assays developed in chapter 5 with the aim of identifying variants with hydroamination activity towards a range of alkenes for the synthesis of a wide variety of amines.

The hydroamination of cinnamic acid using various primary amine nucleophiles also proved unsuccessful. This is likely to be a result of the high K_M values and the low binding affinity of the amine partners. Screening variants for increased activity towards the deamination of *N*-methyl-L-phenylalanine (see 5.2.1: *Measuring the Absorbance of Alkene Products*) may allow the identification of variants with lower K_M values, which may also catalyze the hydroamination reaction with methylamine.

Chapter 5: Assay Development and Screening

5 Assay Development and Screening

5.1 Introduction

For the detection of novel PAL activity towards a broad range of compounds including, D-amino acids, *N*-substituted phenylalanine derivatives and amines, a number of different assays are required. The methods developed in this chapter include both liquid phase screens and colony based colorimetric screens. Liquid phase methods can be used to screen whole cell biocatalysts in solution and are medium-throughput as variants are screened in 96-well plates. The advantage of spectrophotometric screens is that they are semi-quantitative and give an indication of which active variants have the highest activity. However, these assays have a limited screening capacity of 100-1000 variants per day, therefore more focused rationally designed libraries are required which target residues predicted to interact with the chosen substrate. The colony based colorimetric methods developed herein, are used to screen variants expressed in *E. coli* cells grown on nitrocellulose membranes. The methods are not quantitative but they are high-throughput and can be used to rapidly screen thousands of variants in parallel. Therefore colony based assays are compatible with screening large random libraries, which can lead to the identification of important residues for activity and selectivity which may be difficult to predict by rational design. The assays developed have been used to screen both rationally designed libraries and large random libraries of AvPAL variants for increased activity, substrate promiscuity and D-selectivity. Positive hits from the assays were sequenced and the variants were overexpressed and purified for further characterisation.

5.2 Assay Development

5.2.1 Measuring the Absorbance of Alkene Products

PAL catalyzed amino acid deamination can be monitored spectrophotometrically by measuring the change in absorbance at a wavelength corresponding to the formation of the respective cinnamic acid analogue (see 2.2.2: *Spectrophotometric analysis*). This method is compatible with low concentrations of whole cells biocatalysts and can be used to screen libraries in a 96-well plate for deamination activity towards both L- and D-amino acids and *N*-substituted phenylalanine derivatives. This provides a fast and quantitative method of analyzing activity without the need for derivatising the products or coupling the PAL reaction with subsequent enzymatic steps. However, this method cannot be applied to all substrates of interest as some compounds absorb at the same wavelengths as their corresponding products, for example (*R*)-amphetamine (**31**) and *trans*- β -methylstyrene (**52**) (Figure 44).

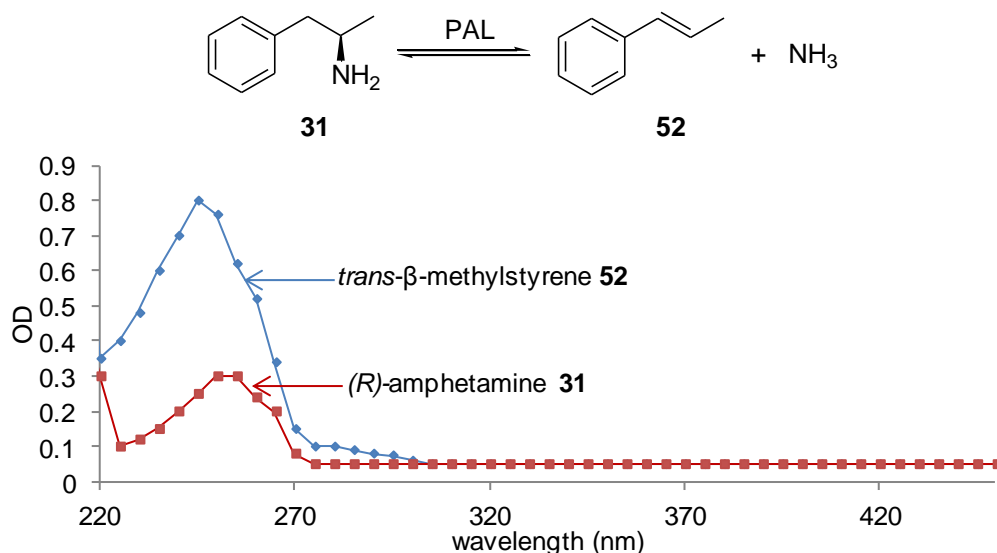


Figure 44: Wavelength scan of (R)-amphetamine, 31 (red) and trans-β-methylstyrene, 52 (blue)

Analogous substrates such as those with nitro-substituents on the aromatic ring were shown to have different substrate and product absorbance profiles. In theory, using these substituted compounds should allow the formation of the β-methylstyrene derivative to be measured spectrophotometrically (Figure 45). Nonetheless, this method suffers from low sensitivity as a result of background absorbance from whole cell contaminants and is not useful for detecting low level PAL activity. Secondly, the methylstyrene derivatives have very low solubility in the aqueous reaction buffers so detecting activity by absorbance measurements is problematic.

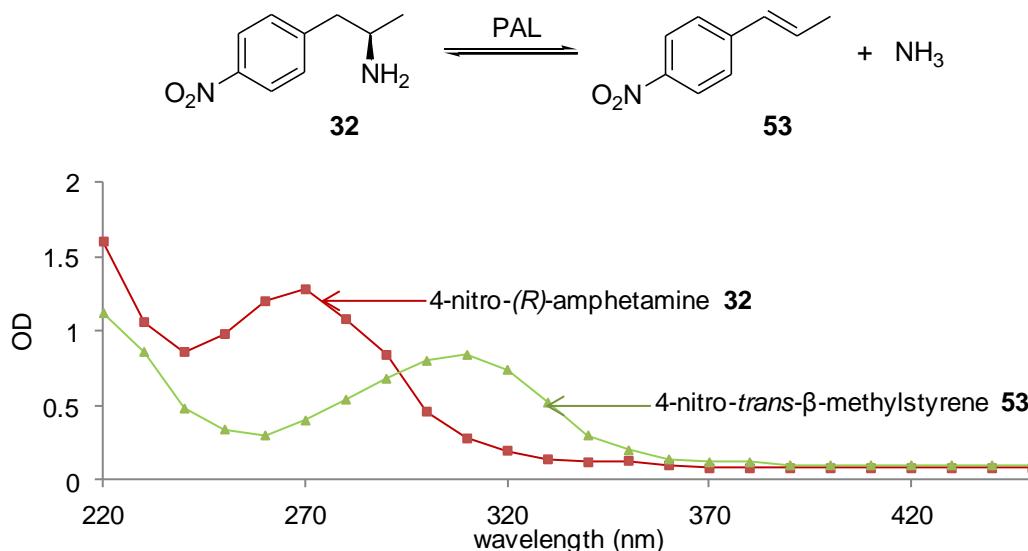


Figure 45: Wavelength scan of 4-nitro-(R)-amphetamine, 32 (red) and 4-nitro-trans-β-methylstyrene, 53 (green)

An alternative method to allow spectrophotometric analysis of PAL catalyzed amphetamine deamination is to extract the trans-β-methylstyrene product into an organic solvent and measure the absorbance of the extract. The pKa of amphetamine is ca. 9.8, therefore under deamination reaction conditions (pH 8.3) the β-methylstyrene product will be extracted

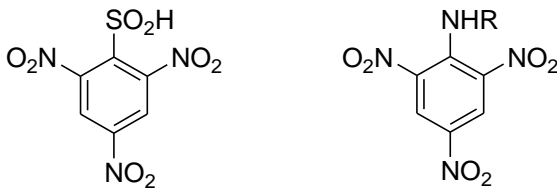
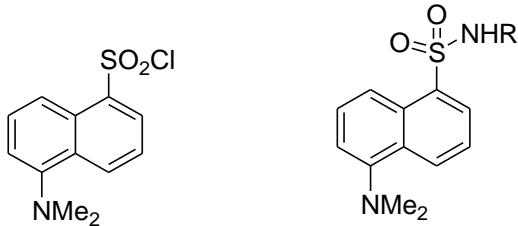
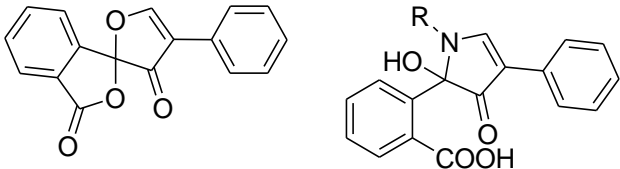
exclusively. Again this method suffers from low sensitivity as a result of large background absorbance from whole cell contaminants at the same wavelengths used to measure β -methylstyrene formation (220-270 nm).

Overall, spectrophotometric methods are only useful for measuring deamination activity towards substrates with high wild-type activity and where the products formed have strong UV-absorbance. Unfortunately, it is not possible to measure hydroamination activity using this assay as very low substrate concentrations are required for the absorbance measurements to be within the limits of detection and small changes in absorbance are sensitive to background interference from whole cell (or cell lysate) contaminants. Furthermore, PAL catalyzed amination is the synthetically useful reaction and an increase in deamination activity does not necessarily correlate to an increase in amination activity (see 2.5 *Determining the kinetic constants for PAL catalyzed reactions*).

5.2.2 Derivatisation Methods

Methods for derivatising the amine products from PAL catalyzed hydroamination reactions were investigated. Formation of an amine derivative allows spectrophotometric analysis at an alternative wavelength, where background signals from the starting materials and whole cell contaminants may be lower. Three derivatising agents were investigated and (*R*)-amphetamine was chosen as the target amine (Table 19).

Table 19: Derivatising agents and methods of detection

Derivatisation reagent	Derivatisation product ^a	Detection
Trinitrobenzene sulphonic acid (TNBS)		Absorbance at 420 nm
Dansyl chloride (Dns-Cl)		Fluorescence excitation 343 nm emission 530 nm
Fluorescamine		Fluorescence excitation 405 nm emission 480 nm

[a] derivatisation of (*R*)-amphetamine NHR= (*R*)-amphetamine

Wild-type PAL enzymes show no activity towards the amination of *trans*- β -methylstyrene, therefore a sensitive assay is required which can detect any low level activity which may be achieved by PAL variants. Hydroamination reactions are typically performed with 5 mM substrate and 10 % conversion was chosen as the limit for detection. Samples of (*R*)-amphetamine in phosphate buffer (100 mM, pH 8.0) were derivatised with trinitrobenzene sulphonic acid (TNBS, 1 % solution) and the absorbance showed a linear correlation with amine concentration. However, in the presence of *E. coli* whole cells no significant difference in absorbance could be detected between samples of (*R*)-amphetamine and controls without amine.

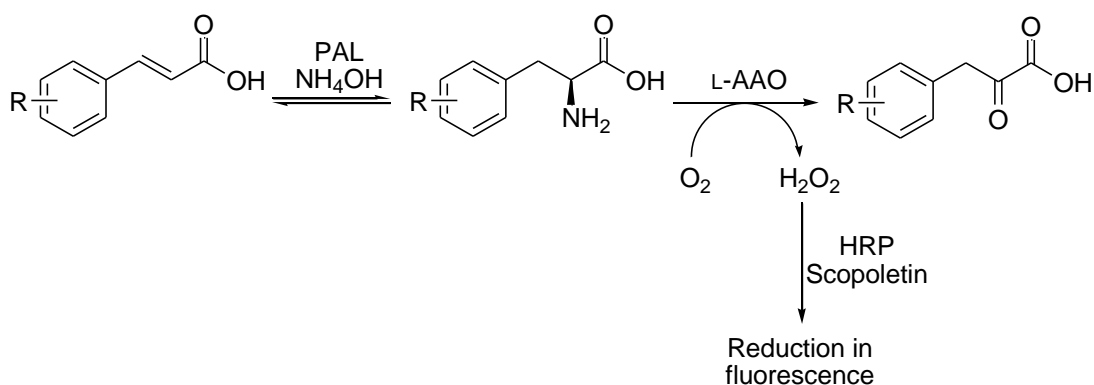
Dansyl chloride and fluorescamine are non-fluorescent reagents which react with amines to give fluorescent products. Unreacted dansyl chloride is hydrolysed and although hydrolysis is slower than dansylation the hydrolysis product fluoresces with a higher intensity than the derivatised amine (hydrolysis detected by TLC using petroleum ether/ethyl acetate, 95:5). The background hydrolysis interferes with the detection of the amine product and therefore dansyl chloride is an unsuitable reagent for this assay. The fluorescamine hydrolysis product is not fluorescent and the rate of derivatisation is 10^4 times faster than the hydrolysis reaction.[131] Nonetheless, fluorescamine was found to be unsuitable for the derivatisation of amines due to interference from amine contaminants from the whole cell biocatalysts.

5.2.3 Enzyme Coupled Assays

To address the issue of high background interference from whole cell contaminants in the spectrophotometric assays, the use of enzyme cascades were investigated. The aim was to couple the PAL catalyzed hydroamination reaction with enzymes such as oxidases, which are selective for the amine or amino acid product and produce hydrogen peroxide as a co-product. Hydrogen peroxide can then be detected using horse radish peroxidase (HRP) and a dye.[132] Using a soluble dye can allow reactions to be monitored spectrophotometrically making the assay quantitative. Alternatively, using an insoluble dye can allow the development of colony based screens.

5.2.3.1 L-Amino Acid Oxidase Coupled Assay

The L-amino acid oxidase (L-AAO) coupled assay for the detection of PAL catalyzed hydroamination of cinnamic acid analogues has been described previously in section 2.2.3: *L-amino acid oxidase coupled assay*. The L-amino acid product from the PAL reaction is oxidised by L-AAO which uses oxygen to regenerate its FAD (flavin adenine dinucleotide) cofactor, concomitantly producing hydrogen peroxide, which is detected using HRP and a dye (Scheme 49).



Scheme 49: L-AAO coupled assay for the detection of L-amino acid formation using the fluorescent dye scopoletin. In the presence of hydrogen peroxide and HRP, scopoletin is oxidised and the fluorescence is quenched

5.2.3.1.1 Liquid Phase Screening

For liquid phase screening commercially available purified L-AAO and HRP enzymes were used. However, this assay is unsuitable for screening PAL hydroamination activity over time using whole cell biocatalysts as L-AAO reacts with amino acids from the cells producing a high background signal. To address this problem, the L-AAO coupled screen can be performed as an endpoint assay on biotransformation samples after the whole cells have been cleared by centrifugation (Figure 46). Scopoletin fluorescence is very sensitive to changes in assay conditions and high concentrations of ammonia present in the reaction. Nonetheless, it gives an initial indication of PAL catalyzed hydroamination activity towards cinnamic acid derivatives. Coloured dyes such as pyrogallol red or ABTS are unsuitable for this assay as the colour formation is affected by high pH.

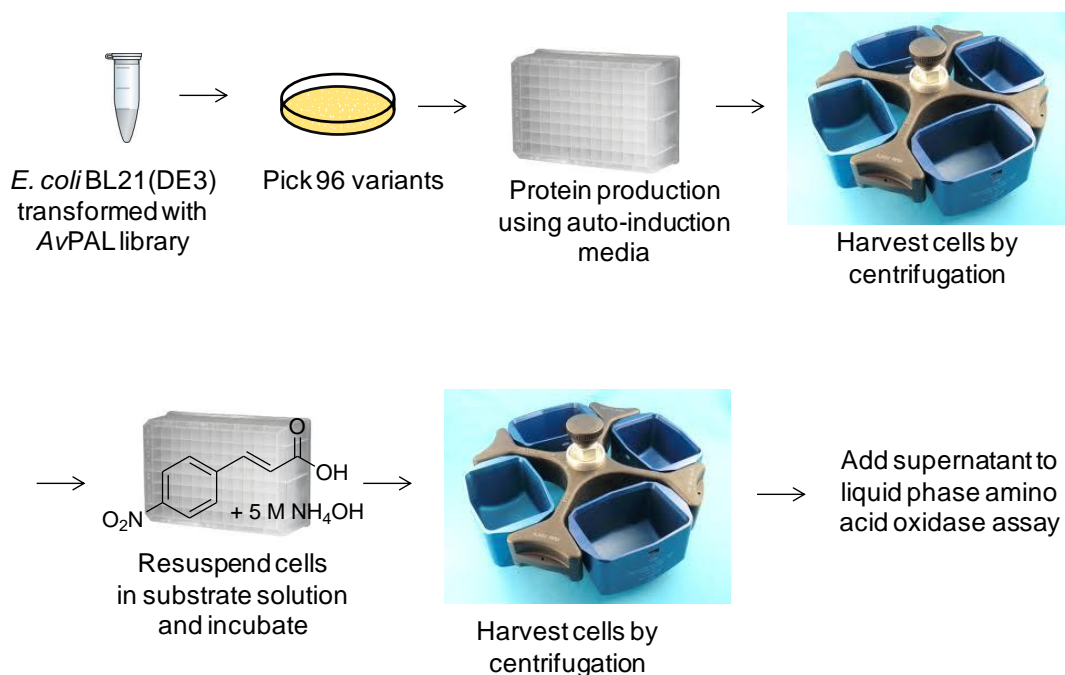


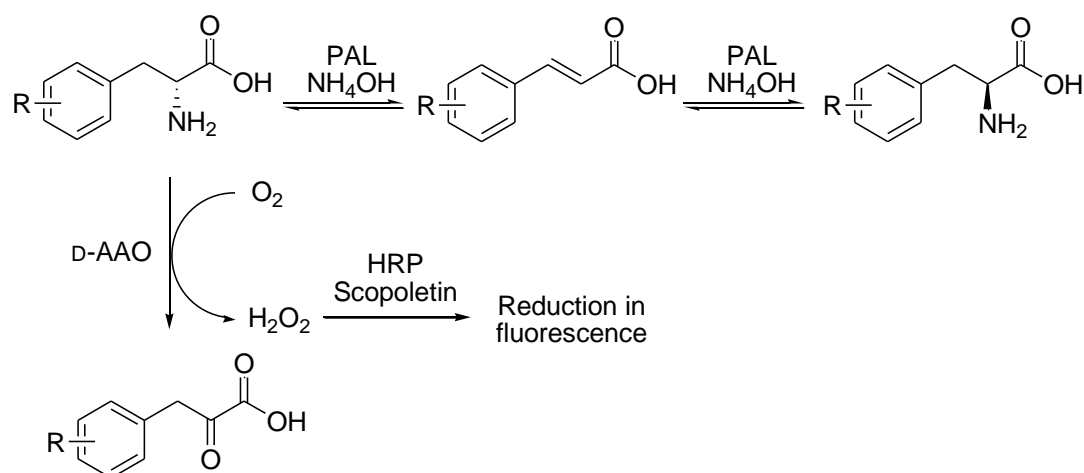
Figure 46: Method for the preparation of libraries and liquid phase screening using the L-AAO coupled assay

5.2.3.1.2 Colony Based Screening

There is potential for an L-AAO coupled assay to be used as a more high-throughput colony based screen if PAL can be co-expressed with an L-AAO in *E. coli* whole cells grown on a nitrocellulose membrane (for details on colony based screening see section 5.2.3.2: *D-amino acid oxidase coupled assay*). The expression of L-AAO's is problematic due to the toxicity of the enzyme.[133] Nonetheless, the L-AAO from the fungus *Hebeloma cylindrosporum* has been expressed in *E. coli* BL21(DE3) as a soluble active protein, although most of the expressed enzyme was found to be insoluble, inactive and in inclusion bodies.[134] With optimization of the *H. cylindrosporum* L-AAO expression system, this enzyme may prove to be useful in the future development of a colony based assay.

5.2.3.2 D-Amino Acid Oxidase Coupled Assay

It has been shown previously in section 2.6.1: *Analytical scale biotransformations*, that for many substrates, PAL catalyzed hydroamination reactions show a time dependence on e.e. Structures which possess electron deficient aromatic rings have the highest k_{cat} values and also show the most pronounced reduction in product e.e. with time. The correlation between the rate of the hydroamination reaction and the rate of D-amino acid formation can be exploited as the basis for a screen. PAL variants with a high catalytic turnover (k_{cat}) can be detected by measuring the formation of D-amino acids using the flavin dependent D-amino acid oxidase coupled to HRP and a dye (Scheme 50). This assay can also be used to screen libraries of variants with a view to develop D-selective catalysts. To achieve this, it would be interesting to screen variants for activity towards substrates such as cinnamic acid, 4-fluorocinnamic acid, 4-chlorocinnamic acid and 3-hydroxycinnamic acid which show excellent wild-type selectivity and yield the L-amino acid product exclusively.



Scheme 50: D-AAO coupled assay for detection of D-amino acid formation

5.2.3.2.1 Liquid Phase Screening

D-AAO from porcine kidney is commercially available as a lyophilized purified protein and can be used to screen for PAL activity in a liquid phase assay. The method used for the detection of D-amino acid formation is the same as described in the previous section 5.2.3.1.1: *Liquid phase screening* by substituting the L-selective AAO for D-AAO.

5.2.3.2.2 Colony Based Screening

The D-AAO coupled assay can also be exploited as a colony based screen by co-expression of both D-AAO and PAL. The gene encoding D-AAO from the yeast *Trigonopsis variabilis* (*Tv*-D-AAO) was codon optimised for *E. coli* expression and synthesized by Life Technologies (Invitrogen division). The D-AAO gene was subcloned into a pRSF-duet vector using NcoI and NotI restriction sites. For screening, *E. coli* BL21(DE3)-Gold cells are co-transformed with a library of pET-16b-PAL and pRSF-D-AAO (Figure 47) and colonies are grown on a permeable nitrocellulose membrane placed on a LB-agar plate. For overproduction of the two enzymes, the membrane is transferred to a second plate containing LB-agar and IPTG (1 mM) and incubated overnight at 20 °C. The membrane is subjected to three cycles of freeze-thawing in liquid nitrogen to partially lyse the cells and it is then placed on a filter paper soaked in the assay solution containing substrate (10 mM), HRP (0.1 mg/mL) and 3,3'-diaminobenzidine (DAB) in 2.5 M NH₄OH pH 9.5. DAB is oxidised in the presence of HRP and hydrogen peroxide to give a dark-brown precipitate, which is localised in the active colony and does not diffuse across the filter paper. This method can be used to screen thousands of colonies in parallel and is compatible with screening large random libraries.

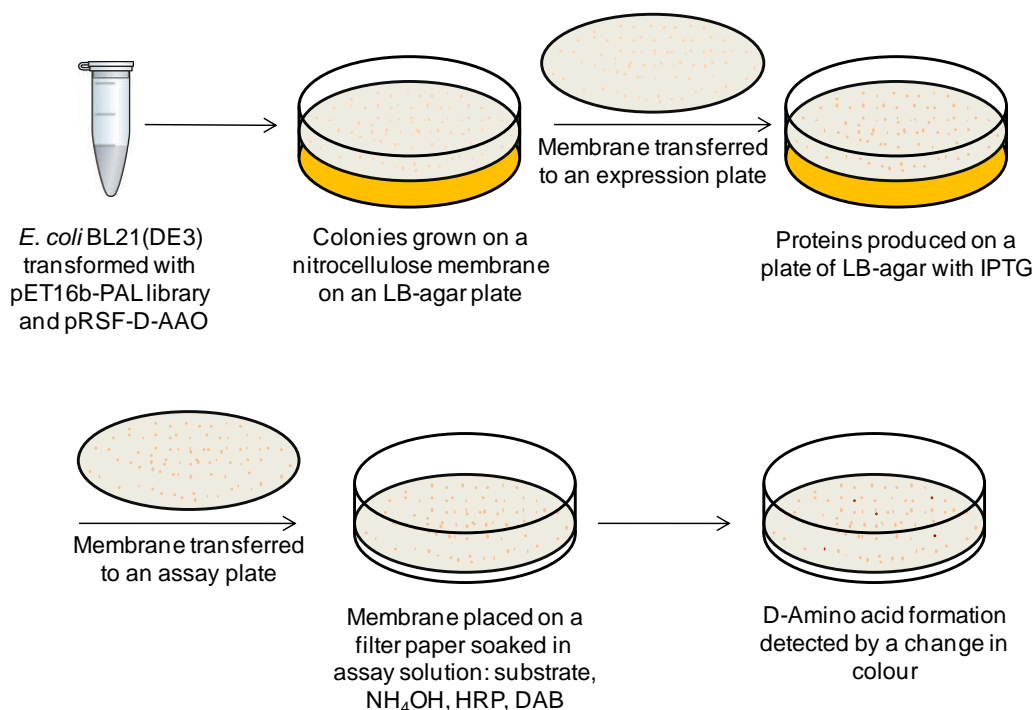
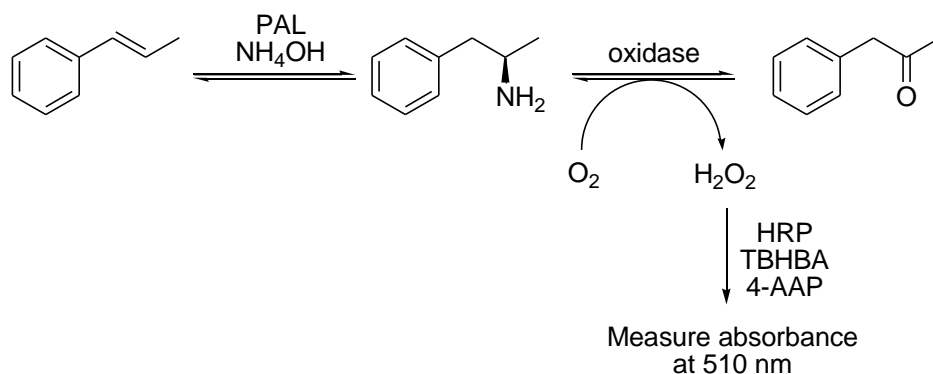


Figure 47: Method of screening libraries using the D-AAO coupled colony based assay

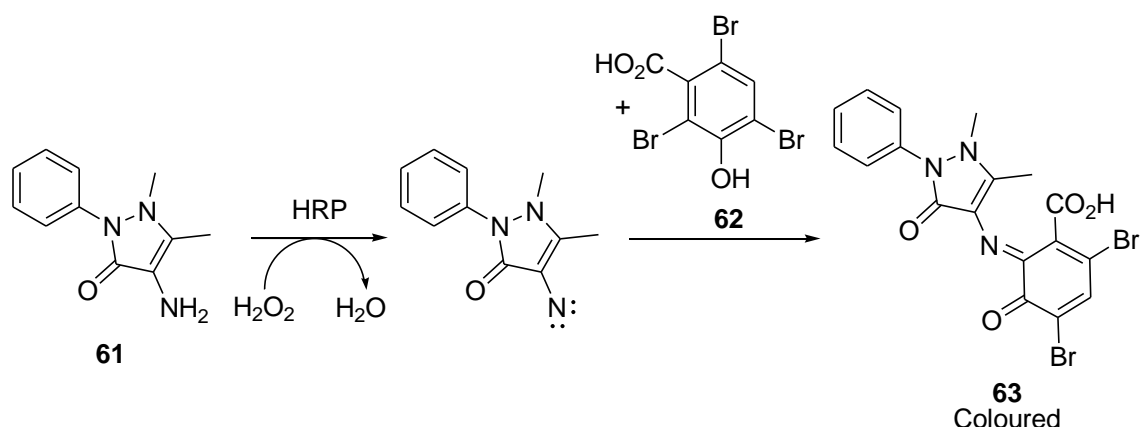
5.2.3.3 Amine-Oxidase Coupled Assay

Amino acid oxidases do not accept amines, therefore for the detection of PAL catalyzed hydroamination activity towards substrates lacking carboxylic acid functionality an alternative enzyme coupled reaction is required. Both FAD-dependent amine oxidases and copper amine oxidases catalyze the transformation of primary amines to imines, use oxygen and release hydrogen peroxide. Therefore the detection of hydrogen peroxide co-product can be used to measure PAL catalyzed amine formation (Scheme 51).



Scheme 51: Assay for the detection of oxidase activity towards (*R*)-amphetamine

Several amine oxidases were screened for their ability to catalyze the oxidation of (*R*)-amphetamine. Purified enzymes were screened spectrophotometrically using the compounds 4-aminoantipyrine **61** (4-AAP) and 2,4,6-tribromo-3-hydroxybenzoic acid **62** (TBHBA), which form a coloured quinone-imine complex **63** in the presence of hydrogen peroxide and HRP (Scheme 52).[135]



Scheme 52: HRP catalyzed oxidation of 4-AAP and subsequent reaction with TBHBA. Amine oxidases generate hydrogen peroxide which drives the peroxidase dependent oxidation of 4-AAP, which subsequently reacts with TBHBA to give coloured quinone-imine complex **63**

Monoamine oxidase from *Aspergillus niger* (MAO-N) has been previously engineered by the Turner research group[9,11-13] and the variants D5, D9 and D11 were screened for activity towards (*R*)- and (*S*)- amphetamine. *E. coli* BL21(DE3) was transformed with the pET-16b

vectors encoding the different MAO-N variants. The variants were overexpressed in LB with IPTG induction (1 mM at OD₆₀₀=0.8) and the His-tagged protein was purified by nickel affinity chromatography (See 6: *Materials and Methods* for details). The purified proteins were assayed spectrophotometrically and the results show that (S)-amphetamine is a good substrate for the MAO-N D9 variant (Figure 48). Unfortunately, the expected product from the PAL catalyzed hydroamination of β -methylstyrene is (R)-amphetamine, which was not accepted by any of the variants screened.

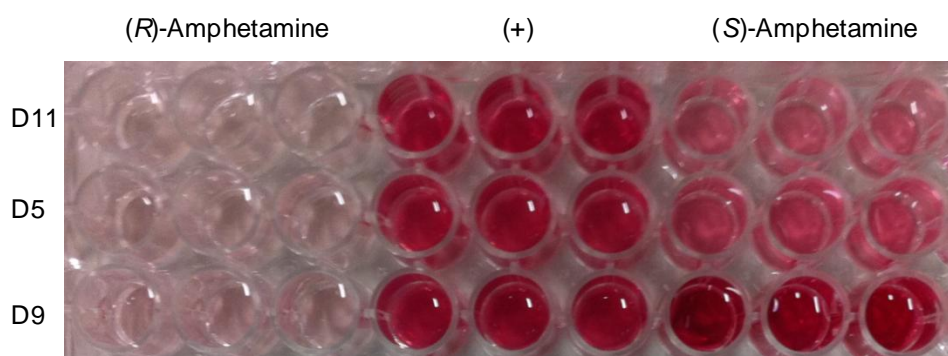


Figure 48: Screening MAO-N D5, D9 and D11 (0.25 mg/mL) for activity towards (R)- and (S)-amphetamine (10 mM) using HRP with TBHBA and 4-AAP. Formation of the red colour was measured at 510 nm and indicates a positive reaction (+)= positive control with (S)-methylbenzylamine (10 mM)

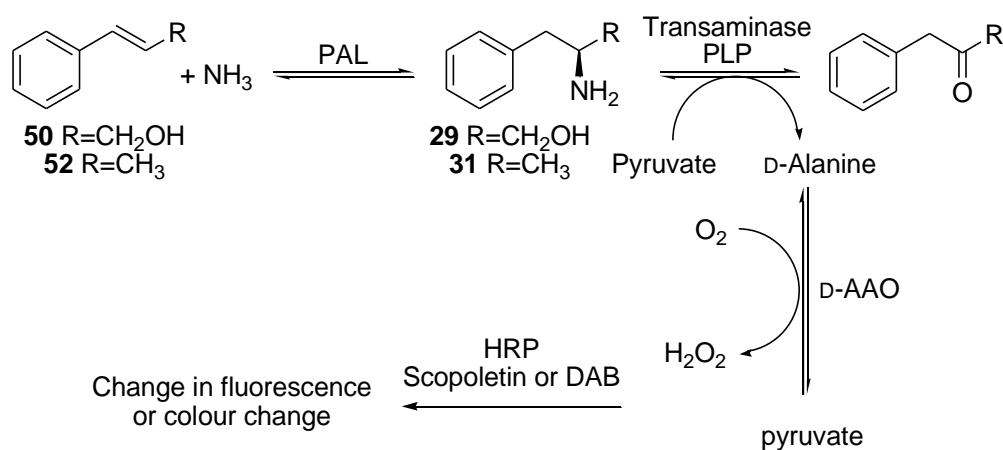
A commercially available diamine oxidase (DAO) from porcine kidney was identified which has natural activity towards phenylethylamine.[136] The DAO has been reported to stereoselectively abstract the pro-S hydrogen from the C₁ position of the substrate. Therefore, it was hypothesised that if amphetamine was accepted as a substrate, the enzyme would favour the (R)-enantiomer. DAO was screened for activity towards both (R)- and (S)-amphetamine using the spectrophotometric assay. Although a positive result was detected for the natural substrate phenylethylamine, DAO did not show any activity towards either enantiomer of amphetamine.

E. coli amine oxidase (EcAO) is a copper containing quinoprotein which is reported to catalyze the oxidation of primary amines such as tyramine and phenylethylamine to the corresponding aldehydes with release of ammonia and hydrogen peroxide.[137] EcAOs contain one copper ion per subunit and have an organic cofactor 2,4,5-trihydroxyphenylalanine quinone (TPQ) which is formed by autocatalytic postranslational modification. Interestingly, it has been reported that EcAO can also catalyze the conversion of the branched amine, (R)-amphetamine.[138] The pkk-2 plasmid carrying the gene for EcAO expression was received as a gift from Prof. Michael McPherson (University of Leeds). EcAO was overexpressed in *E. coli* BL21(DE3) cells using IPTG induction (1 mM at OD₆₀₀=0.6) and the protein was purified by ion exchange chromatography according to the published procedure.[139] The purified enzyme was screened in the liquid phase spectrophotometric assay for activity towards amphetamine and phenylethylamine. Although activity towards phenylethylamine was observed, no activity towards either enantiomer of amphetamine was detected. The previous

study, which suggests that (*R*)-amphetamine is a substrate for EcAO measures the oxygen consumption to determine the activity and does not characterize the ketone product.[138] In agreement with our results, TPQ-dependent amine oxidases have been largely reported to show no conversion of α -branched primary amines to ketones as a result of steric constraints.[137] Consequently amine oxidases were found to be unsuitable for use in the enzyme coupled assay.

5.2.3.4 Transaminase/D-AAO Coupled Assay

A transaminase and D-amino acid oxidase coupled reaction was investigated as a method for detecting PAL catalyzed hydroamination activity towards cinnamyl alcohol (**50**) and β -methylstyrene (**52**) derivatives (Scheme 53). Transaminases are pyridoxal phosphate (PLP) cofactor dependent enzymes which catalyze the transformation of prochiral ketones to chiral amines in the presence of an amine donor. When pyruvate is used as the acceptor substrate, alanine is formed as the product and this can then be oxidised using an amino acid oxidase.



Scheme 53: Assay for the detection of (*R*)-amphetamine and (*S*)-phenylalaninol using a transaminase, D-AAO and HRP

5.2.3.4.1 Liquid Phase Screening

The commercially available (*R*)-selective transaminase ATA-117 from *Arthrobacter sp.* (supplied as purified lyophilized enzyme by Codexis) was screened for activity towards a small panel of amines and amino alcohol substrates (Figure 49). ATA-117 was added to an assay solution of amine substrate, PLP, pyruvate, D-AAO (from porcine kidney), HRP and scopoletin and a reduction in fluorescence indicated transaminase activity. ATA-117 showed good activity towards (*R*)-amphetamine **31** and a clear decrease in scopoletin fluorescence was observed. However, the activity of ATA-117 towards amino alcohols and amine substrates with substituents on the aromatic ring was slightly lower (Figure 49).

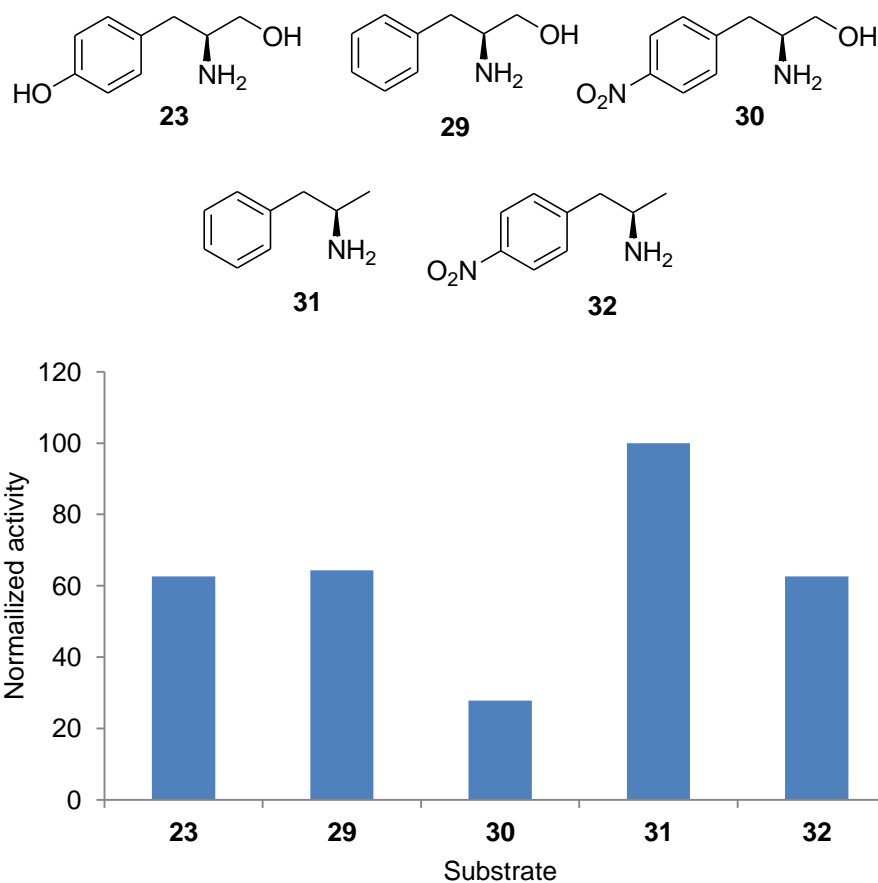


Figure 49: The activity of ATA-117 towards different amine substrates

The (*R*)-selective transaminase from *Arthrobacter sp.* has been engineered by Merck and Codexis for activity towards pro-sitagliptin ketone, the precursor of the antidiabetic compound sitagliptin.[22] This variant was also screened for activity towards the substrates **23** and **26-29**. *E. coli* BL21(DE3) cells were transformed with the plasmid pET-16b carrying the gene for the transaminase variant which was synthesized by Life Technologies (Invitrogen division). The protein was overexpressed in LB media with IPTG induction (1 mM at O.D₆₀₀=0.8) and the His-tagged protein was purified by nickel affinity column chromatography (See section 6: *Materials and Methods* for details). The purified enzyme was screened for activity towards substrates **23** and **26-29** using the hydrogen peroxide detection assay with HRP and scopoletin, but no activity was detected. Therefore for future screening, the commercially available ATA-117 transaminase (Codexis) was used.

5.2.3.4.2 Colony Based Screening

The transaminase/D-AAO coupled screen can be used as a solid phase colony based assay. The genes encoding *Trigonopsis variabilis* D-AAO and *Arthrobacter sp.* transaminase were synthesized by Life Technologies (Invitrogen Division) and subcloned into the pRSF-duet vector by Dr. Rachel Heath. The method for screening libraries of variants using the transaminase/D-AAO coupled assay is similar to the method for the D-AAO coupled screen discussed in *section 5.2.3.2: D-amino acid oxidase coupled assay*. Colonies of *E. coli* BL21(DE3)-Gold are co-transformed with a library of pET-16b-PAL plasmids and the pRSF-duet vector containing the genes for D-AAO and transaminase. Colonies are grown on a nitrocellulose membrane on top of a LB-agar plate. For overproduction of the enzymes, the membrane is transferred to a second plate of LB-agar containing IPTG (1 mM) and the plate is incubated overnight at 20 °C. The membrane is subjected to three cycles of freeze-thawing in liquid nitrogen to partially lyse the cells. The membrane is placed on a filter paper soaked in a pre-assay mix of pyruvate (0.2 mg/mL) and HRP (0.1 mg/ml) to react with any hydrogen peroxide present in the cells. The membrane is then finally placed on a filter paper soaked in the assay solution containing substrate (10 mM), pyruvate (0.2 mg/mL), HRP (0.1 mg/mL) and DAB in 2.5 M NH₄OH pH 9.5 which turns a dark brown colour to indicate a positive reaction. Control reactions were performed by spiking the assay mix with varying concentrations of (*R*)-amphetamine and a significant difference in colour was observed between the different amine concentrations (Figure 50). Colonies transformed with empty vectors, which do not express transaminase, D-AAO or PAL enzymes did not change colour in the presence of (*R*)-amphetamine. This assay is compatible with screening thousands of variants in parallel and can be used to screen large random libraries of PAL variants.

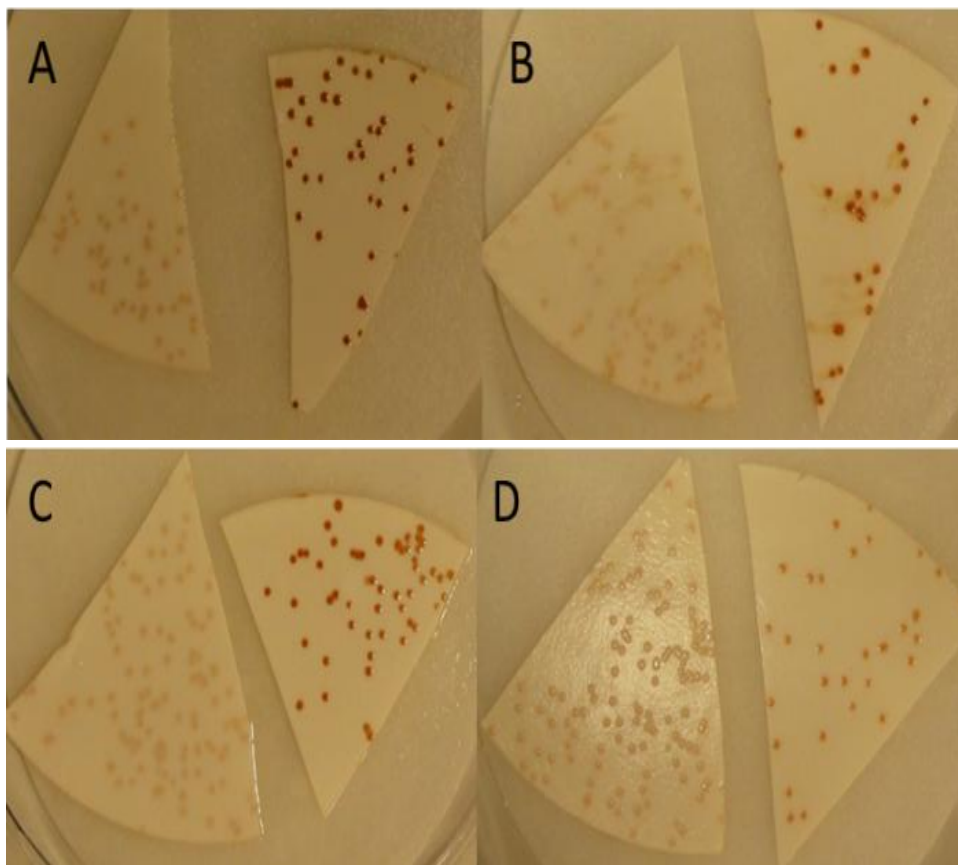


Figure 50: Transaminase coupled assay for the detection of *trans*- β -methylstyrene hydroamination activity. The left membrane has colonies transformed with empty pET-16b and duet-pRSF vectors and the right membrane has colonies expressing PAL, transaminase and D-AAO. Filter papers are soaked in pyruvate, HRP and DAB and spiked with A) 20 mM B) 2 mM C) 0.2 mM and D) no (*R*)-amphetamine. These control reactions were performed by Dr. Rachel Heath

5.2.4 Summary of Assays

Screening methods have been successfully developed to detect the formation of both amino acid and amine products. The assays developed include both liquid phase screens using 96-well plates and colony based screens. The advantages and disadvantages of the different assays are summarised in Table 20.

Table 20: Advantages and disadvantages of the newly developed screening methods

Method	Advantages	Disadvantages
Measuring the absorbance of alkene products <i>Section 5.2.1</i>	<ul style="list-style-type: none"> - Useful for detecting turnover of amino acids and <i>N</i>-substituted amino acids - Quantitative - Uses cheap reagents - No need for derivatisation steps or enzyme coupling reactions 	<ul style="list-style-type: none"> - Not compatible with substrates which have the same absorbance profile as product - Not sensitive enough to detect activity towards products with low UV absorbance - Can't be used to measure hydroamination activity
L-AAO coupled liquid phase assay <i>Section 5.2.3.1.1</i>	<ul style="list-style-type: none"> - Measures hydroamination activity of cinnamic acid analogues - Semi-quantitative - Can be used to detect activity greater than the wild-type enzyme 	<ul style="list-style-type: none"> - Not compatible with colony based screening - Extra steps required to remove whole cell material - Scopoletin fluorescence sensitive to changes in assay conditions
D-AAO coupled liquid phase and colony based assays <i>Section 5.2.3.2</i>	<ul style="list-style-type: none"> - Measures hydroamination activity of cinnamic acid analogues - Liquid phase screen is semi-quantitative - Colony based assay is high-throughput - Positive results can indicate enhanced D-selective or increased activity 	<ul style="list-style-type: none"> - Scopoletin fluorescence used in liquid phase screen is sensitive to changes in assay conditions - High D-activity does not necessarily correlate to enhanced D-selectivity
Transaminase/D-AAO coupled liquid phase and colony based assays <i>Section 5.2.3.4</i>	<ul style="list-style-type: none"> - Measures formation of amines - Liquid phase screen is semi-quantitative - Colony based assay is high-throughput 	<ul style="list-style-type: none"> - Scopoletin fluorescence used in liquid phase screen is sensitive to changes in assay conditions - Transaminase does not accept all amines screened as substrates in chapter 4

5.3 Screening

This section describes the generation of libraries in AvPAL and their subsequent screening using the assays described in the previous section. To screen for D-selective variants, small focused libraries were generated and screened using the liquid phase D-AAO coupled assay (section 5.2.3.2: *D-amino acid oxidase coupled assay*). The transaminase/D-AAO colony based assay (section 5.2.3.4: *Transaminase/D-AAO coupled assay*) was used to screen large libraries of random variants for amine formation.

5.3.1 Screening Variants for Enhanced D-Selectivity

5.3.1.1 Generation of Libraries

The PAL catalyzed hydroamination of 4-nitrocinnamic acid has been shown to favour the formation of 4-nitro-D-phenylalanine (e.e = 14) after prolonged reaction times (see 3.4: *Thermodynamic position of equilibrium*). Therefore 4-nitrocinnamic acid was chosen as a target substrate for screening variants with enhanced D-selectivity. Due to the high wild-type activity towards D-amino acid formation, the semi-quantitative liquid-phase D-AAO coupled assay was chosen in an attempt to detect variants with higher D-activity than the wild-type enzyme. The D-AAO colony based assay was not selected as it does not give quantitative results and a large number of positive hits were expected. The reduced screening capacity of the liquid-phase screen compared to the colony-based screen requires the generation of smaller focused libraries. 4-Nitrocinnamic acid was modelled in the AvPAL active site in order to predict residues which may affect substrate binding (Figure 51). The computational modelling suggested that residues Phe107 and Thr110 directly interact with the nitro-substituent on the substrates aromatic ring. These residues were targeted to investigate if these positions could influence the binding conformation of the substrate in the active site, leading to a change in enantioselectivity.

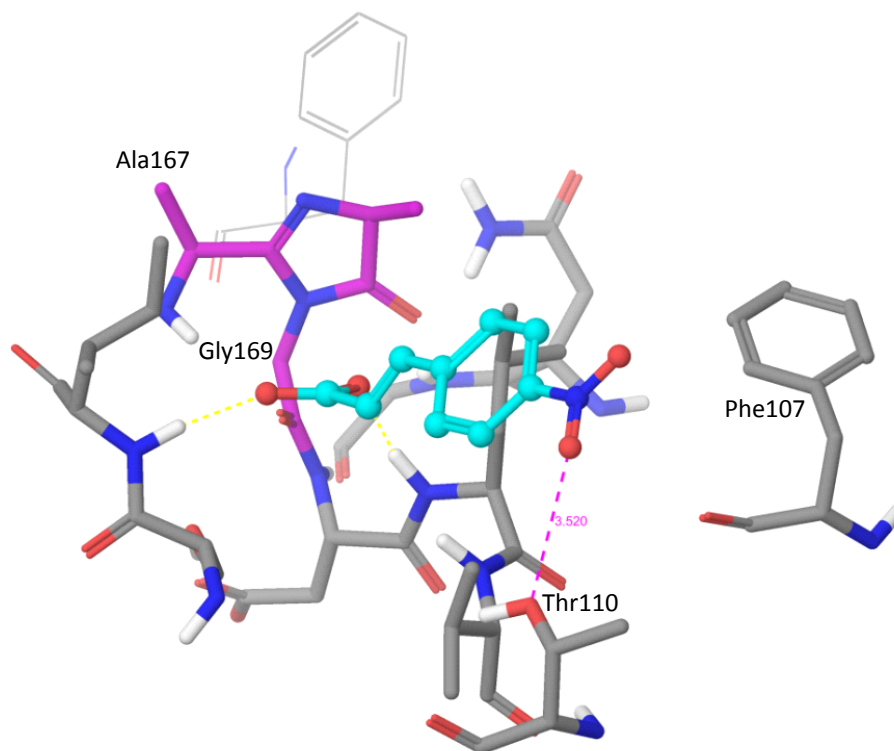


Figure 51: 4-Nitrocinnamic acid modelled in the AvPAL active site with hotspots F107, T110, A167 and G169 for site-directed mutagenesis (modelling by Dr. Sebastian Kroll, Dr. Reddy's)

The mechanistic study of PAL catalyzed D-amino acid formation (chapter 3) suggests that the reaction is MIO-cofactor independent, but the dominant pathway leading to L-amino acid formation is MIO-dependent. Docking L- and D-phenylalanine in the AvPAL active site (see 3.8: *Docking study*) showed that for both enantiomers, the substrates' amine group lies in close proximity to the MIO-cofactor. Therefore the residues Ala167 and G169 which are adjacent to the cofactor are of interest when targeting activity toward D-amino acids. Mutating these residues could have an effect on the electrophilicity of the MIO-cofactor and introducing more bulky residues can influence the substrate's binding conformation in the active site. However, introducing bulky substituents at the positions adjacent to the MIO could also prevent or hinder formation of the cofactor.

Four libraries at positions F107, T110, A167 and G169 were generated using QuikChange site-directed mutagenesis (Agilent) and NNK codons. Sequencing of a sample of 10-15 variants from each library showed in all cases the mutation efficiency was greater than 80 %. For each library 92 variants must be screened to ensure 95 % coverage of mutations and therefore these libraries can be easily screened in 96-well plates.

5.3.1.2 Screening Libraries

E. coli BL21(DE3) cells were transformed with each of the four libraries F107NNK, T110NNK, A167NNK and G169NNK and the variants were prepared as described in section 5.2.3.1, Figure 46. The whole cell biocatalysts were resuspended in a substrate solution of 4-nitrocinnamic acid (5 mM) in NH_4OH (5 M, pH 9.5) and incubated at 30 °C for 2 hours. The cells were cleared by centrifugation and the supernatant was removed and applied to both the L-AAO and D-AAO coupled assays in parallel. The decrease in scopoletin fluorescence was measured spectrophotometrically and the results from the L-AAO and D-AAO assay were compared. Interestingly, active variants showing 4-nitrocinnamic acid amination activity also turned a yellow colour and were easily identified by eye (Figure 52). Unfortunately, comparison of the data from the L-AAO and D-AAO coupled assays did not highlight any variants which demonstrated a significant change in enantioselectivity compared to the wild-type enzyme. Therefore all active variants were selected and the DNA was sequenced.

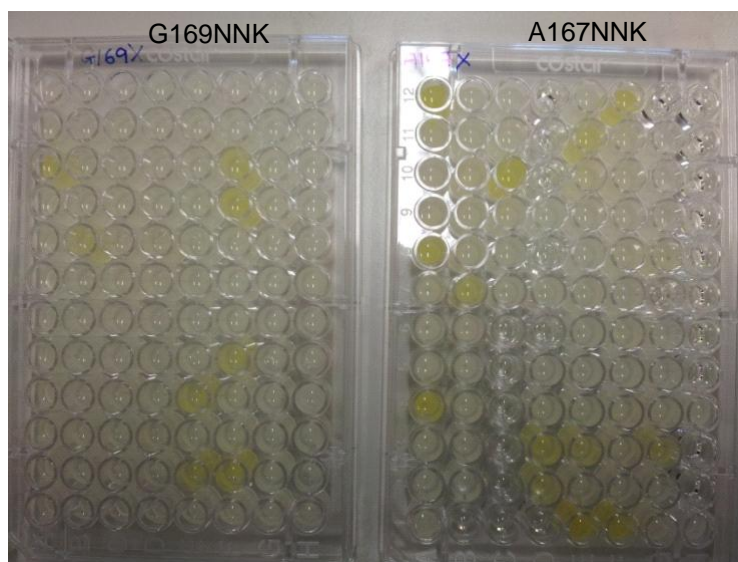


Figure 52: Screening of libraries G169NNK and A167NNK using the L-AAO assay

E. coli BL21(DE3) cells were transformed with all positive variants and the proteins were expressed according to the general protocol. Whole cells, each expressing a single PAL variant, were used in biotransformations and the conversion and product e.e were measured after 24 hours incubation at 30 °C (Table 21). Each set of variants were assayed on different days and for each set of biotransformations a reaction using wild-type AvPAL was performed in parallel. The conversion and product e.e for the wild-type reactions on different days show small variations which may arise from small changes in the reaction conditions such as pH, temperature or substrate concentration. For each variant, reactions starting from 4-nitro-L-phenylalanine and 4-nitro-D-phenylalanine were performed under the same amination reaction conditions to determine the position of equilibrium. Only the reactions catalyzed by wild-type AvPAL and the variants F107L, T110S, T110I and T110N reached the same final ratio of products starting from each of the three components. For each of these variants the final

position of equilibrium was the same as for wild-type AvPAL. Some variants such as A167T, A167C and G169A demonstrated an apparent improved selectivity for the L-enantiomer. However, the same ratio of products was not achieved starting from 4-nitro-L-phenylalanine and 4-nitro-D-phenylalanine. This suggests the reactions may not be at equilibrium and the high L-selectivity may be a consequence of a slow rate of reaction.

Table 21: Percentage conversion and product e.e. (for the L-enantiomer) for the hydroamination reaction of 4-nitrocinnamic acid catalyzed by different AvPAL variants

AvPAL variant	conv. (%) ^a	e.e (%)
wild-type	82	8
A167T	73	90
A167C	74	77
A167S	80	29
G169A	76	66
wild-type	74	-1
F107T	80	69
F107L	79	0
F107I	81	25
F107A	76	5
F107Y	78	13
wild-type	75	2
T110S	72	0
T110I	76	1
T110N	72	0

[a] Substrate (5 mM) in 5 M NH₄OH pH 9.5 at 30 °C after 24 hours

To further characterize the variants A167T, A167C, A167S and G169A for which the equilibrium position could not be determined, the deamination kinetic constants were measured. The kinetic constants were also measured for the variants T110S, T110I and T110N for which the position of equilibrium could be determined. Monitoring the conversion and product e.e over time using whole cell biocatalysts expressing each of the T110 variants, showed a faster rate of conversion and reduction in product e.e compared to the wild-type enzyme (Figure 53). This suggests that T110S, T110I and T110N variants have higher activity than wild-type AvPAL, however after 24 hours all reaction reached the same final composition of products.

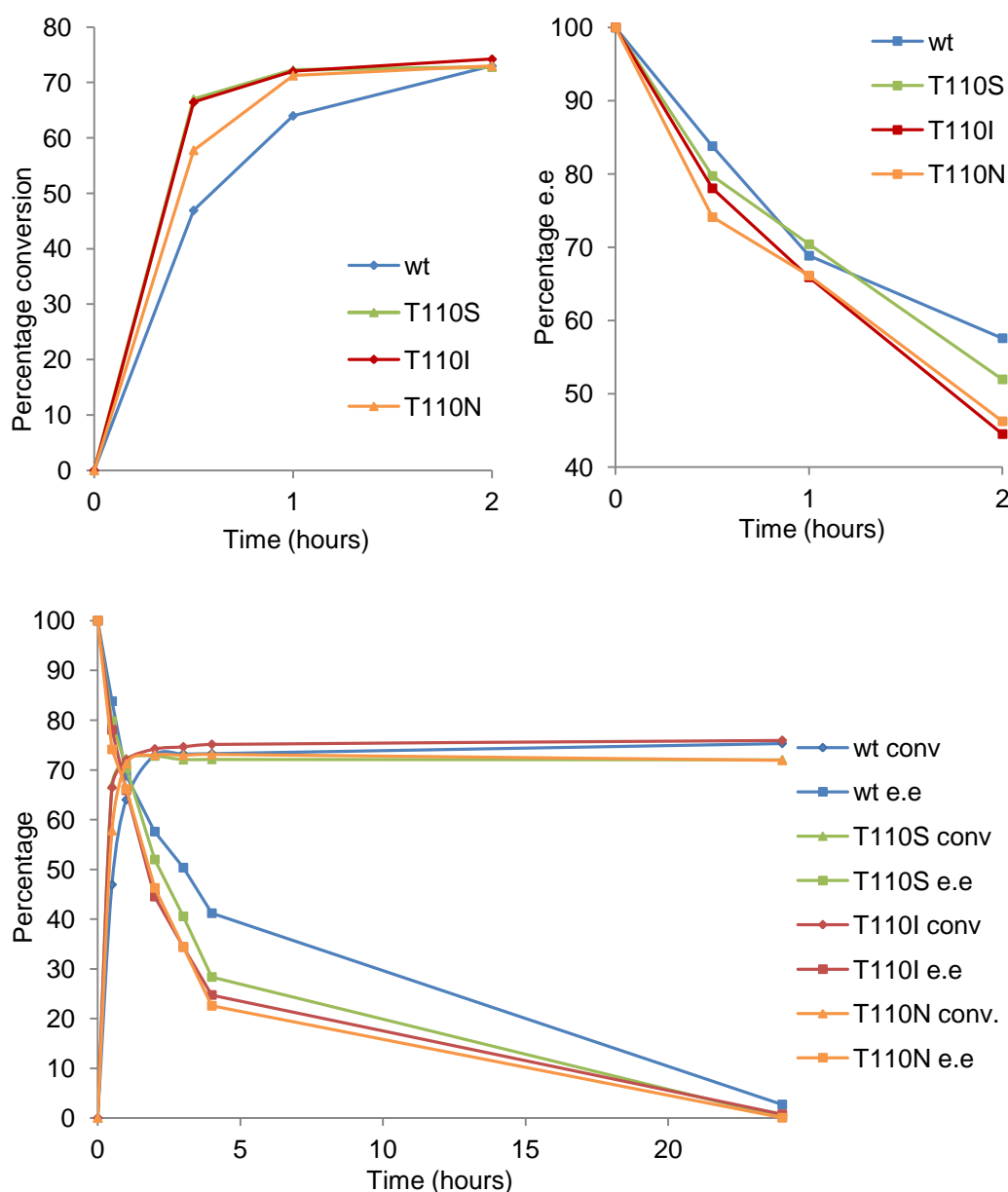


Figure 53: The percentage conversion and product e.e for the hydroamination of 4-nitrocinnamic acid (5 mM in NH_4OH 5 M, pH 9.5, 30 °C) catalyzed by wild-type AvPAL and variants. After 24 hours the variants showed higher substrate conversion and lower product e.e however after 24 hours the reactions had reached the same final composition of products

The variants A167T, A167C, A167S, G169A, T110S, T110I and T110N were each purified using nickel affinity column chromatography and the fractions containing purified proteins were identified by SDS-PAGE, pooled and concentrated (Figure 54).

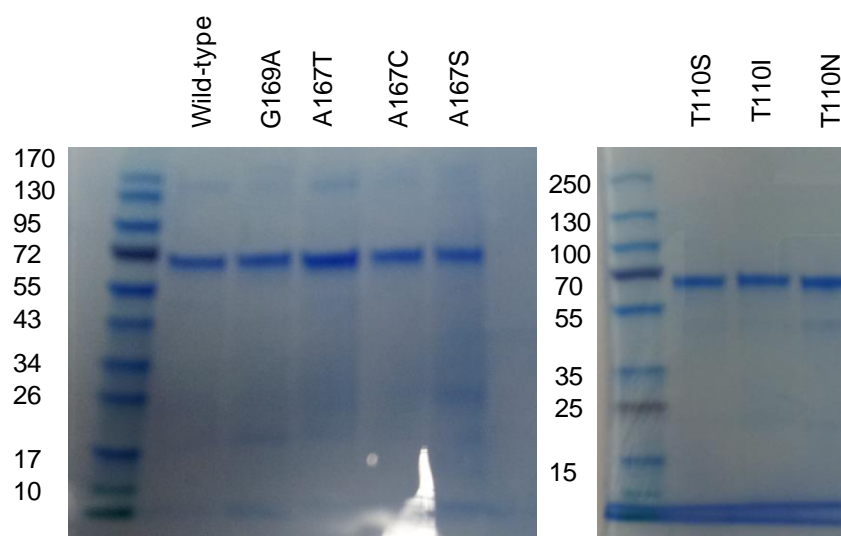


Figure 54: SDS-gels of purified wild-type AvPAL and variants with molecular weight markers and masses shown to the right of the gel

The kinetic constants for the deamination of 4-nitro-L-phenylalanine and 4-nitro-D-phenylalanine were determined spectrophotometrically (see 2.2.2: *Spectrophotometric analysis*) and the results are shown in Table 22. The MIO mutants A167T, A167C, A167S and G169A all showed lower activity (k_{cat}) than the wild-type enzyme towards both enantiomers of 4-nitrophenylalanine. For the deamination of 4-nitro-L-phenylalanine the value of K_M for all MIO mutants with the exception of G169A, were similar to the wild-type enzyme. Interestingly, the K_M value for the deamination of 4-nitro-D-phenylalanine was considerably larger for the MIO mutants than wild-type AvPAL. This suggests that these mutations have unfavourable interactions with the D-enantiomer, causing it to bind more weakly in the active site. The relative rates for the deamination reaction ($k_{cat(L)}/k_{cat(D)}$) catalyzed by A167T shows a preference for the L-enantiomer compared to the wild-type reaction whilst the variant G169A shows an increase in the D-selectivity. The k_{cat} values for A167T and G169A catalyzed deamination of both 4-nitro-L-phenylalanine and 4-nitro-D-phenylalanine are lower than the k_{cat} values for the S168A variant, which cannot form the MIO cofactor by post-translational modification (see 3.6.1: *Kinetic constants for S168A catalyzed reactions*). This suggests the A167T and G169A variants may not have formed the MIO cofactor effectively and the activity observed may be occurring via an MIO-independent pathway.

The T110 variants T110S, T110I and T110N showed two to three fold higher activity (k_{cat}) towards the deamination of both 4-nitro-L-phenylalanine and 4-nitro-D-phenylalanine compared to the wild-type enzyme. Although the variant T110N showed the highest turnover of 4-nitro-L-phenylalanine, T110I showed the highest turnover of 4-nitro-D-phenylalanine.

Furthermore, the relative rates for the deamination reaction ($k_{\text{cat(L)}}/k_{\text{cat(D)}}$) catalyzed by T110I show that the ratio of L-activity to D-activity has decreased representing an increase in the D-selectivity.

Table 22: Kinetic constants for the deamination of 4-nitro-L-phenylalanine and 4-nitro-D-phenylalanine catalyzed by wild-type AvPAL and variants.

Variant	4-nitro-L-phenylalanine ^a			4-nitro-D-phenylalanine ^a			$k_{\text{cat(L)}}/k_{\text{cat(D)}}$
	$k_{\text{cat}} (\text{s}^{-1})$	$K_{\text{M}} (\text{mM})$	R^2	$k_{\text{cat}} (\text{s}^{-1})$	$K_{\text{M}} (\text{mM})$	R^2	
wild-type	1.21	0.46	0.99	0.11	0.06	0.99	11.0
A167T	0.027	0.59	0.97	0.0022	0.70	0.90	12.3
A167C	0.068	0.48	0.99	0.0061	0.78	0.95	11.1
A167S	0.63	0.39	0.99	0.059	0.24	0.99	10.7
G169A	0.0015	0.08	0.99	0.0003	1.0	0.85	5.0
T110S	2.10	0.63	0.99	0.18	0.12	0.99	11.7
T110I	2.14	0.60	0.99	0.34	0.06	0.99	6.3
T110N	2.40	0.56	0.99	0.23	0.05	0.99	10.4
S168A ^b	0.045	0.137	0.90	0.025	0.329	0.86	1.8

[a] Deamination reactions were performed in 0.1 M borate buffer pH 8.3 at 30 °C in a 96-well plate using an Eppendorf BioSpectrometer [b] The kinetics for S168A were determined previously under the same reaction conditions but using cuvettes and a Varian Cary-series UV-Vis spectrophotometer (Agilent)

The kinetic constants were also measured for the 4-nitrocinnamic acid hydroamination reaction catalyzed by wild-type AvPAL and T110S, T110I and T110N variants (Table 23). The results showed that the variants have increased hydroamination activity (k_{cat}) towards 4-nitrocinnamic acid compared to the wild-type enzyme. T110N was the most active variant and showed a two-fold increase in activity (k_{cat}) towards 4-nitrocinnamic acid.

Table 23: Kinetic constants for the amination of 4-nitrocinnamic acid

variant	k_{cat} (s ⁻¹)	K_M (mM)	R^2
wild-type	4.2	0.56	0.92
T110S	6.2	0.91	0.80
T110I	5.6	0.54	0.85
T110N	8.0	0.96	0.71

Amination reactions were performed in 5 M NH₄OH pH 9.5 at 30 °C

5.3.2 Screening Variants for Activity Towards Amine Substrates

5.3.2.1 Generation of Libraries

A large library of AvPAL genes each with a single mutation (and subcloned into pET-16b) were provided by Codexis. The library included 192 amino acid positions randomized using NNK codons and the variants were subdivided into four equal sized pools based on the amino acid residues proximity to the active site (Figure 55). For a full list of the amino acid positions covered in each pool see the appendix. Approximately five-fold oversampling of the theoretical library population size is necessary to observe 95 % of the mutations present.[16] Therefore, complete oversampling of a pool covering 48 positions will require screening of approximately 5,000 variants and these libraries will be screened using the colony based assays.

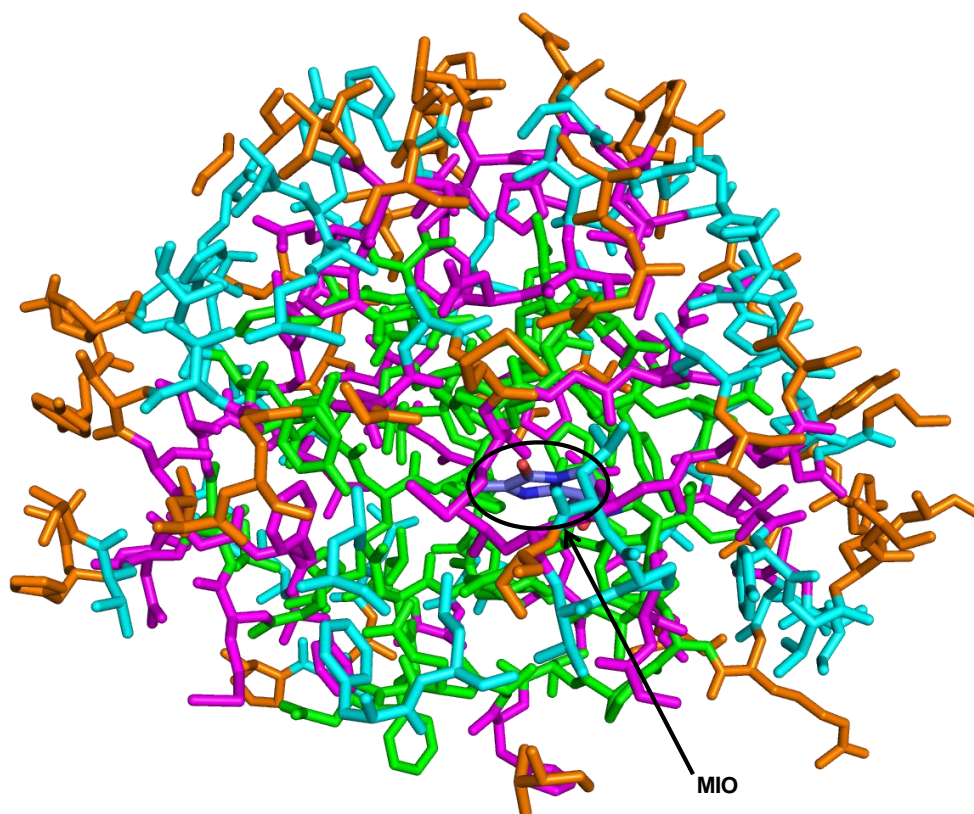


Figure 55: AvPAL amino acid positions incorporated into the library. Residues have been pooled together based on their proximity to the active site. Pool A (green), Pool B (magenta), Pool C (cyan) and Pool D (orange)

5.3.2.2 Screening Libraries

Both Pool A and Pool B were screened for activity using *trans*- β -methylstyrene and cinnamyl alcohol as substrates but unfortunately no colour indicating PAL activity was observed (Figure 56).



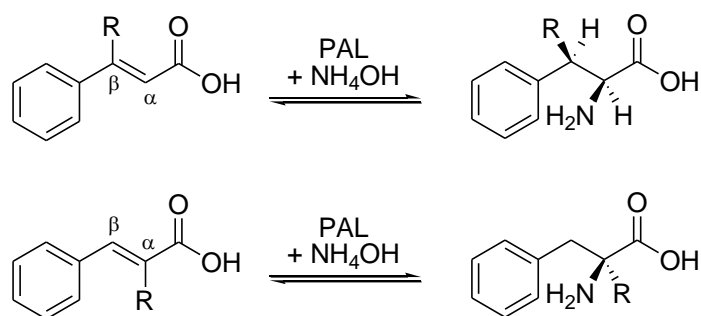
Figure 56: Colony based D-AAO/transaminase screen for PAL activity towards *trans*- β -methylstyrene using Pool A. No colour change was observed in any of the colonies screened

Due to the limited solubility of the substrates screened, 10 % DMSO was added as a co-solvent; nonetheless substrate availability in the whole cells may have presented an issue. Alternatively a single point mutation may not be sufficient to produce activity towards these non-substrates.

5.4 Conclusions and Future Work

A number of screens have been successfully developed including both spectrophotometric and colony based assays. The deamination of amino acids can be monitored by measuring the change in absorbance using whole cell biocatalysts in a 96-well plate. Furthermore the amination of cinnamic acid derivatives can be measured using the L-AAO and D-AAO coupled (endpoint) assays. The liquid phase methods have been used to successfully screen four rationally designed libraries for hydroamination activity towards 4-nitrocinnamic acid. MIO mutants at positions A167 and G169 had lower activity towards the deamination of both L- and D-enantiomers of 4-nitrophenylalanine compared to wild-type AvPAL. Interestingly, T110N was identified as a variant with higher activity (k_{cat}) towards the amination of 4-nitrocinnamic acid than the wild-type enzyme. In addition, the variant T110I showed enhanced D-selectivity in the deamination reactions of 4-nitrophenylalanine, however the final position of equilibrium was unaffected by the point mutation. In order to develop the D-selectivity of AvPAL biocatalysts further, it would be interesting to use the D-AAO solid phase assay to screen the large randomized libraries (Codexis). Targeting substrates such as cinnamic acid, 4-fluorocinnamic acid or 4-chlorocinnamic acid which show excellent wild-type selectivity for the L-amino acid product would be interesting as there is no wild-type activity.

There is potential to develop an L-AAO colony based assay by co-expression of PAL with membrane bound L-AAO enzymes. This could be used to screen for activity towards non-substrates such as β -substituted cinnamic acid derivatives for the formation of diastereoisomers or α -substituted derivatives (Scheme 54). A colony based, L-AAO coupled assay could also be used to screen for cinnamic acid derivatives with electron donating substituents on the aromatic ring, such as methoxy groups as these are currently poor substrates for PAL enzymes.



Scheme 54: PAL catalyzed hydroamination of α - and β -substituted cinnamic acid analogues

Lastly a transaminase and D-AAO coupled assay has been successfully developed to detect PAL catalyzed amine formation. Unfortunately, screening the Codexis libraries for activity towards *trans*- β -methylstyrene and cinnamyl alcohol did not yield any positive hits. Future work should focus on screening the four pools of variants for activity towards activated substrates such as 4-nitro- β -methylstyrene or 4-nitro-substituted cinnamyl alcohol, however these substrates suffer from limited solubility. Alternatively, pyridyl analogues can be screened as substrates which benefit from enhanced solubility.

Chapter 6: Materials and Methods

6 Materials and Methods

6.1 Chemicals and Reagents

Analytical grade chemicals and reagents were obtained from Sigma Aldrich Ltd, Fisher Scientific UK Ltd, AlfaAesar or Apollo Scientific. Auto induction media and LB pre-mix powders were purchased from ForMedium and all reagents were used as received from the supplier.

6.2 Genes and Enzymes

All genes were synthesized by Life Technologies (Invitrogen Division) based on the protein sequences and optimised for expression in *E. coli*. Genes were cloned into their respective vectors (Novagen) by members of the Turner group. For the cloning, plasmids were cut with restriction enzymes (according to Table 24), dephosphorylated with calf alkaline phosphatase and ligated with linearized vectors using a quick ligation kit (NEB). The constructs were transformed into *E. coli* XL1 blue cells (Agilent technologies), colonies were selected, the DNA was isolated using a mini-prep kit (Qiagen) and the correct constructs were confirmed by sequencing (GATC).

Table 24: Vectors containing different genes and restriction sites used for subcloning

Gene	Vector	Restriction site I	Restriction site II
<i>Av</i> PAL	pET-16b	NdeI	BamHI
<i>Rg</i> PAL	pET-16b	NdeI	BamHI
<i>Pc</i> PAL	pET-16b	NdeI	BamHI
<i>Pp</i> Rac	pRSF-Duet1	BamHI	NotI
<i>Tv</i> D-AAO	pRSF-Duet1	NcoI	NotI
transaminase	pRSF-Duet1	NdeI	XhoI

The pRSF-Duet1 vector has multiple cloning sites and both the *Tv* D-AAO and (*R*)-selective ω -transaminase were cloned into the same plasmid according to Figure 57 (performed by Dr. Rachel Heath).

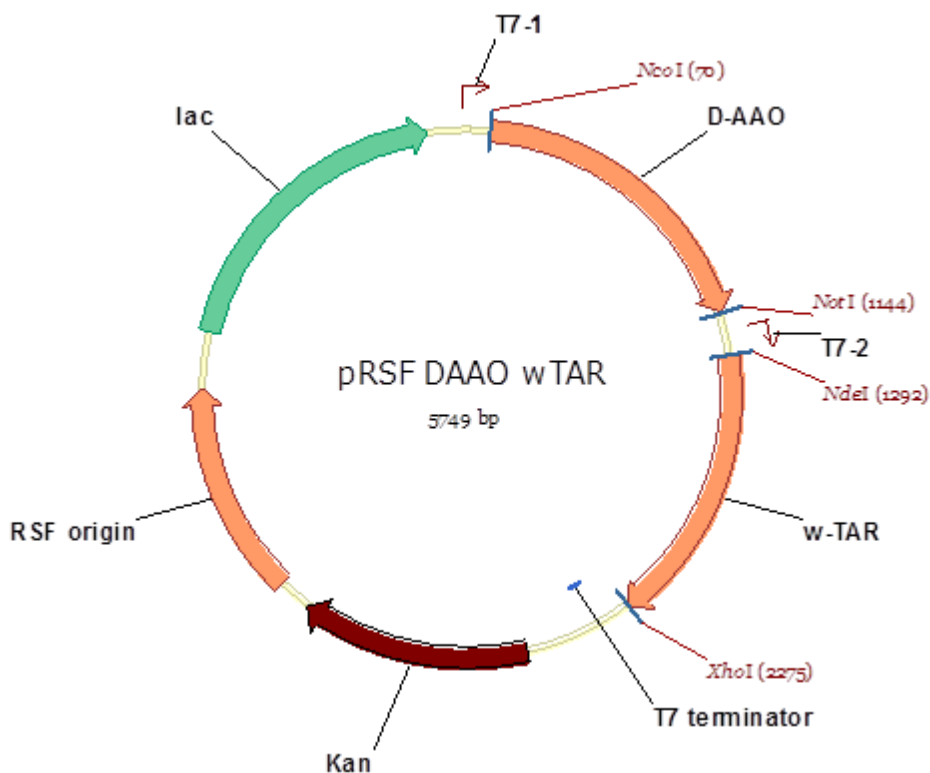


Figure 57: Plasmid map of the D-AAO and transaminase genes cloned into pRSF-Duet1

The *E. coli* amine oxidase gene (in a pkk-2 vector) was kindly donated by Prof. Mike McPherson at the University of Leeds.[139]

The following enzymes were purchased from Sigma Aldrich:

- Lysozyme from chicken egg white (protein \geq 90 %, lyophilized powder)
- Horse radish peroxidase (HRP), type VI-A, essentially salt-free (lyophilized powder)
- L-Amino acid oxidase from *Crotalus adamanteus*, type IV ($>$ 3.0 U/mg, 7.2 mg/mL, aqueous suspension).
- D-Amino acid oxidase from porcine kidney (8.2 U/mg, lyophilized powder)
- Diamine oxidase from porcine kidney (0.11 U/mg, lyophilized powder)
- RgPAL solution containing 60 % glycerol, 3 mM Tris pH 7.5 and up to 0.5 M $(\text{NH}_4)_2\text{SO}_4$ (7.4 mg protein/mL, 0.97 U/mg)

Transaminase ATA-117 was supplied by Codexis as lyophilized purified protein.

N-Acetyl amino acid racemase variant G291D/F323Y was supplied by Dr. Reddy's (lyophilized powder)

D-Acylase was supplied by Amano as a lyophilized powder

6.3 Instruments

Shaker incubators used were from FALC instruments. Centrifugation was performed using a Beckman Coulter™ Avanti™ J-30I Centrifuge (with Beckman JA- 25.50, F-10 and JS-5.3 rotors). The bench-top centrifuges are from Eppendorf. Cell lysis was performed by sonication using a Soniprep 150 (MSE UK Ltd.). Kinetic constants were measured using an Eppendorf BioSpectrometer and a Varian Cary-series UV-Vis spectrophotometer (Agilent) equipped with a Peltier block temperature control.

Reverse phase HPLC was performed on an Agilent system equipped with a G1379A degasser, G1312A binary pump, a G1329 autosampler unit, a G1315B diode array detector and a G1316A temperature controlled column compartment. ¹H and ¹³C NMR spectra were recorded on a Bruker Avance 400 (400.1 MHz or 399.9 MHz for ¹H and 100.6 MHz for ¹³C) without additional internal standards. Chemical shifts are reported as δ in parts per million (ppm) and are calibrated against residual solvent signals. The following abbreviations were used to define the multiplicities: s, singlet; d, doublet; t, triplet; q, quartet; m, multiplet.

6.4 Buffers and Solutions

All bacterial media was autoclaved at 121 °C for 20 minutes and all purification buffers were filtered through a 0.22 μ m pore filter

LB media: LB pre-mix freeze dried powder consisting of yeast extract (5 g/L), tryptone (10 g/L) and NaCl (10 g/L) was dissolved in dH₂O (25 g/L)

LB agar: Agar (15 g/L) was added to LB media

Auto induction media: Auto induction pre-mix powder consisting of tryptone (10 g/L), yeast extract (5 g/L), (NH₄)₂SO₄ (3.3 g/L), KH₂PO₄ (6.8 g/L), Na₂HPO₄ (7.1 g/L), MgSO₄ (150 mg/L), glucose (0.5g/L), lactose (2.0 g/L) and trace elements (30 mg/L) was dissolved in dH₂O (34.85 g/L) and glycerol (50 % v/v, 10 mL) was added

2TY media: Yeast extract (5 g), tryptone (8 g) and NaCl (2.5 g) were dissolved in dH₂O (500 mL)

Borate buffer (100 mM): Boric acid (6.18 g/L) and KCl (7.45 g/L) were dissolved in dH₂O and the solution was adjusted to pH 8.3 or 9.5 with the addition of 10 N NaOH.

Phosphate buffer (100 mM): K₂HPO₄ solution (1 M, 94 ml) and KH₂PO₄ solution (1 M, 6ml) were added to dH₂O (900 mL) to give a buffered solution of pH 8.0.

Buffer A: Imidazole (1.36 g/L, 20 mM) and NaCl (17.53 g/L, 300 mM) were added to 100 mM phosphate buffer (pH 8.0)

Buffer B: Imidazole (10.2 g/L, 150 mM) and NaCl (17.53 g/L, 300 mM) were added to 100 mM phosphate buffer (pH 8.0)

Buffer C: Imidazole (27.2 g/L, 800 mM) and NaCl (17.53 g/L, 300 mM) were added to 100 mM phosphate buffer (pH 8.0)

Saturated scopoletin solution: Scopoletin (10 mg) was added to dH₂O (100 ml) and incubated at 37 °C with shaking (250 rpm) for 1 hour to make a saturated solution. The solution was filtered through a 0.22 µm pore filter to remove remaining solids and to give a working solution with a fluorescence of approximately 40,000 RFU

6.5 Protein Production and Purification

6.5.1 PAL Expression

PAL was expressed from a single colony of *E. coli* BL21(DE3) (New England Biolabs) transformed with a pET-16b vector containing the PAL gene insert. LB media (8 mL) supplemented with ampicillin (100 µg/mL) for selection, was inoculated and incubated overnight (37 °C, 250 rpm). The culture was diluted (1:100) in auto-induction media (800 mL) containing ampicillin (100 µg/mL) and incubated for 3 days (18 °C, 250 rpm). Cells were harvested by centrifugation (8,000 rpm, 20 minutes, 4 °C) washed with potassium phosphate buffer (100 mM, pH 8.0, 25 mL) and harvested (4000 rpm, 20 minutes, 4 °C) for a second time. Cell paste was stored at -20 °C until needed, used directly in whole cell biotransformations or the protein was subsequently purified. Cells were lysed and the PAL proteins were purified following the general procedures.

6.5.2 PpRac Expression

PpRac was expressed from a single colony of *E. coli* BL21(DE3) (New England Biolabs) transformed with the pRSF-Duet vector containing the *PpRac* gene insert. LB media (8 mL) supplemented with kanamycin (30 µg/mL) for selection, was inoculated and incubated overnight (37 °C, 250 rpm). The culture was diluted (1:100) in LB media (800 mL) supplemented with kanamycin (30 µg/mL) which was incubated at 37 °C until the *E. coli* reached exponential growth ($OD_{600} = 0.6-0.8$). Isopropyl-β-D-thiogalactopyranoside (IPTG, 1 mM) was added to induce protein overexpression and the culture was incubated at 30 °C with shaking (250 rpm) for a further 18 hours. Cells were harvested by centrifugation (8,000 rpm, 20 minutes, 4 °C) washed with potassium phosphate buffer and harvested (4000 rpm, 20 minutes, 4 °C) for a second time. Cell paste was stored at -20 °C until needed. Preparation of cell lysate and protein purification was performed according to the general procedures with the exception that a centrifugal concentrator with a 30,000 MW cut off (Vivaspin) was used to concentrate the protein.

6.5.3 MAO-N Expression

MAO-N variants D5, D9 and D11 were expressed from a single colony of *E. coli* C43(DE3) (New England Biolabs) transformed with a pET-16b vector containing the MAO-N gene insert. LB media (8 mL) supplemented with ampicillin (100 µg/mL) for selection, was inoculated and incubated overnight (37 °C, 250 rpm). The culture was diluted (1:100) in LB media (600 mL) containing ampicillin (100 µg/mL) and incubated for 24 hours (37 °C, 250 rpm). Cells were harvested by centrifugation (8,000 rpm, 20 minutes, 4 °C) washed with potassium phosphate buffer (100 mM, pH 8.0, 25 mL) and harvested (4000 rpm, 20 minutes, 4 °C) for a second time. Cell paste was stored at -20 °C until needed for purification. Cells were lysed and the MAO-N proteins were purified following the general procedures with the exception that a centrifugal concentrator with a 30,000 MW cut off (Vivaspin) was used to concentrate the protein.

6.5.4 *E. coli* Amine Oxidase (EcAO) Expression and Purification

EcAO was expressed from a single colony of *E. coli* BL21(DE3) (New England Biolabs) transformed with the pkk-2 vector containing the EcAO gene insert. LB media (5 mL) supplemented with ampicillin (75 µg/mL) for selection, was inoculated and incubated overnight (37 °C, 250 rpm). The culture was diluted (1:100) in 2TY media (500 mL) supplemented with CuSO₄ (150 µM) and ampicillin (75 µg/mL) which was incubated at 37 °C until the *E. coli* reached exponential growth (OD₆₀₀ = 0.6-0.8). Isopropyl-β-D-thiogalactopyranoside (IPTG, 1 mM) was added to induce protein overexpression and the culture was incubated at 37 °C with shaking (250 rpm) for a further 4 hours. Cells were harvested by centrifugation (8,000 rpm, 20 minutes, 4 °C) washed with Tris-HCl buffer (50 mM, pH 8.0) and harvested (4000 rpm, 20 minutes, 4 °C) for a second time. Cell paste was stored at -20 °C until needed.

For cell lysis, the frozen cell paste was thawed on ice and resuspended in Tris-HCl buffer containing 20 % sucrose (50 mM, pH 8.0, 10 mL). EDTA (42 mM, 3 mL) and lysozyme (10 mg/mL in 50 mM Tris-HCl buffer, pH 8.0, 3 mL) were added and the suspension was incubated at 37 °C for 30 minutes. Tris-HCl buffer containing 9 % sucrose (50 mM, pH 8.0, 6 mL) and Tris-HCl buffer containing 15 mM MgCl₂ (50 mM, pH 8.0, 13.5 mL) were added to the suspension. Cell debris was removed by centrifugation (10,000 rpm, 30 minutes, 4 °C) to yield a cell-free extract which was filtered through a syringe filter with a 0.45 µm pore size.

For purification the supernatant was concentrated and repeatedly washed with Tris-HCl buffer (20 mM, pH 7.0). The cell lysate containing crude protein was loaded onto a Q Sepharose ion exchange column (GE Healthcare) equilibrated with Tris-HCl buffer (20 mM, pH 7.0). The column was washed with Tris-HCl buffer (20 mM, pH 7.0) containing 35 mM NaCl to remove any non-specific binding proteins. Elution of purified protein was achieved using Tris-HCl buffer (20 mM, pH 7.0) containing 175 mM NaCl. Fractions containing purified protein were identified by SDS-PAGE, combined, concentrated using a centrifugal concentrator (100,000

MW cut off, Vivaspin) and de-salted using a PD10 column (GE Healthcare) into Tris-HCl buffer (20 mM, pH 7.0). Protein concentration was determined in triplicate using the bicinchoninic acid (BCA) assay according to the manufacturers protocol (Pierce Biotechnology).

6.5.5 General Procedure for the Preparation of Cell Lysate

For cell lysis, frozen cell paste was thawed on ice and resuspended in potassium phosphate buffer (100 mM, pH 8.0, 5 mL per 1 g cell pellet). The resulting suspension was treated with lysozyme (1 mg/mL) and incubated at 37 °C for 45 minutes. Cells were disrupted by sonication using 20 cycles of 20 seconds on, 20 seconds off, 12 micron amplitude. Cell debris was removed by centrifugation (20,000 rpm, 20 minutes, 4 °C) to yield a cell-free extract which was filtered through a syringe filter with a 0.45 µm pore size.

6.5.6 General Procedure for Protein Purification

For purification, the cell lysate containing crude protein was loaded onto a fast flow His-trap chelating column (GE Healthcare) charged with NiSO₄ (100 mM) and equilibrated with Buffer A. The column was washed with Buffer A (10 c.v) followed by Buffer B (10 c.v) to remove any non-specific binding proteins. Elution of purified protein was achieved using Buffer C (20 c.v) and fractions containing purified protein were identified by SDS-PAGE (Figure 58) using a prestained protein molecular weight marker (Fermentas SM 0441) and pre-cast SDS gels (NuSep). Fractions were combined, concentrated using a centrifugal concentrator (100,000 MW cut off, Vivaspin) and de-salted using a PD10 column (GE Healthcare) into phosphate buffer. Protein concentration was determined in triplicate using the bicinchoninic acid (BCA) assay according to the manufacturers protocol (Pierce Biotechnology).

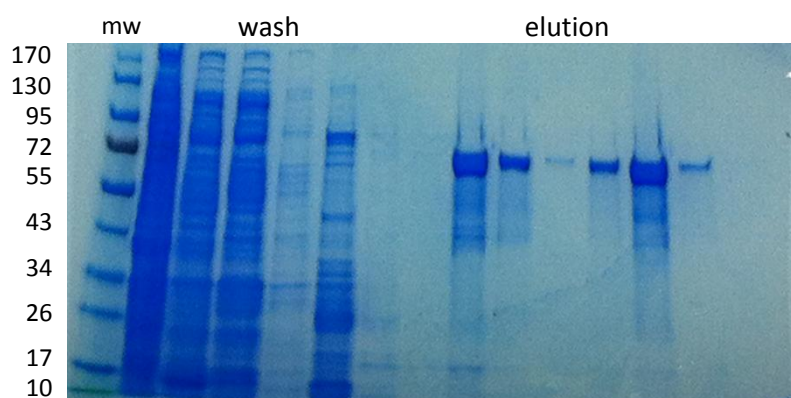


Figure 58: SDS-PAGE of AvPAL purification. Lane 1 contains a protein molecular weight marker and the numbers to the left are given in kDa. Wash fractions contain non-specific binding proteins and elution fractions contain purified AvPAL (64 kDa)

6.6 Biotransformation Procedures

6.6.1 Preparation of Racemic Standards for HPLC Analysis

A solution of purified *PpRac* (100 μ L, 2 mg/mL) was added to L-amino acid solutions **2b-g**, **2k-l** & **2n-o** (10 mM) in phosphate buffer and the reactions were incubated overnight (30 °C, 120 rpm). A sample (300 μ L) was taken from the biotransformation, heated to 100 °C for 5 minutes to quench the reaction and analyzed by chiral HPLC.

6.6.2 General Procedure for PAL Catalyzed Hydroamination of Cinnamic Acid Analogues

E. coli BL21(DE3) whole cells (40 mg/mL) expressing PAL were resuspended in ammonium hydroxide (5 M, pH 9.5). The cell suspension (2.5 mL) was added to substrate solutions **1a-q** (10 mM, 2.5 mL) to give a final substrate concentration of 5 mM and whole cell concentration of 20 mg/mL. The reactions were incubated at 30 °C (250 rpm) and samples (300 μ L) were taken at various time points and analyzed by HPLC. Control reactions were carried out in parallel with *E. coli* BL21(DE3) whole cells containing empty pET-16b plasmids and showed no conversion.

6.6.3 Large Scale PAL Catalyzed Hydroamination Reactions

E. coli BL21(DE3) whole cells expressing AvPAL (7.5 g) were resuspended in a solution of 2-chlorocinnamic acid (**1e**, 1g, 5.48 mmol) in (NH₄)₂CO₃ (2.5M, pH 9.1, 500 mL, without pH adjusting). The reaction was incubated at 30 °C with shaking (250 rpm) and samples were taken over time and analyzed by chiral HPLC. After 8 hours, the reaction had reached 80% conversion and the L-amino acid product had an e.e.>99%. The *E. coli* whole cells were removed by centrifugation (4000 rpm, 4 °C, 20 mins) and the supernatant was lyophilized. The freeze dried sample was re-dissolved in HCl (1 M) to form the hydrochloride salt of the L-amino acid product which was then lyophilized for a second time. The crude product was washed repeatedly with diethyl ether to remove unreacted starting material. Finally the product was dissolved in water and recrystallized with the addition of 5 M NH₄OH until pH 7.0. The product was filtered and washed with ice cold water to give 2-chloro-L-phenylalanine **2e** as a white solid (572 mg, 52% yield, >99% e.e.)

¹H NMR (D₂O+NaOH): δ 7.32 (d, J=6.8, 1H, ArH), 7.20-7.11 (m, 3H, ArH), 3.44 (t, J=7.2, 1H, CHNH₂), 2.98 (dd, J=13.4, 6.4, 1H, CHAr), 2.81 (dd, J=13.4, 8.0, 1H, CHAr)

4-trifluoromethyl-L-phenylalanine **2d** was prepared using the same method starting from 4-trifluoromethyl cinnamic acid **1d**. The product L-**2d** was achieved as a white solid (450 mg, 42% yield, >99% e.e.)

^1H NMR (D_2O): δ 7.53 (d, $J=8.0$, 2H, ArH), 7.28 (d, $J=8.0$, 2H, ArH), 3.39 (t, $J=6.5$, 1H, CHNH₂), 2.91 (dd, $J=13.5$, 5.7, 1H, CHAr), 2.79 (dd, $J=13.4$, 7.3, 1H, CHAr)

6.6.4 D-Amino Acid Synthesis

L-Amino acid oxidase from *Crotalus adamanteus* (5 μL) was added to solutions of racemic amino acids **2b-n** (5 mM) in phosphate buffer (100 mM, pH 8.0, 5 mL). Racemic amino acids were obtained from (i) racemase catalyzed reactions starting from L-amino acids L-**2b-n**, or (ii) PAL catalyzed amination reactions starting from cinnamic acid derivatives **1b-n** after prolonged incubation (22 hours or more). The reactions were incubated overnight (30 °C, 120 rpm) and samples taken from the biotransformations were analyzed by chiral HPLC.

6.6.5 General Procedure for PAL Catalyzed Deamination of Amine Substrates

Purified AvPAL or RgPAL (0.3 mg) was added to amine substrate (5 mM) in 100 mM borate buffer pH 8.3 (5 mL) and incubated at 30 °C for 48 hour with shaking at 120 rpm. Biotransformations were pH adjusted to approximately pH 12 with the addition of NaOH (10 N) and extracted with TBME (3x10 mL). Organic phases were combined, dried over magnesium sulphate and concentrated. The residue was redissolved in TBME (500 μL) and analyzed by normal phase HPLC and GC-FID.

6.6.6 General Procedure for PAL Catalyzed Hydroamination of Alkenes

Purified AvPAL or RgPAL (0.3 mg) was added to amine substrate (5 mM) in 5 M NH₄OH pH 9.5 with 10 % DMSO (5 mL) and incubated at 30 °C for 48 hour with shaking at 120 rpm. Biotransformations were pH adjusted to approximately pH 12 with the addition of NaOH (10 N) and extracted with TBME (3x10 mL). Organic phases were combined, dried over magnesium sulphate and concentrated. The residue was redissolved in TBME (500 μL) and analyzed by normal phase HPLC and GC-FID.

6.7 Site Directed Mutagenesis

Mutagenic oligonucleotide primers were synthesized by MWG as Custom Oligos and were diluted in dH₂O (100 ng/ μL). Primer sequences used for site directed mutagenesis are shown in Table 25.

Table 25: Mutagenic primer sequences for site directed mutagenesis

Mutation	Primer sequences
S168A	Forward: ggtagcattggtgccgcccggatctggttc Reverse: gaaccagatcaccggcggcaccaatgctacc
Y78F	Forward: accgctggtaacaccaaatacggttcaccg Reverse: cgggaaccgattttggtgtaccagcgg
F107X	Forward: ccaatctggttgNNKctgaaaaccggatcagg Reverse: cctgcaccggtttcagMNNcacaaccagattgg
T110X	Forward: gcagtttattacctgcaccNNKtttcagaaacc Reverse: ggttctgaaaMNNggatcaggtaataaactgc
A167X	Forward: ggtagcattggtNNKagcggatctggttccg Reverse: cgggaaccagatcaccgctMNNaccaatgctacc
G169X	Forward: agcattggtgccagcNNKgatctggttccgctgag Reverse: ctgagcgggaaccagatcMNNgctggcaccaatgct

All mutagenesis reactions were performed following the QuikChange protocol (Stratagene). DNA template (50 ng), 10 x reaction buffer (5 μ L), forward and reverse primers (125 ng each), dNTP mix (10 mM of each base, 1 μ L) and DMSO (1 μ L) were made up to 50 μ L in dH₂O. Phusion high-fidelity DNA polymerase (1 μ L) was added and the reactions were carried out in a thermocycler using the parameters given in Table 26.

Table 26: Thermal cycling parameters for site directed mutagenesis. 16 Cycles were used for a single amino acid change and 18 cycles were used for generating libraries of mutations

Cycles	Temperature (°C)	Duration
1	95	30 sec
16-18	95	30 sec
	55	1 min
	68	8 min

To digest the parental DNA template, DpnI restriction enzyme (1 μ L) was added to each amplification reaction and the digests were incubated at 37 °C for 2 hours. The reactions were heated to 80 °C for 20 minutes to denature the DpnI enzyme and *E. coli* XL1-Blue supercompetent cells were transformed with the DpnI treated DNA. Mutations were confirmed by performing mini-preps of the DNA and sequencing reactions were carried out by GATC. *E. coli* BL21(DE3) cells were then transformed with the new plasmids carrying the genes with successful mutations and proteins were expressed and purified following the general protocols.

6.7.1 Sodium Borohydride Reduced PAL

Wild-type AvPAL was reduced according to the method of Schuster and Rétey.[101] Sodium borohydride (10 mg) was added to a solution of wild-type AvPAL (2.5 mL, 2 mg/mL) in phosphate buffer (100 mM, pH 8.0) and incubated at 4 °C for 18 hours. The excess sodium borohydride was removed using a PD10 desalting column (GE Healthcare).

6.7.2 Circular Dichroism

CD spectra of purified PAL enzymes (ca. 1 mg/mL) in phosphate buffer were measured using a spectropolarimeter. Samples in quartz cuvettes were scanned using the following parameters:

Wavelength range: 260–190 nm

Step size: 0.5 nm

Spectral bandwidth: 1 nm

Time per point: 3 seconds.

Path length: 0.1 nm

6.7.3 UV Difference Spectroscopy

The UV spectra of purified wild-type AvPAL and S168A AvPAL (0.8 and 0.4 mg/mL) in phosphate buffer (100 mM, pH 8.0), were measured between 270 and 340 nm using a Varian-Cary series UV-vis spectrophotometer (Agilent). The spectrum of the S168A variant was subtracted from the spectra of wild-type PAL using Microsoft Excel.

6.8 Deuterium Isotope Labelling Study

6.8.1 Amination Reactions

E. coli BL21(DE3) whole cells expressing wild-type AvPAL (20 mg/mL) were resuspended in NH₄OH (5M, pH 9.5, 100 mL) containing deuterated 4-nitrocinnamic acid **18** (230 mg, 1.2 mmol) and incubated for 18 hours at 30 °C with shaking (250 rpm). Chiral HPLC showed 83 % conversion to the corresponding 4-nitrophenylalanine (e.e. 6 % in favour of the L-enantiomer). The whole cell material was cleared from the reaction by centrifugation (4000 rpm, 20 min, 4 °C), the supernatant was decanted and lyophilized. The product was redissolved in 10 % H₂SO₄ and any insoluble material was removed by filtration. The solution was loaded onto a column of Dowex (acidic resin 50 x 8, 50–100 mesh), which was washed with water until pH 7. The product was eluted with 5 M NH₄OH and fractions containing product were lyophilized to give an orange powder (124 mg). The ¹H NMR spectra of the mixture of L- and D-amino acids showed that the reaction proceeded with complete diastereoselectivity to give the (2*R*,3*S*)- and (2*S*,3*R*)-diastereoisomers. To obtain optically pure samples of these products, L-Amino acid oxidase from *Crotalus adamanteus* (5 µL) was added to a solution of half the L- and D-amino acid mixture (60 mg, 5 mM) in phosphate buffer (100 mM, pH 8.0, 10 mL). D-Amino acid

oxidase from *Porcine kidney* (1 mg) was added to the other half of the solution of L- and D-amino acid mixture (60 mg, 5 mM) in phosphate buffer (100 mM, pH 8.0, 10 mL). Both reactions were incubated overnight at 30 °C with shaking (150 rpm). Chiral HPLC confirmed both the reactions had proceeded to completion and the reactions were subsequently lyophilized. The solids were washed with acetone to remove the keto-acid product, redissolved in 1 M HCl and filtered to remove any protein material. The final solution was lyophilized and ¹H NMR showed the products were deuterated 4-nitro-D-phenylalanine **D-13** (31 mg, e.e.>99%) and deuterated 4-nitro-L-phenylalanine **L-13** (24 mg, e.e.>99%)

6.8.2 Deamination Reactions

6.8.2.1 Wild-type AvPAL Catalyzed Deamination Reactions

- Reactions in borate buffer pH 8.3

Whole cell *E. coli* BL21(DE3) (50 mg/mL) expressing AvPAL was added to either **D-13** or **D-16** (100 mg, 10 mM) in borate buffer (100 mM, pH 8.3, 40 mL) and the biotransformations were incubated at 30 °C with shaking (250 rpm) for 48 hours. Chiral HPLC showed 89 % conversion to the corresponding 4-nitrocinnamic acid for each reaction. The whole cell material was removed from the biotransformations by centrifugation (4000 rpm, 20 min, 4 °C) and the supernatant was decanted and acidified to pH 1.0 with 1 M HCl to precipitate the product. The products were collected by filtration and lyophilized to give orange powders, (25 mg and 22 mg respectively). Analysis by ¹H NMR showed that the deamination of **D-13** resulted in a mixture of deuterated product **18** and fully protiated 4-nitrocinnamic acid product **1m** (49% and 71% loss of deuterium incorporation from 2 repeats), whereas the deamination of **D-16** resulted only in fully protiated product **1m**.

- Reactions in borate buffer pH 9.5

Purified AvPAL (0.5 mg) was added to amino acid solutions of **D-13** and **D-16** (5 mM, 2 mL) in borate buffer (0.1 M, pH 9.5) and incubated at 30 °C with shaking (150 rpm) for 18 hours. A sample (400 µL) was taken from the reaction and D₂O (400 µL) was added, ¹H NMR analysis run with a water suppression method showed the formation of the single expected products **18** and **1m** respectively.

- Reactions in D₂O pH 8.3

Borate buffer was prepared using D₂O and pH adjusted with the addition of 10 N NaOH to pH 8.3. A solution of purified AvPAL was buffer exchanged using a PD10 desalting column into D₂O-borate buffer. AvPAL (294 µL, 1.7 mg/mL) was added to amino acid solutions of **D-13** and **D-16** (5 mM, 2 mL) in D₂O-borate buffer at pH 8.3 and the reactions were incubated at 30 °C with shaking (150 rpm) for 18 hours. ¹H NMR analysis run with a water suppression method showed the formation of the single expected products **18** and **1m**.

6.8.2.2 S168A AvPAL Catalyzed Deamination Reactions

Purified S168A (0.5 mg) was added to amino acid solutions D-**13** and D-**16** (5 mM, 2 mL) in borate buffer (0.1 M, pH 9.5 or 8.3) and incubated at 30 °C with shaking (150 rpm) for 18 hours. A sample (400 μ L) was taken from the reaction and D₂O (400 μ L) was added, ¹H NMR analysis was run with a water suppression method. Reactions of substrate D-**16** at both pH 8.3 and 9.5 yielded the formation of the single expected product **1m**, whereas the reaction of substrate D-**13** at both pH 8.3 and pH 9.5 yielded a mixture of products **1m** and **18** (with 63% and 30% loss of deuterium incorporation at pH 8.3 and pH 9.5 respectively).

6.9 Determining the Kinetic Parameters of PAL catalyzed reactions

The molar absorption coefficient for each cinnamic acid derivative was calculated by measuring the absorbance of standards of known concentrations. This value was used to convert values of OD/min to mM/min.

Table 27: Molar absorbance coefficient for cinnamic acid derivatives 1a-d, 1i-j & 1m-n

Substrate	wavelength (nm)	ϵ (M ⁻¹ cm ⁻¹)
1a	300	3865
1b	295	5865
1c	295	6401
1d	285	11296
1i	295	12808
1j	280	4802
1m	335	6256
1n	300	8173

6.9.1 Measurement of Deamination Kinetic Constants

Amino acid solutions at eight different concentrations (100 μ L, 0-20 mM) in borate buffer (100 mM, pH 8.3) were pre-heated to 30 °C in a 96-well microtitre plate. Purified PAL solution (100 μ L, 0.3 mg/mL) was added to the substrate and the initial increase in absorbance was measured spectrophotometrically at 30 °C using an Eppendorf BioSpectrometer. The initial rate (mM/min) was calculated from the initial change in OD per minute using a standard calibration curve for each product. Each substrate concentration was repeated in triplicate and the kinetic parameters were determined using non-linear regression analysis.

To measure the deamination kinetics for determining the catalytic mechanism of D-amino acid formation (chapter 3) reactions were performed using amino acid solutions at six different

concentrations (850 μ L, 0-0.4 mM) in borate buffer (100 mM, pH 8.3) in cuvettes. Purified PAL solution (50 μ L, 0.8 mg/mL) was added to the substrate and the initial increase in absorbance was measured spectrophotometrically at 30 °C using a Varian Cary-series UV-Vis spectrophotometer (Agilent). Each substrate concentration was repeated in triplicate and the kinetic parameters were determined using linear Hanes-Woolf plots.

6.9.2 Measurement of Amination Kinetic Constants

Cinnamic acid solutions at six different concentrations (850 μ L, 0-0.4 mM) in ammonium hydroxide (5 M, pH 9.5) were pre-heated to 30 °C in cuvettes. PAL solution (50 μ L, 0.8 mg/mL) was added and the initial decrease in absorbance was measured spectrophotometrically at 30 °C. The initial rate (mM/min) was calculated from the initial change in OD per minute using a standard calibration curve for each substrate. Each substrate concentration was repeated in triplicate and the kinetic parameters were determined using non-linear regression analysis.

6.10 Derivatisation Methods

6.10.1 Trinitrobenzene Sulphonic Acid (TNBS) Derivatisation

TNBS solution in 100 mM phosphate buffer, pH 8.0 (1 % w/v, 75 μ L) was added to (*R*)-amphetamine standards in 100 mM phosphate buffer, pH 8.0 (0.5-10 mM, 125 μ L) in a 96-well plate. The derivatisation reaction was incubated at 37 °C for 2 hours and the absorbance was measured at 420 nm.

6.10.2 Dansyl Chloride (Dns-Cl) Derivatisation

(*R*)-Amphetamine solutions in dH₂O (0.5-5 mM, 75 μ L), sodium bicarbonate solution (100 mM, pH 9.0, 50 μ L) and Dns-Cl solution in dH₂O (15 mM, 75 μ L) were added to a 96-well plate. The reaction was incubated for 1 hour at 37 °C and the fluorescence was measured using excitation at 343 nm and emission at 530 nm.

6.10.3 Fluorescamine Derivatisation

(*R*)-Amphetamine solutions in dH₂O (0.5-5 mM, 40 μ L), fluorescamine solution in acetonitrile (0.1 % w/v, 90 μ L) and phosphate buffer (100 mM, pH 8, 170 μ L) were added to a 96-well plate. The reaction was incubated at room temperature for 10 minutes and the fluorescence was measured using excitation at 405 nm and emission at 480 nm.

6.11 Amine Oxidase Spectrophotometric Screen

Assay solution: HRP (1 mg), 4-AAP (100 mg/mL in dH₂O, 30 μ L), TBHBA (20 mg/mL in DMSO, 100 μ L) and 1 M phosphate buffer pH 7.7 (1 mL) made up to 10 mL with dH₂O

Purified amine oxidases (100 μ L, 0.5 mg/mL) were added to amine solutions (10 mM, 50 μ L) with assay solution (50 μ L) in a 96-well plate and the change in absorbance was measured at 510 nm

6.12 General Procedures for the Amino Acid Oxidase Coupled Assays

Assay solution (1.6 mL):

- cinnamic acid substrate solutions (5 mM) in 5 M NH_4OH , pH 9.5 (1 mL)
- saturated scopoletin solution (400 μ L)
- HRP solution (1 mg/mL in dH_2O , 100 μ L)
- L-AAO solution (1:10 dilution in dH_2O , 100 μ L) or D-AAO solution (3 mg/mL in dH_2O , 100 μ L)

Purified PAL (ca. 1 mg/mL, 40 μ L) was added to working assay solution (160 μ L) in a 96 well plate and the reactions were incubated at 30 $^\circ\text{C}$. The initial decrease in relative fluorescence units was monitored over time (excitation 380 nm, emission 460 nm).

6.12.1 Liquid Phase Amino Acid Oxidase Coupled Assay

E. coli BL21(DE3) cells transformed with pET16-AvPAL libraries were plated onto LB-agar plates with ampicillin (100 $\mu\text{g}/\text{mL}$) and incubated at 37 $^\circ\text{C}$ overnight. Colonies (96) were picked and used to inoculate starter cultures of LB media (1 mL each) supplemented with ampicillin (100 $\mu\text{g}/\text{mL}$) in a 96 deep-well plate. The plate was incubated overnight (30 $^\circ\text{C}$, 250 rpm) and the starter cultures (100 μ L) were used to inoculate auto-induction media (1 mL) with ampicillin (100 $\mu\text{g}/\text{mL}$) in a 96-well plate which was incubated at 18 $^\circ\text{C}$ for 2 days. Cells were harvested by centrifugation (JS 5.3 rotor, Beckman, 4000 rpm, 10 min, 4 $^\circ\text{C}$) and the supernatant was decanted. The cells were resuspended in 4-nitrocinnamic acid (5 mM) in 5 M NH_4OH , pH 9.5 and incubated for 2 hours at 30 $^\circ\text{C}$. Cells were harvested by centrifugation (4000 rpm, 10 min, 4 $^\circ\text{C}$). An assay mix of saturated scopoletin solution (80 μ L, HRP (1 mg/mL, 10 μ L) and L-AAO (1:10 dilution, 10 μ L) or D-AAO solution (3 mg/mL, 10 μ L) was added to the biotransformation supernatant (100 μ L) in a new 96-well microtitre plate and the decrease in fluorescence was monitored over time (excitation 380 nm, emission 460 nm).

6.12.2 Colony Based D-Amino Acid Oxidase Screen

Assay solution: A DAB tablet (containing 10.5 mg DAB) was dissolved in 5 mL phosphate buffer (100 mM, pH 8.0) until completely dissolved. 5 M NH_4OH pH 9.5 (5 mL) was added to the solution and some of the DAB precipitated. The solution was sonicated for 1 hour and then filtered through filter paper to remove any remaining solids. A solution (10 mL) containing substrate (20 mM) and HRP (0.1 mg/mL) in 5 M NH_4OH pH 9.5 was added to the DAB solution (10 mL).

E. coli BL21(DE3)-Gold cells transformed with pET-16b AvPAL libraries and the D-AAO pRSF-duet vector, were plated onto nitrocellulose membranes placed onto LB-agar plates with

ampicillin (100 µg/mL) and kanamycin (30 µg/mL) and incubated at 30 °C overnight. The membranes were removed from the agar plates and transferred onto second expression LB-agar plates containing IPTG (1 mM) with ampicillin (100 µg/mL) and kanamycin (30 µg/mL). The expression plates were incubated at 20 °C for 24 hours. The membranes were removed from the plates and subjected to three freeze-thaw cycles using liquid nitrogen. For the assay, the membrane was placed onto a filter paper soaked in the assay solution and incubated at room temperature for up to 4 hours or until colour developed. For each assay controls were performed in parallel using empty pET-16b and pRSF-Duet vectors.

Positive variants are picked and grown in LB (5 mL) with ampicillin (100 µg/mL) and kanamycin (30 µg/mL) at 37 °C overnight. Plasmid DNA is recovered by using a mini-prep kit according to the manufacturers protocol (Qiagen). The pRSF vector carrying the D-AAO gene is digested using restriction enzymes XmaI, AflIII or XhoI (NEB) which are unique to the duet vector. Digested DNA is retransformed into *E. coli* XL1-Blue for selection of the PAL containing plasmid which can be isolated following a second mini-prep.

6.12.3 Liquid Phase Transaminase/ D-Amino Acid Oxidase Screen

Assay solution was made up to 10 mL in 5 M NH₄OH, pH 9.5:

- Substrate (10 mM)
- HRP (1 mg)
- Pyruvate (2 mg)
- PLP (5 mg)
- Transaminase ATA-117 (10 mg)
- D-AAO (3 mg)

Purified PAL (ca. 1 mg/mL, 50 µL) was added to assay solution (100 µL) and saturated scopoletin solution (50 µL) in a 96-well plate. The reactions were incubated at 30 °C and the initial decrease in relative fluorescence units was monitored over time (excitation 380 nm, emission 460 nm).

6.12.4 Colony Based Transaminase/D-Amino Acid Oxidase Screen

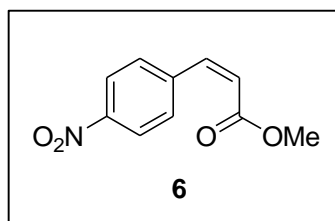
Assay solution: A DAB tablet (containing 10.5 mg DAB) was dissolved in 5 mL phosphate buffer (100 mM, pH 8.0) until completely dissolved. 5 M NH₄OH pH 9.5 (5 mL) was added to the solution and some of the DAB precipitated. The solution was sonicated for 1 hour and then filtered through filter paper to remove any remaining solids. A solution (10 mL) containing substrate (20 mM) and HRP (0.1 mg/mL) and pyruvate (0.2 mg/mL) in 5 M NH₄OH pH 9.5 was added to the DAB solution (10 mL).

E. coli BL21(DE3)-Gold cells transformed with pET-16b AvPAL libraries and the D-AAO/transaminase pRSF-duet vector, were plated onto nitrocellulose membranes placed onto LB-agar plates with ampicillin (100 µg/mL) and kanamycin (30 µg/mL) and incubated at 30 °C

overnight. The membranes were removed from the agar plates and transferred onto second LB-agar expression plates containing IPTG (1 mM) with ampicillin (100 µg/mL) and kanamycin (30 µg/mL). The expression plates were incubated at 20 °C for 24 hours. The membranes were removed from the plates and subjected to three freeze-thaw cycles in liquid nitrogen. To reduce background activity the membranes were first incubated on top of a filter paper pre-soaked in HRP (0.1 mg/mL) and pyruvate (0.2 mg/mL) for 30 minutes. For the assay, the membrane was placed onto a filter paper soaked in the assay solution and incubated at room temperature for up to 4 hours or until colour developed. For each assay controls were performed in parallel using empty pET-16b and pRSF-Duet vectors.

Positive variants are picked and grown in LB (5 mL) with ampicillin (100 µg/mL) and kanamycin (30 µg/mL) at 37 °C overnight. Plasmid DNA is recovered by using a mini-prep kit according to the manufacturer's protocol (Qiagen). The pRSF vector carrying the transaminase ad D-AAO gene is digested using restriction enzymes XmaI, AflIII or XhoI (NEB) which are unique to the duet vector. Digested DNA is retransformed into *E. coli* XL1-Blue for selection of the PAL containing plasmid which can be isolated following a second mini-prep.

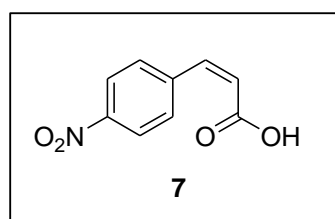
6.13 Chemical Synthesis



6 (*Z*)-methyl-3-(4-nitrophenyl)acrylate: A dry 3-neck flask was charged with Still-Gennari reagent (1 g, 3.16 mmol, 1.4 eq) and 18-crown-6 (1.48 g, 5.6 mmol, 2.5 eq) in THF (20 mL) and cooled to -78 °C. KHMDS solution in toluene (0.5 M, 6.27 mL, 3.16 mmol, 1.4 eq) was added slowly and the reaction was stirred for 30 minutes. 4-Nitrobenzaldehyde (0.34 g, 2.25 mmol,

1 eq) was added to the suspension which was stirred at -78 °C for 4 hours. The reaction was diluted with TBME (50 mL) and washed with NH₄Cl solution (10 %, 50 mL). The organic phase was washed with water (until pH 7), dried over magnesium sulphate and concentrated. The crude product was purified by column chromatography using pet. ether/ ethyl acetate (10:1 then 4:1) to yield **6** (0.39 g, 1.89 mmol, 84 %) as a pale yellow solid.

¹H NMR (CDCl₃): δ 8.19 (d, J=8.8, 2H, ArH), 7.65 (d, J=8.4, 2H, ArH), 7.01 (d, J=12.5, 1H, CH), 6.12 (d, J=12.5, 1H, CH), 3.07 (s, 3H, OCH₃)

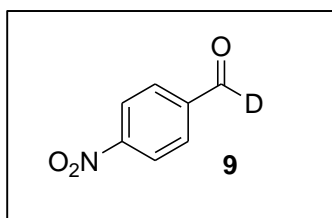


7 (*Z*)-3-(4-nitrophenyl)acrylic acid[140]: To a stirred suspension of **6** (380 mg, 1.8 mmol) in water (3.5 mL), THF (3.5 mL) and methanol (2 mL), was added LiOH·H₂O (228 mg, 5.4 mmol, 3 eq) and the reaction was stirred at room temperature overnight.

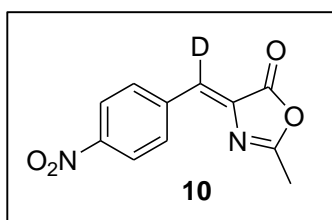
The reaction was acidified with 1 M HCl and extracted with ethyl acetate, dried over magnesium sulphate and concentrated to yield **7** (340 mg, 1.76 mmol, 98 %) as a yellow solid which was used without further purification.

$^1\text{H NMR}$ ($\text{DMSO-}d_6$): δ 8.23 (d, $J=8.9$, 2H, ArH), 7.76 (d, $J=8.6$, 2H ArH), 7.09 (d, $J=12.6$, 1H, CH), 6.19 (d, $J=12.6$, 1H, CH), 1.91 (s, OH)

m/z (ESI) observed 191.9 $[\text{M-H}]^-$, $\text{C}_9\text{H}_7\text{NO}_4$ calculated 193.16



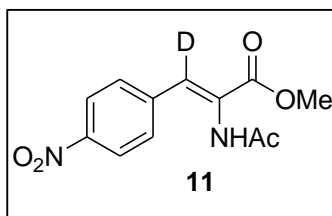
9 4-nitro- ^2H -benzaldehyde: LiAlD_4 (0.6 g, 15.8 mmol, 1.5 eq.) was suspended in diglyme (7 mL) and *tert*-butyl alcohol (5 mL) and stirred at room temperature for 30 minutes. The LiAlD_4 mixture was added dropwise to a solution of 4-nitrobenzoylchloride **8** (2 g, 10.8 mmol, 1 eq.) in diglyme (10 mL) at -78°C . The reaction was stirred for 30 minutes at -78°C when water was added to quench the reaction; the product was extracted with diethyl ether and concentrated. The addition of water to the product in remaining diglyme resulted in precipitation of the product which was collected by filtration. The product was lyophilized to give **9** as a light yellow powder (866 mg, 5.7 mmol, 53 % crude) which was used without further purification.



10 $[4\text{-}^2\text{H}]$ -4(4-nitrobenzylidene)-2-methyl-5(4H)-oxazol-2-one: 4-Nitrobenzaldehyde **9** (0.86 g, 5.7 mmol, 1 eq.) was added to *N*-acetylglycine (664 mg, 5.7 mmol, 1 eq.) and sodium acetate (466 mg, 5.7 mmol, 1 eq.) in acetic anhydride (5 mL) and stirred at 100°C overnight. The reaction was cooled to room temperature, resulting in precipitation of the desired product. The precipitate was washed with diethyl ether and collected by filtration to give **10** as a gold solid (1.30 g, 5.6 mmol, 99 % crude) which was used without further purification.

$^1\text{H NMR}$ (CDCl_3): δ 8.30-8.24 (m, 4H, ArH), 2.45 (s, 3H, CH_3)

$^{13}\text{C NMR}$ (CDCl_3): δ 168.54, 166.90, 148.38, 138.92, 135.55, 132.60, 127.54, 123.91, 15.88

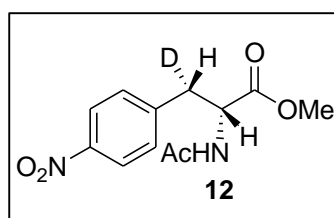


11 $[4\text{-}^2\text{H}]$ -methyl-2-acetamido-3(4-nitrophenyl)acrylate: Sodium methoxide solution in methanol (25 wt %, 1.2 mL) was added to azalactone **10** (1.2 g, 5.2 mmol) in methanol (12 mL) and stirred at room temperature for 30 minutes. The reaction was diluted with dichloromethane (100 mL) and washed with saturated NH_4Cl solution (100 mL). The organic phase was washed with water (2 x 50 mL) dried and concentrated to give **11** as a light yellow solid (0.64 g, 2.4 mmol, 46 % crude) which was used without further purification.

^1H NMR (DMSO- d_6): δ 9.92 (s, 1H, NH), 8.25 (d, $J=9.0$, 2H, ArH), 7.86 (d, $J=9.0$, 2H, ArH), 3.74 (s, 3H, CO_2CH_3), 2.02 (s, 3H, NHCOCH_3)

^{13}C NMR (DMSO- d_6): δ 169.4, 165.2, 145.9, 140.3, 130.6, 129.6, 123.6, 52.4, 22.5

m/z (ESI) observed 288.1 $[\text{M}+\text{Na}]^+$, $\text{C}_{12}\text{H}_{11}\text{N}_2\text{O}_5\text{D}$ calculated 265.24



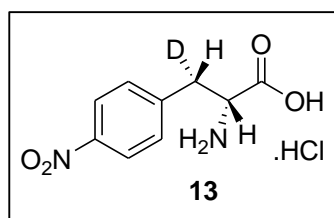
12 (*R*)-methyl-2-acetamido-3- $[[^2\text{H}]$]-3-(4-nitrophenyl) propanoate: Enamide **11** (315 mg, 1.2 mmol) and $[\text{Rh}(\text{R,R})\text{-Ethyl-DuPhos}(\text{COD})]\text{BF}_4$ (7.3 mg, 1 mol%) were stirred in methanol (5 mL) under 100 psi of H_2 for 90 minutes. The methanol was evaporated and the product was redissolved in ethyl acetate,

filtered through a plug of silica and concentrated to give **12** as an orange solid (315 mg, 1.2 mmol, 99 % crude) which was used without further purification.

^1H NMR (CDCl_3): δ 8.17 (d, $J=8.8$, 2H, ArH), 7.29 (d, $J=8.6$, 2H, ArH), 5.99 (d, $J=7.1$, 1H, NH), 4.93 (dd, $J=7.3$, 6.2, 1H, CHCO_2Me), 3.76 (s, 3H, CO_2CH_3), 3.29 (d, $J=6.0$, 1H, CHAr), 2.02 (s, 3H, NHCOCH_3)

^{13}C NMR (DMSO- d_6): δ 171.5, 169.7, 147.2, 143.7, 130.2, 123.7, 52.8, 52.7, 23.2

m/z (ESI) observed 268.1 $[\text{M}+\text{H}]^+$, $\text{C}_{12}\text{H}_{13}\text{N}_2\text{O}_5\text{D}$ calculated 267.26



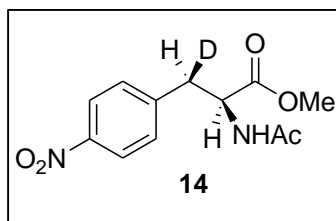
13 (*R*)-2-amino-3- $[[\text{S}-^2\text{H}]$]-3-(4-nitrophenyl)propanoic acid hydrochloride: 4 M HCl (20 mL) was added to a stirring solution of protected amino acid **12** (315 mg, 1.2 mol) in acetone (2.5 mL). The mixture was heated under reflux for 7 hours, after cooling the reaction was treated with decolorizing

charcoal filtered and concentrated. Triturating with acetone gave the product **13** as a light yellow solid (199 mg, 0.8 mmol, 67 % yield, 99 % e.e., 83 % ^2H incorporation).

^1H NMR ($\text{D}_2\text{O} + \text{NaOH}$): δ 8.07 (d, $J=8.5$, 2H, ArH), 7.34 (d, $J=8.5$, 2H, ArH), 3.42 (d, $J=5.9$, 1H, CHNH_2), 2.94 (d, $J=5.7$, 1H, CHAr)

^{13}C NMR ($\text{D}_2\text{O} + \text{NaOH}$): δ 170.0, 145.8, 143.4, 131.0, 123.5, 52.6

m/z (ESI) observed 212.1 $[\text{M}+\text{H}]^+$, $\text{C}_9\text{H}_9\text{N}_2\text{O}_4\text{D}$ calculated 211.19



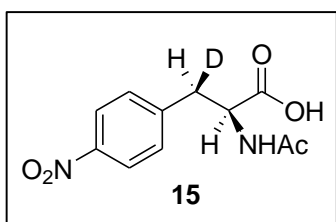
14 (*S*)-methyl-2-acetamido-3-^[2H]-3(4-nitrophenyl) propanoate: Enamide **11** (315 mg, 1.2 mmol) and [Rh(*S,S*)-Ethyl-DuPhos(COD)]BF₄ (7.3 mg, 1 mol %) were stirred in methanol (5 mL) under 100 psi of H₂ for 90 minutes. The methanol was evaporated and the product was redissolved in ethyl acetate,

filtered through a plug of silica and concentrated to give **14** as an orange solid (315 mg, 1.2 mmol, 99 % crude) which was used without further purification.

¹H NMR (CDCl₃): δ 8.16 (d, J=8.7, 2H, ArH), 7.28 (d, J=8.7, 2H, ArH), 5.99 (d, J=7.1, 1H, NH), 4.92 (dd, J=7.3, 6.2, 1H, CHCO₂Me), 3.75 (s, 3H, CO₂CH₃), 3.28 (d, J=6.0, 1H, CHAR), 2.01 (s, 3H, NHCOCH₃)

¹³C NMR (DMSO-d₆): δ 171.5, 169.7, 147.2, 143.8, 130.2, 123.7, 52.8, 52.7, 23.2

m/z (ESI) observed 268.2 [M+H]⁺, C₁₂H₁₃N₂O₅D calculated 267.26



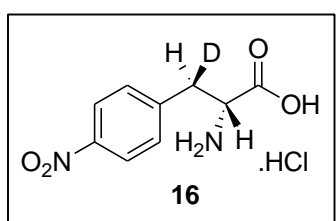
15 (*S*)-2-acetamido-3-^[2H]-3(4-nitrophenyl)propanoic acid: Lithium hydroxide (86 mg, 3.6 mmol, 3 eq) was added to protected amino acid **14** (315 mg, 1.2 mmol, 1 eq) in water (3.5 mL), THF (3.5 mL) and methanol (2 mL), and stirred at room temperature for 2 hours. The reaction was neutralized

with the addition of 1 M HCl, extracted with ethyl acetate (2 x 20 mL) dried and concentrated to give **15** as a light yellow solid (298 mg, 1.2 mmol, 99 %) which was used without further purification.

¹H NMR (DMSO-d₆): δ 8.15 (m, 3H, ArH+NH), 7.50 (d, J=8.7, 2H, ArH), 4.43 (dd, J=8.0, 5.0, 1H, CHCO₂H), 3.18 (d, J=4.9, 1H, CHAR), 1.77 (s, 3H, NHCOCH₃)

¹³C NMR (DMSO-d₆): δ 172.7, 169.1, 145.3, 145.2, 130.4, 123.2, 53.0, 22.3

m/z (ESI) observed 252.0 [M-H]⁻, C₁₁H₁₁N₂O₅D calculated 253.23



16 (*R*)-2-amino-3-[(*R*)-^{2H}]-3(4-nitrophenyl)propanoic acid hydrochloride: *N*-acetyl amino acid **15** (295 mg, 1.2 mmol) was dissolved in Tris-buffer (2 mM, pH 8.0, 8 mL) containing CoCl₂·6H₂O (5 mM). *N*-Acetyl amino acid racemase variant G291D/F323Y (1 mL, 100 U / mL, Dr. Reddy's) and D-acylase

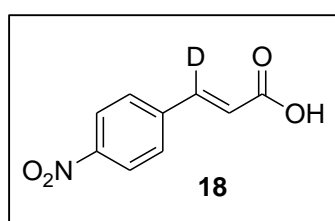
(20 mg, Amano) were added and the reaction was incubated at 37 °C with shaking for 23 hours. To quench the reaction, the pH was adjusted to pH 1.0 with the addition of 6 M HCl and the reaction mixture was incubated for 1 hour with shaking at 37 °C. The enzymes were removed by filtering the reaction mixture through a pad of celite under vacuum, and the filtrate

was lyophilized. The product was triturated in acetone and filtered to give the product **16** as a light yellow solid (231 mg, 0.93 mmol, 78 % yield, 98 % e.e., 83 % ^2H incorporation).

^1H NMR (D_2O + NaOH): δ 8.08 (d, $J=8.6$, 2H, ArH), 7.34 (d, $J=8.6$, 2H, ArH), 3.43 (d, $J=7.2$, 1H, CHNH $_2$), 2.85 (d, $J=7.1$, 1H CHAr)

^{13}C NMR (D_2O + NaOH): δ 170.0, 145.7, 143.4, 131.0, 123.5, 52.6

m/z (ESI) observed 212.1 $[\text{M}+\text{H}]^+$, $\text{C}_9\text{H}_9\text{N}_2\text{O}_4\text{D}$ calculated 211.19

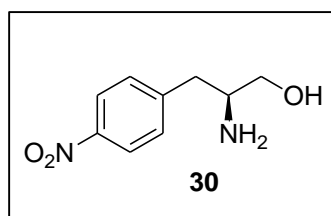


18 *trans*-3- ^2H -3-(4-nitrophenyl)acrylic acid: 4-Nitro- ^2H -benzaldehyde **9** (400 mg, 2.7 mmol, 1 eq.), malonic acid (330 mg, 3.2 mmol, 1.2 eq) and piperidine (32 μL , 0.3 mmol, 0.1 eq) were stirred in pyridine (15 mL) at 80 $^\circ\text{C}$ overnight. The pyridine was evaporated and the solids were washed with cold

water. The product was purified by recrystallisation in dichloromethane to give **18** as a light yellow solid (416 mg, 2.1 mmol, 79 % yield, 99 % ^2H incorporation).

^1H NMR (D_2O): δ 8.13 (d, $J=8.9$, 2H, ArH), 7.65 (d, $J=8.9$, 2H, ArH), 6.52 (s, 1H, CH)

^{13}C NMR (D_2O): δ 164.66, 147.50, 141.98, 130.14, 128.73, 128.32, 123.98, 123.62

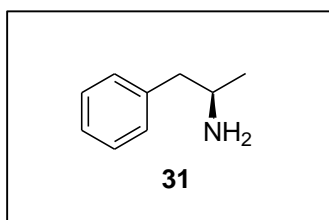


(*S*)-2-amino-3-(4-nitrophenyl)propan-1-ol **30**[141]: 4-nitro-L-phenylalanine methyl ester **28** (1 g, 3.8 mmol) was dissolved in water (7.5 ml) and added dropwise to sodium borohydride (0.56 g, 15 mmol) in water (7.5 ml) in an ice-salt bath. The reaction was stirred for 4 hours. TLC showed there was a small amount

of starting material (DCM/MeOH 9:1). The reaction was extracted with ethyl acetate (3 x 50 ml) and dried over magnesium sulphate. The solvent was evaporated and the crude product was purified by column chromatography (DCM then DCM/MeOH 9:1) to give **30** as a yellow powder (0.35 g, 1.78 mmol, 47 %)

^1H NMR (400 MHz, CDCl_3): δ 8.13 (d, 2H, $J=8.8$, ArH), δ 7.50 (d, 2H, $J=8.4$, ArH), δ 4.69 (s, OH), δ 3.22 (dd, 2H, $J=4.8$, 10.4, CH $_2$), δ 2.84 (dq, 2H, $J=5.2$, 7.2, CH $_2$), δ 2.54 (dd, 1H, $J=7.8$, 10.4, CH)

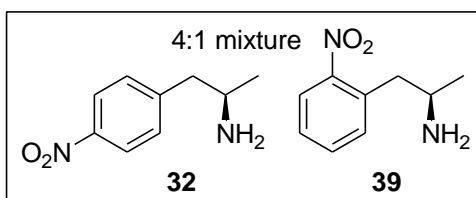
^{13}C NMR (CDCl_3): δ 148.75, 145.79, 130.48, 123.09, 65.93, 54.31



(R)-amphetamine **31**[142]: (*4R*, *5S*)-4-methyl-5-phenyl-2-oxazolidinone (1.8g, 10 mmol) was dissolved in ethanol (20 mL) and Pd/C 10% (100 mg) was added. The flask was flushed with nitrogen followed by hydrogen, and the reaction was stirred under hydrogen at room temperature overnight. TLC showed the reaction had gone to completion (EtOAc/pet ether 40-60 4:1), the reaction was filtered over celite and concentrated to give **31** (1.30 g, 9.5 mmol, 95 %) as a colourless oil which was used without further purification.

^1H NMR (400 MHz, CDCl_3): δ 7.18 (m, 5H, ArH), δ 3.10 (m, 1H, CH), δ 2.66 (dd, 1H, $J=5.2$, 13.6, CH_2), δ 2.46 (dd, 1H, $J=8.0$, 13.2, CH_2), δ 1.05 (d, 3H, $J=6.4$, CH_3)

m/z (ESI) observed 136.1 $[\text{M}+\text{H}]^+$, $\text{C}_9\text{H}_{13}\text{N}$ calculated 135.21



4-nitro-(R)-amphetamine **32**: Amphetamine, **31** (1 g, 5.4 mmol) was added portionwise to fuming nitric acid (5 mL) at -20°C and stirred for 18 hours under nitrogen. The reaction was poured onto ice (50 mL) and extracted with TBME. The aqueous

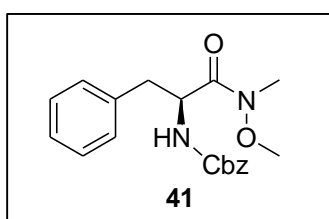
phase was basified to pH 13 with NaOH (6 N) and then re-extracted with TBME (3 x 80 mL). The organic phases were combined, dried over magnesium sulphate and concentrated to give **32** and **39** in a 4:1 mixture (789 mg, 60 %) as a brown oil.

4:1 mixture of 4-nitro-(*R*)-amphetamine **32** and 2-nitro-(*R*)-amphetamine **39**.

4-nitro-(*R*)-amphetamine **32** ^1H NMR (400 MHz, CDCl_3): δ 8.19 (d, 2H, $J=8.8$, ArH), δ 7.38 (d, 2H, $J=8.8$, ArH), δ 3.25 (m, 1H, CH), δ 2.82 (dd, 1H, $J=5.6$, 13.6, CH_2), δ 2.69 (dd, 1H, $J=8.0$, 13.2, CH_2), δ 1.16 (d, 3H, $J=6.3$, CH_3)

2-nitro-(*R*)-amphetamine **39** ^1H NMR (400 MHz, CDCl_3): δ 8.11 (d, 1H, $J=7.7$, ArH), δ 7.93 (d, 1H, $J=8.2$, ArH), δ 7.54 (m, 2H, ArH), δ 3.25 (m, 1H, CH), δ 3.05 (dd, 1H, $J=5.4$, 13.2, CH_2), δ 2.85 (dd, 1H, $J=5.4$, 11.9, CH_2), δ 1.16 (d, 3H, $J=6.3$, CH_3)

m/z (ESI) observed 181.1 $[\text{M}+\text{H}]^+$, $\text{C}_9\text{H}_{12}\text{N}_2\text{O}_2$ calculated 180.2

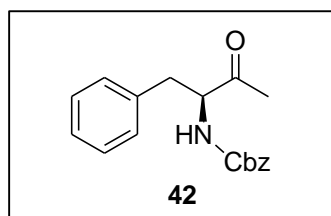


Benzyl-(S)-1-(*N*-methoxy-*N*-methylcarbamoyl)-2-phenylethyl carbamate **41**[128]: Cbz-protected-L-phenylalanine (4 g, 13.4 mmol) was dissolved in DMF (60 mL), HBTU (7.44 g, 20.3 mmol), HOBt.H₂O (3.04 g, 20.3 mmol), DIEA (8.36 g, 11.26 ml, 48 mmol) and *N,O*-dimethylhydroxylamine. HCl (4.48 g, 46.2 mmol) were added and the reaction was stirred at room temperature for 2 hours. TLC showed

the reaction had gone to completion (cyclohexane/EtOAc 1:1). The reaction was diluted with ethyl acetate (400 mL) and washed with NaHCO₃ (3 x 200 mL), 10 % citric acid (3 x 200 mL) and saturated NaCl (3 x 200mL). The organic phase was dried over magnesium sulphate and concentrated to give **41** (5g, 14.6 mmol, 109 % crude) as a thick colourless oil which was used without further purification.

¹H NMR (400 MHz, CDCl₃): δ 7.28 (m, 10H, ArH), δ 5.45 (d, 1H, J=8.0, NH), δ 5.08 (dd, 2H, J=12, 24, CH₂Cbz), δ 5.05 (m, 1H, CHN), δ 3.70 (s 3H, OCH₃), δ 3.20 (s, 3H, NCH₃), δ 3.09 (dd, 1H, J=6, 13.6 CH₂), δ 2.93 (dd, 1H, J=7.2, 16.8, CH₂)

m/z (ESI) observed 365.3 [M+Na]⁺, C₁₉H₂₂N₂O₄ calculated 342.39

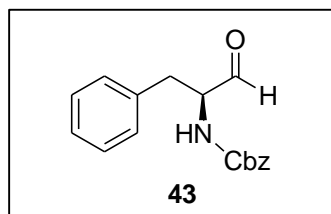


Benzyl-(S)-3-oxo-1-phenylbutan-2-ylcarbamate **42**[143]:

Weinreb amide **41** (1.5 g, 4.3 mmol) dissolved in THF (3 mL) was added dropwise to a solution of MeLi (8.25 mL, 1.6 M in diethyl ether) in THF (37 mL) at -30 °C. The reaction was stirred for 1 hour and TLC showed the reaction had gone to completion (cyclohexane/EtOAc, 3:1). The reaction was decomposed with 1 N HCl and extracted with diethyl ether (2 x 100 mL), dried over magnesium sulphate and concentrated to give a purple oil which crystallised in air. The crude product was purified by column chromatography (cyclohexane/EtOAc 7:1 then 3:1) to give **42** as a yellow solid (0.61 g, 2.03 mmol, 47 %).

¹H NMR (400 MHz, CDCl₃): δ 7.32 (m, 8H, ArH), δ 7.14 (d, 2H, J=6.4, ArH), δ 5.41 (d, 1H, J=7.2, NH), δ 5.11 (s 2H, CH₂Cbz), δ 4.66 (dd, 1H, J=6.4, 13.6, CH), δ 3.15 (dd, 1H, J=6.8, 14.4, CH₂), δ 3.05 (dd, 1H, J=6.0, 14.0, CH₂), δ 2.17 (s, 3H, CH₃)

m/z (ESI) observed 320.3 [M+Na]⁺, C₁₈H₁₉NO₃ calculated 297.14

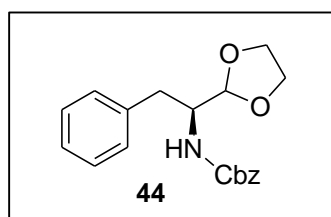


Benzyl-(S)-1-formyl-2-phenylethylcarbamate **43**[128]:

Weinreb amide **41** (1.4 g, 4.0 mmol) was dissolved in dry THF (25 mL) and LiAlH₄ (1 M in THF, 10 mL) was added under nitrogen at 0 °C. The reaction was warmed to room temperature and stirred for 1 hour. Diethyl ether was added (100 mL) and the reaction was quenched with 0.5 M HCl (50 mL). The aqueous phase was extracted with diethyl ether (3 x 20 mL), the organic phases were combined and washed with 1 M HCl (3 x 20 mL), 5 % NaHCO₃ (3 x 20 mL), and saturated NaCl (3 x 20 mL), dried over magnesium sulphate and concentrated to give a light yellow oil. The crude product was purified by column

chromatography (EtOAc/cyclohexane 3:1 then 2:1) to give **43** (0.365 g, 1.2 mmol, 30 %) as a light yellow solid.

^1H NMR (400 MHz, CDCl_3): δ 9.67 (s, 1H, aldehyde), δ 7.34 (m, 8H, ArH), δ 7.16 (d, 2H, $J=6.8$, ArH), δ 5.30 (s, 1H, NH), δ 5.14 (s, 2H, CH_2Cbz), δ 4.55 (dd, 1H, $J=6.8$, 12.8, CH), δ 3.20 (dd, 1H, $J=6.4$, 14.0, CH_2), δ 3.16 (dd, 1H, $J=6.4$, 13.6, CH_2)



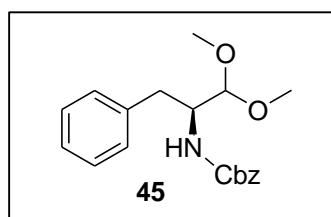
Benzyl-(S)-1-(1,3-dioxolan-2-yl)-2-phenylethylcarbamate

44[128]: Ethylene glycol (297 μl , 5.3 mmol) and TsOH (13 mg, 0.065 mmol) were added to a solution of benzyl-(S)-1-formyl-2-phenylethylcarbamate **43** (0.14 g, 0.53 mmol) in toluene (12 mL). The reaction was stirred under reflux for 6 hours. The

reaction was concentrated and the residue was redissolved in EtOAc (20 mL), washed with water (3 x 20 mL) saturated NaCl (3 x 20 mL), dried over magnesium sulphate and concentrated to give a white solid. The crude product was purified by column chromatography (cyclohexane/EtOAc 2:1) to give **44** (100 mg, 0.31 mmol, 58 %) as a white solid.

^1H NMR (400 MHz, CDCl_3): δ 7.30 (m, 10H, ArH), δ 5.07 (d, 2H, $J=5.2$, CH_2Cbz), δ 4.92 (d, 1H, $J=7.6$, NH), δ 4.87 (d, 1H, $J=2.0$, CH), δ 4.24 (m, 1H, CHN), δ 4.00 (m, 2H, CH_2), δ 3.90 (m, 2H, CH_2), δ 2.89 (dq, 2H, $J=7.2$, 15.6, CH_2)

m/z (ESI) observed 350.4 $[\text{M}+\text{Na}]^+$, $\text{C}_{19}\text{H}_{21}\text{NO}_4$ calculated 327.37



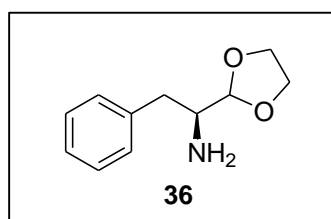
Benzyl-(S)-1,1-dimethoxy-3-phenylpropan-2-yl-carbamate

45[144]: benzyl-(S)-1-formyl-2-phenylethylcarbamate **43** (0.15 g, 0.53 mmol) was dissolved in anhydrous methanol (5 mL), TsOH (10 mg, 0.05 mmol) and trimethylorthoformate (10 % vol) were added and the reaction was stirred under nitrogen at

room temperature for 5 hours. TLC (cyclohexane/EtOAc 2:1) showed the reaction had gone to completion. The reaction was concentrated and NaHCO_3 (10 mL) was added. The product was extracted with dichloromethane (3 x 20 mL), dried over magnesium sulphate and concentrated to give a colourless oil. The crude product was purified by column chromatography (Cyclohexane/EtOAc 2:1) to give **45** (82 mg, 0.025 mmol, 47 %) as a white solid.

^1H NMR (400 MHz, CDCl_3): δ 7.21 (m, 10H, ArH), δ 4.97 (d, 1H, $J=12.4$, CH_2Cbz), δ 4.91 (d, 1H, $J=12.4$, CH_2Cbz), δ 4.88 (d, 1H, $J=9.2$, CH), δ 4.10 (d, 1H, $J=3.6$, NH), δ 4.03 (m, 1H, CHN), δ 4.36 (s, 3H, CH_3), δ 4.32 (s, 3H, CH_3), δ 2.86 (dd, 1H, $J=6.0$, 14.0, CH_2), δ 2.72 (dd, 1H, $J=8.0$, 14.0, CH_2)

m/z (ESI) observed 352.3 [M+Na]⁺, C₁₉H₂₃NO₄ calculated 329.39

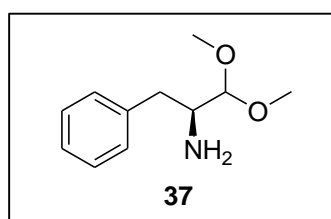


(*S*)-1-(1,3-dioxolan-2-yl)-2-phenylethanamine **36**[128]:

Pd(OH)₂/C (20 wt %, 80 mg) was added to a nitrogen purged solution of benzyl-(*S*)-1-(1,3-dioxolan-2-yl)-2-phenylethylcarbamate **44** (80 mg, 0.25 mmol) in ethyl acetate (2 mL). 1,4-cyclohexadiene (0.24 mL, 2.5 mmol, 10 eq) was added and the reaction was stirred at room temperature for 5 hours. The reaction was filtered over celite and concentrated to give a yellow oil. The crude product was purified by column chromatography (cyclohexane/EtOAc 1:1 then EtOAc) to give **36** (20 mg, 0.10 mmol, 41 %) as a yellow solid.

¹H NMR (400 MHz, CDCl₃): δ 7.19 (m, 5H, ArH), δ 4.78 (d, 1H, J=3.6, CH), δ 4.07 (m, 2H, CH₂), δ 3.94 (m, 2H, CH₂), δ 3.21 (m, 1H, CHN), δ 2.98 (dd, 1H, J=5.6, 13.6, CH₂), δ 2.75 (dd, 1H, J=8.8, 13.6, CH₂)

m/z (ESI) observed 194.2 [M+H]⁺, C₁₁H₁₅NO₂ calculated 193.24

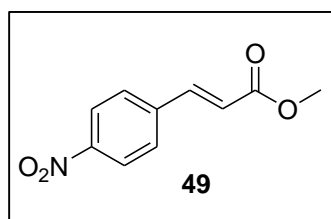


(*S*)-1,1-dimethoxy-3-phenylpropan-2-amine **37**[144]:

Pd(OH)₂/C (20 wt %, 100 mg) was added to a nitrogen purged solution of benzyl-(*S*)-1,1-dimethoxy-3-phenylpropan-2-yl-carbamate **45** (100 mg, 0.4 mmol) in ethyl acetate (2 mL). 1,4-cyclohexadiene (0.38 mL, 4 mmol, 10 eq) was added and the reaction was stirred at room temperature for 5 hours. The reaction was filtered over celite and concentrated. The crude product was purified by column chromatography (cyclohexane/EtOAc 1:1 then EtOAc) to give **37** (35 mg, 0.18 mmol, 45 %) as a yellow oil.

¹H NMR (400 MHz, CDCl₃): δ 7.19 (m, 5H, ArH), δ 4.12 (d, 1H, J=5.2, CH), δ 3.40 (s, 3H, CH₃), δ 3.36 (s, 3H, CH₃), δ 3.17 (m, 1H, CHN), δ 2.94 (dd, 1H, J=5.2, 13.6, CH₂), δ 2.66 (dd, 1H, J=8.4, 13.6, CH₂)

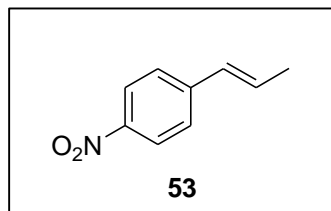
m/z (ESI) observed 196.3 [M+H]⁺, C₁₁H₁₇NO₂ calculated 195.26



trans-methyl-3-(4-nitrophenyl)acrylate **49**[145]: 4-nitro-*trans*-cinnamic acid (**1m**) (0.97 g, 5 mmol) was added portionwise to a stirred solution of thionyl chloride (0.43 mL, 6 mmol) in methanol (60 mL) cooled to 0 °C. The reaction was allowed to warm to room temperature and was stirred overnight. The

precipitate was washed with cold methanol and dried in air to give **49** (0.70 g, 3.4 mmol, 68 %) as a white solid, which was used without further purification.

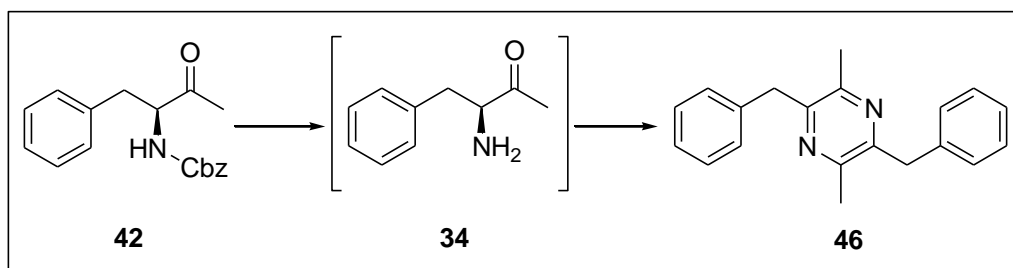
^1H NMR (400 MHz, CDCl_3): δ 8.19 (d, 2H, $J=8.8$, ArH), δ 7.66 (d, 1H, $J=16.0$, CH), δ 7.61 (d, 2H, $J=8.8$, ArH), δ 6.50 (d, 1H, $J=16.0$, CH), δ 3.78 (s, 3H, CH_3)



4-nitro-trans-beta-methylstyrene **53**: 4-nitro-(*R*)-amphetamine **32** (50 mg, 0.278 mmol) was dissolved in methanol (2.5 mL) and acetonitrile (3.75 mL). K_2CO_3 (540 mg, 3.96 mmol, 16 eq) and iodomethane (0.25 mL, 4 mmol, 22 eq) were added and the reaction was stirred at room temperature overnight. The

reaction was concentrated (1 mL), diluted with diethylether (10 mL) and washed with water (10 mL). The water was extracted with diethylether (2 x 10 mL) and the organic phases were combined, dried over MgSO_4 and concentrated. The crude product was purified by column chromatography (pet ether 60-80 then pet ether 60-80/diethylether 9:1) to give **53** (33 mg, 0.20 mol, 73 %) as a white solid.

^1H NMR (400 MHz, CDCl_3): δ 8.09 (d, 2H, $J=9.2$, ArH), δ 7.38 (d, 2H, $J=8.8$, ArH), δ 6.40 (m, 2H, alkene), δ 1.88 (d, 3H, $J=5.2$, CH_3)



Cbz-protected amino ketone **42** (1.0 mmol) was dissolved in ethyl acetate (4 mL) under nitrogen. $\text{Pd}(\text{OH})_2/\text{C}$ (20 % wt, 300 mg) and 1,4 cyclohexadiene (0.9 mL, 10 mmol, 10 eq) were added and the reaction was stirred at room temperature overnight. The reaction was filtered through a pad of celite and the filtrate was concentrate to give the dimerisation product **46**.

2,5-dibenzyl-3,6-dimethylpyrazine **46**

^1H NMR (400 MHz, CDCl_3): δ 7.28-7.14 (m, 8H, ArH), 4.14 (s, 4H, 2x CH_2), 2.46 (s, 6H, 2x CH_3)

^{13}C NMR (CDCl_3): δ 138.2, 128.7, 128.5, 126.38, 41.19, 21.36

m/z (ESI) observed 289.3 $[\text{M}+\text{H}]^+$, $\text{C}_{20}\text{H}_{20}\text{N}_2$ calculated 288.39

7 Appendix

7.1 DNA and Protein Sequences

7.1.1 *Anabaena variabilis* PAL (AvPAL)

1 M K T L S Q A Q S K T S S Q Q F S F T G
1 ATGAAAACCCTGAGCCAGGCACAGAGCAAAACCAGCAGCCAGCAGTTTAGCTTTACCGG
21 N S S A N V I I G N Q K L T I N D V A R
61 AATAGCAGCGCAAATGTGATTATTGGTAATCAGAAACTGACCATCAATGATGTTGCACGT
41 V A R N G T L V S L T N N T D I L Q G I
121 GTTGCCCGTAATGGCACCCCTGGTTAGCCTGACCAATAATACCGATATTCTGCAGGGTATT
61 Q A S C D Y I N N A V E S G E P I Y G V
181 CAGGCCAGCTGTGATTATATCAATAATGCAGTTGAAAGCGGTGAACCGATTTATGGTGT
81 T S G F G G M A N V A I S R E Q A S E L
241 ACCAGCGGTTTTGGTGGTATGGCAAATGTTGCAATTAGCCGTGAACAGGCAAGCGAACTG
101 Q T N L V W F L K T G A G N K L P L A D
301 CAGACCAATCTGGTTTTGGTTTTCTGAAAACCGGTGCAGGTAATAAACTGCCGCTGGCAGAT
121 V R A A M L L R A N S H M R G A S G I R
361 GTTCGTGCAGCAATGCTGCTGCGTGCAAATAGCCACATGCGTGGTGCAAGCGGTATTCGT
141 L E L I K R M E I F L N A G V T P Y V Y
421 CTGGAAGTGAATTAACGCATGGAAATCTTTCTGAATGCCGGTGTACCCCGTATGTTTAT
161 E F G S I G A S G D L V P L S Y I T G S
481 GAATTTGGTAGCATTGGTGCCAGCGGTGATCTGGTTCCGCTGAGCTATATTACCGGTAGC
181 L I G L D P S F K V D F N G K E M D A P
541 CTGATTGGCCTGGACCCGAGCTTTAAAGTTGATTTTAATGGCAAAGAAATGGACGCACCG
201 T A L R Q L N L S P L T L L P K E G L A
601 ACCGCACTGCGTCAGCTGAATCTGAGTCCGCTGACCCTGCTGCCGAAAGAAGGTCTGGCA
221 M M N G T S V M T G I A A N C V Y D T Q
661 ATGATGAATGGCACCAGCGTTATGACCGGTATTGCAGCAAATTGTGTTTATGATACCCAG
241 I L T A I A M G V H A L D I Q A L N G T
721 ATTCTGACCGCAATTGCAATGGGTGTTTCATGCACTGGATATTCAGGCACTGAATGGTACA
261 N Q S F H P F I H N S K P H P G Q L W A
781 AATCAGAGCTTTCATCCGTTTATCCATAACAGCAAACCGCATCCGGGTCAGCTGTGGGCA
281 A D Q M I S L L A N S Q L V R D E L D G
841 GCAGATCAGATGATTAGCCTGCTGGCCAATAGCCAGCTGGTTTCGTGATGAACTGGATGGT
301 K H D Y R D H E L I Q D R Y S L R C L P
901 AAACATGATTATCGTGATCATGAACTGATCCAGGATCGTTATAGCCTGCGTTGTCTGCCG
321 Q Y L G P I V D G I S Q I A K Q I E I E
961 CAGTATCTGGGTCCGATTGTTGATGGTATTAGCCAGATTGCCAAACAAATCGAAATTGAG

341 I N S V T D N P L I D V D N Q A S Y H G
 1021 ATTAACAGCGTTACCGATAACCCGCTGATTGATGTTGATAATCAGGCAAGCTATCATGGT
 361 G N F L G Q Y V G M G M D H L R Y Y I G
 1081 GGTAATTTTCTGGGTGAGTATGTTGGTATGGGTATGGATCATCTGCGCTATTATATCGGT
 381 L L A K H L D V Q I A L L A S P E F S N
 1141 CTGCTGGCAAAACATCTGGATGTTGAGATTGCACTGCTGGCATCACCGAATTTAGCAAT
 401 G L P P S L L G N R E R K V N M G L K G
 1201 GGTCTGCCTCCGAGTCTGCTGGGTAATCGTGAACGTAAGTTAATATGGGTCTGAAAGGT
 421 L Q I C G N S I M P L L T F Y G N S I A
 1261 CTGCAGATTTGCGGTAATAGCATTATGCCGCTGCTGACCTTTTATGGTAATAGTATTGCA
 441 D R F P T H A E Q F N Q N I N S Q G Y T
 1321 GATCGTTTTCCGACCCATGCCGAACAGTTTAACCAGAATATTAACAGCCAGGGTTATACC
 461 S A T L A R R S V D I F Q N Y V A I A L
 1381 AGCGCAACCCTGGCACGTCGTAGCGTTGATATTTTTTCAGAATTATGTTGCCATTGCCCTG
 481 M F G V Q A V D L R T Y K K T G H Y D A
 1441 ATGTTTGGTGTTCAGGCAGTTGATCTGCGTACCTACAAAAAACCGGTCATTATGATGCA
 501 R A C L S P A T E R L Y S A V R H V V G
 1501 CGTGCCTGTCTGTCACCGCAACCGAACGTCGTATAGCGCAGTTCGTCATGTTGTTGGT
 521 Q K P T S D R P Y I W N D N E Q G L D E
 1561 CAGAAACCGACCTCAGATCGTCCGTATATTTGGAATGATAATGAACAGGGTCTGGATGAA
 541 H I A R I S A D I A A G G V I V Q A V Q
 1621 CATATTGCACGTATTAGTGCAGATATTGCAGCCGGTGGTGTATTGTTTCAGGCCGTTTCAG
 561 D I L P C L H *
 1681 GACATTCTGCCGTGTCTGCATTAA

7.1.2 *Petroselinum crispum* PAL (PcPAL)

1 M E N G N G A I T N G H V N G N G M D F
 1 ATGGAGAACGGCAATGGTGCAATTACAAATGGACATGTAAACGGGAACCGAATGGATTTT
 21 C M K T E D P L Y W G I A A E A M T G S
 61 TGCATGAAGACCGAAGATCCGTTGTTACTGGGGAATCGCGGCGGAGGCAATGACAGGGAGT
 41 H L D E V K K M V A E Y R K P V V K L G
 121 CATTTGGATGAAGTGAAGAAGATGGTGGCTGAGTATAGGAAGCCGTTGTGAAGTTAGGA
 61 G E T L T I S Q V A A I S A R D G S G V
 181 GGAGAAACATTGACTATTTCTCAAGTGGCAGCTATTTTCGGCTAGGGATGGTAGTGGTGTCT
 81 T V E L S E A A R A G V K A S S D W V M
 241 ACGGTGGAGCTTTCCGAGGCGGCGAGAGCTGGCGTTAAGGCTAGTAGTATTGGGTGATG
 101 D S M N K G T D S Y G V T T G F G A T S
 301 GATAGTATGAACAAAGGGACGGATAGTTATGGTGTAACTACTGGTTTTGGTGTCTACTTCT
 121 H R R T K Q G G A L Q K E L I R F L N A
 361 CATAGGAGGACTAAGCAAGGTGGTGTCTTTCAGAAAAGAGCTCATTAGGTTCTTGAATGCT

141 G I F G N G S D N T L P H S A T R A A M
421 GGAATATTTGGTAATGGATCAGATAATACATTACCACACTCAGCAACAAGAGCTGCAATG
161 L V R I N T L L Q G Y S G I R F E I L E
481 TTAGTGAGGATCAACACTCTGCTCCAGGGATACTCTGGAATCCGATTCGAAATTTCTCGAA
181 A I T K F L N Q N I T P C L P L R G T I
541 GCGATTACTAAGTTTCTAAACCAGAACATTACTCCTTGTTTGCCACTCCGGGGTACAATC
201 T A S G D L V P L S Y I A G L L T G R P
601 ACTGCTTCTGGTGATCTTGTGCCATTGTCTTACATTGCTGGACTTCTCACTGGCCGTCCG
221 N S K A V G P T G V I L S P E E A F K L
661 AATTCTAAGGCTGTTGGACCTACTGGAGTAATTCTTAGCCCCGAAGAAGCGTTTAAACTT
241 A G V E G G F F E L Q P K E G L A L V N
721 GCTGGAGTGGAAGGAGGTTTTTTTCGAGTTGCAGCCTAAAGAAGGCCTTGCACTTGTTAAT
261 G T A V G S G M A S M V L F E A N I L A
781 GGAACAGCTGTTGGTTCTGGTATGGCCTCTATGGTACTTTTTCGAGGCTAATATATTAGCT
281 V L A E V M S A I F A E V M Q G K P E F
841 GTTTTGGCTGAAGTTATGTCAGCGATTTTTCGCTGAAGTGATGCAAGGAAAGCCTGAGTTC
301 T D H L T H K L K H H P G Q I E A A A I
901 ACTGACCATTTGACGCATAAGTTGAAGCACCATCCGGGCCAAATTGAGGCTGCAGCTATA
321 M E H I L D G S A Y V K A A Q K L H E M
961 ATGGAACACATTTTTGGATGGAAGCGCTTATGTTAAGGCTGCTCAGAAGCTACATGAAATG
341 D P L Q K P K Q D R Y A L R T S P Q W L
1021 GATCCATTGCAGAAGCCGAAACAGGACAGATATGCTCTTAGAACATCTCCTCAGTGGCCT
361 G P Q I E V I R S S T K M I E R E I N S
1081 GGTCCCTCAGATTGAAGTGATTTCGATCATCGACTAAGATGATTGAAAGAGAGATTA ACTCT
381 V N D N P L I D V S R N K A I H G G N F
1141 GTCAATGATAACCCGTTGATTGATGTTTTCGAGGAACAAGGCTATTCACGGTGGCAATTTTC
401 Q G T P I G M S M D N T R L A I A A I G
1201 CAGGGCACACCTATTGGAATGTCGATGGACAATACACGTTTGGCTATTGCCGCGATAGGA
421 K L M F A Q F S E L V N D F Y N N G L P
1261 AAGCTCATGTTTGTCTCAATTTTCTGAACTTGTAACGACTTTTACAACAATGGGTTGCCA
441 S N L S G G R N P S L D Y G F K G A E I
1321 TCAAATTTGTCTGGAGGGCGTAATCCAAGTTTGGATTATGGATTCAAGGGTGCTGAAATT
461 A M A S Y C S E L Q F L A N P V T N H V
1381 GCGATGGCTAGTTACTGCTCTGAACTTCAATTTTTAGCCAATCCAGTGACCAACCATGTT
481 Q S A E Q H N Q D V N S L G L I S S R K
1441 CAAAGTGCTGAACAACACAATCAAGATGTAAACTCCTTGGGCTTAATCTCTTCAAGGAAA
501 T S E A V E I L K L M S T T F L V G L C
1501 ACATCAGAAGCTGTTGAAATCTTGAAACTCATGTCTACTACATTTTTAGTAGGCCTCTGC
521 Q A I D L R H L E E N L K S T V K N T V
1561 CAAGCAATAGACTTGAGGCATTTGGAGGAGAATTTAAAAAGCACTGTCAAAAACACAGTA

541 S S V A K R V L T M G V N G E L H P S R
 1621 AGCTCAGTAGCTAAGCGAGTACTAACTATGGGTGTCAACGGAGAACTCCACCCCTCAAGA
 561 F C E K D L L R F V D R E Y I F A Y I D
 1681 TTCTGTGAGAAAGATTTACTCAGATTTGTGGACCGGAATACATTTTTGCATATATTGAT
 581 D P C S A T Y P L M Q K L R Q T L V E H
 1741 GATCCCTGCAGCGCAACCTACCCATTGATGCAAAAATTAAGACAAACACTAGTTGAGCAT
 601 A L K N G D N E R N M N T S I F Q K I A
 1801 GCATTGAAGAATGGTGACAACGAGAGAAAACATGAACACTTCCATCTTCCAAAAGATTGCG
 621 T F E D E L K A L L P K E V E S A R A A
 1861 ACCTTTGAGGATGAACTAAAGGCCCTATTGCCTAAAGAAGTTGAAAGTGCTAGAGCTGCA
 641 L E S G N P A I P N R I E E C R S Y P L
 1921 CTCGAAAGTGAAATCCAGCAATCCCAAACAGGATCGAGGAGTGCAGGTCTTACCCATTG
 661 Y K F V R K E L G I E Y L T G E K V T S
 1981 TACAAGTTTGTGAGGAAAAGAGTTGGGAATTGAGTATCTTACAGGAGAAAAAGTAACGTCA
 681 P G E E F D K V F I A M S K G E I I D P
 2041 CCTGGAGAAGAGTTTCGATAAGGTATTTATAGCAATGAGCAAAGGAGAGATCATTGATCCA
 701 L L E C L E S W N G A P L P I C *
 2101 TTGTTAGAGTGCCTGGAGTCATGGAATGGTGCTCCTCTTCCAATCTGTAA

7.1.3 *Rhodotorula glutinis* PAL (*RgPAL*)

1 M A P S L D S I S H S F A N G V A S A K
 1 ATGGCACCGAGCCTGGATAGCATTAGCCATAGCTTTGCGAACGGCGTGGCGAGCGCGAAA
 21 Q A V N G A S T N L A V A G S H L P T T
 61 CAGGCGGTGAATGGCGGAGCACCAATCTGGCCGTGGCGGGTAGCCATCTGCCGACCACC
 41 Q V T Q V D I V E K M L A A P T D S T L
 121 CAGGTGACCCAGGTTGATATTGTGGAAAAATGCTGGCAGCGCCGACCGATAGCACCCCTG
 61 E L D G Y S L N L G D V V S A A R K G R
 181 GAACTGGATGGCTATAGCCTGAACCTGGGTGATGTGGTGAGCGCAGCGCTAAAGTTCGT
 81 P V R V K D S D E I R S K I D K S V E F
 241 CCGGTGCGTGTGAAAGATAGCGATGAAATCCGCAGCAAAATCGATAAAAAGCGTGGAATTT
 101 L R S Q L S M S V Y G V T T G F G G S A
 301 CTGCGTAGCCAGCTGTCTATGAGCGTGTATGGCGTGACCACCGCTTTGGCGGTAGCGCG
 121 D T R T E D A I S L Q K A L L E H Q L C
 361 GATACCCGTACCGAAGATGCGATTAGCCTGCAGAAAGCGCTGCTGGAACATCAGCTGTGC
 141 G V L P S S F D S F R L G R G L E N S L
 421 GCGGTGCTGCCGAGCAGCTTTGATAGCTTTCGTCTGGGCCGTGGCCTGGAAAATAGCCTG
 161 P L E V V R G A M T I R V N S L T R G H
 481 CCGCTGGAAGTGGTGCGTGGCGCCATGACCATTTCGTGTGAACAGCCTGACCCGTGGCCAT
 181 S A V R L V V L E A L T N F L N H G I T
 541 AGCGCGGTGCGTCTGGTGGTTCTGGAAGCGCTGACCAACTTCTGAATCATGGCATTACC

201 P I V P L R G T I S A S G D L S P L S Y
601 CCGATTGTGCCGCTGCGTGGCACCATTAGCGCGAGCGGCGATCTGAGCCCGCTGTCTTAT
221 I A A A I S G H P D S K V H V V H E G K
661 ATTGCAGCGGCGATTAGCGCCATCCGGATAGCAAAGTGCATGTGGTGCATGAAGGCAAA
241 E K I L Y A R E A M A L F N L E P V V L
721 GAAAAAATTCTGTATGCGCGTGAAGCGATGGCGCTGTTTAACTGGAACCGGTGGTGCTG
261 G P K E G L G L V N G T A V S A S M A T
781 GGCCCCGAAAGAAGGCCTGGGCCTGGTTAATGGCACGGCGGTTAGCGCGAGCATGGCGACC
281 L A L H D A H M L S L L S Q S L T A M T
841 CTGGCCCTGCACGATGCACACATGCTGAGTCTGCTGTCTCAGAGCCTGACCGCCATGACC
301 V E A M V G H A G S F H P F L H D V T R
901 GTGGAAGCGATGGTGGGCCATGCGGGCAGCTTTCATCCGTTTCTGCATGATGTGACCCGT
321 P H P T Q I E V A G N I R K L L E G S R
961 CCGCATCCGACCCAGATTGAAGTGGCGGGCAACATTCGTAAACTGCTGGAAGGCAGCCGT
341 F A V H H E E E V K V K D D E G I L R Q
1021 TTTGCGGTGCATCATGAAGAAGAAGTAAAAGTAAAAGACGATGAAGGCATTCTGCGTCAG
361 D R Y P L R T S P Q W L G P L V S D L I
1081 GATCGTTATCCGCTGCGTACCAGCCCCGAGTGGCTGGGTCCGCTGGTGAGCGATCTGATT
381 H A H A V L T I E A G Q S T T D N P L I
1141 CATGCGCATGCGGTGCTGACCATTGAAGCGGGCCAGAGCACCACCGATAATCCGCTGATT
401 D V E N K T S H H G G N F Q A A A V A N
1201 GATGTGAAAAACAAAACCAGCCATCATGGCGGCAACTTTCAGGCGGCAGCGGTGGCGAAC
421 T M E K T R L G L A Q I G K L N F T Q L
1261 ACGATGGAAAAAACCCGTCTGGGCCTGGCGCAGATTGGCAAACCTGAACTTTACCCAGCTG
441 T E M L N A G M N R G L P S C L A A E D
1321 ACCGAAATGCTGAACGCGGGCATGAACCGTGGTCTGCCGAGCTGTCTGGCCGCGGAAGAT
461 P S L S Y H C K G L D I A A A A Y T S E
1381 CCGAGCCTGAGCTATCATTGCAAAGGCCTGGATATCGCGGCAGCGGCGTATACCAGCGAA
481 L G H L A N P V T T H V Q P A E M A N Q
1441 CTGGGCCATCTGGCCAATCCGGTGACCACCCATGTGCAGCCGCGGAAATGGCGAACCAG
501 A V N S L A L I S A R R T T E S N D V L
1501 GCGGTAACTCTCTGGCCCTGATTAGCGCGCGTCTGACCACCGAAAGCAACGATGTTCTG
521 S L L L A T H L Y C V L Q A I D L R A I
1561 AGCCTGCTGCTGGCCACCCATCTGTATTGCGTGCTGCAGGCGATTGATCTGCGTGCGATC
541 E F E F K K Q F G P A I V S L I D Q H F
1621 GAGTTCGAATTCAAAAAACAGTTTGGTCCGCGGATTGTGAGCCTGATTGATCAGCATT
561 G S A M T G S N L R D E L V E K V N K T
1681 GGCAGCGCCATGACCGGCAGCAACCTGCGTGACGAACTGGTTGAAAAAGTGAACAAAACC
581 L A K R L E Q T N S Y D L V P R W H D A
1741 CTGGCCAAACGTCTGGAACAGACCAACAGCTATGATCTGGTGCCGCTTGGCATGATGCG

601 F S F A A G T V V E V L S S T S L S L A
 1801 TTTAGCTTTGCAGCGGGCACCGTGGTGGAAAGTTCTGAGCAGCACCAGCCTGAGCCTGGCC
 621 A V N A W K V A A A E S A I S L T R Q V
 1861 GCGGTGAACGCGTGGAAAGTGGCGGCAGCGGAAAGCGCCATTAGCCTGACCCGCCAGGTG
 641 R E T F W S A A S T S S P A L S Y L S P
 1921 CGTGAAACCTTTTGGAGCGCGGCGAGCACCAGCAGCCCGGCACTGAGCTACCTGAGCCCCG
 661 R T Q I L Y A F V R E E L G V K A R R G
 1981 CGTACCCAGATCCTGTATGCGTTTGTGCGTGAAGAAGTGGGCGTGAAAGCGCGTCTGTGGT
 681 D V F L G K Q E V T I G S N V S K I Y E
 2041 GATGTGTTTCTGGGCAAACAGGAAGTGACCATTGGCAGCAACGTGAGCAAAAATTTATGAA
 701 A I K S G R I N N V L L K M L A *
 2101 GCGATTAAAAGCGGCCGTATTAACAACGTGCTGCTGAAAATGCTGGCCTAA

7.1.4 *Pseudomonas putida* Alanine Racemase (PpRac)

1 M P F R R T L L A A S L A L L I T G Q A
 1 ATGCCGTTTTGTCGTACCCTGCTGGCAGCAAGCCTGGCACTGCTGATTACCGGTCAGGCA
 21 P L Y A A P P L S M D N G T N T L T V Q
 61 CCGCTGTATGCAGCACCAGCCTCTGAGCATGGATAATGGCACCAATACCCTGACCGTTCAG
 41 N S N A W V E V S A S A L Q H N I R T L
 121 AATAGCAATGCATGGGTTGAAGTTAGCGCAAGCGCACTGCAGCATAATATTCGCACCCTG
 61 Q A E L A G K S K L C A V L K A D A Y G
 181 CAGGCAGAACTGGCAGGTAAGCAAACTGTGTGCAGTTCTGAAAGCAGATGCATATGGT
 81 H G I G L V M P S I I A Q G V P C V A V
 241 CATGGCATTGGTCTGGTTATGCCGAGCATTATTGCACAGGGTGTTCGGTGTGTTGCAGTT
 101 A S N E E A R V V R A S G F T G Q L V R
 301 GCAAGCAATGAAGAGGCACGTGTTGTTGTCGCAAGCGGTTTTACAGGTCAGCTGGTTCGT
 121 V R L A S L S E L E D G L Q Y D M E E L
 361 GTTCGTCTGGCAAGCCTGAGCGAACTGGAAGATGGTCTGCAGTATGATATGGAAGAACTG
 141 V G S A E F A R Q A D A I A A R H G K T
 421 GTTGGTAGCGCAGAATTTGCACGTCAGGCAGATGCAATTGCCGCACGTCATGGTAAAACC
 161 L R I H M A L N S S G M S R N G V E M A
 481 CTGCGTATTCATATGGCACTGAATAGCAGCGGTATGAGCCGTAATGGTGTGAAATGGCA
 181 T W S G R G E A L Q I T D Q K H L K L V
 541 ACCTGGTCAGGTGCTGGTGAAGCCCTGCAGATTACAGATCAGAAACATCTGAAACTGGTT
 201 A L M T H F A V E D K D D V R K G L A A
 601 GCACTGATGACCCATTTTGCAGTGGAAAGATAAAGATGATGTTTCGTAAAGGTCTGGCAGCC
 221 F N E Q T D W L I K H A R L D R S K L T
 661 TTTAATGAACAGACCGATTGGCTGATTAACATGCACGTCTGGATCGTAGCAAACTGACC

241 L H A A N S F A T L E V P E A R L D M V
 721 CTGCATGCCGCAAATAGCTTTGCAACCCTGGAAGTTCCGGAAGCCCGTCTGGATATGGTT
 261 R T G G A L F G D T V P A R T E Y K R A
 781 CGTACCGGTGGTGCACGTGTTTGGTGATACCGTTCGGGCACGTACCGAATATAAACGTGCA
 281 M Q F K S H V A A V H S Y P A G N T V G
 841 ATGCAGTTTTAAAAGCCATGTTGCAGCAGTTCATAGCTATCCGGCAGGTAATACCGTTGGT
 301 Y D R T F T L A R D S R L A N I T V G Y
 901 TATGATCGTACCTTTACCCTGGCACGTGATAGCCGTCTGGCCAATATCACCGTGGGTTAT
 321 S D G Y R R V F T N K G H V L I N G H R
 961 AGTGATGGTTATCGTCGTGTGTTTACCAATAAAGGTCATGTGCTGATTAATGGTCATCGT
 341 V P V V G K V S M N T L M V D V T D F P
 1021 GTTCCGGTTGTTGGTAAAGTTAGCATGAATACACTGATGGTTGATGTGACCGATTTTCCG
 361 D V K G G N E V V L F G K Q A G G E I T
 1081 GATGTTAAAGGTGGTAATGAAGTTGTGCTGTTTGGAAAACAGGCAGGCCGGTGAAATTACC
 381 Q A E M E E I N G A L L A D L Y T V W G
 1141 CAGGCAGAAATGGAAGAAATTAATGGTGCCTGCTGGCCGATCTGTATACCGTTTGGGGT
 401 N S N P K I L V D *
 1201 AATAGCAATCCGAAAATCCTGGTGGATTAA

7.1.5 *Trigonopsis variabilis* D-Amino Acid Oxidase (Tv-D-AAO)

1 M A K I V V I G A G V A G L T T A L Q L
 1 ATGGCCAAAATTGTTGTTATTGGTGCCGGTGTTCAGGTCTGACCACCGCACTGCAGCTG
 21 L R K G H E V T I V S E F T P G D L S I
 61 CTGCGTAAAGGTCATGAAGTTACCATTGTGAGCGAATTTACACCGGGTGATCTGAGCATT
 41 G Y T S P W A G A N W L T F Y D G G K L
 121 GGTTATACCAGCCCGTGGGCAGGCGCAAATTTGGCTGACCTTTTATGATGGTGGTAAACTG
 61 A D Y D A V S Y P I L R E L A R S S P E
 181 GCAGATTATGATGCAGTTAGCTATCCGATTCTGCGTGAACCTGGCACGTAGCAGTCCGGAA
 81 A G I R L I N Q R S H V L K R D L P K L
 241 GCAGGTATTCGTCTGATTAATCAGCGTAGCCATGTTCTGAAAACGTGATCTGCCGAAACTG
 101 E G A M S A I C Q R N P W F K N T V D S
 301 GAAGGTGCAATGAGCGCAATTTGTCAGCGTAATCCGTGGTTTAAAAATACCGTGGATAGC
 121 F E I I E D R S R I V H D D V A Y L V E
 361 TTTGAGATCATTGAAGATCGTAGCCGTATCGTTCATGATGATGTTGCATATCTGGTTGAA
 141 F A S V C I H A G V Y L N W L M S Q C L
 421 TTTGCCAGCGTTTGTATTTCATGCCGGTGTATCTGAATTGGCTGATGAGCCAGTGTCTG
 161 S L G A T V D K R R V N H I K D A N L L
 481 AGCCTGGGTGCAACCGTTGATAAACGTCGTGTGAACCATATTAAGATGCCAATCTGCTG
 181 H S S G S R P D V I V N C S G L F A R F
 541 CATAGCAGCGGTAGCCGTCCGGATGTTATTGTTAATTGTAGCGGTCTGTTTGCACGTTTT

201 L G G V E D K K M Y P I R G Q V V L V R
 601 CTGGGTGGTGGTTGAGGACAAAAAATGTATCCGATTCGTGGTCAGGTTGTTCTGGTTCGT
 221 N S L P F M A S F S S T P E K E N E D E
 661 AATAGCCTGCCGTTTATGGCAAGCTTTAGCAGCACACCTGAAAAAGAAAACGAAGACGAA
 241 A L Y I M T R F D G T S I I G G C F Q P
 721 GCCCTGTATATCATGACCCGTTTTGATGGCACCAGCATTATTGGTGGTGTTCAGCCG
 261 N N W S S E P D P S L T H R I L S R A L
 781 AATAATTGGAGCAGCGAACCGGATCCGAGCCTGACCCATCGTATTCTGAGCCGTGCACTG
 281 D R F P E L T K D G P L D I V R G C V G
 841 GATCGTTTTCCGGAAGTACCAAAGATGGTCCGCTGGATATTGTTCTGGTGTGTGGT
 301 H R P G R E G G P R V E L E K I P G V G
 901 CATCGTCCGGGTCGTGAAGGTGGTCCGCGTGTGAACTGGAAAAAATCCGGGTGTTGGT
 321 F V V H N Y G A A G A G Y Q S S Y G M A
 961 TTTGTGGTGCATAATTATGGTGCAGCCGGTGCAGGTTATCAGAGCAGCTATGGTATGGCA
 341 D E A V S Y V E R A L T R P N L *
 1021 GATGAAGCCGTTAGCTATGTTGAACGTGCACTGACCCGTCGGAATCTGTAA

7.1.6 *Arthrobacter* sp. ω -Transaminase

1 M T S E I V Y T H D T G L D Y I T Y S D
 1 ATGACCAGCGAAATTGTTTATACCCATGATACCGGTCTGGATTATATCACCTATAGCGAT
 21 Y E L D P A N P L A G G A A W I E G A F
 61 TATGAACTGGATCCGGCAAATCCGCTGGCAGGCGGTGCAGCATGGATTGAAGGTGCATTT
 41 V P P S E A R I S I F D Q G Y L H S D V
 121 GTTCCGCCTAGCGAAGCACGTATTAGCATTTTTGATCAGGGCTATCTGCATAGTGATGTT
 61 T Y T V F H V W N G N A F R L D D H I E
 181 ACCTATACCGTGTTCATGTGTGGAATGGTAATGCATTTCCGCTGGATGATCATATTGAA
 81 R L F S N A E S M R I I P P L T Q D E V
 241 CGTCTGTTTAGCAATGCAGAAAGCATGCGTATTATTCCGCTCTGACCCAGGATGAAGTT
 101 K E I A L E L V A K T E L R E A F V S V
 301 AAAGAAATTGCACTGGAAGTGGTTGCAAAAACCGAACTGCGTGAAGCATTTGTTAGCGTT
 121 S I T R G Y S S T P G E R D I T K H R P
 361 AGCATTACCCGTGGTTATAGCAGCACACCGGGTGAACGTGATATTACCAAACATCGTCCG
 141 Q V Y M Y A V P Y Q W I V P F D R I R D
 421 CAGGTTTATATGTATGCAGTTCCGTATCAGTGGATTGTTCCGTTTGTATCGTATTTCGTGAT
 161 G V H A M V A Q S V R R T P R S S I D P
 481 GGTGTTTCATGCAATGGTTGCACAGAGCGTTCGTCTGACCCGCTAGCAGCATGATCCG
 181 Q V K N F Q W G D L I R A V Q E T H D R
 541 CAGGTTAAAAATTTTCAGTGGGGTGATCTGATTCGTGCAGTTCAAGAAACCATGATCGT
 201 G F E A P L L L D G D G L L A E G S G F
 601 GGTTTTGAAGCACCGCTGCTGCTGGATGGTGGTCTGCTGGCCGAAGGTAGCGGTTTT

221 N V V V I K D G V V R S P G R A A L P G
 661 AATGTTGTTGTGATTAAAGATGGTGTGGTTCGTAGTCCGGGTCGTGCAGCACTGCCTGGT
 241 I T R K T V L E I A E S L G H E A I L A
 721 ATTACCCGTAAAACCGTTCTGGAAATTGCAGAAAAGCCTGGGTTCATGAAGCAATTCTGGCA
 261 D I T L A E L L D A D E V L G C T T A G
 781 GATATTACCCTGGCAGAACTGCTGGATGCAGATGAAGTTCTGGGTTGTACCACCGCAGGC
 281 G V W P F V S V D G N P I S D G V P G P
 841 GGTGTTTGGCCGTTTGTAGCGTGGATGGTAATCCGATTTTCAGATGGTGTTCGGGTCCTCG
 301 I T Q S I I R R Y W E L N V E S S S L L
 901 ATTACCCAGAGCATTATTCGTTCGTTATTGGGAACTGAATGTTGAAAGCAGCAGCCTGCTG
 321 T P V Q Y *
 961 ACACCGGTTTCAGTATTAA

7.1.7 Monoamine Oxidase from *Aspergillus niger* (MAO-N) Protein Sequence

Protein sequence for the wild-type mono amino acid oxidase from *Aspergillus niger* (MAO-N) with mutations shown in Table 28.

<u>10</u>	<u>20</u>	<u>30</u>	<u>40</u>	<u>50</u>	<u>60</u>
MTSRDGYQWT	PETGLTQGV	SLGVISPTN	IEDTDKDGW	DVIVIGGGYC	GLTATRDLT
<u>70</u>	<u>80</u>	<u>90</u>	<u>100</u>	<u>110</u>	<u>120</u>
AGFKTLLEA	RDRIGGRSWS	SNIDGYPYEM	GGTWVHHWQS	HVWREITRYK	MHNALSPSFN
<u>130</u>	<u>140</u>	<u>150</u>	<u>160</u>	<u>170</u>	<u>180</u>
FSRGNVHFQL	RTNPTTSTYM	THEAEDELLR	SALHKFTNVD	GTNGRTVLPF	PHDMFYVPEF
<u>190</u>	<u>200</u>	<u>210</u>	<u>220</u>	<u>230</u>	<u>240</u>
RKYDEMSYSE	RIDQIRDELS	LNERSSLEAF	ILLCSGGTLE	NSSFGEFLHW	WAMSGYTYQG
<u>250</u>	<u>260</u>	<u>270</u>	<u>280</u>	<u>290</u>	<u>300</u>
CMDCLISYKF	KDQSAFARR	FWEEAAGTGR	LGYVFGCPVR	SVVNERDAAR	VTARDGREFA
<u>310</u>	<u>320</u>	<u>330</u>	<u>340</u>	<u>350</u>	<u>360</u>
AKRLVCTIPL	NVLSTIQFSP	ALSTERISAM	QAGHVMCTK	VHAEVDNKDM	RSWTGIAYPF
<u>370</u>	<u>380</u>	<u>390</u>	<u>400</u>	<u>410</u>	<u>420</u>
NKLCYAIGDG	TTPAGNTHLV	CFGTDANHIQ	PDEDVRETLK	AVGQLAPGTF	GVKRLVFHNW
<u>430</u>	<u>440</u>	<u>450</u>	<u>460</u>	<u>470</u>	<u>480</u>
VKDEFKAGAW	FFSRPGMVSE	CLQGLREKHR	GVVFANSDWA	LGWRSFIDGA	IEEGTRAARV
<u>490</u>					
VLEELGTKRE	VKARL				

Table 28: Mutations in the protein sequence of each MAO-N variant

Variant	Phe210	Leu213	Met242	Ile246	Asn336	Thr384	Asp385	Trp430
D5	-	-	-	Met	Ser	Asn	Ser	-
D9	Leu	Thr	Gln	Thr	Ser	Asn	Ser	His
D11	Leu	Thr	Gln	Thr	Ser	Asn	Ser	Gly

7.1.8 *E. coli* Amine Oxidase

10 20 30 40 50 60
 MGSPSLYSAR KTTLLAVAL SFAWQAPVFA HGGEAHMVPV DETLKEFGAD VQWDDYQIF

70 80 90 100 110 120
 TLIKDGAYVK VKPGAQTAIV NGQPLALQVP VVMKDNKAWV SDTFINDVFQ SGLDQTFQVE

130 140 150 160 170 180
 KRPHPLNALT ADEIKQAVEI VKASADFKPN TRFTEISLLP PDKEAVWAFAL ENKPVDPQR

190 200 210 220 230 240
 KADVIMLDGK HIIEAVVDLQ NNKLLSQPI KDAHGMVLLD DFASVQNIIN NSEEFAAAVK

250 260 270 280 290 300
 KRGITDAQKV ITTPLTVGYF DGKDGLKQDA RLLKVISYLD VGDGNYWAHP IENLVAVVDL

310 320 330 340 350 360
 EQKKIVKIEE GPVVPVPMTA RPFQGRDRVA PAVKPMQIEE PEGKNYTITG DMIHWRNWDF

370 380 390 400 410 420
 HLSMNSRVGP MISTVTYNDN GTKRKVMYEG SLGGMIVPYG DPDIGWYFKA YLDSDYDGMG

430 440 450 460 470 480
 TLTSPARGK DAPSNVLLN ETIADYTGVP MEIPRAIAVF ERYAGPEYKH QEMQPNVST

490 500 510 520 530 540
 ERRELVVRWI STVGNVDYIF DWIFHENGTI GIDAGATGIE AVKGVKAKTM HDETAKDDTR

550 560 570 580 590 600
 YGTLIDHNIV GTTHQHIYNF RLDDVDGEN NSLVAMDPVV KPNTAGGPRT STMQVNQYNI

610 620 630 640 650 660
 GNEQDAAQKF DPGTIRLLSN PNKENRMGNP VSYQIIPYAG GTHPVAKGAQ FAPDEWIYHR

670 680 690 700 710 720
LSFMDKQLWV TRYHPGERFP EGKYPNRSTH DTGLGQYSKD NESLDNTDAV VWMTTGTHV
730 740 750
ARAEWPIMP TEWVHTLLKP WNFDETPTL GALKKDK

7.2 PAL Catalyzed Hydroamination Reactions

Whole cell *E. coli* BL21(DE3) expressing *RgPAL*, *PcPAL* and *AvPAL* were resuspended in ammonium hydroxide (5 M, pH 9.5) containing substrates **1a-n** (5 mM) and the reactions were incubated at 30 °C with shaking (250 rpm). Samples (300 µL) were taken over time and methanol (300 µL) was added. After centrifugation (13,000 rpm, 4 °C, 2 minutes), the supernatant was filtered and injected directly onto a reverse phase HPLC for analysis. The percentage conversion and product e.e are given in Table 29-Table 31.

Table 29: RgPAL catalyzed amination reactions of cinnamic acid derivatives 1a-n

		20 min	40 min	60 min	2h	3h	6h	22h
1a	conv.	50	51	50	51	52	52	55
	e.e.	<99	<99	<99	<99	<99	<99	<99
1b	conv.	61	62	60	63	63	63	71
	e.e.	96	88	85	71	67	58	2
1c	conv.	59	60	60	60	60	60	61
	e.e.	<99	<99	<99	<99	<99	<99	<99
1d	conv.	30	46	57	71	73	73	75
	e.e.	<99	<99	<99	<99	<99	<99	93
1e	conv.	80	90	91	91	91	91	93
	e.e.	96	94	90	82	76	59	13
1f	conv.	66	66	66	67	67	72	76
	e.e.	72	63	56	46	41	28	7
1g	conv.	35	47	51	52	51	51	51
	e.e.	<99	<99	<99	<99	<99	<99	<99
1h	conv.	3	9	14	54	58	60	62
	e.e.	<99	<99	<99	89	70	66	38
1i	conv.	79	81	81	82	83	84	85
	e.e.	<99	<99	<99	84	79	63	28
1j	conv.	77	82	87	87	88	88	89
	e.e.	<99	<99	66	49	43	18	1
1k	conv.	86	87	87	89	89	87	86
	e.e.	57	38	22	2	-8	-13	-14
1l	conv.	82	84	83	84	84	84	83
	e.e.	46	33	27	18	15	10	7
1m	conv.	48	67	75	83	85	85	85
	e.e.	72	70	66	57	52	37	5
1n	conv.	19	31	40	49	50	48	48
	e.e.	<99	<99	<99	<99	<99	<99	<99

Percentage conversion and e.e

Table 30: PcPAL catalyzed amination reactions of cinnamic acid derivatives 1a-n

		20 min	40 min	60 min	2h	3h	6h	22h
1a	conv.	54	55	54	55	55	57	58
	e.e.	>99	>99	>99	>99	>99	>99	>99
1b	conv.	62	62	62	65	69	67	75
	e.e.	88	84	83	68	61	39	6
1c	conv.	61	61	57	55	57	61	60
	e.e.	>99	>99	>99	>99	>99	>99	>99
1d	conv.	42	62	69	73	75	75	75
	e.e.	>99	>99	98	98	97	96	96
1e	conv.	90	91	91	92	89	93	94
	e.e.	>99	89	81	69	72	31	0
1f	conv.	74	69	70	71	72	73	72
	e.e.	43	34	29	25	23	15	14
1g	conv.	47	50	50	50	50	49	50
	e.e.	>99	>99	>99	>99	>99	>99	>99
1h	conv.	2	29	39	46	50	54	49
	e.e.	>99	>99	>99	>99	91	40	-8
1i	conv.	81	82	80	83	83	84	87
	e.e.	>99	>99	>99	77	69	48	10
1j	conv.	82	87	87	88	88	90	89
	e.e.	>99	70	61	46	36	15	0
1k	conv.	87	88	88	89	88	87	87
	e.e.	51	22	6	-1	-7	-7	-11
1l	conv.	84	85	85	85	85	84	84
	e.e.	35	24	18	12	10	6	7
1m	conv.	61	77	82	85	86	86	86
	e.e.	71	78	70	52	38	18	-4
1n	conv.	18	32	41	50	50	50	50
	e.e.	>99	>99	>99	>99	>99	>99	>99

Percentage conversion and e.e

Table 31: AvPAL catalyzed amination reactions of cinnamic acid derivatives 1a-n

		20 min	40 min	60 min	2h	3h	6h	22h
1a	conv.	3	4	6	12	17	30	49
	e.e.	>99	>99	>99	>99	>99	>99	>99
1b	conv.	1	17	23	43	49	56	59
	e.e.	>99	>99	>99	>99	>99	>99	>99
1c	conv.	6	13	17	31	37	50	59
	e.e.	>99	>99	>99	>99	>99	>99	>99
1d	conv.	58	69	71	71	73	73	76
	e.e.	>99	>99	98	94	90	82	71
1e	conv.	22	39	50	75	83	91	91
	e.e.	>99	>99	>99	>99	>99	>99	>99
1f	conv.	7	15	21	34	42	59	62
	e.e.	>99	>99	>99	>99	>99	>99	>99
1g	conv.	18	30	37	49	51	53	53
	e.e.	>99	>99	>99	>99	>99	>99	>99
1h	conv.	20	43	54	61	61	61	61
	e.e.	>99	>99	>99	>99	>99	>99	>99
1i	conv.	9	19	27	51	61	77	80
	e.e.	>99	>99	>99	>99	>99	>99	>99
1j	conv.	83	83	85	85	85	85	85
	e.e.	>99	>99	>99	>99	>99	>99	75
1k	conv.	38	69	83	87	87	87	86
	e.e.	50	40	36	21	13	-3	-9
1l	conv.	6	12	18	35	43	65	78
	e.e.	>99	>99	>99	>99	>99	>99	92
1m	conv.	81	78	79	80	81	81	79
	e.e.	72	55	44	19	10	-2	-6
1n	conv.	7	13	16	46	48	50	50
	e.e.	>99	>99	>99	>99	>99	>99	>99

Percentage conversion and e.e.

7.3 Amino Acid Positions in Pools A-D

Pool A		Pool B		Pool C		Pool D	
Number	Mutation	Number	Mutation	Number	Mutation	Number	Mutation
1	Y314X	49	G224X	97	Y367X	145	G218X
2	Q452X	50	L171X	98	P325X	146	G380X
3	R317X	51	H446X	99	V368X	147	V249X
4	N451X	52	F398X	100	I390X	148	A246X
5	I454X	53	F84X	101	A280X	149	R442X
6	C318X	54	Q457X	102	V172X	150	V227X
7	N453X	55	I310X	103	R295X	151	S461X
8	S315X	56	D346X	104	L382X	152	A394X
9	R313X	57	L323X	105	Y358X	153	V294X
10	F363X	58	F264X	106	N261X	154	Q255X
11	G361X	59	T260X	107	S399X	155	T229X
12	L364X	60	S164X	108	L393X	156	L288X
13	N455X	61	P348X	109	M284X	157	M429X
14	L316X	62	K384X	110	H302X	158	L278X
15	M168X	63	D170X	111	L108X	159	F267X
16	D312X	64	I254X	112	A383X	160	S137X
17	G360X	65	H250X	113	M370X	161	Y304X
18	Q311X	66	T225X	114	V344X	162	T81X
19	E448X	67	M87X	115	N400X	163	H307X
20	G85X	68	G83X	116	N258X	164	R128X
21	A447X	69	T345X	117	Y459X	165	G300X
22	Q321X	70	G259X	118	S395X	166	P266X
23	G166X	71	I268X	119	D441X	167	P396X
24	L319X	72	L219X	120	E340X	168	M221X
25	I165X	73	Q262X	121	I326X	169	V327X
26	Y322X	74	A391X	122	A220X	170	I285X
27	S456X	75	L257X	123	I77X	171	D306X
28	N347X	76	Q277X	124	L104X	172	P76X
29	G86X	77	E308X	125	A251X	173	Q101X
30	H385X	78	G458X	126	E397X	174	L252X
31	T445X	79	G79X	127	F107X	175	G248X
32	V388X	80	A440X	128	I439X	176	L298X
33	N362X	81	K272X	129	V90X	177	L100X
34	Y78X	82	H269X	130	H274X	178	I350X
35	S263X	83	L386X	131	H265X	179	A136X

Pool A		Pool B		Pool C		Pool D	
Number	Mutation	Number	Mutation	Number	Mutation	Number	Mutation
37	P320X	85	D253X	133	E297X	181	P273X
38	F443X	86	L349X	134	L174X	182	T110X
39	L309X	87	D387X	135	M247X	183	Y377X
40	N223X	88	S82X	136	T460X	184	D303X
41	G365X	89	G324X	137	P173X	185	A91X
42	P444X	90	N89X	138	K216X	186	S131X
43	H359X	91	R305X	139	S226X	187	Y378X
44	Q389X	92	G369X	140	V80X	188	N270X
45	Q449X	93	G163X	141	A256X	189	G371X
46	Q366X	94	M222X	142	G276X	190	A462X
47	L392X	95	A281X	143	S271X	191	D373X
48	A88X	96	M228X	144	S343X	192	W279X

7.4 Publications

Phenylalanine Ammonia Lyase Catalyzed Synthesis of Amino Acids via an MIO-Cofactor Independent Pathway

Sarah. L. Lovelock, Richard. C. Lloyd and Nicholas. J. Turner*

Phenylalanine ammonia lyases (PALs) belong to a family of 4-methylideneimidazole-5-one (MIO) cofactor-dependent enzymes that are responsible for the conversion of *L*-phenylalanine to *trans*-cinnamic acid in eukaryotic and prokaryotic organisms. Under conditions of high ammonia concentration, this deamination reaction is reversible and hence there is considerable interest in the development of PALs as biocatalysts for the enantioselective synthesis of non-natural amino acids. Herein we report the discovery of a previously unobserved competing MIO-independent reaction pathway which proceeds in a non-stereoselective manner and results in the generation of both *L*- and *D*-phenylalanine derivatives. The mechanism of the MIO-independent pathway is explored through isotopic labelling studies and mutagenesis of key active-site residues. The results obtained are consistent with amino acid deamination occurring via a stepwise E_{1cB} elimination mechanism.

Optically active amino acids are fundamental building blocks for the synthesis of a wide range of bioactive natural products, pharmaceuticals and agrochemicals. For example, there is significant interest in the development of therapeutic peptides and proteins which can contain both natural and non-natural amino acids.^[1] Non-proteinogenic amino acids have also been used independently as drug molecules, including Levodopa (*L*-dopa), the main drug used for the treatment of Parkinson's disease.^[2] Furthermore, asymmetric synthesis frequently relies on amino acids as chiral starting materials and auxiliaries.^[3] The increasing demand to access amino acids in optically pure form has led to the development of a number of biotechnological approaches.^[4] A particularly attractive method for the synthesis of aromatic amino acids involves the use of phenylalanine ammonia lyases (PALs), a class of enzymes which catalyze the reversible regio- and stereoselective hydroamination of *trans*-cinnamic acid derivatives.^[5] These reactions are compatible with aqueous and metal free conditions and have the distinct advantage that no protecting group

chemistry is required. Additionally PALs utilize readily available achiral cinnamic acid derivatives as starting materials and they do not rely on external cofactors or recycling systems making them particularly suitable as industrial biocatalysts.^[6] This feature is highlighted by the recent application of PAL in the synthesis of 2'-chloro-*L*-phenylalanine on a tonne scale, by DSM Pharma Chemicals.^[7]

To allow structure-guided rational engineering for the development of biocatalysts with desirable properties, a detailed understanding of the enzyme's catalytic mechanism is highly advantageous; however the PAL catalytic mechanism is still under investigation. PALs belong to a family of 4-methylideneimidazole-5-one (MIO) cofactor dependent enzymes, which also include histidine and tyrosine ammonia lyases (HALs and TALs) and aminomutases (AMs), the latter catalyzing the isomerization of α - and β -amino acids.^[8] The MIO cofactor is formed by an autocatalytic condensation reaction of a conserved Ala-Ser-Gly motif. Mechanistic studies suggest the presence of a covalent intermediate formed via the addition of the substrate amine onto the exocyclic methylene group of the cofactor (figure 1).^[9] Subsequent elimination of the amine to form cinnamic acid is generally reported to occur via an E_{1cB} mechanism, although evidence in favor of an E_2 elimination pathway has also been presented.^[10] An alternative Friedel-Crafts mechanism has been proposed on the basis that the elimination mechanisms involve unfavorable abstraction of a non-acidic proton from the β -position of the amino acid.^[11] Nonetheless, there is considerable evidence to support the formation of an amine-MIO intermediate including crystallographic data,^[12] molecular mechanics calculations^[13] and kinetic isotope studies.^[14]

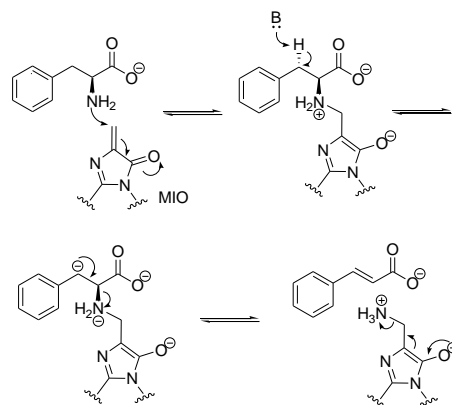


Figure 1. Proposed E_{1cB} mechanism for the PAL catalyzed *L*-phenylalanine deamination reaction

[*] S. L. Lovelock, Prof. N. J. Turner
School of Chemistry, University of Manchester
Manchester Institute of Biotechnology
131 Princess Street, Manchester, M1 7DN, UK
E-mail: Nicholas.turner@manchester.ac.uk

Dr. R. C. Lloyd
Dr. Reddy's Laboratories, Chirotech Technology Centre
410 Cambridge Science Park
Milton Road, Cambridge, CB4 0PE, UK

[**] Financial support from the Centre of Excellence in Biocatalysis, Biotransformation and Biocatalytic Manufacture (CoEBio3: www.coebio3.org) and a Royal Society Wolfson Research Merit Award are gratefully acknowledged.



The substrate range of eukaryotic PALs from the plant *Petroselinum crispum* (PcPAL) and yeast *Rhodotorula glutinis* (RgPAL) have been well characterized and show activity towards a range of substituted phenylalanine derivatives. The nature of the aromatic substituent has been shown to greatly influence activity, providing insights into the enzyme's catalytic mechanism.^[15] To date, there have been few reported examples of bacterial PALs and they have not been previously exploited as biocatalysts for non-natural amino acid synthesis. Recently, the crystal structure of a double mutant of PAL from the bacteria *Anabaena variabilis* (AvPAL) was solved, representing the first structure showing the flexible catalytic loops well resolved and in the active conformation for catalysis.^[12c] Availability of a detailed crystal structure makes AvPAL an attractive candidate for directed evolution. In order to investigate the suitability of AvPAL as a biocatalyst for amino acid synthesis, the activity of wt AvPAL was determined alongside the eukaryotic PcPAL and RgPAL. The conversion of a panel of cinnamic acid derivatives (**1a-n**) to their corresponding amino acids were monitored over time using *E. coli* BL21(DE3) whole cells expressing the individual PALs. The activity of AvPAL was largely comparable to that of PcPAL and RgPAL, with all three enzymes catalyzing the conversion of substrates **1a-n** with high to moderate conversions. All reactions initially proceeded with excellent enantioselectivity in favour of the L-amino acids (see supplementary information). Interestingly, it was observed that the e.e. of products **2b**, **2d-f** & **2h-m** diminished significantly following prolonged reaction times with all three PAL biocatalysts (table 1). These products all possess electron-withdrawing substituents on the aromatic ring, suggesting that PALs are able to catalyze the formation of the D-enantiomers of electron-deficient structures. D-amino acid formation is especially prominent with substrates which are able to stabilize negative charge at the benzylic position, for

Table 1. The conversion and e.e. of cinnamic acid derivatives **1a-n** (5 mM) after 22 hours

	AvPAL		PcPAL		RgPAL	
	conv.	e.e.	conv.	e.e.	conv.	e.e.
1a	49	>99	58	>99	55	>99
1b	59	>99	75	6	71	2
1c	59	>99	60	>99	61	>99
1d	76	71	75	96	75	93
1e	91	>99	94	0	93	13
1f	62	>99	72	14	76	7
1g	53	>99	50	>99	51	>99
1h	61	76	49	-8	62	38
1i	80	>99	87	10	85	28
1j	77	75	89	0	89	1
1k	86	-9	87	-11	86	-14
1l	78	92	84	7	83	7
1m	79	-6	86	-4	85	5
1n	50	>99	50	>99	48	>99

Percentage conversion and product e.e. (for the L-enantiomer) were determined by chiral HPLC. *E. coli* BL21(DE3) whole cells (20 mg/ml) expressing each PAL were incubated with 5 mM substrate in 5 M NH₄OH pH 9.5 at 30 °C

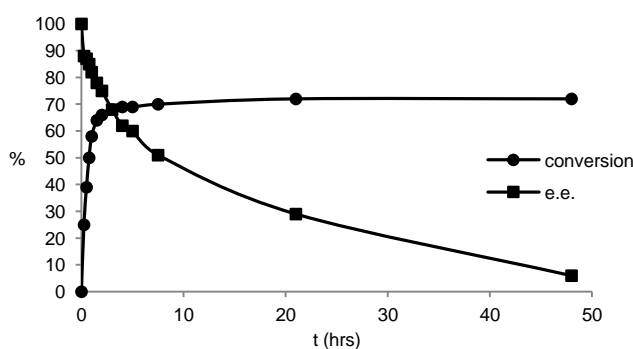


Figure 2. The amination reaction of 4-nitrocinnamic acid (**1m**) mediated by *E. coli* BL21(DE3) cells (15 mg/ml) expressing AvPAL in 5 M NH₄OH pH 9.5, 30 °C

example in the cases of substrates **1k** and **1m** which possess *ortho* and *para* nitro-substituents respectively. The AvPAL mediated amination reaction of **1b**, **1e-f**, **1h-j** & **1l** demonstrated significantly higher enantioselectivity compared with PcPAL and RgPAL under the conditions employed. Although the application of PALs as biocatalysts for the amination of cinnamic acid analogues has been described extensively in literature and implemented in industrial processes,^[7] the formation of D-amino acids has not been reported. Furthermore to our knowledge the time-dependence on e.e. has not been described previously.

To gain insight into the origin of D-amino acid synthesis, the AvPAL mediated amination of 4-nitrocinnamic acid (**1m**) was studied in detail. The reactions were repeated with purified PAL enzymes which confirmed that the variation in e.e. over time did not occur as a result of background reactions taking place in the *E. coli* whole cells. Control reactions in the absence of enzyme showed (i) no conversion to either L- or D- product and (ii) no racemization of either L- or D-amino acids, eliminating the possibility of non-selective background chemical reactions. The amination of **1m** was monitored over time using whole cell AvPAL biocatalysts (15 mg/mL). The reaction profile is consistent with initial (reversible) formation of the L-amino acid as the kinetic product followed by a slower process in which formation of the D-enantiomer occurs (figure 2). The observation that the same equilibrium composition (4-nitrocinnamic acid **1m** 14%, 4-nitrophenylalanine **2m** 86%, e.e. = -9%) was obtained starting from each of the three components (i.e. **1m**, L-**2m**, D-**2m**) under standard amination reaction conditions supports this proposal.

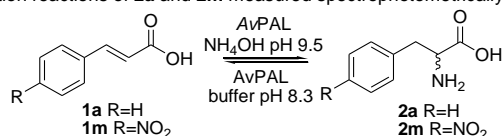
The active-site loop contains an essential Tyr78 residue, believed to be responsible for abstraction of the substrate's C-3 benzylic proton.^[12c] To assess the role of the catalytic base Tyr78 in D-amino acid formation, the Y78F variant of AvPAL was expressed and purified, and was shown to be correctly folded by circular dichroism. Y78F showed no activity towards the deamination of either enantiomer of phenylalanine (**2a**) or 4-nitrophenylalanine (**2m**) and it was also inactive towards the amination of cinnamic acid (**1a**) and 4-nitrocinnamic acid (**1m**). Our results confirm that Tyr78 plays a vital role in the AvPAL catalyzed deamination of L-**2a** and also demonstrates that it is an essential catalytic residue for activity towards production of D-amino acids.

To examine the role of the prosthetic group in D-amino acid formation the AvPAL S168A variant was expressed, which can no longer form MIO by post-translational modification. The absence of cofactor in this variant was confirmed by analysis of the UV difference spectra. The discrete maxima at ca. 310 nm, associated with the presence of cofactor in wt AvPAL is diminished in the S168A variant.^[16] The kinetic parameters for S168A and wt AvPAL were determined. Surprisingly, the *k*_{cat} for wt AvPAL catalyzed amination of 4-nitrocinnamic acid (**1m**) was 140 times greater than

cinnamic acid (**1a**) (table 2). The S168A mutation resulted in complete loss of activity towards the amination of **1a** and deamination of L-**2a**. However, S168A retained low level activity towards the amination of **1m** and towards the deamination of L-**2m**, although a significant reduction (293 and 31 fold respectively) in k_{cat} was observed. Interestingly, the k_{cat} for 4-nitro-D-phenylalanine (D-**2m**) deamination was not significantly affected by the absence of the MIO cofactor.

These results suggest that the dominant pathway for the formation (or consumption) of L-amino acids is dependent on the MIO cofactor, whereas the analogous reactions involving the D-enantiomers occur via an MIO-independent pathway. Comparable k_{cat} values are observed for the S168A catalyzed deamination of both L-**2m** and D-**2m**, demonstrating that the cofactor-independent pathway proceeds in a non-stereoselective manner. Reduction of the MIO exocyclic methylene group represents an alternative method of cofactor inactivation.^[11a] Treatment of wt AvPAL with NaBH₄ led to reduced enzyme which displayed similar activity to S168A (see supplementary information). A Y78F/S168A double mutant was expressed and displayed no activity towards **1m**, L-**2m** or D-**2m**, demonstrating that the Tyr78 residue is essential for the cofactor independent reactions and that the non-selective pathway occurs in the active site rather than an alternative binding site.

Table 2. Kinetic constants for the amination reactions of **1a** and **1m** and the deamination reactions of **2a** and **2m** measured spectrophotometrically



Substrate	wt AvPAL			S168A AvPAL		
	k_{cat} (s ⁻¹)	K_{M} (mM)	$k_{\text{cat}}/K_{\text{M}}$ (s ⁻¹ mM ⁻¹)	k_{cat} (s ⁻¹)	K_{M} (mM)	$k_{\text{cat}}/K_{\text{M}}$ (s ⁻¹ mM ⁻¹)
amination ^[a]						
1a	0.029	0.039	0.744	n.d.	n.d.	n.d.
1m	4.106	0.720	5.703	0.014	0.062	0.225
deamination ^[b]						
L- 2a	0.491	0.298	1.648	n.d.	n.d.	n.d.
D- 2a	n.d.	n.d.	n.d.	n.d.	n.d.	n.d.
L- 2m	1.380	0.478	2.887	0.045	0.137	0.328
D- 2m	0.090	0.089	1.011	0.025	0.329	0.076

n.d = kinetic constants could not be measured [a] amination reaction in 5 M NH₄OH, pH 9.5, 30 °C [b] deamination reactions in 0.1 M buffer, pH 8.3, 30 °C

It has been previously shown that PAL mediated deamination of L-phenylalanine proceeds in a stereoselective manner with loss of the *pro-S* benzylic proton.^[17] In order to investigate the stereoselectivity of D-amino acid formation and deamination, deuterated 4-nitrocinnamic acid **3** (>99% deuterium incorporation) and deuterated 4-nitro-D-phenylalanine diastereoisomers D-**4** (99% e.e. 83% ²H incorporation) and D-**5** (98% e.e. 83% ²H incorporation) were synthesized via a chemoenzymatic strategy. Of particular interest was the application of *N*-acetyl amino acid racemase (NAAAR G291D/F323Y)^[18] in combination with a commercially available D-acylase to invert the C-2 stereocentre to the required (*R*)-configuration for the synthesis of D-**5** (see supplementary information).

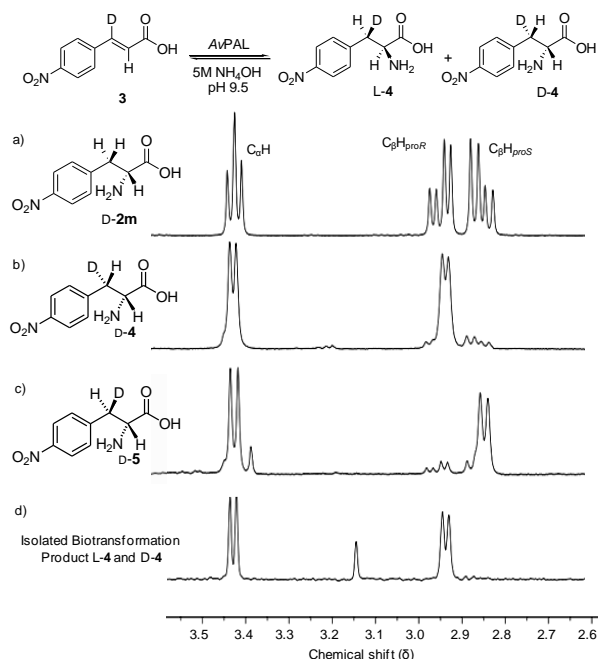


Figure 3. ¹H NMRs of (a) unlabeled 4-nitro-D-phenylalanine D-**2m**, (b and c) deuterated 4-nitro-D-phenylalanine standards **4** and **5** and (d) the isolated product from the AvPAL catalyzed amination of 4-nitro-(3-²H)-cinnamic acid **3**

Amination of **3** was carried out in the presence of AvPAL, producing a mixture of L- and D- amino acids (e.e. = 6 %) which were isolated by ion-exchange chromatography. ¹H NMR of this product shows the presence of a single diastereoisomer resulting from *anti*-addition of ammonia across the double bond, as judged by comparison with chemo-enzymatically synthesized standards **4** and **5** (figure 3). Single enantiomers (e.e. >99%) of the deuterated biotransformation products (L-**4** and D-**4**) could be obtained by kinetic resolution using commercially available D-amino acid oxidase from porcine kidney and L-amino acid oxidase from *Crotalus adamanteus*.

The stereoselectivity of AvPAL deamination reactions was also investigated using the isotopically labelled substrates D-**4** and D-**5**. Although substrate **5** yielded a single fully protiated product **1m** consistent with the exclusive *anti*-elimination of the (*3R*)-deuterium, substrate **4** gave a mixture of products **1m** and **3**. The ratio of products produced is variable and appears to be influenced by subtle changes in reaction conditions. This result was somewhat unexpected considering the (reversible) amination of 4-nitro-(3-²H)-cinnamic acid **3** was completely stereoselective to produce isomer **4**. PAL catalyzed deamination reactions are performed at pH 8.3 whereas reactions in the amine synthesis direction are conducted at pH 9.5 which leads to a more favourable equilibrium position. Deamination of **4** and **5** were repeated at pH 9.5 and in both cases were shown to result in the formation of a single product due to *anti*-elimination of the (*3R*)-proton or deuterium respectively. Deamination of substrates **4** and **5** catalyzed by S168A (lacking the MIO cofactor) showed a similar trend to wt AvPAL. At both pH 8.3 and pH 9.5 substrate **5** yielded fully protiated product **1m** exclusively, whereas deamination of substrate **4** gave a mixture of products **1m** and **3**. The loss of deuterium incorporation was significantly higher at pH 8.3 than at pH 9.5.

These observations are consistent with the deamination of D-amino acids proceeding via a stepwise E_cB mechanism, with initial stereoselective deprotonation of the *pro-R* benzylic proton catalyzed by Tyr78, followed by elimination of ammonia. At pH 8.3 non-stereoselective reprotonation of the carbanion intermediate from either bulk solvent or active-site residues competes with amine

elimination resulting in partial loss of the deuterium in the final product. The rate of reprotonation is pH dependent and is slower at pH 9.5 than at pH 8.3. This is consistent with studies regarding the mechanism of aminomutases *CcTAM* and *TcPAM* (from *Taxus* plants), which report a loss in the product deuterium incorporation and demonstrate that proton exchange with bulk solvent is pH dependent.^[19] Docking L- and D-phenylalanine into the AvPAL active-site (see supplementary information) demonstrates that only the *pro-S* benzylic proton of L-phenylalanine and *pro-R* proton of D-phenylalanine interact with the catalytic Tyr78 residue, consistent with the results of the isotopic labelling study.

Combined, the kinetic data obtained with wt AvPAL and selected variants along with isotopic labelling studies and molecular modelling have provided significant mechanistic insights into a competing MIO-independent pathway. This pathway proceeds in a non-selective manner, leading to the formation of both L- and D-amino acids. Hydroamination has been shown to occur via *anti*-addition of the amine and the benzylic proton. The key catalytic base (Tyr78) in the well established MIO-dependent pathway remains an essential catalytic residue in the cofactor-independent pathway, demonstrating that this 'enzyme assisted' reaction occurs within the PAL active site. The deamination of D-amino acids proceeds via a stepwise E₁cB mechanism with initial deprotonation at the benzylic position catalyzed by Tyr78. We propose that electron deficient substrates increase the stability of this intermediate carbanion with respect to reprotonation, allowing a slow MIO-independent amine elimination step to occur. Our observations further suggest that cinnamic acid derivatives are able to adopt two productive binding modes in the PAL active site (figure 4). Although two binding modes of cinnamic acid have been reported to occur in the closely related mutases, a second binding conformation has not been described for lyases.^[14, 19a]

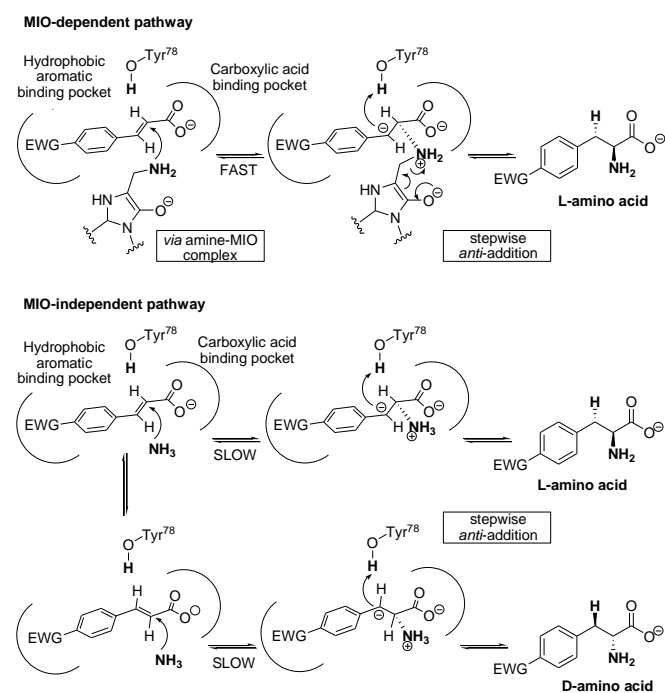


Figure 4. Proposed MIO-dependent and independent pathways

In conclusion, amination reactions catalyzed by both bacterial AvPAL and eukaryotic PcPAL and RgPAL led to the significant formation of D-amino acids in addition to the expected L-amino acid products. For substrates possessing an electron deficient aromatic ring, a significant reduction in e.e. was observed over time.

Mutagenesis of key active site residues and the determination of kinetic parameters has shown that D-amino acids are formed via an 'enzyme assisted' MIO-independent pathway. The mechanism of this pathway has been explored and the results are consistent with a stepwise E₁cB elimination process. The discovery of this alternative pathway may provide insights for future studies on the mechanism of the MIO-dependent pathway. Moreover, these results may have broader implications for the future development of selective biocatalysts for the synthesis of non-natural amino acids.

Keywords: α-amino acids • ammonia lyases • catalytic mechanism • enzyme catalysis • enzymes

- [1] D. J. Craik, D. P. Fairlie, S. Liras, D. Price, *Chem. Biol. Drug. Des* **2013**, *81*, 136-147.
- [2] C. W. Olanow, Y. Agid, Y. Mizuno, A. Albanese, U. Bonucelli, P. Damier, J. D. Yebenes, O. Gershanik, M. Guttman, F. Grandas, M. Hallet, O. Hornykiewicz, P. Jenner, R. Katzenschlager, W. J. Langston, P. LeWitt, E. Melamed, M. A. Mena, P. P. Michel, C. Mytilineou, J. A. Obeso, W. Poewe, N. Quinn, R. Raisman-Vozari, A. H. Rajput, O. Rascol, C. Sampaio, F. Stocchi, *Movement Disorders* **2004**, *19*, 997-1005.
- [3] U. Kazmaier, *Angew. Chem.* **2005**, *117*, 3575; *Angew. Chem. Int. Ed.* **2005**, *44*, 2186-2188.
- [4] a) S. Panke, M. Held, M. Wubbolts, *Curr. Opin. Biotechnol.* **2004**, *15*, 272-279; b) D. Zhu, L. Hua, *J. Biotechnol.* **2009**, *4*, 1420-1431; J. Altenbucher, M. Siemann-Herzberg, C. Syldatk, *Curr. Opin. Biotechnol.* **2001**, *12*, 559-563.
- [5] N. J. Turner, *Current Opin. Chem. Bio.* **2011**, *15*, 234-240.
- [6] M. M. Heberling, B. Wu, S. Bartsch, D. B. Janssen, *Curr. Opin. Chem. Bio.* **2013**, *17*, 250-260.
- [7] B. de Lange, D. J. Hyett, P. J. D. Maas, D. Mink, F. B. J. van Assema, N. Sereing, A. H. M. de Vries, J. G. de Vries, *ChemCatChem* **2011**, *3*, 289-292.
- [8] H. A. Cooke, C. V. Christianson, S. D. Bruner, *Curr. Opin. Chem. Bio.* **2009**, *13*, 460-468.
- [9] a) A. Peterkofsky, *J. Biol. Chem.* **1962**, *237*, 787-795; b) J. D. Hermes, P. M. Weiss, W. W. Cleland, *Biochemistry* **1985**, *24*, 2959-2967.
- [10] S. Pilbák, Ö. Farkas, L. Poppe, *Chem. Eur. J.* **2012**, *18*, 7793-7802.
- [11] a) B. Schuster, J. Rétey, *Proc. Natl. Acad. Sci* **1995**, *92*, 8433-8437; b) L. Poppe, J. Rétey, *Angew. Chem.* **2005**, *117*, 3734-3754; *Angew. Chem. Int. Ed.* **2005**, *44*, 3668-3688; c) A. Gloge, B. Langer, L. Poppe, J. Rétey, *Arch. Biochem. Biophys.* **1998**, *359*, 1-7.
- [12] a) T. F. Schwede, J. Rétey, G. E. Schulz, *Biochemistry* **1999**, *38*, 5355-5361; b) S. Strom, U. Wanninayake, N. D. Ratnayake, K. D. Walker, *Angew. Chem.* **2012**, *124*, 2952-2956; *Angew. Chem. Int. Ed.* **2012**, *51*, 2898-2902; c) L. Wang, A. Gamez, H. Archer, E. E. Abola, C. N. Sarkissian, P. Fitzpatrick, D. Wendt, Y. Zhang, M. Vellard, J. Bliesath, S. M. Bell, J. F. Lemontt, C. R. Sriver, R. C. Stevens, *J. Mol. Biol.* **2008**, *380*, 623-635.
- [13] A.-L. Seff, S. Pilbák, I. Silaghi-Dumitrescu, L. Poppe, *J. Mol. Model* **2011**, *17*, 1551-1563.
- [14] N. D. Ratnayake, U. Wanninayake, J. H. Geiger, K. D. Walker, *J. Am. Chem. Soc.* **2011**, *133*, 8531-8533.
- [15] a) A. Gloge, J. Zon, A. Kövári, L. Poppe, J. Rétey, *Chem. Eur. J.* **2000**, *6*, 3386-3390; b) C. Paizs, A. Katona, J. Rétey, *Eur. J. Org. Chem.* **2006**, 1113-1116; c) S. Bartsch, U. T. Bornscheuer, *Angew. Chem.* **2009**, *121*, 3412-3415; *Angew. Chem. Int. Ed.* **2009**, *48*, 3362-3365.
- [16] D. Röther, D. Merkel and J. Rétey, *Angew. Chem.* **2000**, *112*, 2592-2594; *Angew. Chem. Int. Ed.* **2000**, *39*, 2462-2464
- [17] R. H. Wightman, J. Staunton, A. R. Battersby, *J. Chem. Soc., Perkin Transactions 1: Org. and Bio-Org. Chem.* **1972**, *18*, 2355-2364.
- [18] S. Baxter, S. Royer, G. Grogan, F. Brown, K. E. Holt-Tiffin, I. N. Taylor, I. G. Fotheringham, D. J. Campopiano, *J. Am. Chem. Soc.* **2012**, *134*, 19310-19313.
- [19] a) U. Wanninayake, K. D. Walker, *J. Am. Chem. Soc.* **2013**, *135*, 11193-11206; b) W. Matatu, K. L. Klette, C. Foster, K. D. Walker, *Biochemistry* **2007**, *46*, 9785-9794.

8 References

1. Bornscheuer UT, Huisman GW, Kazlauskas RJ, Lutz S, Moore JC, Robins K: **Engineering the third wave of biocatalysis.** *Nature* 2012, **485**:185-194.
2. Reetz MT: **Biocatalysis in organic chemistry and biotechnology: past, present and future.** *J. Am. Chem. Soc.* 2013, **135**:12480-12496.
3. Turner NJ: **Directed evolution for enzymes in applied catalysis.** *Trends Biotechnol* 2003, **21**:474-478.
4. Turner NJ: **Directed evolution drives the next generation of biocatalysts.** *Nature Chem. Biol.* 2009, **5**:567-573.
5. Stremmer WP: **Rapid evolution of a protein *in vitro* by DNA shuffling.** *Nature* 1994, **370**:389-391.
6. Mastrobattista E, Taly V, Chanudet E, Treacy P, Kelly BT, Griffiths AD: **High-throughput screening of enzyme libraries: *in vitro* evolution of a β -galactosidase by fluorescence-activated sorting of double emulsions.** *Chem. Biol.* 2005, **12**:1291-1300.
7. Fernandez-Gacio A, Uguen M, Fastrez J: **Phage display as a tool for the directed evolution of enzymes.** *Trends Biotechnol* 2003, **21**:408-414.
8. Lipovsek D, Antipov E, Armstrong KA, Olsen MJ, Klibanov AM, Tidor B, Wittrup KD: **Selection of horseradish peroxidase variants with enhanced enantioselectivity by yeast surface display.** *Chem. Biol.* 2007, **14**:1176-1185.
9. Ghislieri D, Green AP, Pontini M, Willies SC, Rowles I, Frank A, Grogan G, Turner NJ: **Engineering an enantioselective amine oxidase for the synthesis of pharmaceutical building blocks and alkaloid natural products.** *J. Am. Chem. Soc.* 2013, **135**:10863-10869.
10. Alexeeva M, Enright A, Dawson MJ, Mahmoudian M, Turner NJ: **Deracemization of α -methylbenzylamine using an enzyme obtained by *in vitro* evolution.** *Angew. Chem. Int. Ed* 2002, **41**:3177-3180.
11. Carr R, Alexeeva M, Dawson MJ, Gotor-Fernández V, Humphrey CE, Turner NJ: **Directed evolution of a monoamine oxidase for the preparative deracemization of cyclic secondary amines.** *Chem. Comm* 2005, **6**:637-639.
12. Carr R, Alexeeva M, Enright A, Eve TSC, Dawson MJ, Turner NJ: **Directed evolution of a monoamine oxidase possessing both broad substrates specificity and high enantioselectivity.** *Angew. Chem. Int. Ed* 2003, **42**:4807-4810.
13. Dunsmore CJ, Carr R, Fleming T, Turner NJ: **A chemo-enzymatic route to enantiomerically pure cyclic tertiary amines** *J. Am. Chem. Soc.* 2006, **128**:2224-2225.
14. Reetz MT, Peyralens JD, Höbenreich H, Maichele A, Vogel A: **Expanding the substrate scope of enzymes: combining mutations obtained by CASTing.** *Chem. Eur. J.* 2006, **12**:6031-6038.
15. Reetz MT, Wang L-W, Bocola M: **Directed evolution of enantioselective enzymes: iterative cycles of CASTing for probing protein-sequence space.** *Angew. Chem. Int. Ed* 2006, **45**:1236-1241.
16. Reetz MT, Kahakeaw D, Lohmer R: **Addressing the numbers problem in directed evolution.** *ChemBioChem* 2008, **9**:1797-1804.
17. Reetz MT, Kahakeaw D, Lohmer R, Wu S: **Greatly reduced amino acid alphabets in directed evolution: making the right choice for saturation mutagenesis at homologous enzyme positions.** *Chem. Comm* 2008:5499-5501.
18. Abrahamson MJ, Vázquez-Figueroa E, Woodall NB, Moore JC, Bommarius AS: **Development of an amine dehydrogenase for synthesis of chiral amines.** *Angew. Chem. Int. Ed* 2012, **51**:3969-3972.
19. Panke S, Held M, Wubbolts M: **Trends and innovations in industrial biocatalysis for the production of fine chemicals.** *Curr. Opin. Biotechnol.* 2004, **15**:272-279.
20. Balkenhohl F, Dietrich K, Hauer B, Ladner W: **Optically active amines via lipase-catalyzed methoxyacetylation.** *J. Prakt. Chem* 1997, **339**:381-384.

21. Znabet A, Polak MM, Janssen E, Kanter FJJd, Turner NJ, Orru RVA, Ruijter E: **A highly efficient synthesis of telaprevir by strategic use of biocatalysis and multicomponent reactions.** *Chem. Commun* 2010, **46**:7918-7920.
22. Saville CK, Janey JM, Mundorff EC, Moore JC, Tam S, Jarvis WR, Colbeck JC, Krebber A, Fleitz FJ, Brands J, et al.: **Biocatalytic asymmetric synthesis of chiral amines from ketones applied to sitagliptin manufacture.** *Science* 2010, **329**:305-308.
23. Leuchtenberger W, Huthmacher K, Drauz K: **Biotechnological production of amino acids and derivatives: current status and prospects.** *Appl. Microbiol. Biotechnol* 2005, **69**:1-8.
24. De Lange B, Hyett DJ, Maas PJD, Mink D, Van Assema FBJ, Sereing N, De Vries AHM, De Vries JG: **Asymmetric synthesis of (S)-2-indolinecarboxylic acid by combining biocatalysis and homogeneous catalysis.** *ChemCatChem* 2011, **3**:289-292.
25. Mink D, Van Assema FBJ, Maas PJD, Hyett DJ: **Process for the preparation of enantiomerically enriched indoline-2-carboxylic acid.** US Patent 2006.
26. Cotzias GC, Paavasilou PS, Gellene R: **L-Dopa in Parkinson's syndrome.** *The New England Journal of Medicine* 1969, **281**:272.
27. Craik DJ, Fairlie DP, Liras S, Price D: **The future of peptide-based drugs.** *Chem. Biol. Drug. Des* 2013, **81**:136.
28. Gfeller D, Michielin O, Zoete V: **SwissSidechain: A molecular and structural database of non-natural sidechains.** *Nucleic Acids Research* 2013, **41**:327-332.
29. List B, Lerner RA, Barbas III CF: **Proline-catalyzed direct asymmetric aldol reactions.** *J. Am. Chem. Soc.* 2000, **122**:2395-2396.
30. Paradowska J, Stodulski M, Mlynarski J: **Catalysts based on amino acids for asymmetric reactions in water.** *Angew. Chem. Int. Ed* 2009, **48**:4288-4297.
31. Xu L-W, Lu Y: **Primary amino acids: privileged catalysts in enantioselective organocatalysis.** *Org. Biomol. Chem.* 2008, **6**:2047.
32. Najera C, Sansano JM: **Catalytic asymmetric synthesis of α -amino acids.** *Chem. Rev.* 2007, **107**:4584-4671.
33. Ma J-A: **Recent developments in the catalytic asymmetric synthesis of α - and β -amino acids.** *Angew. Chem. Int. Ed* 2003, **42**:4290-4299.
34. Yet L: **Recent developments in catalytic asymmetric Strecker-type reactions.** *Angew. Chem. Int. Ed* 2001, **40**:875-877.
35. Martens J: **Enantioselective organocatalytic Strecker reactions in the synthesis of α -amino acids.** *ChemCatChem* 2010, **2**:379-381.
36. Ishitani H, Komiyama S, Hasegawa Y, Kobayashi S: **Catalytic asymmetric Strecker synthesis. Preparation of enantiomerically pure α -amino acid derivatives from aldimines and tributyltin cyanide or achiral aldehydes, amines, and hydrogen cyanide using a chiral zirconium catalyst.** *J. Am. Chem. Soc.* 2000, **122**:762-766.
37. Corey EJ, Grogan MJ: **Enantioselective synthesis of α -amino nitriles from *N*-benzhydryl imines and HCN with a chiral bicyclic guanidine as catalyst.** *Org. Lett.* 1999, **1**:157-160.
38. Trost BM, Dogra K: **Synthesis of novel quaternary amino acids using molybdenum-catalyzed asymmetric allylic alkylation.** *J. Am. Chem. Soc.* 2002, **124**:7256-7257.
39. Corey EJ, Xu F, Noe MC: **A rational approach to catalytic enantioselective enolate alkylation using a structurally rigidified and defined chiral quaternary ammonium salt under phase transfer conditions.** *J. Am. Chem. Soc.* 1997, **119**:12414-12415.
40. Kobayashi S, Hamada T, Manabe K: **The catalytic asymmetric Mannich-type reactions in aqueous media.** *J. Am. Chem. Soc.* 2002, **124**:5640-5641.
41. Burk MJ: **Modular phospholane ligands in asymmetric catalysis.** *Acc. Chem. Res* 2000, **33**:363-372.
42. Rossen K: **Ru- and Rh- catalyzed asymmetric hydrogenations: Recent surprises from an old reaction.** *J. Am. Chem. Soc.* 2001, **40**:4611-4613.
43. Roy J: **Pharmaceutical impurities- a mini-review.** *AAPS PharmSciTech* 2002, **3**:1-8.
44. Altenbuchner J, Siemann-Herzberg M, Sylatk C: **Hydantoinases and related enzymes as biocatalysts for the synthesis of unnatural chiral amino acids.** *Curr. Opin. Biotechnol.* 2001, **12**:559-563.
45. Turner NJ: **Ammonia lyases and aminomutases as biocatalysts for the synthesis of α -amino and β -amino acids.** *Current opinion in Chem. Bio.* 2011, **15**:234-240.

46. Cooke HA, Christianson CV, Bruner SD: **Structure and chemistry of 4-methylideneimidazole-5-one containing enzymes.** *Curr. Opin. Chem. Bio.* 2009, **13**:460-468.
47. Asano Y, Kato Y, Levy C, Baker P, Rice D: **Structure and function of amino acid ammonia lyases.** *Biocatalysis and Biotransformations* 2004, **22**:131-138.
48. De Villiers M, Veetil VP, Raj H, De Villiers J, Poelarends GJ: **Catalytic mechanisms and biocatalytic applications of aspartate and methylaspartate ammonia lyases.** *Chem. Biol.* 2012, **7**:1618-1628.
49. Hodgins D, Abeles RH: **The presence of covalently bound pyruvate in D-proline reductase and its participation in the catalytic process.** *J. Biol. Chem.* 1967, **242**:5158-5159.
50. Wickner RB: **Dehydroalanine in histidine ammonia lyase.** *J. Biol. Chem.* 1969, **244**:6550-6552.
51. Schwede TF, Retey J, Schulz GE: **Crystal structure of histidine ammonia-lyase revealing a novel polypeptide modification as the catalytic electrophile.** *Biochemistry* 1999, **38**:5355-5361.
52. Kyndt JA, Meyer TE, Cusanovich MA, Van Beeumen JJ: **Characterization of a bacterial tyrosine ammonia lyase, a biosynthetic enzyme for the photoactive yellow protein.** *FEBS lett.* 2002, **512**:240-244.
53. Xue Z, McCluskey M, Cantera K, Sariaslani FS, Huang L: **Identification, characterization and functional expression of a tyrosine ammonia-lyase and its mutants from the photosynthetic bacterium *Rhodobacter sphaeroides*.** *J. Ind. Microbiol. Biotechnol.* 2007, **34**:599-604.
54. Zhang Y, Li SZ, Li J, Pan X, Cahoon RE, Jaworski JG, Wang X, Jez JM, Chen F, Yu O: **Using unnatural protein fusions to engineer resveratrol biosynthesis in yeast and mammalian cells.** *J. Am. Chem. Soc.* 2006, **128**:13030–13031.
55. Fritz. RR, Hodgins DS, Abell CW: **Phenylalanine ammonia lyase: induction and purification from yeast and clearance in mammals.** *J. Biol. Chem.* 1976, **251**:4646-4650.
56. Koukol J, Conn EE: **Metabolism of aromatic compounds in higher plants.** *J. Biol. Chem.* 1961, **236**:2692-2698.
57. Paizs C, Katona A, Retey J: **The Interaction of heteroaryl-acrylates and alanines with phenylalanine ammonia-lyase from parsley.** *Chem. Eur. J.* 2006, **12**:2739-2744.
58. Shadle GL, Wesley SV, Korth KL, Chen F, Lamb C, Dixon RA: **Phenylpropanoid compounds and disease resistance in transgenic tobacco with altered expression on L-phenylalanine ammonia lyase.** *Phytochemistry* 2003, **64**:153-161.
59. Dixon RA: **Natural products and disease resistance.** *Nature* 2001, **411**:843-847.
60. Williams JS, Thomas M, Clarke DJ: **The gene *stIA* encodes a phenylalanine ammonia-lyase that is involved in the production of a stilbene antibiotic in *Photorhabdus luminescens* TT01.** *Microbiology* 2005, **151**:2543-2550.
61. Bezanson GS, Desaty D, Emes AV, Vining LC: **Biosynthesis of cinnamamide and detection of phenylalanine ammonia-lyase in *Streptomyces verticillatus*.** *Can. J. Microbiol.* 1970, **16**:147-151.
62. Xiang L, Moore BS: **Inactivation, complementation and heterologous expression of *encP*, a novel bacterial phenylalanine ammonia-lyase gene.** *J. Biol. Chem.* 2002, **277**:32505-32509.
63. Chesters C, Wilding M, Goodall M, Micklefield J: **Thermal bifunctionality of bacterial phenylalanine aminomutase and ammonia lyase enzymes.** *Angew. Chem. Int. Ed* 2012, **51**:TBC.
64. Moffitt MC, Louie GV, Bowman ME, Pence J, Noel JP, Moore BS: **Discovery of two cyanobacterial phenylalanine ammonia lyases: kinetic and structural characterization.** *Biochemistry* 2007, **46**:1004-1012.
65. Wang L, Gamez A, Archer H, Abola EE, Sarkissian CN, Fitzpatrick P, Wendt D, Zhang Y, Vellard M, Bliesath J, et al.: **Structural and biochemical characterization of the therapeutic *Anabaena variabilis* phenylalanine ammonia lyase** *J. Mol. Biol* 2008, **380**:623-635.
66. Wang L, Gamez A, Sarkissian CN, Straub M, Patch MG, Han GW, Striepeke S, Fitzpatrick P, Scriver CR, Stevens RC: **Structure based chemical modification**

- strategy for enzyme replacement treatment of phenylketonuria.** *Mol. Genet. Metab.* 2005, **86**:134-140.
67. Hanson H, Havir EA: **L-Phenylalanine ammonia lyase II: Mechanism and kinetic properties of the enzyme from potato tubers.** *Biochemistry* 1968, **7**:1904-1914.
 68. Hanson KR, Havir EA, Ressler C: **Phenylalanine ammonia-lyase: enzymatic conversion of 3-(1,4-cyclohexadienyl)-L-alanine to trans-3-(1,4-cyclohexadienyl)acrylic acid.** *Biochemistry* 1979, **18**:1431-1438.
 69. Gloge A, Langer B, Poppe L, Retey J: **The behaviour of substrate analogues and secondary deuterium isotope effects in the phenylalanine ammonia-lyase reaction.** *Arch. Biochem. Biophys.* 1998, **359**:1-7.
 70. Gloge A, Zon J, Kovari A, Poppe L, Retey J: **Phenylalanine ammonia-lyase: The use of its broad substrate specificity for mechanistic investigation and biocatalysis- synthesis of L-arylalanines.** *Chem. Eur. J.* 2000, **6**:3386-3390.
 71. Bartsch S, Bornscheuer UT: **Mutational analysis of phenylalanine lyase to improve reaction rates for various substrates.** *Protein Engineering, Design and Selection* 2010, **23**:929-933.
 72. Paizs C, Tosa MI, Bencze LC, Brem J, Irimie FD, Retey J: **2-amino-3-(5-phenylfuran-2-yl)propanoic acids and 5-phenylfuran-2-ylacrylic acids are novel substrates of phenylalanine ammonia-lyase.** *Heterocycles* 2011, **82**:1217-1228.
 73. Calabrese JC, Jordan DB, Boodhoo A, Sariaslani S, Vannelli T: **Crystal structure of phenylalanine ammonia lyase: multiple helix dipoles implicated in catalysis.** *Biochemistry* 2004, **43**:11403-11416.
 74. Ritter H, Schulz GE: **Structural basis for the entrance into the phenylpropanoid metabolism catalysed by phenylalanine ammonia-lyase.** *Plant cell* 2004, **16**:3426-3436.
 75. Smith TA, Cordelle FH, Abeles RH: **Inactivation of histidine deaminase by carbonyl reagents.** *Arch. Biochem. Biophys.* 1967, **120**:724-725.
 76. Ohmiya Y, Hayashi H, Kondo T, Kondo Y: **Location of dehydroalanine residues in the amino acid sequence of bovine thyroglobulin. Identification of "donor" tyrosine sites for hormonogenesis in thyroglobulin.** *J. Biol. Chem.* 1990, **265**:9066-9071.
 77. Schuster B, Retey J: **Serine-202 is the putative precursor of the active site dehydroalanine of phenylalanine ammonia lyase.** *FEBS Lett.* 1994, **349**:252-254.
 78. Rother D, Merkel D, Retey D: **Spectroscopic evidence for a 4-methylidene imidazol-5-one in histidine and phenylalanine ammonia-lyases.** *Angew. Chem. Int. Ed* 2000, **39**:2462-2464.
 79. Langer B, Langer M, Retey J: **Methylidene imidazolone (MIO) from histidine and phenylalanine ammonia lyase.** *Biochem. Biophys. Acta* 2001, **1647**:179-184.
 80. Baedeker M, Schulz GE: **Autocatalytic peptide cyclization during chain folding of histidine ammonia lyase.** *Structure* 2002, **10**:61-67.
 81. Pilbak S, Tomin A, Retey J, Poppe L: **The essential tyrosine-containing loop conformation and the role of the C-terminal multi-helix region in eukaryotic phenylalanine ammonia-lyase.** *FEBS* 2006, **273**:1004-1019.
 82. Christianson CV, Montavon TJ, Lanen SGV, Shen B, Bruner SD: **The structure of L-tyrosine 2,3-from the C-1027 enediyne antitumor antibiotic biosynthetic pathway.** *Biochemistry* 2007, **46**:7205-7214.
 83. Watts KT, Mijts BN, Lee PC, Manning AJ, Schmitt-Dannert C: **Discovery of a substrate selectivity switch in tyrosine ammonia-lyase, a member of the aromatic amino acid lyase family.** *Chemistry and Biology* 2006, **13**:1317-1326.
 84. Christianson SD, Wu W, Spies MA, Shen B, Toney MD: **Kinetic analysis of the 4-methylideneimidazole-5-one containing tyrosine amino mutase in enediyne antitumor antibiotic C-1027 biosynthesis.** *Biochemistry* 2003, **42**:12708-12718.
 85. Steele CL, Chen Y, Dougherty BA, Li W, Hofstead S, Lam KS, Xiang Z, Chiang S-J: **Purification cloning and functional expression of phenylalanine aminomutase: The first committed step in taxol side-chain biosynthesis.** *Biochem. Biophys.* 2005, **438**:1-10.
 86. Krug D, Muller R: **Discovery of additional members of the tyrosine aminomutase enzyme family and the mutational analysis of CmdF.** *ChemBioChem* 2009, **10**:741-750.

87. Bartsch S, Wybenga GG, Jansen M, Herbling MM, Wu B, Dijkstra BW, Janssen DB: **Redesign of a phenylalanine aminomutase into a phenylalanine ammonia lyase.** *ChemCatChem* 2013, **5**:1797-1802.
88. Tabor H, Mehler AH, Hayaishi O, White J: **Urocanic acid as an intermediate in the enzymatic conversion of histidine to glutamic and formic acids.** *J. Biol. Chem.* 1952, **196**:121-128.
89. Hanson KR, Wightman RH, Stauton J, Battersby AR: **Stereochemical course of the elimination catalyzed by L-phenylalanine ammonia lyase and the configuration of 2-benzamidocinnamic azlactone.** *Chem. Comm* 1971, **D**:185-186.
90. Peterkofsky A: **The mechanism of action of histidase: amino-enzyme formation and partial reaction.** *J. Biol. Chem.* 1962, **237**:787-795.
91. Hermes JD, Weiss PM, Cleland WW: **Use of Nitrogen-15 and deuterium isotope effect to determine the chemical mechanism of phenylalanine ammonia lyase.** *Biochemistry* 1985, **24**:2959-2967.
92. Furuta T, Takahashi H, Shibasaki H, Kasuya Y: **Reversible stepwise mechanism involving a carbanion intermediate in the elimination ammonia from L-histidine catalyzed by histidine ammonia-lyase.** *J. Biol. Chem.* 1992, **267**:12600-12605.
93. Pilbak S, Farkas O, Poppe L: **Mechanism of the tyrosine ammonia lyase reaction-tandem nucleophilic and electrophilic enhancement by a proton transfer.** *Chem. Eur. J.* 2013, **18**:7793-3802.
94. Seff A-L, Pilbak S, Silaghi-Dumitrescu I, Poppe L: **Computational investigation of the histidine ammonia-lyase reaction: a modified loop conformation and the role of the zinc(II) ion.** *J. Mol. Model* 2011, **17**:1551-1563.
95. Louie GV, Bowman ME, Moffitt MC, Baiga TJ, Moore BS, Noel JP: **Structural determinants and modulation of substrate specificity in phenylalanine-tyrosine ammonia lyases.** *Chem. Biol.* 2006, **13**:1327-1338.
96. Christianson CV, Montavon TJ, Festin GM, Cooke HA, Shen B, Bruner SD: **The mechanism of MIO based aminomutases in β -amino acid biosynthesis.** *J. Am. Chem. Soc.* 2007, **129**:15744-15745.
97. Montavon TJ, Christianson CV, Festin GM, Shen B, Bruner SD: **Design and characterization of mechanism-based inhibitors for the tyrosine aminomutase SgTAM.** *Bioorg. Med. Chem. Lett* 2008, **18**:3099-3102.
98. Strom S, Wanninayake U, Ratnayake ND, Walker KD: **Insights into the mechanistic pathway of the *Pantoea agglomerans* phenylalanine aminomutase.** *Angew. Chem. Int. Ed* 2012, **51**:2898-2902.
99. Yongyu Zhao, Bordwell FG: **Bond dissociation free energies of the H-A bonds in HA²⁻ dianions.** *J. Org. Chem* 1995, **60**:3932-3933.
100. Langer M, Pauling A, Retey J: **The role of dehydroalanine in catalysis by histidine ammonia lyase.** *Angew. Chem. Int. Ed* 1995, **34**:1464-1465.
101. Schuster B, Retey J: **The mechanism of action of phenylalanine ammonia-lyase: the role of the prosthetic dehydroalanine.** *Proc. Natl. Acad. Sci* 1995, **92**:8433-8437.
102. Poppe L, Retey J: **Friedel-Crafts-type mechanism for the enzymatic elimination of ammonia from histidine and phenylalanine.** *Angew. Chem. Int. Ed.* 2005, **44**:3668-3688.
103. Bartsch S, Bornscheuer UT: **A single residue influences the reaction mechanism of ammonia lyases and mutases.** *Angew. Chem. Int. Ed* 2009, **48**:3362-3365.
104. Rother D, Poppe L, Morlock G, Vieregutz S, Retey J: **An active site homology model of phenylalanine ammonia-lyase from *Petroselinum crispum*.** *Eur. J. Biochem.* 2002, **269**:3065-3075.
105. Khan NU, Vaidyanathan CS: **A new simple spectrophotometric assay of phenylalanine ammonia-lyase.** *Current Sci* 1986, **55**:391-393.
106. Rowles I: **Development of novel ammonia-lyase biocatalysts for the production of unnatural amino acids for industry.** Manchester, UK: University of Manchester: 2009.
107. Studier FW: **Protein production by auto-induction in high-density shaking cultures.** *protein expression and purification* 2005, **41**:207-234.
108. Paizs C, Katona A, J.Retey: **Chemoenzymatic one-pot synthesis of enantiopure L-arylalanine from arylaldehydes.** *Eur. J. Org. Chem* 2006:1113-1116.

109. Viergutz S, Poppe L, Tomin A, Rezey J: **Mechanistic investigation of phenylalanine ammonia lyase by using *N*-methylated phenylalanines.** *Helvetica Chimica Acta* 2003, **86**:3601-3612.
110. Kemmer G, Keller S: **Nonlinear least-squares data fitting in Excel spreadsheets.** *Nature Protocols* 2010, **5**:267-281.
111. Bommarius AS, Shwarm M, Drauz K: **Biocatalysis to amino acid-based chiral pharmaceuticals-examples and perspectives.** *J. Mol. Cat. B: Enzymatic* 1998, **5**:1-11.
112. Ratnayake ND, Wanninayake U, Geiger JH, Walker KD: **Stereochemistry and mechanism of a microbial phenylalanine aminomutase.** *J. Am. Chem. Soc.* 2011, **133**:8531-8533.
113. Still WC, Gennari C: **Direct synthesis of Z-unsaturated esters. A useful modification of the Horner-Emmons olefination.** *Tetrahedron Lett.* 1983, **24**:4405-4408.
114. Erlenmeyer E: **Ueber die Condensation der Hippursäure mit Phtalensäureanhydrid und mit benzaldehyd.** *Eur. J. Org. Chem* 1893, **275**:1-8.
115. Wightman RH, Staunton J, Battersby AR: **Studies of enzyme-mediated reactions. Part 1. Syntheses of deuterium or tritium labelled (3*S*)- and (3*R*)-phenylalanines: Stereochemical course of the elimination catalysed by L-phenylalanine ammonia-lyase.** *J. Chem. Soc., Perkin Transactions 1: Org. and Bio-Org. Chem.* 1972, **18**:2355-2364.
116. Roff GJ, Lloyd RC, Turner NJ: **A versatile chemo-enzymatic route to enantiomerically pure β -branched α -amino acids.** *J. Am. Chem. Soc.* 2004, **126**:4098-4099.
117. Baxter S, Royer S, Grogan G, Brown F, Holt-Tiffin KE, Taylor IN, Fotheringham IG, Campopiano DJ: **An improved racemase/acylase biotransformation for the preparation of enantiomerically pure amino acids.** *J. Am. Chem. Soc.* 2012, **134**:19310-19313.
118. Li D-D, Lv P-C, Zhang H, Zhang H-J, Hou Y-P, Liu K, Ye Y-H, Zhu H-L: **The combination of 4-anilinoquinazoline and cinnamic acid: a novel mode of binding to the epidermal growth factor receptor tyrosine kinase.** *Bioorg. Med. Chem* 2011, **19**:5012-5022.
119. Wanninayake U, Walker KD: **A bacterial tyrosine aminomutase proceeds through retention or inversion of stereochemistry to catalyze its isomerization reaction.** *J. Am. Chem. Soc.* 2013, **135**:11193-11206.
120. Mutatu W, Klettke KL, Foster C, Walker KD: **Unusual mechanism for an aminomutase rearrangement: retention of configuration at the migration termini.** *Biochemistry* 2007, **46**:9785-9794.
121. D'Cunha GB, Satyanarayan V, Nair PM: **Novel direct synthesis of L-Phenylalanine methylester by using *Rhodotorula glutinis* phenylalanine ammonia lyase in an organic-aqueous biphasic system.** *Enzyme Microb. Tech* 1994, **16**:318-322.
122. D'Cunha GB, Satyanarayan V, Nair PM: **Stabilization of phenylalanine ammonia lyase from *Rhodotorula glutinis* cells for the continuous synthesis of L-phenylalanine methyl-ester.** *Enzyme Microb. Tech* 1996, **19**:421-427.
123. Weiner B, Poelarends GJ, Janssen DB, Feringa BL: **Biocatalytic enantioselective synthesis of *N*-substituted aspartic acids by aspartate ammonia lyase.** *Chem. Eur. J.* 2008, **14**:10094-10100.
124. Xu B, Huang Z, Liu C, Cai Z, Pan W, Cao P, Hao X, Liang G: **Synthesis and anti-hepatitis B virus activities of Matijing-Su derivatives.** *Bioorg. Med. Chem* 2009, **17**:3118-31125.
125. James J. Mencil, Fishbein P: **Method for making pharmaceutical compounds.** US Patent 2010, US 2012/0125146 A1.
126. Duterte D, Morier E, Poncin-Lafitte ML, Rapin JR, Rips R: **Synthesis of *p*-iodoamphetamine-125I.** *Journal of labelled compounds and radiopharmaceuticals* 1983, **20**:149-155.
127. Nahm S, Weinreb SM: ***N*-Methoxy-*N*-methylamides as effective acylating agents.** *Tetrahedron Lett.* 1981, **22**:3815-3818.
128. Kappel JC, Barany G: **Backbone amide linker (BAL) strategy for *N*-9-fluorenylmethoxycarbonyl (Fmoc) solid-phase synthesis of peptide aldehydes.** *J. Peptide Sci.* 2005, **11**:525-535.

129. Millian L, Estelles R, Abarca B, Ballesteros R, Sanz MJ, Blazquez MA: **Reactive oxygen species (ROS) generation inhibited by aporphine and phenanthrene alkaloids semi-synthesized from natural boldine.** *Chem. Pharm. Bull.* 2004, **52**:696-699.
130. Evans CT, Conrad D, Hanna K, Peterson W, Choma C, Misawa M: **Novel stabilization of phenylalanine ammonia-lyase catalyst during bioconversion of *trans*-cinnamic acid to L-phenylalanine.** *Appl. Microbiol. Biotechnol* 1987, **25**:399-405.
131. Udenfriend S, Stein S, Bohlen P: **Fluorescamine: a reagent for assay of amino acids, peptides, proteins and primary amines in the picomole range.** *Science* 1972, **178**:871-872.
132. Rhee SG, Chang T-S, Jeong W, Kang D: **Methods for detection and measurement of hydrogen peroxide inside and outside of cells.** *Mol. Cells* 2010, **29**:539-549.
133. Pollegioni L, Motta P, Molla G: **L-Amino acid oxidase as biocatalyst: a dream too far?** *Appl. Microbiol. Biotechnol* 2013, **97**:9323-9341.
134. Nuutinen JT, Marttinen E, Soliymani R, Hilden K, Timonen S: **L-Amino acid oxidase of the fungus *Hebeloma cylindrosporium* displays substrate preference towards glutamate.** *Microbiology* 2012, **158**:272-283.
135. Holt A, Palacic MM: **A peroxidase-coupled continuous absorbance plate-reader assay for flavin monoamine oxidases, copper-containing amine oxidases and related enzymes.** *Nature Protocols* 2006, **1**:2498-2505.
136. Coleman AA, Scaman CH, Kang YJ, Palacic MM: **Stereochemical trends in copper amine oxidase reactions.** *J. Biol. Chem.* 1991, **266**:6795-6800.
137. Qiao C, Ling K-Q, Shepard EM, Dooley DM, Sayre LM: **Mechanism-based cofactor derivatization of a copper amine oxidase by a branched primary amine recruits the oxidase activity of the enzyme to turn inactivator into substrate.** *J. Am. Chem. Soc.* 2006, **128**:6206-6219.
138. Hacısalihoglu A, Jongejan A, Jongejan JA, Duine JA: **Enantioselective oxidation of amphetamine by copper-containing quinoprotein amine oxidases from *Escherichia coli* and *Klebsiella oxytoca*.** *Journal of molecular catalysis B: Enzymatic* 2000, **11**:81-88.
139. Smith MA, Pirrat P, Pearson AR, Kurtis CRP, Trinh CH, Gaule TG, Knowles PF, Phillips SEV, McPherson MJ: **Exploring the roles of the metal ions in *Escherichia coli* copper amine oxidase.** *Biochemistry* 2010, **49**:1268-1280.
140. Nicholas L, Beugelmans-Verrier M, Guihem J: **Interactions between aromatic and neighbouring polar groups. Part III. Synthesis and physicochemical study of *p*-substituted 3-phenyl bicyclohept-5-ene-2-carboxylic acids and their methyl esters.** *Tetrahedron* 1981, **37**:3847-3860.
141. Bosch MP, Campos F, Niubo I, Rosell G, Diaz JL, Brea J, Loza MI, Guerrero A: **Synthesis and biological activity of new potential agonists for the human adenosine A_{2A} Receptor.** *J. Med. Chem.* 2004, **47**:4041-4053.
142. Mencil JJ, Fishbein P: **Method for making pharmaceutical compounds.** US Patent 2010, US 2012/0125146 A1.
143. Kano S, Yokomatsu T, Iwasawa H, Shibuya S: **Highly diastereoselective synthesis of (3*R*, 4*R*)- and (3*R*, 4*S*)- β,γ -diamino acids from D-phenylalanine.** *Chem. Pharm. Bull.* 1988, **39**:3341-3347.
144. Waibel M, Hasserodt J: **Diversity-oriented synthesis of a drug-like system displaying the distinctive N-C=O interaction.** *J. Org. Chem.* 2008, **73**:6119-6126.
145. Tomasic T, Zidar N, Sink R, Kovac A, Blanot D, Contreras-Martel C, Dessen A, Muller-Premru M, Zega A, Gobec S, et al.: **Structure-based design of a new series of D-glutamic acid based inhibitors of bacterial UDP-N-acetylmuramoyl-L-alanine: D-glutamate ligase (MurD).** *J. Med. Chem.* 2011, **54**:4600-4610.